PEPTIDES TARGETING PROTEIN-PROTEIN INTERACTIONS: METHODS AND APPLICATIONS

EDITED BY: Luca Domenico D'Andrea, Laura Belvisi and M. Angeles Jimenez

PUBLISHED IN: Frontiers in Molecular Biosciences

frontiers Research Topics

frontiers

ISSN 1664-8714
ISBN 978-2-88971-820-7
DOI 10.3389/978-2-88971-820-7

About Frontiers

Frontiers is more than just an open-access publisher of scholarly articles: it is a pioneering approach to the world of academia, radically improving the way scholarly research is managed. The grand vision of Frontiers is a world where all people have an equal opportunity to seek, share and generate knowledge. Frontiers provides immediate and permanent online open access to all its publications, but this alone is not enough to realize our grand goals.

Frontiers Journal Series

The Frontiers Journal Series is a multi-tier and interdisciplinary set of open-access, online journals, promising a paradigm shift from the current review, selection and dissemination processes in academic publishing. All Frontiers journals are driven by researchers for researchers; therefore, they constitute a service to the scholarly community. At the same time, the Frontiers Journal Series operates on a revolutionary invention, the tiered publishing system, initially addressing specific communities of scholars, and gradually climbing up to broader public understanding, thus serving the interests of the lay society, too.

Dedication to Quality

Each Frontiers article is a landmark of the highest quality, thanks to genuinely collaborative interactions between authors and review editors, who include some of the world's best academicians. Research must be certified by peers before entering a stream of knowledge that may eventually reach the public - and shape society; therefore, Frontiers only applies the most rigorous and unbiased reviews.
Frontiers revolutionizes research publishing by freely delivering the most outstanding research, evaluated with no bias from both the academic and social point of view. By applying the most advanced information technologies, Frontiers is catapulting scholarly publishing into a new generation.

What are Frontiers Research Topics?

Frontiers Research Topics are very popular trademarks of the Frontiers Journals Series: they are collections of at least ten articles, all centered on a particular subject. With their unique mix of varied contributions from Original Research to Review Articles, Frontiers Research Topics unify the most influential researchers, the latest key findings and historical advances in a hot research area! Find out more on how to host your own Frontiers Research Topic or contribute to one as an author by contacting the Frontiers Editorial Office: frontiersin.org/about/contact

PEPTIDES TARGETING PROTEIN-PROTEIN INTERACTIONS: METHODS AND APPLICATIONS

Topic Editors:
Luca Domenico D'Andrea, National Research Council (CNR), Italy
Laura Belvisi, University of Milan, Italy
M. Angeles Jimenez, Spanish National Research Council (CSIC), Spain

Citation: D'Andrea, L. D., Belvisi, L., Jimenez, M. A., eds. (2021). Peptides Targeting Protein-Protein Interactions: Methods and Applications. Lausanne: Frontiers Media SA. doi: 10.3389/978-2-88971-820-7

Table of Contents

frontiers in Molecular Biosciences

EDITORIAL
published: 14 October 2021
doi: 10.3389/fmolb.2021.780106

Editorial: Peptides Targeting Protein-Protein Interactions: Methods and Applications

Laura Belvisi[1], *Luca Domenico D'Andrea*[2]* *and María Angeles Jiménez*[3]

[1]Dipartimento di Chimica, Università Degli Studi di Milano, Milano, Italy, [2]Istituto di Scienze e Tecnologie Chimiche "G. Natta", Consiglio Nazionale Delle Ricerche, Milano, Italy, [3]Instituto de Química Física Rocasolano (IQFR), CSIC, Madrid, Spain

Keywords: peptide, protein-protein interaction, computational design, bioactive peptide, molecular recognition

Editorial on the Research Topic

Peptides Targeting Protein-Protein Interactions: Methods and Applications

OPEN ACCESS

Edited by:
Ray Luo,
University of California, Irvine, United States

Reviewed by:
Wei Yang,
State College of Florida, Manatee–Sarasota, United States
Thomas Simonson,
École Polytechnique, France

***Correspondence:**
Luca Domenico D'Andrea
luca.dandrea@cnr.it

Specialty section:
This article was submitted to Molecular Recognition, a section of the journal Frontiers in Molecular Biosciences

Received: *20 September 2021*
Accepted: *30 September 2021*
Published: *14 October 2021*

Citation:
Belvisi L, D'Andrea LD and Jiménez MA (2021) Editorial: Peptides Targeting Protein-Protein Interactions: Methods and Applications. Front. Mol. Biosci. 8:780106. doi: 10.3389/fmolb.2021.780106

INTRODUCTION

Proteins perform a myriad of crucial roles in biological systems that depend mainly on the interaction with one or more proteins. Many physiological and pathological conditions are regulated by recognition and association among proteins. Therefore, the development of molecules able to modulate these protein-protein interactions (PPIs) open the way towards novel drugs, diagnostics and molecular tools for chemical biology and therapeutic applications. Peptides represent a class of compounds well suited for protein recognition and, of course, to modulate protein-protein interactions. More, considering the pharmaceutical field peptides are the best candidate to fill the gap between small molecule drugs and protein therapeutics.

This Research Topic aims to provide an overview of the current state and recent advances of the field. To that end, it includes both review and original research contributions that highlight promising and compelling computational tools developed to design bioactive peptides/peptidomimetics as well as successful examples of peptides, which targeting a protein-protein recognition site, are able to modulate a biological response or bind to a specific protein.

COMPUTATIONAL APPROACHES TO DESIGN PROTEIN-TARGETING PEPTIDES

Peptides targeting PPIs have been found by serendipity, screening libraries or designed by structure-based computational methods. In particular, the *in silico* approaches are gained much popularity as the methodology is coming robust. In this Topic Hashemi et al. review the recent advances in the field of in silico approaches for the design of interfering peptides against PPIs, covering many aspects and stages of the peptide design process. The review by Pérez et al. summarizes well established computational tools used to study protein/peptide interactions and provide examples of their applications in conjunction with other techniques to a few cases in drug discovery and tissue engineering. Hassankalhori et al. describes novel frontiers in computational studies applying their Supervised Molecular Dynamics protocol to explore the molecular recognition and the binding mode of macrocyclic peptides to thrombin.

APPLICATIONS OF PROTEIN-TARGETING PEPTIDES

Modulation of PPIs constitutes a promising, but challenging, way to find novel therapeutic agents to fight numerous pathologies. The fact that PPIs exhibit large surface contact areas, but lack deep binding cavities, make them difficult to target for with small molecules. Because of their physical properties, peptides are, instead, more suitable to target PPIs. The contributions included in this Topic provide a view of the advances in finding peptide modulators. The review by Cabri et al. provides us quite a thorough overview of the peptides that are currently in different phases of clinical development. These peptides are directed to diverse pathologies, i.e. cancer and related diseases, inflammation and autoimmune disorders, genetic and hormonal diseases, diabetes, obesity, cardiovascular, and neurodegenerative diseases, as well as bacterial and viral infections. Pluda et al. reviews linear and cyclic peptide-based inhibitors of two metalloproteinases, whose dysregulation leads to several pathologies (cancer, inflammatory, neurodegenerative, and cardiovascular diseases). The strategies to find these peptides include traditional medicinal chemistry, rational design, and combinatorial peptide display technologies. The review by Yang et al. focuses on the interaction between APC and ASEF, two proteins involved in metastatic colorectal cancer, and their structure-based designed peptide inhibitors. Alexa et al. describe their experimental results on finding peptides inhibiting mitogen-activated protein kinases (MAPK), involved in the regulation of many cellular functions such as cell division, differentiation and apoptosis. A 15-mer peptide derived from the RHDF1 protein, which is able to bind MAPK, is taken as starting hit and modified to optimize cell-penetrating capacity and decrease its length without affecting its binding affinity. Orea-Ordóñez et al. proposes to disrupt ribosome assembly as a novel approach for cancer therapy. Based on the crystal structure of the complex between the Erb1 and Ytm1 ribosome assembly factors, a series of peptides potentially able to interfere with that interaction are designed and assayed *in vitro*. Singh et al. focus on the interaction between a voltage-gated Na^+ channel (NAV1.6) and the fibroblast growth factor 14 (FGF14), which participates in the regulation of neuron excitability in clinically relevant regions of the central nervous system. They found that two 4-mer FGF14-derived peptides inhibit the formation of the FGF14/NAV1.6 complex.

FUTURE PERSPECTIVES

On the whole, the review and original research contributions gathered in this Research Topic provide an excellent view of the current state of the field of peptides targeting protein-protein interactions. Based on them, we can envisage a growing and successful future of the field. The modulation of PPIs with peptides has turned out a valuable approach for a number of different pathologies with many peptides already in clinical development, however the area is expected to broaden and improve applications in the near future as a huge number of PPIs are still unexplored or unknown. In this framework the availability of powerful and innovative methodologies, both experimental and computational, can support the progresses in the challenging effort of discovering novel peptide as PPI modulators endowed of optimal properties.

AUTHOR CONTRIBUTIONS

All authors listed have made a substantial, direct, and intellectual contribution to the work and approved it for publication.

Conflict of Interest: The authors declare that the research was conducted in the absence of any commercial or financial relationships that could be construed as a potential conflict of interest.

Publisher's Note: All claims expressed in this article are solely those of the authors and do not necessarily represent those of their affiliated organizations, or those of the publisher, the editors and the reviewers. Any product that may be evaluated in this article, or claim that may be made by its manufacturer, is not guaranteed or endorsed by the publisher.

frontiers in Molecular Biosciences

REVIEW
published: 22 April 2021
doi: 10.3389/fmolb.2021.662579

Advances and Insights of APC-Asef Inhibitors for Metastatic Colorectal Cancer Therapy

Xiuyan Yang[1], Jie Zhong[2], Qiufen Zhang[2], Li Feng[2], Zhen Zheng[2], Jian Zhang[1,2]* and Shaoyong Lu[1]**

[1] Department of Pathophysiology, Key Laboratory of Cell Differentiation and Apoptosis of Chinese Ministry of Education, Shanghai Jiao Tong University School of Medicine, Shanghai, China, [2] Medicinal Chemistry and Bioinformatics Center, Shanghai Jiao Tong University School of Medicine, Shanghai, China

In Colorectal cancer (CRC), adenomatous polyposis coli (APC) directly interacts with the Rho guanine nucleotide exchange factor 4 (Asef) and releases its GEF activity. Activated Asef promotes the aberrant migration and invasion of CRC cell through a CDC42-mediated pathway. Knockdown of either APC or Asef significantly decreases the migration of CRC cells. Therefore, disrupting the APC-Asef interaction is a promising strategy for the treatment of invasive CRC. With the growth of structural information, APC-Asef inhibitors have been designed, providing hope for CRC therapy. Here, we will review the APC-Asef interaction in cancer biology, the structural complex of APC-Asef, two generations of peptide inhibitors of APC-Asef, and small molecule inhibitors of APC-Asef, focusing on research articles over the past 30 years. We posit that these advances in the discovery of APC-Asef inhibitors establish the protein-protein interaction (PPI) as targetable and provide a framework for other PPI programs.

Keywords: APC-Asef inhibitors, structure based drug design, peptide inhibitors, small molecule inhibitors, colorectal cancer therapy

OPEN ACCESS

Edited by:
Luca Domenico D'Andrea, National Research Council (CNR), Italy

Reviewed by:
Ernesto Jorge Fuentes, The University of Iowa, United States
Trevor P. Creamer, University of Kentucky, United States

****Correspondence:***
Shaoyong Lu
lushaoyong@yeah.net
Xiuyan Yang
yangxy@shsmu.edu.cn
Jian Zhang
jian.zhang@sjtu.edu.cn

Specialty section:
This article was submitted to Molecular Recognition, a section of the journal Frontiers in Molecular Biosciences

Received: *01 February 2021*
Accepted: *24 March 2021*
Published: *22 April 2021*

Citation:
Yang X, Zhong J, Zhang Q, Feng L, Zheng Z, Zhang J and Lu S (2021) Advances and Insights of APC-Asef Inhibitors for Metastatic Colorectal Cancer Therapy. Front. Mol. Biosci. 8:662579. doi: 10.3389/fmolb.2021.662579

INTRODUCTION

Colorectal cancer (CRC), which results from the complex factors of genes and the environment, is the world's fourth most deadly cancer. The incidence of CRC is increasing with the rapid economic growth and global aging population (Steffen, 1986; Lise et al., 1987; Kemeny, 1992; Weekes et al., 2009). In the early stage of CRC, the 5-year survival rate is up to 90 percent after surgical excision. In contrast, those with the advanced stages usually need to treat with combination therapy of chemotherapy and surgery, and the 5-year survival rate presents a decline to varying degrees. Despite the dramatic improvement in CRC treatment, metastatic CRC is still an unmet challenge (Gallina et al., 2006; Aliev and Aliev, 2007; Haggar and Boushey, 2009; Zheng et al., 2014; Liu et al., 2015; Jideh and Bourke, 2018). Therefore, there is an urgent need for innovative and effective drug candidates, especially for metastatic CRC patients.

The Adenomatous polyposis coli (APC) protein plays a pivotal role in sporadic and familial CRCs. APC was first characterized as a mutated gene in CRC by Groden et al. (1991; **Figure 1**). The following work explained how APC exerted its effect as a tumor suppressor in the traditional Wnt signaling pathway. APC could form APC/Axin/GSK3-β destruction complex and downregulate β-catenin. Mutated APC resulted in the aberrant stabilization and accumulation of β-catenin, which could activate the transcription of the TCF/LEF family transcription factors associated with proliferation (Korinek et al., 1997; Morin et al., 1997; He et al., 1998; Tetsu and McCormick, 1999). APC contains multiple domains and interacts with other proteins, suggesting APC act in non-traditional roles outside the Wnt pathway in CRC. Kawasaki et al. identified

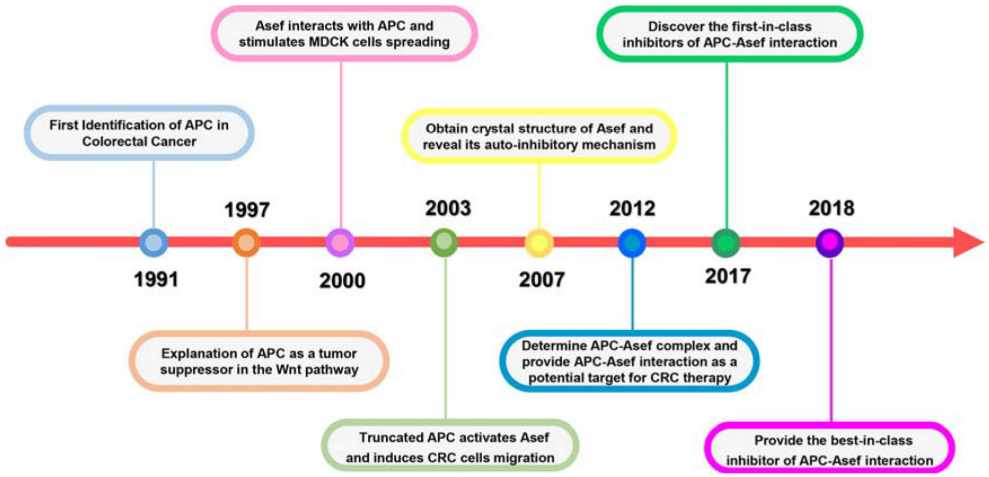

FIGURE 1 | Significant milestones in the history of APC-Asef Interaction.

Rho guanine nucleotide exchange factor 4 (Asef) released its auto-inhibited activity by interacting with the armadillo repeat domain (ARM) of APC, thereby stimulating Asef-mediated MDCK cell flattening, lamellipodia formation, and cell spreading (Kawasaki et al., 2000). In addition, the expression of truncated APC could activate Asef in CRC, inducing inappropriate cell migration and invasion (Kawasaki et al., 2003). In 2007, the crystal structure of Asef was solved and demonstrated its auto-inhibitory mechanism caused by the intramolecular interaction between the SH3 domain and DH domain (Murayama et al., 2007). Zhang et al. (2012) reported the APC-Asef complex's structures and elucidated the molecular mechanism of Asef recognition by APC, which provided APC-Asef interaction as a potential target for CRC therapy (Zhang et al., 2012). Since the characterization of the APC-Asef co-complex, remarkable progress has been made in the development of APC-Asef inhibitors. Based on these structures, MAIT-203, the first-in-class inhibitor of APC-Asef interaction, was generated, which could efficiently reduce the migration and invasion of CRC cells by blocking APC-Asef interaction (Jiang et al., 2017). After multiple optimizations, MAI-400, the best-in-class inhibitor of APC-Asef interaction, was discovered with an IC_{50} of 250 nM (Yang et al., 2018). This article reviews these processes and breakthroughs on APC-Asef interaction as a valuable target for CRC therapy. We hope that it will conduct a longitudinal analysis of critical issues, limitations, and opportunities to develop new CRC candidates and make significant contributions to medical research.

APC-ASEF INTERACTION PROMOTES COLORECTAL CANCER CELL MIGRATION AND CANCER PROGRESSION

APC is a multifunctional protein, which plays crucial and diverse functions in cellular processes, including Wnt/β-catenin signaling (Ha et al., 2004; Xing et al., 2004; MacDonald et al., 2009; Wang et al., 2014) and non-traditional Wnt pathway (Hamada and Bienz, 2002; Bienz and Hamada, 2004; Akiyama and Kawasaki, 2006; Etienne-Manneville, 2009; **Figure 2**). The human APC protein mainly contains an oligomerization domain (OD), an ARM domain, a β-catenin binding region, a basic domain, and an end-binding protein 1 (EB1)/ discs large (DLG) binding domain (**Figure 2A**). APC can interact with various proteins, including β-catenin, Asef, IQGAP1, Sam68, KAP-3, Kinesin-2, and Amer1. APC binds to β-catenin and recruits it to a destruction complex that contains axin, glycogen synthase kinase 3β (GSK3β), and casein kinase 1α. The destruction complex promotes the phosphorylation of β-catenin and induces its proteasome-mediated degradation, thus suppressing the canonical Wnt signaling pathway (**Figure 2A**; Li et al., 1998; Sieber et al., 2000; Zhang et al., 2011). Other PPIs are investigated to elucidate the function of APC in non-traditional pathways comprehensively. APC's interaction with Asef stimulates the GEF activity of Asef and promotes Asef-mediated cell flatting, cell membrane ruffling, lamellipodia formation, and cell spreading (Kawasaki et al., 2000). APC also interacts with IQGAP1 at the leading edge of migrating cells to regulate cell polarization and migration (Watanabe et al., 2004). APC can bind to the tyrosine-rich domain of Sam68 and regulate alternative splicing of TCF-1 (Morishita et al., 2011). APC interacts with KAP-3 to form a complex with β-catenin and the kinesin superfamily proteins KIF3A-KIF3B, leading to increased cell migration (Mahajan et al., 2015). The interaction between APC and Kinesin-2 plays an essential role at dendrite branch points to resolve microtubule collisions (Weiner et al., 2016). APC interacts with Amer1 and regulates the APC-dependent maintenance of intercellular junctions and negatively regulates the Wnt/β-catenin signal transduction pathway (Grohmann et al., 2007; Tanneberger et al., 2011; Zhang et al., 2015). These PPIs explain the function of APC in tumor formation and migration.

APC mutations have been identified in most sporadic and family CRCs and are considered an early event for tumorigenesis.

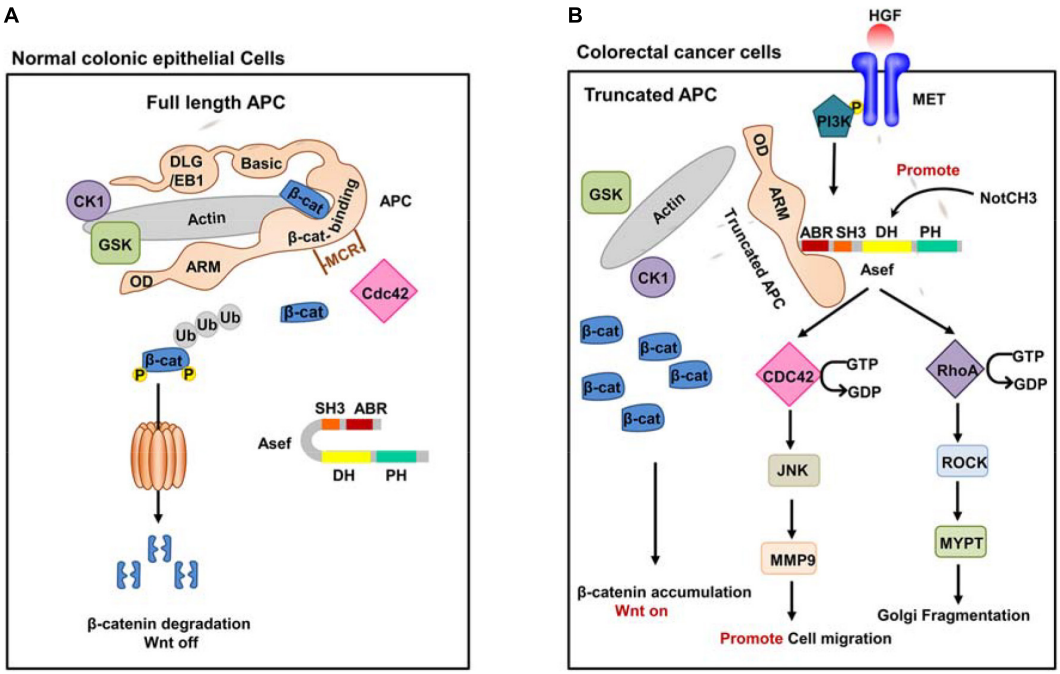

FIGURE 2 | The function of Wile-type APC and truncated APC. **(A)** Wild-type full-length APC in normal colonic epithelial cells. In normal colonic epithelial cells, APC acts as a tumor suppressor in the traditional Wnt signaling pathway. APC could interact with β-catenin and form APC/Axin/GSK3-β destruction complex. The destruction complex promotes phosphorylation of β-catenin and induces its proteasome-mediated degradation, thus suppressing the canonical Wnt signaling pathway. **(B)** A representative truncated APC in CRC cells. In CRC cells, truncated APC interacts with Asef instead of β-catenin and stimulates the GEF activity of Asef. Activated Asef promotes cell migration and Golgi fragmentation through the downstream pathway.

The presence of APC mutations in premalignant lesions detected by exome sequencing of human colorectal adenomas and the surrounding mucosa confirmed its role in the early growth of colon adenoma. APC mutant mouse models have proved that the alterations in the APC gene are essential for the initiation of intestinal tumor (Miyoshi et al., 1992; Sen-Gupta et al., 1993; Su et al., 1993; Iwama et al., 1999; Iwama, 2001; Nikolaev et al., 2012; Borras et al., 2016; Zhang and Shay, 2017). Most APC mutations are confined to their central region, referred to as the mutation cluster region (MCR). Alterations in the APC gene generate C-terminal truncated APC fragment and cause loss of the domains required for binding to β-catenin and microtubules. Therefore, truncated APC is disabled to degrade β-catenin, resulting in the accumulating of β-catenin, which constitutively activates the Wnt signaling pathway in CRC cells (Tominaga et al., 1998; Norris et al., 2000; Schneikert and Behrens, 2006; Schneikert et al., 2007, 2011). In addition, the truncated APC effectively interacts with Asef via its ARM domain (**Figure 2B**). Asef, one of the human Dbl-family of guanine nucleotide exchange factors (GEFs), consists of an APC-binding region (ABR), an Src homology 3 (SH3) region, a Dbl homology (DH) region, and a pleckstrin homology (PH) region. Asef is usually auto-inhibited by binding between its SH3 domain and DH-PH domains (Kawasaki et al., 2000; Gotthardt and Ahmadian, 2007; Mitin et al., 2007; Murayama et al., 2007; Muroya et al., 2007; Yoshihiro et al., 2008). Zhang et al. (2012) suggested that the intramolecular interaction strength between the DH and SH3 domain of Asef was less than that of Asef-APC. The isothermal titration calorimetry (ITC) assay revealed a tight binding between APC and Asef with a K_d value of 17.8 nM. Therefore, the interaction of the Asef-DH and Asef-SH3 was easily separated once APC binding with Asef.

Upon binding to the truncated APC, Asef releases its auto-inhibition and stimulates its GEF activity, thereby catalyzing the exchange of GDP for GTP in CDC42. The activated Asef and CDC42 upregulate the expression of matrix metalloproteinase 9 (MMP9) mainly through the c-Jun N-terminal kinase (JNK) pathway, thereby stimulating cell flattening, membrane ruffing, and lamellipodia formation and ultimately promoting cancer cell migration (Kawasaki et al., 2000, 2003, 2009a; Gotthardt and Ahmadian, 2007; Mitin et al., 2007; Murayama et al., 2007; Itoh et al., 2008).

It has also been shown that epidermal growth factor (EGF), hepatocyte growth factor (HGF), and basic fibroblast growth factor (bFGF) increase the amount of the APC-Asef complex and induce its accumulation and co-localization in membrane ruffles and lamellipodia, thereby promoting cell migration (Itoh et al., 2008; Kawasaki et al., 2009a,b). In addition, upstream PI3K may affect APC and Asef in the HGF signaling pathway (Kawasaki et al., 2009b). These increase the possibility that HGF and PI3K activate the migration activity of CRC cells by inducing the accumulation of APC-Asef complex in membrane ruffles and lamellipodia. Additionally, the miR-1-NOTCH3 signaling plays

a critical role in CRC cell migration and cancer angiogenesis by up-regulating Asef expression (Furukawa et al., 2013).

Recently, Kim et al. found that truncated APC activated Asef and then induced Golgi fragmentation by stimulating the RhoA-ROCK-MLC2 pathway. Golgi fragmentation led to the loss of cell polarity and disordered direction of cell migration, which facilitated CRC initiation and progression. This phenomenon may be an early event in CRC development, which affects the regular directed cell migration, promoting cancer initiation and progression (Rodriguez-Cruz et al., 2018).

In conclusion, truncated APC is disabled to play its suppressor role but constitutively activates Asef, promoting the migration of CRC cells and the progression to invasive malignancy.

DISRUPTING APC-ASEF INTERACTION COULD BE A POTENT TARGET FOR CRC THERAPY

Recently, PPIs are becoming ponderable therapeutic targets for various diseases. APC-Asef interaction plays an essential role in the progression, invasion, and metastasis of CRC. Whether knocking down APC or Asef, it significantly decreased the migration of several types of CRC cells, such as HCT116 and SW480 (Kawasaki et al., 2003). Further study showed that the number and size of the intestinal adenomas in $Apc^{Min/+}$ mice were significantly reduced (Kawasaki et al., 2009a). These results suggest that the APC-Asef interaction has an essential impact on intestinal adenoma formation and tumor progression. Therefore, the APC-Asef interaction might be a novel target for the treatment of CRC. APC-Asef inhibitors might provide therapeutic options for the treatment of metastatic CRC.

STRUCTURE CHARACTERIZATION OF APC-ASEF INTERACTION

Based on the critical influence of APC-Asef on the CRC migration, Zhang et al. (2015) attempted to solve the crystal structure of APC-Asef to provide a structural basis for drug development. The ARM domain of APC (residues 443-767), consisting of seven armadillo repeats, interacts with the ABR region of Asef. Another conserved region preceding the seven armadillo repeats was referred to as the PreARM region (residues 326-442). In addition, APC mutations usually result in a truncated APC fragment with intact PreARM and ARM in CRCs. The entire APC-PreARM-ARM region might form an ARM. Therefore, they determined the crystal structure of APC-PreARM-ARM (PDB: 3NMW), APC-PreARM-ARM/Asef-ABR-SH3 (PDB: 3NMX), and APC-PreARM-ARM/Asef-ABR (PDB: 3NMZ) (Zhang et al., 2012). Zhang et al. (2015) first detailed the APC-PreARM domain (residues 326-442), which consisted of four α helices (Arm-1-H3, Arm0-H1, Arm0-H2, and Arm0-H3) and a long helix insertion (H-Ins) (**Figure 3A**). The APC-PreARM domain packed widely with the ARM domain of APC, and together formed a single-folding unit (**Figure 3B**). The APC-PreARM-ARM/Asef-ABR-SH3 complex structure revealed that Asef-ABR bound to the concave surface of the APC-ARM, formed by the Arm1-H3, Arm2-H3, Arm3-H3, Arm4-H3, and Arm3-H1 (**Figure 3C**). However, the resolution is only 3.0 Å, so the APC-PreARM-ARM/Asef-ABR complex with a higher resolution (2.3 Å) was determined (**Figure 3D**) to obtain the precise binding information. The binding interface between APC and Asef is up to 1,300 Å. Many hydrogen bond networks and van der Waal contacts in APC-ARM/Asef-ABR complex interface stabilize the interaction of APC and Asef. The mutation analysis of APC and Asef demonstrated that APC-Asn507, APC-Asn550, Asef-Glu183, and Asef-Ala186 are critical in the interaction between APC and Asef. These works reveal the molecular mechanism by which APC recognizes Asef and provide a structural basis for the inhibitors design of APC-Asef interaction.

STRUCTURE-BASED DESIGN OF FIRST-IN-CLASS APC-ASEF INHIBITORS

Although the crystal structure of APC-Asef complex has been solved, the interaction area of APC-Asef is generally flat and large. It is still a challenge to develop inhibitors of APC-Asef interaction. To identify potent inhibitors of APC-Asef interaction, Jiang et al. (2017) first determined the hot spots of APC-Asef binding (Jiang et al., 2017). The structural analysis of the APC-Asef interaction revealed that the flexible segment of Asef-ABR (^{176}SHPGGGGEQLAINELISDG^{194}, referred to as ORIGIN) fit into the flat pocket of APC-ARM with 36 pairs of residue-residue interactions. Based on this ORIGIN sequence, Jiang et al. (2017) first designed a fluorescent probe (Ac-GGGGEQLAINELISDGK-FITC) and established a fluorescence polarization (FP) competitive assay. They synthesized various truncated peptides based on the ORIGIN, such as ^{179}GGGGEQLAINELISDG^{193} (K_i = 17.1 ± 3.52 μM), ^{181}GGEQLAINELISD^{192} (K_i = 49.1 ± 13.2 μM), ^{81}GGEQLAI^{187} (K_i = 44.62 ± 0.99 μM), ^{183}EQLAINEL^{190} (K_i > 300 μM), and ^{187}INELISD^{192} (K_i > 300 μM). As a result, the peptide MAI-005 (^{181}GGEQLAI^{187}) with an acceptable activity (K_i = 44.62 ± 0.99 μM) and moderate size was considered as a hit peptide for further optimization (**Figure 4A**). They also replaced residues in each position of MAI-005 and synthesized these mutated peptides to establish a peptide library. High throughput screening of the peptide library by FP assay suggested that the favorable mutations at positions Gly181, Gln184, and Ile187 of MAI-005 could increase 4–14% binding affinities separately. Combining these favorable mutations, they developed three peptides MAI-102 (^{181}GGEALAW^{187}, K_i = 3.12 ± 0.70 μM), MAI-107 (^{181}GGEALAD^{187}, K_i = 3.80 ± 0.72 μM), and MAI-108 (^{181}AGEALAD^{187}, K_i = 2.41 ± 0.88 μM), with more than 12-fold increased affinity than MAI-005.

The crystal structures of APC/MAI-102, APC/MAI-107, and APC/MAI-108 revealed that MAI-108 induced conformational changes in the APC-ARM pocket at the position of Arg549, Lys586, and Gln542. All three compounds could induce the conformational changes of the side chain of APC Arg549 (**Figures 4B–D**), resulting in a doughnut shape of the APC-ARM

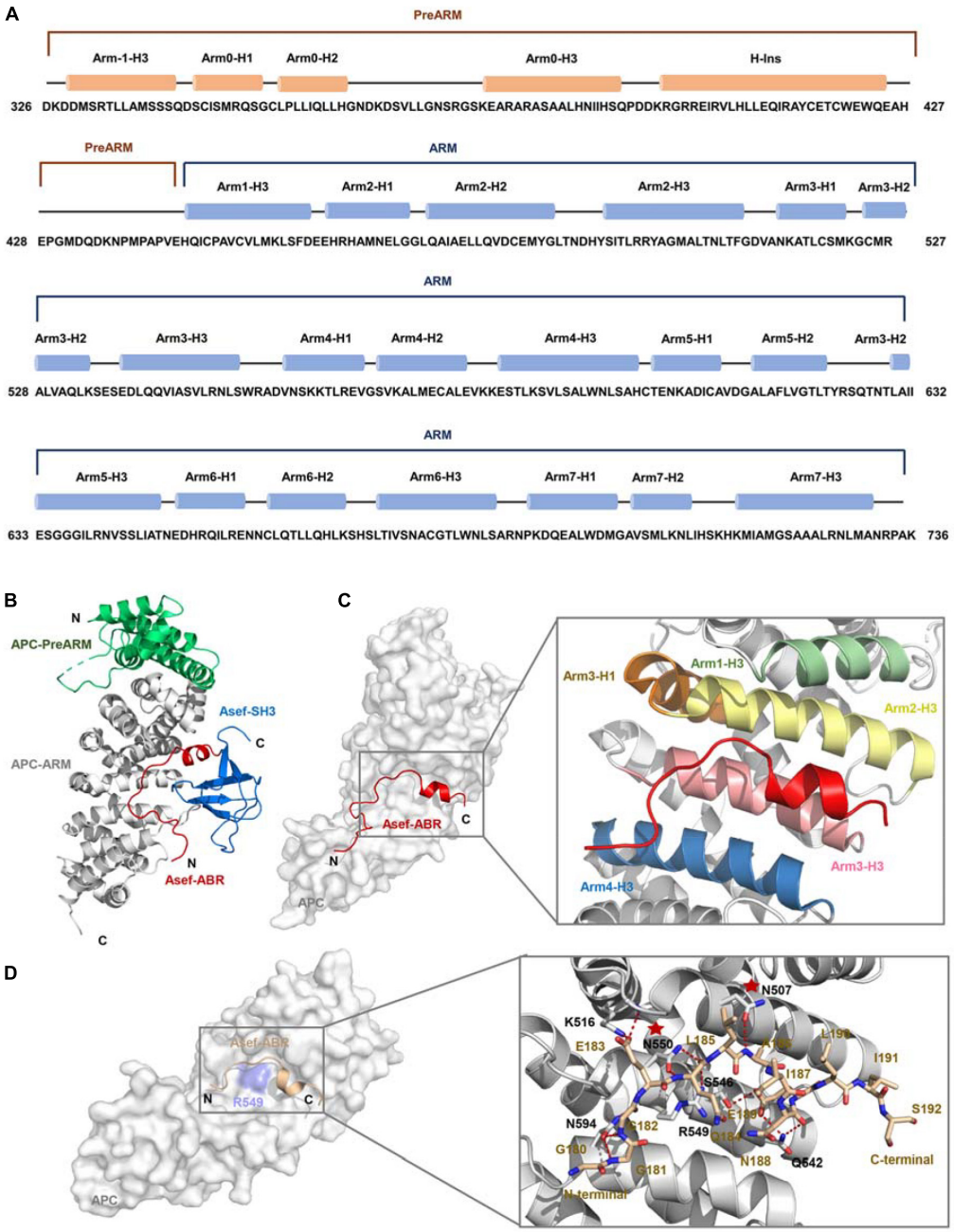

FIGURE 3 | The crystal structure of APC and Asef **(A)** Sequence of human APC (residues 326-736). APC-PreARM residues (326-442) are labeled orange, and APC-ARM (453-767) are labeled blue. APC-PreARM consists of five α helices: Arm-1-H3, Arm0-H1, Arm0-H2, Arm0-H3, and the long helix insertion (H-Ins). APC-ARM contains seven armadillo repeats Arm1 to Arm7. **(B)** APC (PreARM-ARM)/Asef (ABR-SH3) complex structure, the PreARM portion of APC is shown in green, and the ARM portions of APC are shown in gray. The ABR domain of Asef is shown in red, and the SH3 domain of Asef is shown in blue. **(C)** Detailed information of the interface of APC and Asef complex. Asef is shown in red. Arm1-H3, Arm2-H3, Arm3-H1, Arm3-H3, and Arm4-H3 are shown in green, yellow, orange, pink, and blue, respectively. **(D)** Left: The interactions of APC and Asef-ABR. The ABR domain of Asef is shown in champagne, and APC is shown in gray. Right: Close-up view of interactions between APC and Asef. APC is shown as a gray carton, and Asef is shown as a champagne stick. Red dashed lines represent hydrogen bonds. The red stars represent APC-Asn507 and APC-Asn550 are critical in the interaction of APC and Asef.

pocket with the more druggable property. Compared with the flat interaction surface of APC-Asef, the doughnut shape pocket of APC provided a potential druggable target for the development of APC-Asef inhibitors. Moreover, the overlapped structures of MAI-102, MAI-107, and MAI-108 in the binding site provided new information for the next optimization. The residues 181–185 of MAI-102, MAI-107, and MAI-108 had similar binding confirmation, but the C terminus exhibited diverse conformation

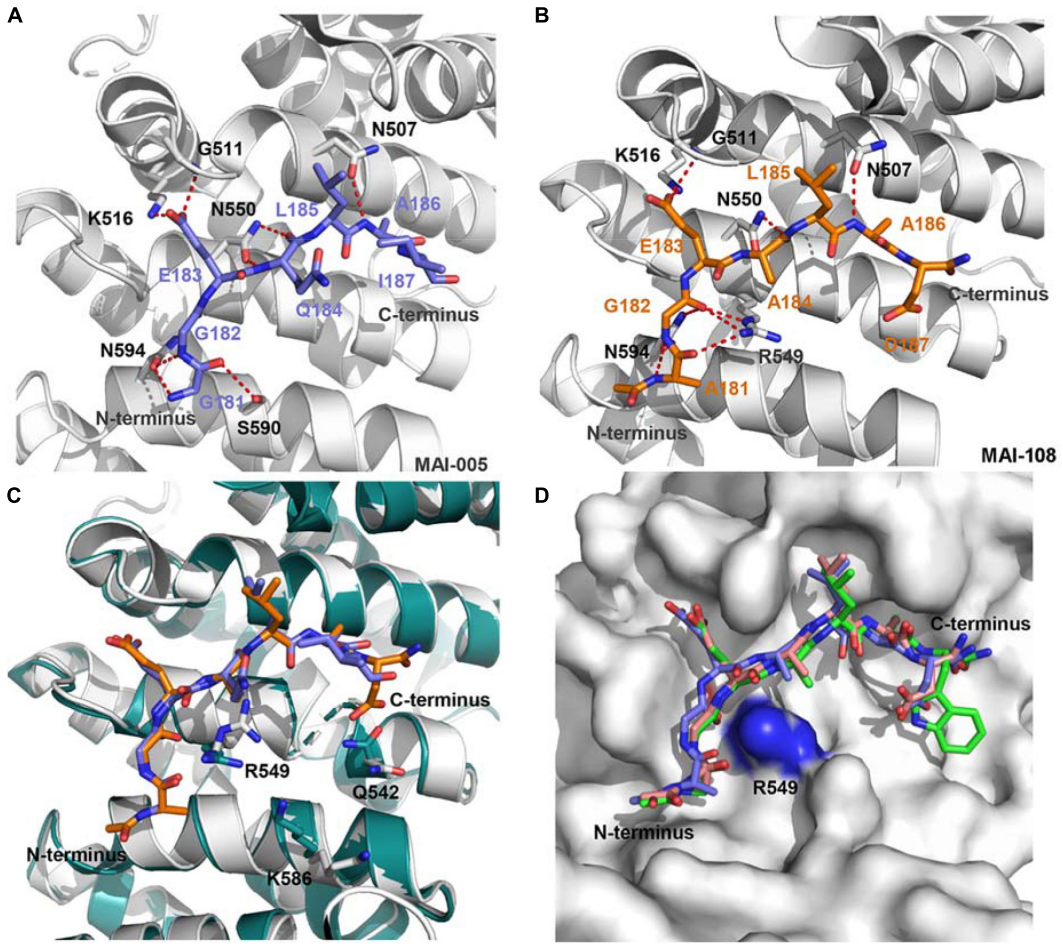

FIGURE 4 | (A) The interactions of APC and MAI-005. APC is shown as a cartoon representation (gray), and MAI-005 is shown as a stick representation (purple). Red dashed lines represent hydrogen bonds. **(B)** Crystal structure of APC and MAI-108 (5IZ8). APC is shown as a cartoon representation (gray), and MAI-108 is shown as a stick representation (orange). Red dashed lines represent hydrogen bonds. **(C)** Structure comparison of APC/MAI-005 (APC, cartoon, gray; MAI-005, stick, purple) and APC/MAI-108 (APC, cartoon, cyan; MAI-108, stick, orange). **(D)** Superimposition of APC/MAI-102 (5IZA), APC/MAI-107 (5IZ9), and APC/MAI-108 (5IZ8) (APC, surface, gray; MAI-102, stick, green; MAI-107, stick, light pink; MAI-108, stick, purple).

(**Figure 4D**). The optimization of C-terminal peptide residues might improve the binding affinity via adding additional interactions. Therefore, they established a next-generation library of peptides based on the scaffold of ^{181}AGEAL^{185}. The new peptides library involved various N-terminal groups, entirely stochastic diverse residues at position 186, and the confined acidic or polar residues at position 187. Finally, they found MAI-150 (^{181}AGEALYE^{187}, $K_i = 0.12 \pm 0.02$ μM) was a better inhibitor of APC-Asef. The binding affinity of MAI-150 increased more than 20-fold in comparison to MAI-108 and 370-fold to MAI-005. The crystal structure and mutation analysis showed that the improved binding affinity might be caused by forming the additional interactions through residue Tyr186, Glu187, and the N-terminal benzyloxycarbonyl group of MAI-150 (**Figures 5A,B**).

Next, peptidomimetic inhibitors were designed to improve the binding affinity based on the APC/MAI-150 complex structure. The optimization of the N-terminal group and residues at positions 185 and 186 resulted in the peptidomimetic compound MAI-203 with cyclopentylalanine residue at position 185. The K_i value of MAI-203 to APC was as high as 0.015 ± 0.001 μM, equivalent to the dissociation constant of APC-Asef (K_d = 0.018 μM). The binding affinity of MAI-203 improved more than nine-fold compared to MAI-150 and 2,900-fold to MAI-005. The crystal structure of APC/MAI-203 was determined to explain the high binding affinity of MAI-203 to APC. MAI-203 induced the subsite formed by Arg463 and Phe510 of the APC larger to adapt to the cyclopentylalanine residue of MAI-203. This might facilitate tighter hydrophobic interactions and account for the improved binding affinity of MAI-203 (**Figures 5C,D**). The cell permeability of MAI-203 is low because of the large size and peptide properties. Jiang et al. (2017) connected the penetrating peptide TAT (trans-activating transcriptional activator) to the C-terminal of MAI-203 and MAI-150 and obtained the cell-permeable peptide MAIT-203 and MAIT-150.

To determine the effect of peptides *in vivo*, Jiang et al. (2017) performed co-immunoprecipitation experiments in HEK293T

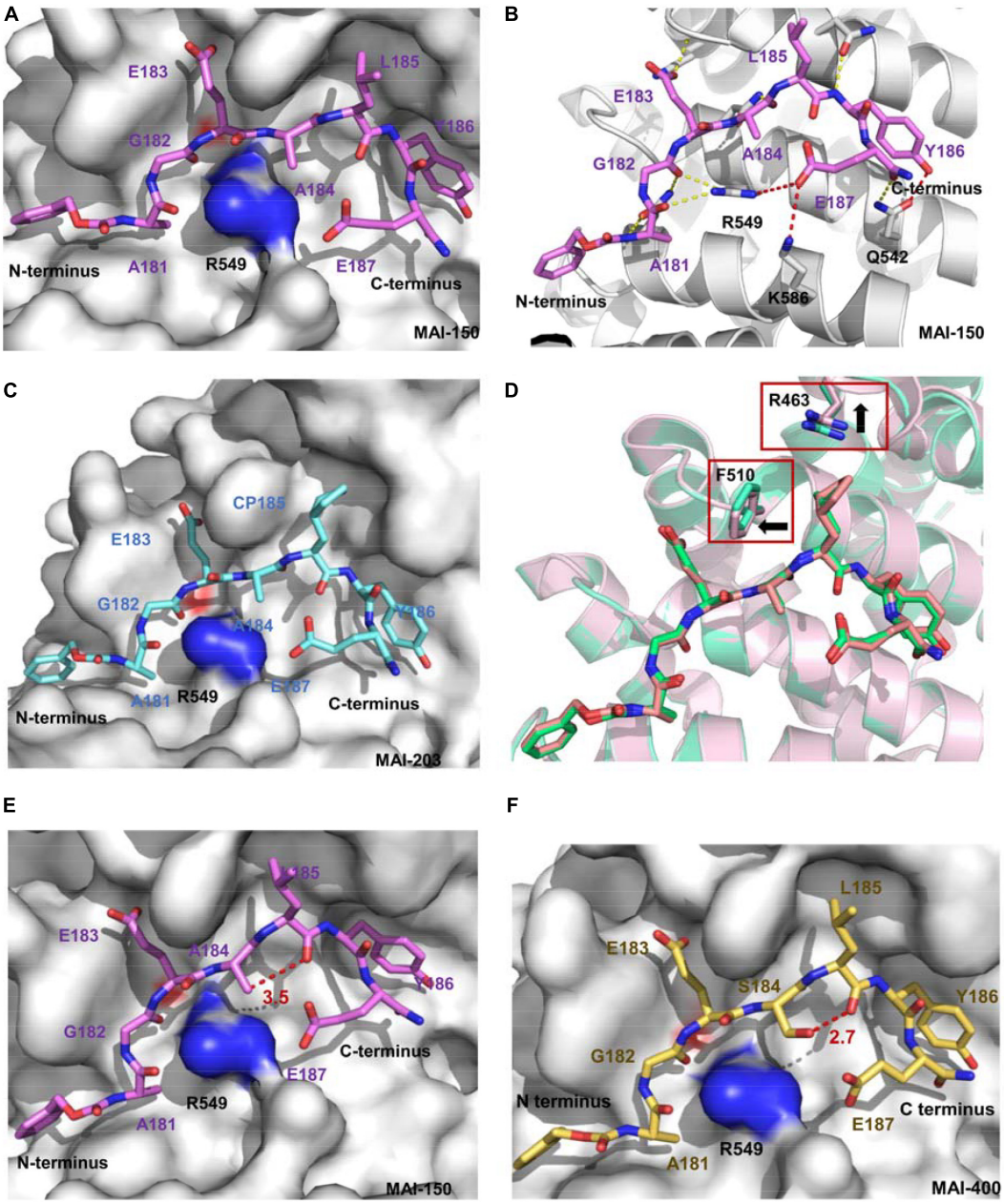

FIGURE 5 | (A) Crystal structure of APC and MAI-150 (5IZ6). APC is shown as a surface representation (gray), and MAI-150 is shown as a stick representation (pink). **(B)** The interactions of APC and MAI-150 (APC, cartoon, gray; MAI-150, stick, pink). Yellow dashed lines represent hydrogen bonds. Red dashed lines represent new hydrogen bonds. **(C)** Crystal structure of APC and MAI-203 (5B6G). APC is shown as a surface representation (gray), and MAI-150 is shown as a stick representation (blue). **(D)** A structural comparison of APC/MAI-150 (APC, cartoon, pink; MAI-150, stick, pink) and APC/MAI-203 (APC, cartoon, cyan; MAI-203, stick, cyan). **(E)** Crystal structure of APC and MAI-150. APC is shown as a surface representation (gray), and MAI-150 is shown as a stick representation (pink). **(F)** Crystal structure of APC and MAI-400 (5Z8H). APC is shown as a surface representation (gray), and MAI-400 is shown as a stick representation (yellow). Red dashed lines represent hydrogen bonds.

cells and SW480 cells. The results showed that MAI-203 and MAI-150 reduced the APC-Asef interaction in a dose-dependent manner. The cellular thermal shift assay in SW480 cells revealed that MAIT peptides could increase the thermal denaturation temperature (ΔT_m = 6.92 ± 0.94°C), which indicated that the MAIT peptides directly interacted with APC in cells. Next, the function of MAIT peptides in CRC cells was investigated. RCTA, transwell and wound-healing assays were performed to evaluate the anti-migratory effect of MAIT peptides. The results showed that MAIT peptides at 10 μM caused significant repression of cell migration and invasion in SW480 and HCT116 cells. Cell vitality and proliferation

experiments showed that MAIT peptides at concentrations up to 100 μM had no effect on the morphology or growth of SW480 and HCT116 cells. In the biology assays, MAIT-203 could effectively block the APC–Asef interaction, thereby inhibiting the migration and invasion of two types of CRC cells without affecting cell proliferation. In a fluorescence-based GEF assay with GTP-bound GTPases, MAIT-203 was used as a chemical probe to identify the downstream GTPase substrate of activated-Asef by APC-ARM. The results suggested that the GEF activity of CDC42 was stimulated by APC-Asef interaction and decreased by treatment of MAIT-203. Therefore, the downstream GTPase in the Asef activation pathway stimulated by APC was CDC42. Future research will focus on the mechanism of cell migration and invasion through the APC-Asef-CDC42 pathway.

OPTIMIZATION STRATEGY LEADING TO THE BEST-IN-CLASS INHIBITOR

To obtain highly effective new APC-Asef inhibitors, Yang et al. (2018) further optimized MAI-150 via a rational structure-based strategy. According to the complex structure of MAI-150/APC (PDB code 5IZ6), the hydrogen atom in the side chain of residue A184 and the oxygen atom in the backbone of residue L185 have a suitable angel (120.9°) and distance (3.5 Å) to form an intramolecular hydrogen bond (**Figure 5E**). Then, Yang et al. (2018) designed and synthesized a series of MAI-150 derivatives by replacing the A184 residue with polar amino acids, whose side chains provided hydrogen-bond donors. These efforts led to discovering MAI-400, a best-in-class APC-Asef inhibitor with a K_d of 0.012 μM and an IC_{50} of 0.25 ± 0.01 μM. The complex of APC/ MAI-400 was determined, and the formation of intramolecular hydrogen bond was confirmed (**Figure 5F**). Surface Plasmon Resonance (SPR) and ITC assay revealed the binding affinity of MAI-400 to APC and explained the contribution of the intramolecular hydrogen bond. Co-immunoprecipitation (co-IP) assay showed that MAI-400 efficiently disrupted the APC-Asef interaction in a dose-dependent manner. Their successful strategy may be a useful approach for peptide optimization.

SMALL MOLECULE INHIBITORS OF APC-ASEF PROTEIN-PROTEIN INTERACTION

Zhu et al. reported numbers of 2-H pyrazole derivatives containing morpholine groups as inhibitors of APC-Asef (Yan et al., 2019) (**Figure 6**). Based on the structure of APC-PreARM-ARM/Asef-ABR (PDB: 3NMZ), they found 2-H pyrazole derivatives showed good estimated binding free energy from −56.45 to −35.46 kcal/mol by molecular docking. Among these compounds, compound 7g had the best-estimated binding free energy of −56.45 kcal/mol. The estimated binding mode of 7g-APC suggested 7g bound to the central position of the APC-Asef interact surface through six conventional hydrogen bonds, two carbon-hydrogen bonds, and six Pi bonds. These predicted interactions reflected the stability of APC-7g binding.

Next, 2-H pyrazole derivatives 7a–7y were synthesized through a 5-step route. The structure of 7g was identified by NMR, MS, elemental analysis, and single-crystal X-ray diffraction analysis. The efficacies of derivatives 7a–7y were evaluated by the FP competitive assay. The IC_{50} values of these compounds ranged from 0.18 to 22.68 μM, and the typical compound 7g showed the best IC_{50} values of 0.18 μM. ITC furtherly verified the binding affinity of 7g-APC and 7g-Asef. The results showed that 7g could interact to APC with a K_d value of 12.8 μM

Compound 7g exhibited anti-proliferative activity against six cancer cell lines, especially against HCT-116 cells. Compound 7g also induced HCT-116 cell apoptosis at a concentration of 2–4 μM. Further studies showed that 7g could increase ROS level and induce apoptosis of HCT-116 cells. Compound 7g could weaken the adhesion and invasion of HCT-116 cells

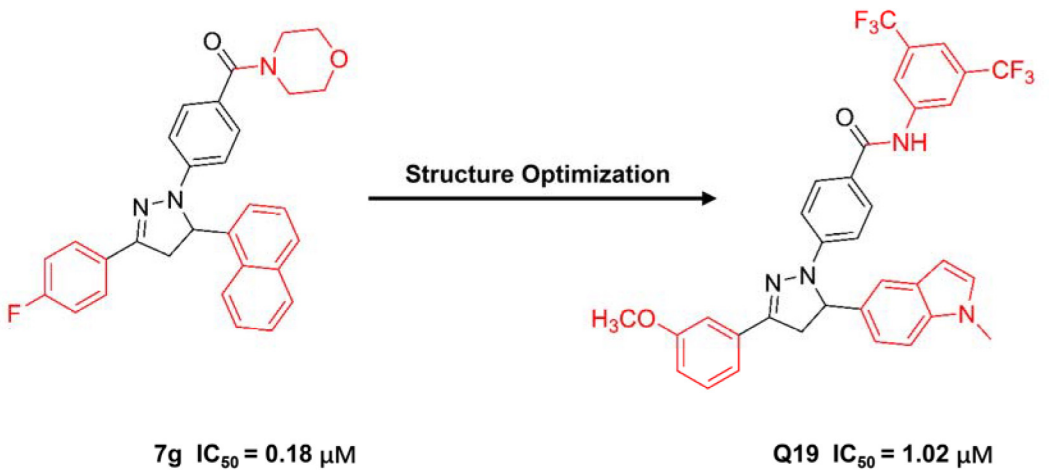

FIGURE 6 | The structure of compound 7g and Q19.

at a concentration of 2 μM. Besides the in vitro bioactivity, the in vivo anti-tumor efficacy of 7g was also investigated. The mouse xenograft and orthotopic transplantation models were established to evaluate the in vivo anti-tumor efficacy of 7g. The average weight of the excised tumor and tumor volume in 7g treated mice significantly reduced compared to the vehicle group. The results showed 7g significantly suppressed tumor growth.

Through further optimization of 7g, compound Q19 was obtained as the following generation inhibitor of APC-Asef with the IC_{50} values of 1 μM (Qi et al., 2020). Compound Q19 could inhibit the proliferation of HCT-116 cells with the GC_{50} values of 1.37 μM. Besides, compound Q19 could induce the mitochondria depolarization and apoptosis of HCT-116 cells. However, Q19 was not as potent as 7g in FP assay and anti-proliferation assay.

Based on these results, it is hard to determine the direct target of compounds 7g and Q19. The only evidence to verify the direct binding of APC and 7g is the ITC assays. However, the original data of ITC results suggest that the molar ratio is not less than 1, indicating that the APC is not saturated by 7g. It is theoretically impossible to calculate the accurate K_d value due to its atypical curve and appropriate molar ratio. The current K_d value of 7g to APC is not convincing, and the binding affinity of 7g-APC still needs further confirmation. More convincing binding affinity assays and co-crystal structure need to be provided to assure the target of 7g. Besides, the interaction of APC-Asef with ROS-induced apoptosis and mitochondria depolarization needs to be clarified.

Another group was interested in developing APC-Asef inhibitors and tried to identify new small molecular inhibitors of APC-Asef through a combination of docking methods and molecular dynamics simulations (Jadav et al., 2020). They analyzed and validated the central binding region of APC bind to MAI-peptide, including Arg539, Lys516, Asn507, and Trp553 of APC. Then, structure-based virtual screening (SBVS) of ZINC13, NCI, and Maybridge public compound library were carried out. The top-scoring hits were explored by induced fit docking analysis and molecular dynamic simulations. Finally, the 16 ligand hits with amide groups were predicted to be APC-Asef inhibitors with the pretty similarity of known anti-cancer β-carbolines and pharmacological profile. However, bioassays are still required to prove the actual targets and activities of these molecules.

BIOASSAYS FOR EVALUATING THE BINDING AFFINITY AND EFFICACY OF APC-ASEF INHIBITORS

Binding Assays

Appropriate methods that can sensitively evaluate the binding affinity of screening candidates help identify and validate PPI inhibitors, including FP assay, ITC, SPR, Thermal shift assay (TSA), and cellular thermal shift assay (CETSA). In the initial screening process, an FP competitive assay was established to screen APC-Asef inhibitors. In this assay, the formation of the APC-inhibitor complex was deduced from a decrease in FP, and the IC_{50} and K_i values were determined. The FP assay is a convenient and effective competition binding assay for screening PPIs inhibitors. However, the applications of FP is limited to screening inhibitors that competitively bind to the receptors at a stoichiometry of 1:1 (Huang, 2003). As the gold standard technique for measuring direct binding affinity, ITC experiments are usually carried out in the following confirmation processes (Zeiss and Bauer-Brandl, 2006; Wiebke, 2015). ITC assays further confirmed the binding affinity of MAI-peptides to APC or Asef. The ITC results showed that the stoichiometry ratio of MAI-peptide and APC was 1:1, which was suitable for the FP assay. The K_d value measured by ITC is consistent with the IC_{50} and K_i value by FP. The enthalpy change and entropy change during the binding of peptides to APC provided useful information for hit-to-lead optimization. ITC is not suitable for high throughput screening. SPR is also used to determine the direct binding affinity and thermodynamic parameters of MAI-peptides to APC (Yan, 2015). The dissociation and association rate constants help to understand the structure-activity relationships (SAR) of MAI-peptides. TSA and CETSA are reliable methods to measure the interaction between MAI-peptides and APC by determining the melting temperature (T_m) of the protein complex (Zhang and Monsma, 2010; Rogez-Florent et al., 2014; Letourneau et al., 2019; Henderson et al., 2020; Rodriguez-Furlan and Hicks, 2021). The results of TSA and CETSA showed that MAI-peptides directly bind to APC *in vitro*.

Functional Assays

Co-immunoprecipitation (co-IP), Real-Time Cell Analysis (RCTA), wound-healing and Transwell assay were performed to determine the function of MAI-peptides in CRC cells. Co-IP experiments in HEK293T cells and SW480 cells demonstrated the inhibitory effect of MAIT-peptides on physiologically APC-Asef interaction. RCTA can detect electrical impedance through microelectronic biosensor technology and measure the migration and invasion of CRC cells. The RCTA results showed that MAIT-203 remarkably inhibited the migration and invasion of SW480 and HCT116 cells better than MAIT-150. The wound-healing assay was used to detect the influence of MAIT-peptides on the spreading tendency of SW480 and HCT116 cells. MAIT-203 significantly inhibited cell migration, especially at the leading edges. In addition, a Transwell assay was performed to confirm the anti-migration effect of MAIT-peptides. Consistent with the previous results, MAIT-203 reduced the migration of SW480 and HCT116 cells. To evaluate the anti-migration efficacy of MAIT-peptides *in vivo*, researchers need to establish a mouse model of CRC with liver metastasis. The following research may focus on the efficacy of APC-Asef inhibitors on CRC metastasis *in vivo*.

CHALLENGES IN TARGETING APC-ASEF PPI

Targeting the APC-Asef interaction using peptidomimetic inhibitors as a new therapy for CRC migration has achieved exciting results. MAIT-203 and its derivatives have been found

to inhibit the migration and invasion of SW480 cells efficiently. However, undesirable physicochemical properties of peptides, such as poor oral bioavailability, low permeability, and instability, limit their further development.

The Asef binding site on APC is tremendous, and it is still a challenge to block this site with small molecules. Small molecule inhibitors possess several distinct advantages, such as higher membrane permeability, better selectivity, and higher affinity than peptides. With the current complex structures of peptide-APC, the discovery of small-molecule inhibitors of APC-Asef might be feasible. The hot spots in APC and the binding mode of peptides provide essential information for the design of small-molecule inhibitors. Peptides simplification also provides an available method for the design of small molecule inhibitors.

Besides, allosteric modulation could provide a new strategy to regulate PPI via conformational changes to avoid the flat and large interaction surface of PPI. Allosteric inhibitors targeting APC might be another way to discover small molecule inhibitors. Most allosteric PPI modulators were discovered fortuitously. However, the rapid progress in chemical and structural biology facilitates the rational design of allosteric PPI modulators. The first step is to identify the allosteric site of APC-Asef based on the APC-Asef co-complex structure. Multiple computational approaches are feasible to predict allosteric sites, such as statistical coupling analysis (SCA) (Lockless and Ranganathan, 1999), FRpred (Fischer et al., 2008), ConSeq (Berezin et al., 2004), ConCavity (Capra et al., 2009), and Allosite (Huang et al., 2013). These methods help us analyze and select potential allosteric sites of APC-Asef. Once the allosteric site is uncovered, virtual screening of allosteric modulators and standard-precision (SP) docking are performed. The commercial screening hits are chosen based on the comprehensive analysis of their binding modes and physiochemical properties. Finally, experimental screening and site validation could yield the possible hit compounds as the allosteric inhibitors of APC-Asef. These rational design strategies might inspire other research of allosteric PPI-based drug discovery.

Degradation of truncated APC by PROTACs technology might disturb the APC-Asef interaction and inhibit CRC migration, which provides a new method for CRC therapy.

Additionally, the APC-Asef interaction is regulated by HGF and phosphatidylinositol-3-kinase. Multiple-target therapy might be a more efficient method in cancer treatment. Therefore, the combination of APC-Asef interaction inhibitors and HGF inhibitors, as well as PI3K inhibitors, might be tolerable and effective for the treatment of CRC.

The APC-Asef interaction could be a promising target for CRC therapy. The development of APC-Asef interaction inhibitors is still in the early stages. The discovery of druggable APC-Asef inhibitors is needed for CRC therapy. Further studies will focus on the preclinical studies of APC-Asef inhibitors to provide new options for the treatment of CRC.

CONCLUSION

Protein-protein interactions are attractive drug targets in many diseases. Most of the disease-relevant PPIs are considered undruggable because of their flat, featureless and expansive interface. The structure-based design has been an important strategy for discovering PPI inhibitors. The discovery of APC-Asef inhibitors is an example of rational design utilizing PPI structural information. Firstly, the crystal structures of APC-Asef provided a molecular basis for rational inhibitor discovery. Hotspot identification helped to characterize the key binding site and served as the starting point for the optimization of APC-Asef inhibitors. Next, mutagenesis and structural studies of APC-lead peptide provided the SAR. Multiple optimizations based on the structure resulted in the desirable inhibitor with high binding affinity. Finally, the evaluation of the binding affinity and efficacy of APC-Asef inhibitors *in vitro* and *in vivo* not only demonstrated that APC-Asef PPI was a druggable target of metastatic CRC but also provided a potential lead inhibitor for CRC drug discovery. The successful discovery of APC-Asef inhibitors validated an effective paradigm in structure-based PPI inhibitors design. It provided proof-of-principle for other PPI programs and enabled the development of numerous drugs that target PPIs.

AUTHOR CONTRIBUTIONS

SL, XY, and JZha conceived the study. XY reviewed and edited the manuscript. JZho, QZ, and LF contributed analysis tools. All authors wrote the manuscript.

FUNDING

Financial support of this work by the Science and Technology Commission of Shanghai Municipality (grant 19ZR1476400 to XY).

REFERENCES

Akiyama, T., and Kawasaki, Y. (2006). Wnt signalling and the actin cytoskeleton. *Oncogene* 25, 7538–7544. doi: 10.1038/sj.onc.1210063

Aliev, S. A., and Aliev, E. S. (2007). [Colorectal cancer: incidence, mortality rate, invalidity, certain risk factors]. *Vestn Khir Im I I Grek* 166, 118–122.

Berezin, C., Glaser, F., Rosenberg, J., Paz, I., Pupko, T., Fariselli, P., et al. (2004). ConSeq: the identification of functionally and structurally important residues in protein sequences. *Bioinformatics* 20, 1322–1324. doi: 10.1093/bioinformatics/bth070

Bienz, M., and Hamada, F. (2004). Adenomatous polyposis coli proteins and cell adhesion. *Curr. Opin. Cell Biol.* 16, 528–535. doi: 10.1016/j.ceb.2004.08.001

Borras, E., San Lucas, F. A., Chang, K., Zhou, R. J., Masand, G., Fowler, J., et al. (2016). Genomic landscape of colorectal mucosa and adenomas. *Cancer Prev. Res.* 9, 417–427. doi: 10.1158/1940-6207.CAPR-16-0081

Capra, J. A., Laskowski, R. A., Thornton, J. M., Singh, M., and Funkhouser, T. A. (2009). Predicting protein ligand binding sites by combining evolutionary sequence conservation and 3D structure. *PLoS Comput. Biol.* 5:e1000585. doi: 10.1371/journal.pcbi.1000585

Etienne-Manneville, S. (2009). APC in cell migration. *APC Proteins* 656, 30–40. doi: 10.1007/978-1-4419-1145-2_3

Fischer, J. D., Mayer, C. E., and Soding, J. (2008). Prediction of protein functional residues from sequence by probability density estimation. *Bioinformatics* 24, 613–620. doi: 10.1093/bioinformatics/btm626

Furukawa, S., Kawasaki, Y., Miyamoto, M., Hiyoshi, M., Kitayama, J., and Akiyama, T. (2013). The miR-1-NOTCH3-Asef pathway is important for colorectal tumor cell migration. *PLoS One* 8:e80609. doi: 10.1371/journal.pone.0080609

Gallina, S., Proposito, D., Veltri, S., Montemurro, L. A., Negro, P., and Carboni, M. (2006). [Colorectal cancer surgery. Analysis of risk factors in relation to incidence of morbidity and mortality]. *Chir. Ital.* 58, 723–732.

Gotthardt, K., and Ahmadian, M. R. (2007). Asef is a Cdc42-specific guanine nucleotide exchange factor. *Biol. Chem.* 388, 67–71. doi: 10.1515/Bc.2007.008

Groden, J., Thliveris, A., Samowitz, W., Carlson, M., Gelbert, L., Albertsen, H., et al. (1991). Identification and characterization of the familial adenomatous polyposis coli gene. *Cell* 66, 589–600. doi: 10.1016/0092-8674(81)90021-0

Grohmann, A., Tanneberger, K., Alzner, A., Schneikert, J., and Behrens, J. (2007). AMER1 regulates the distribution of the tumor suppressor APC between microtubules and the plasma membrane. *J. Cell Sci.* 120, 3738–3747. doi: 10.1242/jcs.011320

Ha, N. C., Tonozuka, T., Stamos, J. L., Choi, H. J., and Weis, W. I. (2004). Mechanism of phosphorylation-dependent binding of APC to beta-catenin and its role in beta-catenin degradation. *Mol. Cell* 15, 511–521. doi: 10.1016/j.molcel.2004.08.010

Haggar, F. A., and Boushey, R. P. (2009). Colorectal cancer epidemiology: incidence, mortality, survival, and risk factors. *Clin. Colon Rectal Surg.* 22, 191–197. doi: 10.1055/s-0029-1242458

Hamada, F., and Bienz, M. (2002). A Drosophila APC tumour suppressor homologue functions in cellular adhesion. *Nat. Cell Biol.* 4, 208–213. doi: 10.1038/ncb755

He, T. C., Sparks, A. B., Rago, C., Hermeking, H., Zawel, L., da Costa, L. T., et al. (1998). Identification of c-MYC as a target of the APC pathway. *Science* 281, 1509–1512. doi: 10.1126/science.281.5382.1509

Henderson, M. J., Holbert, M. A., Simeonov, A., and Kallal, L. A. (2020). High-throughput cellular thermal shift assays in research and drug discovery. *SLAS Discov.* 25, 137–147. doi: 10.1177/2472555219877183

Huang, W., Lu, S., Huang, Z., Liu, X., Mou, L., Luo, Y., et al. (2013). Allosite: a method for predicting allosteric sites. *Bioinformatics* 29, 2357–2359. doi: 10.1093/bioinformatics/btt399

Huang, X. Y. (2003). Fluorescence polarization competition assay: the range of resolvable inhibitor potency is limited by the affinity of the fluorescent ligand. *J. Biomol. Screen.* 8, 34–38. doi: 10.1177/1087057102239666

Itoh, R. E., Kiyokawa, E., Aoki, K., Nishioka, T., Akiyama, T., and Matsuda, M. (2008). Phosphorylation and activation of the Rac1 and Cdc42 GEF Asef in A431 cells stimulated by EGF. *J. Cell Sci.* 121(Pt 16), 2635–2642. doi: 10.1242/jcs.028647

Iwama, T. (2001). Somatic mutation rate of the APC gene. *Jpn. J. Clin. Oncol.* 31, 185–187. doi: 10.1093/jjco/hye042

Iwama, T., Konishi, M., Iijima, T., Yoshinaga, K., Tominaga, T., Koike, M., et al. (1999). Somatic mutation of the APC gene in thyroid carcinoma associated with familial adenomatous polyposis. *Jpn. J. Cancer Res.* 90, 372–376. doi: 10.1111/j.1349-7006.1999.tb00757.x

Jadav, S. S., Macalino, S. J. Y., and Alluri, R. (2020). Structure-based discovery of small molecule APC-Asef interaction inhibitors: In silico approaches and molecular dynamics simulations. *J. Mol. Model.* 26:207.

Jiang, H. M., Deng, R., Yang, X. Y., Shang, J. L., Lu, S. Y., Zhao, Y. L., et al. (2017). Peptidomimetic inhibitors of APC-Asef interaction block colorectal cancer migration. *Nat. Chem. Biol.* 13, 994–1001. doi: 10.1038/Nchembio.2442

Jideh, B., and Bourke, M. J. (2018). Colorectal cancer screening reduces incidence, mortality and morbidity. *Med. J. Aust.* 208, 483–484. doi: 10.5694/mja18.00279

Kawasaki, Y., Sato, R., and Akiyama, T. (2003). Mutated APC and Asef are involved in the migration of colorectal tumour cells. *Nat. Cell Biol.* 5, 211–215. doi: 10.1038/ncb937

Kawasaki, Y., Senda, T., Ishidate, T., Koyama, R., Morishita, T., Iwayama, Y., et al. (2000). Asef, a link between the tumor suppressor APC and G-protein signaling. *Science* 289, 1194–1197. doi: 10.1126/science.289.5482.1194

Kawasaki, Y., Tsuji, S., Muroya, K., Furukawa, S., Shibata, Y., Okuno, M., et al. (2009a). The adenomatous polyposis coli-associated exchange factors Asef and Asef2 are required for adenoma formation in Apc(Min/+)mice. *EMBO Rep.* 10, 1355–1362. doi: 10.1038/embor.2009.233

Kawasaki, Y., Tsuji, S., Sagara, M., Echizen, K., Shibata, Y., and Akiyama, T. (2009b). Adenomatous polyposis coli and Asef function downstream of hepatocyte growth factor and phosphatidylinositol 3-kinase. *J. Biol. Chem.* 284, 22436–22443. doi: 10.1074/jbc.M109.020768

Kemeny, N. (1992). Review of regional therapy of liver metastases in colorectal cancer. *Semin. Oncol.* 19(2 Suppl 3), 155–162.

Korinek, V., Barker, N., Morin, P. J., van Wichen, D., de Weger, R., Kinzler, K. W., et al. (1997). Constitutive transcriptional activation by a beta-catenin-Tcf complex in APC-/- colon carcinoma. *Science* 275, 1784–1787. doi: 10.1126/science.275.5307.1784

Letourneau, D., LeHoux, J. G., and Lavigne, P. (2019). Determination of ligand binding affinity and specificity of purified START domains by thermal shift assays using circular dichroism. *Methods Mol. Biol.* 1949, 293–306. doi: 10.1007/978-1-4939-9136-5_20

Li, C., Bapat, B., and Alman, B. A. (1998). Adenomatous polyposis coli gene mutation alters proliferation through its beta-catenin regulatory function in aggressive fibromatosis (desmoid tumor). *Am. J. Pathol.* 153, 709–714. doi: 10.1016/S0002-9440(10)65614-3

Lise, M., Gerard, A., Nitti, D., Zane, D., Buyse, M., Duez, N., et al. (1987). Adjuvant therapy for colorectal cancer. The EORTC experience and a review of the literature. *Dis. Colon Rectum* 30, 847–854.

Liu, S., Zheng, R., Zhang, M., Zhang, S., Sun, X., and Chen, W. (2015). Incidence and mortality of colorectal cancer in China, 2011. *Chin. J. Cancer Res.* 27, 22–28. doi: 10.3978/j.issn.1000-9604.2015.02.01

Lockless, S. W., and Ranganathan, R. (1999). Evolutionarily conserved pathways of energetic connectivity in protein families. *Science* 286, 295–299. doi: 10.1126/science.286.5438.295

MacDonald, B. T., Tamai, K., and He, X. (2009). Wnt/beta-Catenin signaling: components, mechanisms, and diseases. *Dev. Cell* 17, 9–26. doi: 10.1016/j.devcel.2009.06.016

Mahajan, V., Das, A. K., Taggar, R. K., Kumar, D., and Kumar, N. (2015). Polymorphism of keratin-associated protein (KAP) 3.2 gene and its association with wool traits in Rambouillet sheep. *Indian J. Anim. Sci.* 85, 262–265.

Mitin, N., Betts, L., Yohe, M. E., Der, C. J., Sondek, J., and Rossman, K. L. (2007). Release of autoinhibition of ASEF by APC leads to CDC42 activation and tumor suppression. *Nat. Struct. Mol. Biol.* 14, 814–823. doi: 10.1038/nsmb1290

Miyoshi, Y., Nagase, H., Ando, H., Horii, A., Ichii, S., Nakatsuru, S., et al. (1992). Somatic mutations of the APC gene in colorectal tumors: mutation cluster region in the APC gene. *Hum. Mol. Genet.* 1, 229–233. doi: 10.1093/hmg/1.4.229

Morin, P. J., Sparks, A. B., Korinek, V., Barker, N., Clevers, H., Vogelstein, B., et al. (1997). Activation of beta-catenin-Tcf signaling in colon cancer by mutations in beta-catenin or APC. *Science* 275, 1787–1790. doi: 10.1126/science.275.5307.1787

Morishita, E. C., Murayama, K., Kato-Murayama, M., Ishizuka-Katsura, Y., Tomabechi, Y., Hayashi, T., et al. (2011). Crystal structures of the armadillo repeat domain of adenomatous polyposis coli and its complex with the tyrosine-rich domain of Sam68. *Structure* 19, 1496–1508. doi: 10.1016/j.str.2011.07.013

Murayama, K., Shirouzu, M., Kawasaki, Y., Kato-Murayama, M., Hanawa-Suetsugu, K., Sakamoto, A., et al. (2007). Crystal structure of the Rac activator, Asef, reveals its autoinhibitory mechanism. *J. Biol. Chem.* 282, 4238–4242. doi: 10.1074/jbc.C600234200

Muroya, K., Kawasaki, Y., Hayashi, T., Ohwada, S., and Akiyama, T. (2007). PH domain-mediated membrane targeting of Asef. *Biochem. Biophys. Res. Commun.* 355, 85–88. doi: 10.1016/j.bbrc.2007.01.131

Nikolaev, S. I., Sotiriou, S. K., Pateras, I. S., Santoni, F., Sougioultzis, S., Edgren, H., et al. (2012). A single-nucleotide substitution mutator phenotype revealed by exome sequencing of human colon adenomas. *Cancer Res.* 72, 6279–6289. doi: 10.1158/0008-5472.CAN-12-3869

Norris, A. L., Clissold, P. M., Askham, J. M., Morrison, E. E., Moncur, P., McCall, S. H., et al. (2000). Truncated adenomatous polyposis coli (APC) tumour suppressor protein can undergo tyrosine phosphorylation. *Eur. J. Cancer* 36, 525–532. doi: 10.1016/s0959-8049(99)00305-6

Qi, P. F., Fang, L., Li, H., Li, S. K., Yang, Y. S., Qi, J. L., et al. (2020). Discovery of novel pyrazoline derivatives containing methyl-1H-indole moiety as potential

inhibitors for blocking APC-Asef interactions. *Bioorg. Chem.* 99:103838. doi: 10.1016/j.bioorg.2020.103838

Rodriguez-Cruz, F., Torres-Cruz, F. M., Monroy-Ramirez, H. C., Escobar-Herrera, J., Basurto-Islas, G., Avila, J., et al. (2018). Fragmentation of the golgi apparatus in neuroblastoma cells is associated with tau-induced ring-shaped microtubule bundles. *J. Alzheimers Dis.* 65, 1185–1207. doi: 10.3233/Jad-180547

Rodriguez-Furlan, C., and Hicks, G. R. (2021). Label-free target identification and confirmation using thermal stability shift assays. *Methods Mol. Biol.* 2213, 163–173. doi: 10.1007/978-1-0716-0954-5_14

Rogez-Florent, T., Duhamel, L., Goossens, L., Six, P., Drucbert, A. S., Depreux, P., et al. (2014). Label-free characterization of carbonic anhydrase-novel inhibitor interactions using surface plasmon resonance, isothermal titration calorimetry and fluorescence-based thermal shift assays. *J. Mol. Recognit.* 27, 46–56. doi: 10.1002/jmr.2330

Schneikert, J., and Behrens, J. (2006). Truncated APC is required for cell proliferation and DNA replication. *Int. J. Cancer* 119, 74–79. doi: 10.1002/ijc.21826

Schneikert, J., Brauburger, K., and Behrens, J. (2011). APC mutations in colorectal tumours from FAP patients are selected for CtBP-mediated oligomerization of truncated APC. *Hum. Mol. Genet* 20, 3554–3564. doi: 10.1093/hmg/ddr273

Schneikert, J., Grohmann, A., and Behrens, J. (2007). Truncated APC regulates the transcriptional activity of beta-catenin in a cell cycle dependent manner. *Hum. Mol. Genet.* 16, 199–209. doi: 10.1093/hmg/ddl464

Sen-Gupta, S., Van der Luijt, R. B., Bowles, L. V., Meera Khan, P., and Delhanty, J. D. (1993). Somatic mutation of APC gene in desmoid tumour in familial adenomatous polyposis. *Lancet* 342, 552–553. doi: 10.1016/0140-6736(93)91677-e

Sieber, O. M., Tomlinson, I. P., and Lamlum, H. (2000). The adenomatous polyposis coli (APC) tumour suppressor - genetics, function and disease. *Mol. Med. Today* 6, 462–469. doi: 10.1016/s1357-4310(00)01828-1

Steffen, R. (1986). [Therapy of liver metastases of colorectal cancer. Review of the present status]. *Schweiz. Rundsch. Med. Prax.* 75, 1258–1262.

Su, L. K., Johnson, K. A., Smith, K. J., Hill, D. E., Vogelstein, B., and Kinzler, K. W. (1993). Association between wild type and mutant APC gene products. *Cancer Res.* 53, 2728–2731.

Tanneberger, K., Pfister, A. S., Kriz, V., Bryja, V., Schambony, A., and Behrens, J. (2011). Structural and functional characterization of the Wnt inhibitor APC membrane recruitment 1 (Amer1). *J. Biol. Chem.* 286, 19204–19214. doi: 10.1074/jbc.M111.224881

Tetsu, O., and McCormick, F. (1999). Beta-catenin regulates expression of cyclin D1 in colon carcinoma cells. *Nature* 398, 422–426. doi: 10.1038/18884

Tominaga, O., Nita, M. E., Nagawa, H., and Muto, T. (1998). Screening for APC mutations based on detection of truncated APC proteins. *Dig. Dis. Sci.* 43, 306–310.

Wang, L. L., Liu, X. Y., Gusev, E., Wang, C. X., and Fagotto, F. (2014). Regulation of the phosphorylation and nuclear import and export of beta-catenin by APC and its cancer-related truncated form. *J. Cell Sci.* 127, 1647–1659. doi: 10.1242/jcs.131045

Watanabe, T., Wang, S. J., Noritake, J., Sato, K., Fukata, M., Takefuji, M., et al. (2004). Interaction with IQGAP1 links APC to Rac1, Cdc42, and actin filaments during cell polarization and migration. *Dev. Cell* 7, 871–883. doi: 10.1016/j.devcel.2004.10.017

Weekes, J., Lam, A. K., Sebesan, S., and Ho, Y. H. (2009). Irinotecan therapy and molecular targets in colorectal cancer: a systemic review. *World J. Gastroenterol.* 15, 3597–3602. doi: 10.3748/wjg.15.3597

Weiner, A. T., Lanz, M. C., Goetschius, D. J., Hancock, W. O., and Rolls, M. M. (2016). Kinesin-2 and APC function at dendrite branch points to resolve microtubule collisions. *Cytoskeleton* 73, 35–44. doi: 10.1002/cm.21270

Wiebke, F. (2015). Innovative advances in isothermal titration calorimetry (ITC). *Abstr. Pap. Am. Chem. Soc.* 250:177.

Xing, Y., Clements, W. K., Le Trong, I., Hinds, T. R., Stenkamp, R., Kimelman, D., et al. (2004). Crystal structure of a beta-Catenin/APC complex reveals a critical role for APC phosphorylation in APC function. *Mol. Cell* 15, 523–533. doi: 10.1016/j.molcel.2004.08.001

Yan, W. D. (2015). Binding time-not just affinity-gains stature in drug design. *Nat. Med.* 21:545. doi: 10.1038/Nm0615-545

Yan, X. Q., Wang, Z. C., Qi, P. F., Li, G. G., and Zhu, H. L. (2019). Design, synthesis and biological evaluation of 2-H pyrazole derivatives containing morpholine moieties as highly potent small molecule inhibitors of APC-Asef interaction. *Eur. J. Med. Chem.* 177, 425–447. doi: 10.1016/j.ejmech.2019.05.056

Yang, X. Y., Zhong, J., Zhang, Q. F., Qian, J. X., Song, K., Ruan, C., et al. (2018). Rational design and structure validation of a novel peptide inhibitor of the adenomatous-polyposis-coli (APC)-rho-guanine-nucleotide-exchange-factor-4 (Asef) interaction. *J. Med. Chem.* 61, 8017–8028. doi: 10.1021/acs.jmedchem.8b01112

Yoshihiro, K., S-Nosuke, T., Masaki, S., Takafumi, J., Shiori, F., Ken, M., et al. (2008). Function of the tumor suppressor APC and guanine-nucleotide exchange factor Asef. *Febs J.* 275:300.

Zeiss, D., and Bauer-Brandl, A. (2006). Isothermal titration calorimetry (ITC) method to study drug/ion exchanger interaction. *J. Therm. Anal. Calorim.* 83, 309–312. doi: 10.1007/s10973-005-7234-2

Zhang, L., and Shay, J. W. (2017). Multiple roles of APC and its therapeutic implications in colorectal cancer. *J. Natl. Cancer Inst.* 109:djw332. doi: 10.1093/jnci/djw332

Zhang, R., and Monsma, F. (2010). Fluorescence-based thermal shift assays. *Curr. Opin. Drug Discov. Dev.* 13, 389–402.

Zhang, Z. Y., Akyildiz, S., Xiao, Y. F., Gai, Z. C., An, Y., Behrens, J., et al. (2015). Structures of the APC-ARM domain in complexes with discrete Amer1/WTX fragments reveal that it uses a consensus mode to recognize its binding partners. *Cell Disc.* 1:15016.

Zhang, Z. Y., Chen, L. Y., Gao, L., Lin, K., Zhu, L., Lu, Y., et al. (2012). Structural basis for the recognition of Asef by adenomatous polyposis coli. *Cell Res.* 22, 372–386. doi: 10.1038/cr.2011.119

Zhang, Z. Y., Lin, K., Gao, L., Chen, L. Y., Shi, X. S., and Wu, G. (2011). Crystal structure of the armadillo repeat domain of adenomatous polyposis coli which reveals its inherent flexibility. *Biochem. Biophys. Res. Commun.* 412, 732–736. doi: 10.1016/j.bbrc.2011.08.044

Zheng, Z. X., Zheng, R. S., Zhang, S. W., and Chen, W. Q. (2014). Colorectal cancer incidence and mortality in China, 2010. *Asian Pac. J. Cancer Prev.* 15, 8455–8460. doi: 10.7314/apjcp.2014.15.19.8455

Conflict of Interest: The authors declare that the research was conducted in the absence of any commercial or financial relationships that could be construed as a potential conflict of interest.

frontiers in Molecular Biosciences

REVIEW
published: 28 April 2021
doi: 10.3389/fmolb.2021.669431

In silico Approaches for the Design and Optimization of Interfering Peptides Against Protein–Protein Interactions

*Zahra Sadat Hashemi[1], Mahboubeh Zarei[2], Mohsen Karami Fath[3], Mahmoud Ganji[4], Mahboube Shahrabi Farahani[4], Fatemeh Afsharnouri[4], Navid Pourzardosht[5,6], Bahman Khalesi[7], Abolfazl Jahangiri[8], Mohammad Reza Rahbar[9] and Saeed Khalili[10]**

[1] ATMP Department, Breast Cancer Research Center, Motamed Cancer Institute, Academic Center for Education, Culture and Research, Tehran, Iran, [2] Pharmaceutical Sciences Research Center, Shiraz University of Medical Sciences, Shiraz, Iran, [3] Department of Cellular and Molecular Biology, Faculty of Biological Sciences, Kharazmi University, Tehran, Iran, [4] Department of Medical Biotechnology, Faculty of Medical Sciences, Tarbiat Modares University, Tehran, Iran, [5] Cellular and Molecular Research Center, Faculty of Medicine, Guilan University of Medical Sciences, Rasht, Iran, [6] Department of Biochemistry, Guilan University of Medical Sciences, Rasht, Iran, [7] Department of Research and Production of Poultry Viral Vaccine, Razi Vaccine and Serum Research Institute, Agricultural Research Education and Extension Organization, Karaj, Iran, [8] Applied Microbiology Research Center, Systems Biology and Poisonings Institute, Baqiyatallah University of Medical Sciences, Tehran, Iran, [9] Pharmaceutical Sciences Research Center, Shiraz University of Medical Sciences, Shiraz, Iran, [10] Department of Biology Sciences, Shahid Rajaee Teacher Training University, Tehran, Iran

OPEN ACCESS

Edited by:
Luca Domenico D'Andrea, National Research Council, Consiglio Nazionale delle Ricerche (CNR), Italy

Reviewed by:
Denis Colum Shields, University College Dublin, Ireland
Helen Mott, University of Cambridge, United Kingdom

***Correspondence:**
Saeed Khalili
saeed.khalili@sru.ac.ir

Specialty section:
This article was submitted to Molecular Recognition, a section of the journal Frontiers in Molecular Biosciences

Received: *18 February 2021*
Accepted: *06 April 2021*
Published: *28 April 2021*

Citation:
Hashemi ZS, Zarei M, Fath MK, Ganji M, Farahani MS, Afsharnouri F, Pourzardosht N, Khalesi B, Jahangiri A, Rahbar MR and Khalili S (2021) In silico Approaches for the Design and Optimization of Interfering Peptides Against Protein–Protein Interactions. Front. Mol. Biosci. 8:669431. doi: 10.3389/fmolb.2021.669431

Large contact surfaces of protein–protein interactions (PPIs) remain to be an ongoing issue in the discovery and design of small molecule modulators. Peptides are intrinsically capable of exploring larger surfaces, stable, and bioavailable, and therefore bear a high therapeutic value in the treatment of various diseases, including cancer, infectious diseases, and neurodegenerative diseases. Given these promising properties, a long way has been covered in the field of targeting PPIs *via* peptide design strategies. *In silico* tools have recently become an inevitable approach for the design and optimization of these interfering peptides. Various algorithms have been developed to scrutinize the PPI interfaces. Moreover, different databases and software tools have been created to predict the peptide structures and their interactions with target protein complexes. High-throughput screening of large peptide libraries against PPIs; "hotspot" identification; structure-based and off-structure approaches of peptide design; 3D peptide modeling; peptide optimization strategies like cyclization; and peptide binding energy evaluation are among the capabilities of *in silico* tools. In the present study, the most recent advances in the field of *in silico* approaches for the design of interfering peptides against PPIs will be reviewed. The future perspective of the field and its advantages and limitations will also be pinpointed.

Keywords: peptide, protein–protein interactions, *in silico*, bioinformatics 3, interfering peptides

INTRODUCTION

The survival of a cell naturally depends on the connections between its proteins. In a single organism, countless cells are connected to form an interactome. The interactome is an enormous network system composed of a whole set of molecular interactions, particularly protein–protein interactions (PPIs). These interactions could be held together *via* electrostatic forces, hydrogen

bonding, and hydrophobic effect. Approximately 130,000–600,000 PPIs are correlated with the human interactome and make up the PPI networks (Bruzzoni-Giovanelli et al., 2018). These PPIs modulate the systematic function of cells and signaling pathways of the body and are essential to understanding the medicinal chemistry and chemical biology of the cells. They catalyze the critical cellular processes such as replication, transcription, translation, and transmembrane signal transduction (Lu et al., 2020). Proteins and consequently PPIs are the functional building blocks of a living cell. The slightest error in PPIs, especially in a central node (or hub) in a network, could lead to even fatal disease (such as infectious diseases, cancer, and neurodegenerative diseases) and disturb the cell homeostasis. Therefore, focusing on aberrant PPIs holds the promise of curing various diseases and has the therapeutic potential of being attractive targets for developing new drugs and novel diagnostics.

Deliniation of the interaction between a protein domain and a peptide or another protein domain, is the central concept of PPIs (Nevola and Giralt, 2015). A linear sequence of residues, or a short protein domain, evokes the concept of peptides and peptide mimetics (Stone and Deber, 2017). Recently, various drugs have been presented that are relying on the relationship between two proteins. These drugs could mimic the 3D shape of targeted proteins and can specifically fine-tune their interactions. The peptides are capable of adapting secondary structures, which are usually α-helixes, which could also be completely disordered (Nevola and Giralt, 2015).

To provide the desired peptide or small molecule drug, clinical- and molecular-level information is needed (Bakail and Ochsenbein, 2016). Bioinformaticians widely apply high-throughput data obtained from the studies of genomics, RNAomics, proteomics, metabolomics, and glycomics. These collected data are rich sources of the molecular-level information of PPIs and could be useful for personalized treatments (Bakail and Ochsenbein, 2016). *In silico* methods have been widely used in various aspects of biological studies (Khalili et al., 2017; Mard-Soltani et al., 2018; Khodashenas et al., 2019; Rahbar et al., 2019). *In silico* methods could be used to screen for the specific topological surface of peptides capable of specific modulation of PPIs. There is a wide variety of software and algorithms for scrutinizing PPIs to design and optimize these interfering peptides.

Basic *in silico* research about the PPIs (from the 1990s to the 2000s) has significantly contributed to the production of a vast number of constrained peptides and peptide–drug conjugates. The first approvals of the peptide therapeutics were issued for six peptides in 2012. Pasireotide is a somatostatin analog for the treatment of Cushing's disease. Lucinactant is a pulmonary surfactant for the treatment of infant respiratory distress syndrome. Peginesatide is an erythropoietin analog for the treatment of anemia associated with chronic kidney disease (CKD). Carfilzomib is an epoxomicin analog (proteasome inhibitor) that is used as an anticancer medication. Linaclotide is an oligo-peptide agonist of guanylate cyclase 2C used to treat irritable bowel syndrome with constipation and chronic constipation with no known causes. Teduglutide is a 33-membered polypeptide and glucagon-like peptide-2 (GLP-2) analog for the treatment of short bowel syndrome. A new field has opened up for scientists to treat different diseases with the help of various *in silico* algorithms, tools, and software designs by discovering therapeutic peptides and small molecules (Kaspar and Reichert, 2013). The results of *in silico* studies should be confirmed *in vitro* and *in vivo* to pass the phases of clinical trials. The PPI networks would be disturbed and therefore restrained the usage of these therapeutic PPI-targeting peptides (Kaspar and Reichert, 2013).

In silico methods of peptide analyses could include different approaches such as homology modeling, molecular dynamics, protein docking, and PPI targeting. Structural characterization of the peptides could be carried out by x-ray crystallography, NMR spectroscopy, and cryo-electron microscopy. The obtained structural data are stored and available in structural deposition databases like the Protein Data Bank (PDB). The advantages of computational *in silico* methods over empirical methods are their low cost, faster procedure speed, simple process, and reliability to target PPIs using peptides. This approach can lead to the atomic-level identification of PPIs (Murakami et al., 2017). The information about the PPIs is crucial for designing desired peptides or small molecules *via* virtual screening of drug candidates (Nevola and Giralt, 2015). Peptides are reported to have some advantages over small molecule drugs. Small molecules are not sufficient for the complete coverage of the large contact surfaces involved in PPIs. This surface area could practically be from 1,500 to 3,000 Å (Cunningham et al., 2017). Using small molecules, some target sites of the PPI surfaces such as pockets, grooves, or clefts could be missed. Advanced and sophisticated design and modeling of new remedial small molecules will be needed to circumvent this drawback. However, interfering peptides (IPs), natural or synthetic, are superior in this respect and would be reconciled with large or flat PPI surfaces (Bruzzoni-Giovanelli et al., 2018). The studies have shown that the ADME properties of IP therapeutic agents are better than those of small molecules. ADME is correlated with the absorption, distribution, metabolism, excretion, and toxicity of a drug molecule. IPs could be simply designed as valuable therapeutic tools to block various PPI networks. Peptides have been analyzed to block PPIs of the nervous system (Zhai et al., 2014; Shi et al., 2016), cardiovascular system (Pleasant-Jenkins et al., 2017), and even cancer (Jouaux et al., 2008; Mine et al., 2016; Ellert-Miklaszewska et al., 2017). IPs are also associated with low molecular weight, high flexibility, and minimal toxicity, which could offer a new class of biopharmaceuticals. These small peptides could also act as cargo carriers due to their cell penetration property. These cargoes could be linked *via* covalent or non-covalent bonds to some short peptides (5–30 amino acids). These peptides, which could have positive charges, are called cell-penetrating peptides (CPPs). CPPs facilitate cellular delivery and uptake of their cargo commonly through endocytosis (Guidotti et al., 2017). The prospect of IP drugs shows a robust pipeline and an unrivaled

number of marketing opportunities for the treatment of a wide range of diseases.

DATABASES FOR PEPTIDE SEQUENCES AND STRUCTURES

Peptides, once neglected, have now offered tremendous therapeutic applications (Antosova et al., 2009) and have obtained quite an expansion in the pharmaceutical industry. Numerous databases have already been developed to store different kinds of peptides by collecting information from public databases and published scientific articles (**Table 1**). These repositories can be categorized into three classes, namely antimicrobial peptide (AMP) databases, targeted delivery-related databases, and disease-specific databases.

Antimicrobial peptides have garnered a lot of attention for several decades due to their biological activity and their ability to make the pathogens resistant to existing drugs. The AMP databases are the most available among the peptide databases. Some AMP databases are specialized to one type of AMP family, like the Defensins Knowledgebase (defensins) (Seebah et al., 2007), BAGEL4 (bacteriocins) (van Heel et al., 2018), BACTIBASE (bacteriocins) (Hammami et al., 2010), PhytAMP (plant AMPs) (Hammami et al., 2009), the Peptaibol Database (peptaibols) (Whitmore and Wallace, 2004), and InverPep (invertebrates AMPs) (Gómez et al., 2017). Meanwhile, others are general AMP databases, such as APD (Wang et al., 2016), CAMP (Waghu et al., 2016), and DBAASP (Pirtskhalava et al., 2016). APD (antimicrobial peptide database) (Wang and Wang, 2004) initially went online in 2003 with 525 AMPs. It has been extensively accepted and referred to since then. In 2009, an updated version of APD was released (Wang et al., 2009), called APD2, which contains about 1,228 entries and has been consistently updated and further expanded into the APD3 version (Wang et al., 2016). This database is currently focused on collecting natural AMPs with defined sequences and activities. It contains 2,619 AMPs with 261 bacteriocins from bacteria, and 7, 13, 4, and 321 from protists, fungi, archaea, and plants, respectively, with an additional 1,972 animal host defense peptides. Another resource for AMPs is CAMP (collection of antimicrobial peptides) (Thomas et al., 2010). It contains information on sequences of natural as well as synthetic AMPs. The inclusion of the structure of the AMPs and family information constituted the second version of the CAMP (Waghu et al., 2014) known as the CAMPR2. Moreover, CAMPR2 contains the newly identified AMPs sequences. CAMPR3 (Waghu et al., 2016) was introduced in 2016 to include AMP family specific signatures. CAMPR3 provides comprehensive information about the sequences, structures, family signatures, activity profile, sources, target organisms, and hemolytic activity for AMPs, and also links to several external databases. DBAASP (Database of Antimicrobial Activity and Structure of Peptides) was started in 2014 with a collection of published information about the AMPs and the corresponding resources (Gogoladze et al., 2014). In 2016, it was updated to DBAASP v2, with about 8,000 entries, including structural information (Pirtskhalava et al., 2016). It also contributed to the development of several databases such as dbAMP (Jhong et al., 2019), LAMP2 (Ye et al., 2020), PlantPepDB (Das et al., 2020), ADAPTABLE (Ramos-Martín et al., 2019), and starPepDB (Aguilera-Mendoza et al., 2019). Most recently, another updated version of DBAASP (DBAASP v3) (Pirtskhalava et al., 2021) has been released to include new content and additional user services. This database has continuously developed its predictive tools to be employed in the *de novo* design of peptide-based drugs. Its efficacy for the design of peptide-based antimicrobial agents against both gram-positive and gram-negative bacteria has been experimentally confirmed (Vishnepolsky et al., 2019a,b). The BaAMPs database was developed for AMPs with the property of disrupting microbial biofilms (Di Luca et al., 2015). MBPDB is a database of the bioactive peptides of milk origin (Nielsen et al., 2017). CPPsite and TumorHoPe are targeted delivery-related databases. CPPsite (Gautam et al., 2012) is the first database of CPPs that contains 843 entries along with the sequence information, subcellular localization, physicochemical properties, and uptake efficiency. The updated version of CPPsite (Agrawal et al., 2016), called CPPsite 2.0, contains 1,850 entries, including the model system, cargo information, chemical modifications, predicted tertiary structure, and other information. The TumorHoPe database (Kapoor et al., 2012) contains 744 peptides that can recognize tumor tissues and tumor-associated microenvironments.

Disease-specific databases encompass peptides that can be used to design therapeutic peptides capable of targeting specific diseases. PDB (Usmani et al., 2017) is a database of FDA-approved peptides and protein therapeutics, CancerPPD (Tyagi et al., 2015) is a database of anticancer peptides (ACPs) and proteins, and AntiTbPdb (Usmani et al., 2018) is a database of experimentally verified anti-mycobacterial and anti-tubercular peptides. The HIPdb database was established to provide information about 981 HIV-inhibiting peptides (Qureshi et al., 2013), including their sequences and half-maximal inhibitory concentrations (IC_{50}). AVPdb contains 2,683 antiviral peptides and the data about their sequences, efficacy, modifications, and predicted structures (Qureshi et al., 2014). ParaPep (Mehta et al., 2014) is a database of experimentally validated anti-parasitic peptide sequences and their structures curated and compiled from literature, patents, and various other databases. This database was created by Mehta et al. (2014) and contains 863 entries that include 519 unique peptides whose anti-parasitic activities were evaluated against multiple species of *Plasmodium*, *Leishmania*, and *Trypanosoma*. In ParaPep, the structures of peptides consisting of natural, and modified, amino acids have been predicted using the PEPstr software. The Hemolytik database (Gautam et al., 2014) is an information system for experimentally determined hemolytic and non-hemolytic peptides obtained by manual extraction from numerous scientific papers and various databases. This database was created by Gautam et al. (2014) and contains 3,000 entries that include 2,000 unique peptides whose hemolytic activities were assessed on erythrocytes isolated from as many as 17 different sources. WALTZ-DB (Beerten et al., 2015) is the largest available database of experimentally characterized

TABLE 1 | List of peptide sequences and databases containing their structures.

Database	Peptide type		URL	References
Antimicrobial peptides (AMPs) database				
Peptaibol	Peptaibol	Sequence and structure resource for the unusual class of peptides known as peptaibols	http://www.cryst.bbk.ac.uk/peptaibol	Whitmore and Wallace, 2004
Defensins Knowledgebase	Defensins	A manually curated database of more than 350 defensin records each containing sequence, structure and activity information	http://defensins.bii.a-star.edu.sg	Seebah et al., 2007
PhytAMP	Plant AMPs	A specialized database for plant AMPs containing sequence information and physicochemical or biological data, along with a set of tools for sequence analysis	http://phytamp.hammamilab.org/	Hammami et al., 2009
BACTIBASE	Bacteriocins	A manually curated database of bacterial antimicrobial peptides, along with various tools for bacteriocin analysis, such as homology search, multiple sequence alignments, Hidden Markov Models, molecular modeling	http://bactibase.hammamilab.org/main.php	Hammami et al., 2010
BaAMPs	AMP	A manually curated database of AMPs specifically assayed against microbial biofilms	http://www.baamps.it	Di Luca et al., 2015
APD3	AMP	A AMPs database including a total of 2619 peptides, which currently focuses on natural AMPs with defined sequences and activities and also provides other searchable annotations, including target pathogens, molecule-binding partners, post-translational modifications and animal models.	https://wangapd3.com/main.php	Wang et al., 2016
CAMPR3	AMP	A database of sequences, structures and family-specific signatures of prokaryotic and eukaryotic AMPs containing 10247 sequences, 757 structures and 114 family-specific signatures	www.camp3.bicnirrh.res.in.	Waghu et al., 2016
InverPep	Invertebrates AMPs	A manually curated database specialized in experimentally validated AMPs from invertebrates and its information	ciencias.medellin.unal.edu.co/gruposdeinvestigacion/prospeccionydisenobiomoleculas/InverPep/public/home_en	Gómez et al., 2017
MBPDB	Milk bioactive peptide	A comprehensive database of bioactive peptides derived from milk proteins from any mammalian source	http://mbpdb.nws.oregonstate.edu	Nielsen et al., 2017
BAGEL4	Bacteriocins	A mining web server of RiPPs (ribosomally synthesized and posttranslationally modified peptides) and bacteriocins	http://bagel4.molgenrug.nl	van Heel et al., 2018
DBAASP v3	AMP	A continuously updated database of antimicrobial activity and structure of peptides	http://dbaasp.org.	Pirtskhalava et al., 2021
Targeted delivery-related databases				
TumorHope	Therapeutic Peptides	A database of experimentally validated tumor homing peptides containing 744 peptides with information on sequence, target tumor, target cell, peptide receptor, techniques of identification, and also providing secondary/tertiary structure, amino acid composition, and physicochemical properties of peptides which derived from their sequences	http://crdd.osdd.net/raghava/tumorhope/.	Kapoor et al., 2012
CPPsite 2.0	Cell penetrating peptide	A manually curated database of cell-penetrating peptides containing around 1850 peptide entries and providing predicted tertiary structure of peptides, possessing both modified and natural residues	http://crdd.osdd.net/raghava/cppsite/	Agrawal et al., 2016
Disease-specific databases				
Hemolytik	Hemolytic and non-hemolytic peptides	A manually curated resource of experimentally determined hemolytic and non-hemolytic peptides containing 3000 entries that include ∼2000 unique peptides with information on sequence, name, origin, reported function, property such as chirality, types (linear and cyclic), end modifications as well as providing predicted tertiary structure of each peptide	http://crdd.osdd.net/raghava/hemolytik/	Gautam et al., 2014
AVPdb	Antiviral peptides	A resource of experimentally verified antiviral peptides targeting over 60 medically important viruses including Influenza, HCV, HSV, RSV, HBV, DENV, SARS, etc. containing detailed information of 2683 peptides, including 624 modified peptides experimentally tested for antiviral activity	http://crdd.osdd.net/servers/avpdb/	Qureshi et al., 2014
ParaPep	Antiparasitic peptides	A repository of experimentally validated antiparasitic peptide sequences and their structures	http://webs.iiitd.edu.in/raghava/parapep/	Mehta et al., 2014

(Continued)

TABLE 1 | Continued

Database	Peptide type		URL	References
CancerPPD	Anticancer peptides	A manually curated resource of experimentally verified anticancer peptides (ACPs) and anticancer proteins, consists of 3491 ACP and 121 anticancer protein entries, and contains peptides having non-natural, chemically modified residues and D-amino acids	http://crdd.osdd.net/raghava/cancerppd/	Tyagi et al., 2015
SATPdb	Bioactive peptide	A database of structurally annotated therapeutic peptides, holds 19192 unique experimentally validated therapeutic peptide sequences having length between 2 and 50 amino acids, and covers peptides having natural, non-natural, and modified residues	http://crdd.osdd.net/raghava/satpdb/	Singh et al., 2016
THPdb	FDA- approved therapeutic peptides	A manually curated resource of FDA-approved therapeutic peptides and proteins with information on their sequences, chemical properties, composition, disease area, mode of activity, physical appearance, category or pharmacological class, pharmacodynamics, route of administration, toxicity, and target of activity	http://crdd.osdd.net/raghava/thpdb/	Usmani et al., 2017
StraPep	Bioactive peptide	Collection of all the bioactive peptides with known structure, containing 3791 bioactive peptide structures, which belong to 1312 unique bioactive peptide sequences	http://isyslab.info/StraPep	Wang et al., 2018
BIOPEP-UWM	Bioactive peptide	A continuously updated database of bioactive peptides derived from foods	http://www.uwm.edu.pl/biochemia	Minkiewicz et al., 2019
WALTZ-DB 2.0	Amyloid-forming peptide	A database providing information on experimentally determined amyloid-forming hexapeptide sequences	http://waltzdb.switchlab.org/	Louros et al., 2020
Special peptides databases				
NeuroPedia	Neuropeptides	A Neuropeptide Database, provided through hyperlinks to bioinformatic databases on genome and transcripts, protein structure and brain expression of Neuropeptides	www.neuropeptides.nl	Burbach, 2010
NeuroPedia	Neuropeptides	A neuropeptide databank of peptide sequences (including genomic and taxonomic information) and spectral libraries of identified MS/MS spectra of homolog neuropeptides from multiple species	http://proteomics.ucsd.edu/Software/NeuroPedia/	Kim et al., 2011
ConoServer	(Venom toxin peptide) conopeptides	A specialized database of sequence and structures of conopeptides (expressed in carnivorous marine cone snails)	http://www.conoserver.org	Kaas et al., 2012
DADP	Anuran defense peptides	A manually curated resource of anuran defense peptides containing 2571 entries with a total of 1923 non-identical bioactive sequences	http://split4.pmfst.hr/dadp/	Novković et al., 2012
Quorumpeps?	Quorum sensing peptides	A database of quorum sensing peptides with information on structure, activity, physicochemical properties, and related literature	http://quorumpeps.ugent.be/	Wynendaele et al., 2013
NeuroPep	Neuropeptides	A comprehensive and most complete resource of neuropeptides, which holds 5949 non-redundant neuropeptides together with information on source organisms, tissue specificity, families, names, post-translational modifications, 3D structures (if available) and literature references	http://isyslab.info/NeuroPep	Wang et al., 2015
ArachnoServer 3.0	(Venom toxin peptide) (Spider venom)	A manually collection of information on the sequence, structure, function and pharmacology of spider-venom toxin peptides	http://arachnoserver.org/	Pineda et al., 2018
Norin	Non-ribosomal peptides	A database of non-ribosomal peptides together with tools for their analysis containing 1740 peptides	https://bioinfo.cristal.univ-lille.fr/norine/	Flissi et al., 2020

amyloid-forming short sequences. This open-access database was created by Beerten et al. (2015). It contains 1,089 entries that provide primary information about amyloid aggregation incorporated in related databases. Louros et al. (2020) released an updated and significantly expanded version of this database, called WALTZ-DB 2.0. With WALTZ-DB 2.0, the structural model and information were added to the entries. The 3D models of the amyloid fibril cores of the entries were generated using a computational methodology developed in the Switch lab. It also provides a user-friendly option for data filtering and browsing. BIOPEP (Minkiewicz et al., 2008; Iwaniak et al., 2016), currently BIOPEP-UWM (Minkiewicz et al., 2019), is a widely used resource for the identification of bioactive peptides and bioactivity prediction as well as for *in silico* approaches.

The structural information of bioactive peptides is essential for the development of peptide-based drugs. Two databases, namely StraPep and SATPdb, are structural databases that are dedicated to the collection of bioactive peptides with known structures. StraPep (Wang et al., 2018) is dedicated to collecting all of the bioactive peptides with known structures. It displays the structures for 3,791 peptides and provides detailed information for each one (i.e., post-translational modification, experimental structure, secondary structure, the location of disulfide bonds, etc.). SATPdb (Singh et al., 2016) is a database of structurally annotated therapeutic peptides. It has been curated from 22 public peptide databases and has 19,192 unique, experimentally validated therapeutic peptide sequences. Several databases have been designed for unique peptides as well. Quorumpeps (Wynendaele et al., 2012) is developed for quorum sensing peptides, ConoServer (Kaas et al., 2012) and ArachnoServer (Pineda et al., 2018) are focused on venom toxin peptides; NORINE (Flissi et al., 2020) contains information on non-ribosomal peptides; DADP (Novković et al., 2012) is a database of defense peptides; and the NeuroPep, Neuropedia, and Neuropeptides[1] databases contain information on neuropeptides. Besides, databases covering proteins are also considered valuable resources for peptides; for example, UniProt (Universal Protein Resource)[2], which is a central resource of protein data, and protein structure databases such as PDB[3] (Abes et al., 2007), which contain the 3D structure of biomolecules.

IN SILICO TOOLS AND ALGORITHMS FOR PEPTIDE DESIGN

Peptides are the most amenable modulators that can be used to tackle the high surface area of PPIs. They can easily be synthesized, closely mimic the principal features of a protein, and be modified to attain higher stability, bioavailability, and binding strength. Sequence-based design and structure-based design are two major approaches for peptide design. Sequence-based peptide designing involves various physiochemical properties of the peptides and optimizing the peptide stability, toxicity, immunogenicity, and antibody specificity. In this regard, a plethora of *in silico* tools have been developed for sequence-based designing of novel peptides with therapeutic properties ranging from cell-penetrating to anti-microbial, anti-parasitic, anti-cancer, and anti-hypertension (**Table 2**).

Numerous methods, which are classified into general and specific methods, have been developed to predict AMPs. The APD3 (Wang et al., 2016) and CAMPR3 (Waghu et al., 2016) databases are among the general method predictors. They are designed to predict whether a given peptide is AMP or non-AMP. APD3 is developed for the classification, prediction, and design of AMPs using the parameter space defined by all available natural peptides in the database. The CAMPR3 implements four different machine-learning (ML) techniques to develop a peptide model. Deep-AmPEP30 (Yan et al., 2020) is a recently developed method that is used to predict bioactive sequences from genomes. This tool uses a short-length AMP prediction method based on the optimal feature set of PseKRAAC, reduced amino acid composition, and convolutional neural networks. The second group of methods is designed to predict AMPs, specifically on viruses, fungi, bacteria, or parasites. AVPpred (Thakur et al., 2012), AVCpred (Qureshi et al., 2017), and Meta-iAV (Schaduangrat et al., 2019b) are the more commonly used tools for the prediction of antiviral peptides. AVPpred (Thakur et al., 2012) is a web server used for the collection and detection of highly effective antiviral peptides (AVPs) using ML techniques such as support vector machine (SVM), features like the amino acid composition, and physicochemical properties. The AVCpred method is an SVM-based AVP prediction method. The experimental inhibitory percentage from ChEMBL (a large-scale bioactivity database for drug discovery) predicts the antiviral compounds against HIV, hepatitis C virus, hepatitis B virus, human herpesvirus, and 26 other viruses. Meta-iAVP is a sequence-based meta-predictor with an efficient feature representation (Schaduangrat et al., 2019b). It is designed for the accurate prediction of AVPs from peptide sequences. Antifp (Agrawal et al., 2018) is designed to predict antifungal peptides using features like amino acid composition, and similarly, Antibp2 (Lata et al., 2010) is another SVM-based method developed to predict antibacterial peptides. AtbPpred (Manavalan et al., 2019a) is a two-layer ML-based predictor for the identification of anti-*Mycobacterium tuberculosis* peptides. Moreover, ClassAMP (Joseph et al., 2012) and iAMPpred (Meher et al., 2017) are two methods used to predict the AMP class (e.g., antibacterial, antifungal, and antiviral). iAMPpred (Meher et al., 2017) predicts the probability of a peptide to be an antibacterial, antifungal, and antiviral agent by providing the probability score for all of the three classes.

The discovery of ACPs has provided an alternative approach to treating cancer. iACP (Chen et al., 2016), MLACP (Manavalan et al., 2017), ACPred (Schaduangrat et al., 2019a), and AntiCP 2.0 (Agrawal et al., 2020) are some famous *in silico* tools for the prediction and design of ACPs. The discovery of anti-angiogenic peptides is a promising therapeutic route for cancer treatment. TargetAntiAngio (Laengsri et al., 2019) was developed for the prediction and characterization of anti-angiogenic peptides using the random forest classifier in conjunction with various classes of peptide features and was demonstrated to be superior to other existing methods. mAHTPred (Manavalan et al., 2019b) was developed to predict anti-hypertension peptides using six different ML algorithms and showed superior performance compared to existing methods. HLP (half-life prediction) (Sharma et al., 2014) was developed for the prediction and design of peptides with desired half-life using SVM methods.

ToxinPred (Gupta et al., 2013) is one of the most applied SVM-based tools for predicting peptides toxicity. HLPpred-Fuse (Hasan et al., 2020) is the only tool that simultaneously identifies hemolytic peptides and their activities. It has fused six different ML classifiers in a robust hemolytic peptide prediction method. ProInflam (Gupta et al., 2016) was developed to predict the pro-inflammatory antigenicity of peptides using an ML-based

[1] www.neuropeptides.nl

[2] http://www.uniprot.org

[3] https://www.rcsb.org

TABLE 2 | Sequence-based peptide design tools.

Description	Name URL	Method	References
Prediction of AMPs	APD3: https://wangapd3.com/main.php	Support vector machine	Wang et al., 2016
	CAMPR3: http://www.camp3.bicnirrh.res.in/prediction.php	[Support Vector Machines (SVMs), Random Forests (RF) and Discriminant analysis (DA)]	Waghu et al., 2016
	Deep-AmPEP3: https://cbbio.cis.um.edu.mo/AxPEP	Optimal feature set of PseKRAAC reduced amino acids composition and convolutional neural network	Yan et al., 2020
Prediction of Antiviral peptide	AVPpred: http://crdd.osdd.net/servers/avppred	Support Vector Machine	Thakur et al., 2012
	AVCpred: http://crdd.osdd.net/servers/avcpred	Support vector machine	Qureshi et al., 2017
	Meta-iAV http://codes.bio/meta-iavp/	Sequence-based meta-predictor	Schaduangrat et al., 2019b
Prediction of Antifungal Peptides	Antifp: http://webs.iiitd.edu.in/raghava/antifp	Support vector machine based model developed using compositional features of peptides	Agrawal et al., 2018
Prediction of antibacterial peptide	Antibp2: http://www.imtech.res.in/raghava/antibp2/	Support Vector Machine (SVM)	Lata et al., 2010
Prediction of Anti-Tubercular Peptides	AtbPpred: http://thegleelab.org/AtbPpred	Two-layer machine learning (ML)-based predictor	Manavalan et al., 2019a
Prediction and classification of antimicrobial peptides	ClassAM: http://www.bicnirrh.res.in/classamp/	Support vector machine	Joseph et al., 2012
Prediction of antimicrobial peptides	iAMPpred: http://cabgrid.res.in:8080/amppred/	Support vector machine	Meher et al., 2017
Anticancer peptide prediction	iACP: https://bio.tools/iacp	Support vector machine (SVM)	Chen et al., 2016
	MLACP: http://www.thegleelab.org/MLCPP/	Support vector machine- and random forest-based machine-learning methods	Manavalan et al., 2017
	ACPred: http://codes.bio/acpred/	Machine learning models (support vector machine and random forest) and various classes of peptide features	Schaduangrat et al., 2019a
	AntiCP 2.0: https://webs.iiitd.edu.in/raghava/anticp2	Various input features and implementing different machine learning classifiers	Agrawal et al., 2020
Prediction and Analysis of Anti-Angiogenic Peptides	TargetAntiAngio: http://codes.bio/targetantiangio/	Random forest classifier in conjunction with various classes of peptide features.	Laengsri et al., 2019
Prediction of anti-hypertensive peptides	mAHTPred: http://thegleelab.org/mAHTPred	Six different ML algorithms, namely, Adaboost, extremely randomized tree (ERT), gradient boosting (GB), k-nearest neighbor, random forest (RF), and support vector machine (SVM) using 51 feature descriptors derived from eight different feature encoding	Manavalan et al., 2019b
Half Life Prediction	HLP: http://www.imtech.res.in/raghava/hlp/	SVM based models	Sharma et al., 2014
Predict and design toxic/non-toxic peptides	ToxinPred: https://webs.iiitd.edu.in/raghava/toxinpred	Machine learning technique and quantitative matrix using various properties of peptides	Gupta et al., 2013
Improved and robust prediction of hemolytic peptide and its activity	HLPpred-Fuse: http://thegleelab.org/HLPpred-Fuse/	Integrating six different machine learning classifiers and nine different sequence-based encoding	Hasan et al., 2020
Prediction of pro-inflammatory antigenicity of peptides	ProInflam: http://metagenomics.iiserb.ac.in/proinflam/	Machine learning-based prediction	Gupta et al., 2016
Prediction of Cell penetrating peptide	CellPPD : http://webs.iiitd.edu.in/raghava/cellppd/	Support vector machine and motif 2013 based	Gautam et al., 2013
	CPPpred: http://bioware.ucd.ie/cpppred	Neural networks	Holton et al., 2013
	CPPred-RF: http://server.malab.cn/CPPred-RF	Two-layer prediction framework based on the random forest algorithm	Wei et al., 2017
Prediction of bioactive peptide	PeptideRanker: http://bioware.ucd.ie/	Neural Network	Mooney et al., 2012

prediction tool. CellPPD (Gautam et al., 2013) is an SVM-based method that has been widely used to predict CPPs. CPPpred (Holton et al., 2013) is another server used to predict CPPs based on artificial neural networks. In CPPred-RF (Wei et al., 2017), the random forest algorithm can simultaneously predict the CPPs and their uptake efficiency. PeptideRanker (Mooney et al., 2012) is also a webserver used to predict the probability of the peptides being bioactive and ranks the bioactive peptides.

IN SILICO TOOLS AND ALGORITHMS FOR PEPTIDE MODELING

Bioactive peptides are critical in industrial, medical, and biological applications, and they play pivotal roles in regulating various biological processes (Gesell et al., 1997; Liu et al., 2008). There are several conventional methods to identify the tertiary structure of peptide molecules, including CD, electron paramagnetic resonance (EPR), Fourier-transform infrared (FTIR), and NMR spectroscopies and x-ray crystallography. However, these empirical methods are labor-intensive, time-consuming, and expensive to perform. Moreover, the employed solvent may have a significant influence on the peptide structure in some instances. Given these circumstances, computational methods for predicting the 3D structures of the peptide have emerged to circumvent these limitations. These methods are expected to contribute significantly to the delineation of peptide sequence to function relationships and the promotion of efficient designs for new peptide molecules. Like the methods for predicting protein 3D structure, peptides could be modeled by employing the homology, threading, and *ab initio* approach. The peptide modeling tools use one or a combination of these methods to predict the 3D structures of the peptides. The homology and threading methods rely on suitable template structures. Previously resolved peptide structures stored in PDB have a crucial influence on the accuracy of homology-based peptide modeling (Sali, 1995; Sanchez and Šali, 1997). The threading method is performed using the existing folds of proteins as the modeling templates (Bowie et al., 1991; Jones et al., 1992). Unlike the homology and threading methods, the *ab initio* approach is not template-based and exploits the physicochemical features to predict low-energy folding of the peptides (Monge et al., 1994; Bradley et al., 2005). In this regard, the bioinformatic tools involved in peptide modeling are classified into template-based and template-free methods. Various tools and servers have been developed for the prediction of peptide structures. Among the various available tools, six highly referred servers (PEPstr, Protinfo, PEP-FOLD, PEP-FOLD3, Hmmstr/Rosetta, PepLook, and PepSite & FlexPepDock server) are introduced in the following sections.

PEPstr Server

This server can predict the 3D structures of the peptide with an average length of 7–25 and sometimes 27 amino acids. It uses valuable and vital information about the beta-turns in predicting the 3D structure of the peptide. This server acts through different steps to model the peptide 3D structure. Primarily, all residues of the peptide get an extended conformation (phi = Psi = 180°). The secondary structure information from regular secondary structures (helices, beta-strands, and coil) and the beta-turns method help to detect the 2D structure of the peptide. Then, the conformational shape is created by assigning the Psi (Ψ) and phi (Φ) angles of the main chain. The standard Dunbrack backbone-dependent Rotamer library is used to determine the side chain angles. Ultimately, the obtained peptide model is refined by molecular dynamics (MD) simulation and energy minimization. The modeled 3D structure of the peptide will be stored in PDB format. Of note is that MD simulation can be accomplished in vacuum, hydrophilic, and hydrophobic states. The web server of PEPstr[4] was evaluated for the modeling of short peptides (Kaur et al., 2007). This server can model natural and non-natural amino acids, D amino acids, terminal modifications, peptide cyclization, post-translational and advanced modifications of residues, and structure simulations.

Protinfo Server

This server is highly suitable for the prediction of complicated protein structures. The function of this server is based on the interolog approach for the detection of experimental samples. Using the interolog approach is helpful for the identification of similar results found in the existing databases. Following this step, this server modeled input queries based on the determined homologous samples. One of the prominent features of the Protinfo server is that it can support a wide range of templates, from small amino acid subunits to a large number of them. The Protinfo PPC web server is available at http://protinfo.compbio.washington.edu/ppc/ (Hung et al., 2005).

PEP-FOLD Server

This is a high-performance server for *de novo* prediction of peptide structures from amino acid sequences. It utilizes a hidden Markov model (HMM) to make the predictions. It functions through the identification of primary structural alphabet (SA) letters in each sequence. The SA letters extracted by the HMM are necessary to describe the correct conformations of four consecutive residues (Zemla, 2003). It couples the predicted series of SA letters to a greedy algorithm and a coarse-grained force field (Souza et al., 2020). PEP-FOLD can handle peptides with 9–25 amino acids (Maupetit et al., 2009, 2010). PEP-FOLD3 is an improved version of the PEP-FOLD server. It is also a *de novo* approach with a more advanced and faster peptide structure modeling system. It can accommodate a vast range of peptide sizes ranging from 5 to 50 amino acids (Lamiable et al., 2016). PEP-FOLD and PEP-FOLD3 are respectively accessible at https://bioserv.rpbs.univ-paris-diderot.fr/services/PEP-FOLD/ and https://bioserv.rpbs.univ-paris-diderot.fr/services/PEP-FOLD3/.

I-Sites/Hmmstr/Rosetta Server

This server can predict the secondary, local, super-secondary, and tertiary structures of the protein sequences. This server also uses a hidden Markov model (HMMSTR) for local and secondary structure prediction, based on the I-sites library. It

[4]http://www.imtech.res.in/raghava/pepstr/

has three parts: I-site, Hmmstr, and Rosetta. I-site-motifs is a library that contains an extensive collection of small motif sequences (3–19 motifs). The I-site library is connected with numerous structured databases and encompasses about one-third of database sequences (Bystroff et al., 2000). According to the literature, the combination of I-sites and Rosetta is advantageous. Rosetta *ab initio* 3D predictor is a Monte Carlo (MC) Fragment Insertion protein-folding program that can use the results of Critical Assessment of Fully Automated Structure Prediction (CAFASP2) during the process (Fischer et al., 2001). There are some steps in the execution process of this server. The first step is the creation of a profile sequence through multiple alignments of the input sequence using PSI-BLAST (Position-Specific Iterative Basic Local Alignment Search Tool). The second step is the prediction of I-site motifs with a determined profile sequence. The third step is the preparation of fragment movesets from predicted I-site motifs. The fourth step is the modeling of secondary and local structures *via* HMMstr or the analysis of fragment moveset by the Rosetta server (Bystroff and Shao, 2002). Moreover, the I-sites/Hmmstr/Rosetta web server[5] is developed for 3D prediction.

PepLook Server

PepLook is another 3D peptide modeling web server that can model sequences with more than 30 residues. This server prepares many randomly produced peptide structures by altering the SA angles (Φ/Ψ). Modeling cyclic peptide conformation using distance restraint is one of the vital beneficial aspects of this server (Etchebest et al., 2005). Moreover, this server can model the 3D structure of post-translationally modified amino acids (carboxylated or hydroxylated), synthetic amino acids, and ribosomal peptides. PepLook can measure the energy factor of some features, including internal and external hydrophobicity, complete peptide structures (all atoms), and electrostatic and van der Waals interactions (Thomas et al., 2006). The PepLook server could be found at https://orbi.uliege.be/handle/2268/135016.

PepSite and FlexPepDock Server

Protein–peptide interactions are a vital part of many cellular signaling pathways. Getting a good grasp of these interactions would bring about a mechanistic understanding of how cell networks are regulated. The PepSite server can predict the binding of a given peptide onto a protein structure which unveils the details of the interaction of interest. PepSite 2[6] is a complete rewrite of the original PepSite, which can speed up the presentation of results to a fraction of a second. The surface position-specific scoring matrix (S-PSSMs) algorithm is used in this server to detect the binding sites for each peptide residue. Ultimately, a suitable peptide sequence can be generated against predicted biding sites considering certain distance limitations (Trabuco et al., 2012). FlexPepDock[7] is a high-resolution peptide-protein docking (refinement) protocol for the modeling of peptide–protein complexes. It is implemented in the Rosetta framework, which can be combined with the result of PepSite to design atomic models for given peptides in the vicinity of binding sites (London et al., 2011; Raveh et al., 2011). The summary of the information on the mentioned servers is presented in **Table 3**.

[5]http://www.bioinfo.rpi.edu/~bystrc/hmmstr/about.html

[6]http://pepsite2.russelllab.org

[7]http://flexpepdock.furmanlab.cs.huji.ac.il/

IN SILICO TOOLS FOR THE PREDICTION OF PROTEIN–PROTEIN INTERFACES

Proteins are vital agents that carry out all biological activities in the cells. PPIs play a pivotal role in the execution of these functions. Hence, investigating the changes that occur in the space between two proteins can be highly beneficial in the elucidation of disease etiology and the adaptation of appropriate treatment strategies. Various experimental methods exist for detecting biological changes in the PPI interface, including NMR, x-ray crystallography, mass spectrometry, and alanine scanning mutagenesis. NMR and x-ray crystallography can identify the interfaces at the atomic level, while the other methods like alanine scanning act at the residue level. Although the information about some of the PPI interface networks is extracted from high-throughput experiments, these experimental methods have their constraints mainly because they are expensive and time-consuming (Chen and Liu, 2005; Shoemaker and Panchenko, 2007; Casals et al., 2012; Koboldt et al., 2013). In this study, we focus on some computational methods for predicting the properties of the PPIs that can be valuable in circumventing the limitation of traditional pipelines. There are various computational approaches for the analysis of PPI interfaces. The existing strategies could be divided into information-based approaches and docking-based approaches (**Figure 1**). Docking is an important method that can facilitate the reconstruction of binary residue connections between two protein sections.

Information-Based Approach

A wide variety of *in silico* methods has been developed for data-based approaches. This approach is instituted on the information that is extracted from the results of conventional experiments. Three main strategies have been established for data-based approaches to analyze the PPI interfaces, namely the similarity-based method, the ML method, and the evolutionary-based method.

Similarity-Based Method

This method, also known as the "template-based" method, is one of the most widespread searching approaches for annotating the genome function. Instead of using partial sequence and statistical features of the sequence, the method relies on the similarity of whole protein sequences. Several biological properties can be obtained by multiple sequence alignments that are practical for identifying PPIs. These properties include the conservation of amino acids, the similarity between interfacing proteins, and gene fusion. Different behaviors can be expected from the proteins using this method. For example, unstable proteins tend to utilize different interfacial binding patterns. Therefore, using homology search for the extraction of interface residues

TABLE 3 | List of important *in silico* peptide modeling servers.

Type	Brief description	URL	References
Hmmstr/Rosetta	The HMMSTR/Rosetta Server predicts the structure of proteins from the sequence: secondary, local, supersecondary, and tertiary	http://www.bioinfo.rpi.edu/~bystrc/hmmstr/about.html	Bystroff et al., 2000; Bystroff and Shao, 2002
Protinfo	Protinfo PPC is a web server that predicts atomic level structures of interacting proteins from their amino-acid sequences	http://protinfo.compbio.washington.edu/ppc/	Hung et al., 2005; Kittichotirat et al., 2009
Pepstr	This server predicts the tertiary structure of short peptides with sequence length varying between 7 to 25 residues	http://www.imtech.res.in/raghava/pepstr/	Kaur et al., 2007
FlexPepDock	The Rosetta FlexPepDock protocol for high-resolution docking of flexible peptides which mainly consists of two alternating modules that optimize the peptide backbone and rigid body orientation, respectively, using the Monte-Carlo with Minimization approach.	http://flexpepdock.furmanlab.cs.huji.ac.il/	Raveh et al., 2010
PepLook	Peplook server, an efficient tool to predict peptide conformation	https://orbi.uliege.be/handle/2268/135016	Beaufays et al., 2012
PepSite	This server is a tool for accurate prediction of peptide binding sites on protein surfaces	http://pepsite2.russelllab.org	Trabuco et al., 2012
Pep-Fold	PEP-FOLD is a *de novo* approach aimed at predicting peptide structures from amino acid sequences. This method, based on structural alphabet letters	https://bioserv.rpbs.univ-paris-diderot.fr/services/PEP-FOLD/	Maupetit et al., 2009; Thevenet et al., 2012
Pep-Fold3	PEP-FOLD3 latest evolution comes with a *new 3D generation engine*, based on a new Hidden Markov Model sub-optimal conformation sampling approach, faster by one order of magnitude than the previous greedy strategy, while not affecting performance	https://bioserv.rpbs.univ-paris-diderot.fr/services/PEP-FOLD3/	Lamiable et al., 2016

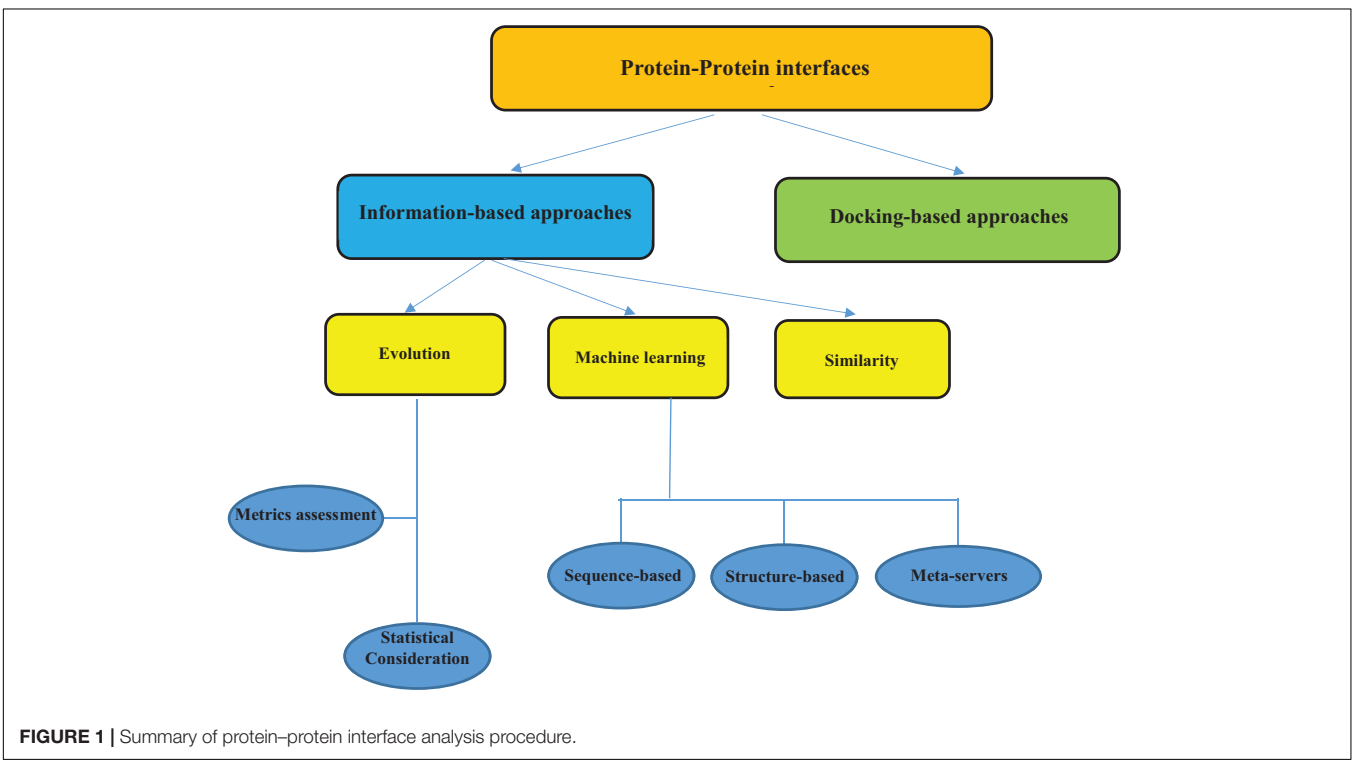

FIGURE 1 | Summary of protein–protein interface analysis procedure.

remains a controversial issue (Grishin and Phillips, 1994; Caffrey et al., 2004; Esmaielbeiki et al., 2016). A list of similarity-based prediction tools for PPI interfaces is represented in **Table 4**.

ML Method

Although there are beneficial aspects for the similarity-based method of predicting PPIs, it suffers from restrictions such as lack of accessible interfaces for experimental homologs and low

TABLE 4 | Similarity-based prediction databases (information-based approach).

Type	Brief introduction	URL	References
IBIS	IBIS is practical server that can sever and identify most of interaction (protein-protein, RNA-protein and etc.)	http://www.ncbi.nlm.nih.gov/Structure/ibis/ibis.cgi	Shoemaker et al., 2010
PredUS	PredUS is a structural similarity-based method and it is useful for detection of several features including designing of adjacent protein, mapping the interfacial space residues, measurement of residue interface score	https://bhapp.c2b2.columbia.edu/PredUs/	Zhang et al., 2011
PrISEC	This server measures surface patch which its function algorithm based on surface residues and atomic formation.	http://prise.cs.iastate.edu/	Jordan et al., 2012
PS-HomPP*	Extracting of interfacial residues via similar residues between binding proteins(intelligent server)	http://ailab1.ist.psu.edu/PSHOMPPIv1.2/	Esmaielbeiki and Nebel, 2014
NPS-HomPPI*	Prediction of probable interacting residues with different proteins(unintelligent server)	http://ailab1.ist.psu.edu/NPSHOMPPI/	Esmaielbeiki and Nebel, 2014
ProBiS	Using local structure alignment for identification of protein-protein interfaces	http://probis.cmm.ki.si/	Esmaielbeiki et al., 2016

** Intelligent server means a server that is considered protein with special connector.*
**Unintelligent server means a server that is considered protein with different connectors.*

quality (de Vries and Bonvin, 2008). ML methods operate based on a comparative pattern between interfacial protein residues and non-interfacial residues. This method could compensate for the limitations of the similarity-based methods. This approach can be categorized within the sequence and structural-based methods and consensus identifiers (Xie et al., 2020). Moreover, the use of ML methods for the prediction of PPIs has represented improved performance in comparison to other conventional approaches, such as neural networks. Thus, ML methods could play a significant role in therapeutic peptide development (Yang, 2008).

Sequence- and structural-based method

The sequence-based interface identifiers operate according to the features of the protein sequences. Most of these tools rely on evolutionary information from multiple sequence alignments (MSA) projected on the protein surfaces (Jordan et al., 2012). Therefore, these methods are inadequate in detecting interfaces of proteins with sparse homolog sequences and evolutionary variable regions. Advancements in structural proteomics have justified the establishment of structure-based automated methods for the prediction of functional surfaces of proteins (Jordan et al., 2012). The performance of this method depends on two 3D mappings and the 3D identifier. The 3D mapping is pertinent to the detection of close structures, and the 3D identifier is related to specific features such as protein surface accessibility (Hoofnagle et al., 2003; Heinig and Frishman, 2004), B-Factor (Halabi et al., 2009), the formation of the protein surface, and the 2D structure (Heinig and Frishman, 2004; Hamer et al., 2010) (**Table 5**).

Meta-servers

Meta-servers combine several interface prediction methods into a consensus predictor to attain more reliable and stable predictions compared to the results of each predictor on its own. This means that meta-servers can act creatively to use different databases as complementary units to improve their function (Kozlowski and Bujnicki, 2012). Three common meta-servers are presented in **Table 6**.

Evolutionary-Based Approach

The prediction of PPI interfaces using evolutionary data is one of the most well-known interface classifiers. This approach is deemed as a realistic approach for the identification of the biological features of PPI interfaces. The EPPIC (Evolutionary Protein–Protein Interface Classifier) server[8] is a tool designed to predict the quaternary structure of proteins from their crystal structures. Primarily, it classifies the interfaces of the crystal structure to determine their biological relevance. All topologically valid assemblies are computed, and the individual interface scores are used to predict the most likely quaternary assembly (Duarte et al., 2012).

Docking-Based Approach

Docking is one of the most well-known computational methods that are highly advantageous for predicting interfaces of biological targets and molecules (Kitchen et al., 2004). This method is practical for atomic-level investigation of molecular interactions. There are several different docking methods, and the selection of each server depends on the complexity of the problem and structure sources. Some structures are extracted *via* NMR or x-ray crystallography, which are suitable for the available docking servers. However, the template-based approach is the best candidate for predicting complex structures (Porter et al., 2019). Testing the accuracy of computational docking algorithms in blind predictions is managed by the CAPRI (Critical Assessment of Predicted Interactions) project (Janin et al., 2003). Molecular docking can be accomplished by a vast range of tools that are already accessible. Many docking tools act on the principle of rigid-body interactions, which results in a suitable match between the surfaces of tertiary (3D) structures. However, working with them has many restrictions such as protein flexibility, which is not considered. Given the importance of molecular docking in the determination of interface residues, many efforts have been made to mend the existing limitations (Luiz Folador et al., 2015; Pinzi and Rastelli, 2019).

[8]http://www.eppic-web.org/ewui/

TABLE 5 | Sequence- and structural-based databases (ML approach).

Type	Brief introduction	URL	References
ProMate(Str)*	Circling of surface residues and Possible estimation of the binding affinity in each selected residues	bioinfo41.weizmann.ac.il/promate/promate.html	Neuvirth et al., 2004
WHISCY	It is a versatile server that is capable to use sequence and structure and its function is measurement of similarity score based on Dayhoff matrix	http://nmr.chem.uu.nl/Software/whiscy/	de Vries et al., 2006
PINUP(Str)*	Presentation of scoring function such as conservation score	http://sysbio.unl.edu/services/PINUP/	Liang et al., 2006
PIER(Str)*	Recognition of interfacial & un-interfacial surface residues	http://abagyan.ucsd.edu/PIER/	Kufareva et al., 2007
SPPIDER (Str)*	Identification of measured (RSA)* and real (RSA)	http://sppider.cchmc.org/	Porollo and Meller, 2007
PSIVER(Seq)*	Detection of binding sites between two proteins via Naïve Bayes and PSSM	http://tardis.nibio.go.jp/PSIVER/	Murakami and Mizuguchi, 2010

(Str), structure; (Seq)*, sequence; (RSA)*, relative solvent accessibility.*

TABLE 6 | Three main meta-servers for prediction of interfaces (ML approach).

Type	Brief introduction	URL	References
Cons-PPISP(Str)	A server that is able to identify interaction sites by using some features such as specific position of surface residue, accessibility of surface residue	https://pipe.scs.fsu.edu/ppisp.html	Chen and Zhou, 2005
meta-PPISP(Str)	Strength incorporation of recognizing sections of three servers (PINUP, Cons-PPISP, ProMate)	http://pipe.scs.fsu.edu/meta-ppisp.html	Qin and Zhou, 2007
CPORT(Str)	Incorporation of six servers (PINUP, Cons-PPISP, ProMate, SPPIDER, PIER, WHISCY)	http://alcazar.science.uu.nl/services/CPORT/	de Vries and Bonvin, 2011

IN SILICO HOTSPOT PREDICTION TOOLS

It is well established that the energy distribution is not uniform in PPI interfaces, and a small number of residues have the largest share in binding free energy. Wells and Clackson, who studied the binding of the growth hormone to its receptor, discovered these residues and used the term hotspot for them (Wells, 1991; Clackson and Wells, 1995; Schreiber and Fersht, 1995; Stites, 1997; Bogan and Thorn, 1998; Clackson et al., 1998; Hu et al., 2000; Keskin et al., 2005; Kouadio et al., 2005). Subsequent studies showed that hotspots form a small number (about 9.5%) of residues of the interface area. Therefore, a more precise definition of hotspots has been proposed, which states that a hotspot is a residue whose mutation to alanine reduces at least 2 kcal/mol in binding free energy ($\Delta\Delta G = \Delta G^{mutanttype} - \Delta G^{wildtype}$) (Bogan and Thorn, 1998; Thorn and Bogan, 2001; Moreira et al., 2007). Hotspot residues are mainly composed of tyrosine (12.3%), arginine (13.3%), and tryptophan (21%) amino acids (Lichtarge et al., 1996; Bogan and Thorn, 1998). Studies have shown that hotspots have conserved structures and predictable physicochemical properties (DeLano, 2002; Moreira et al., 2007; Kenneth Morrow and Zhang, 2012). Impaired PPIs can cause many diseases, such as neurological disorders and cancer. Moreover, the conserved structure of hotspots, as well as their great impact on the binding energy, has made them attractive medical targets for the design of inhibitor drugs. Thus, many unwanted PPIs can be avoided by the use of these inhibitors, and they could be more effective in treating various diseases (Livnah et al., 1996; Wrighton et al., 1996; Tilley et al., 1997; Li et al., 1998; DeLano et al., 2000; Sidhu et al., 2000; Arkin and Wells, 2004; Thanos et al., 2006; Moreira et al., 2007; Wells and McClendon, 2007; White et al., 2008; Blazer and Neubig, 2009). As mentioned, hotspots are predictable, and it is worth mentioning that one of the prediction methods is based on the experimental alanine scanning method. For example, when a large tryptophan residue (as one of the three main hotspot residues) mutates into alanine, this difference in size causes the formation of a cavity, resulting in instability of the complex due to binding energy reduction. Alanine scanning means that when a residue mutates into alanine, the amount of binding energy decreases; if this decreased energy is significant (10-fold or more), then that mutated residue is considered as a hotspot (Bogan and Thorn, 1998; DeLano, 2002). Mutation to alanine residue removes the side chain effect. The methyl side chain of the alanine residue is relatively neutral and also lacks the additional flexibility contribution (Cunningham and Wells, 1989; Wells, 1990; Skolnick et al., 2000). Although glycine mutagenesis removes the contribution of the side chain, it can cause flexibility in the protein backbone (Morrison and Weiss, 2001). Hence, glycine mutagenesis is not considered for hotspot detection. The Alanine Scanning Energetics Database (ASEdb) contains the results of alanine scanning experiments. The Binding Interface Database (BID) has verified experimental hotspots in the literature (Thorn and Bogan, 2001; Fischer et al., 2003). Despite their advantages, these databases also are associated with several drawbacks. The hotspots obtained from experimental studies can only be attributed to a limited number of complexes. Moreover, it is recommended to avoid these data to interpret specific residual interactions (DeLano, 2002). Experimental mutagenesis

of proteins to find hotspots is not practical and useful on a large scale because individual mutated proteins must be purified and analyzed separately. It should also be noted that alanine scanning and other experimental hotspot analysis methods are highly time-consuming and costly. Given these circumstances, theoretical and computational prediction methods seem attractive for hotspot residue prediction (Kenneth Morrow and Zhang, 2012). FoldX[9] is a hotspot prediction tool and server which uses the FOLDEF algorithm developed by Guerois et al. (2002). This server predicts the hotspots of PPIs by using an energy-based method. It finds the PPI energy changes with the computational alanine scanning technique (Schymkowitz et al., 2005; Kenneth Morrow and Zhang, 2012). The Robetta server[10] developed by Baker and Kortemme includes various parameters such as implicit solvation and hydrogen bonding, packing interactions, solvation interactions, and Lennard-Jones interactions to calculate the interaction free energy. The method employed in this server is similar to that in FoldX (energy-based method), and the technique used is computational alanine scanning (Kim et al., 2004). Similar to FoldX, the parameters obtained from the Robetta server are based on changes in protein stability. This server mutates the side chains to alanine and then locally repacks the parts of the structure that fall in a 5-Å radius of the mutated residue. The rest of the protein structure remains unchanged. The changes in binding energies of PPIs result from these mutations and form the basis for hotspot predictions (Kortemme et al., 2004). The Robetta server can accurately predict 79% of hotspot residues with a 1.0 kcal/mol cutoff. However, it enables us to find the hotspots involved in hydrogen bonds with water molecules (Kenneth Morrow and Zhang, 2012). PP_Site is a structure-based tool with a simple algorithm technique based on three factors, namely van der Waals interactions, hydrophobic interactions, and H-Bond, developed by Gao et al. (2004) and Kenneth Morrow and Zhang (2012). FTMAP[11] is an energy-based hotspot prediction tool and server. It uses a probe-based rigid-body docking with fast Fourier transform correlation. The users of FTMAP only need the PDB code or the PDB file of the protein for the prediction (Brenke et al., 2009; Kenneth Morrow and Zhang, 2012). PCRPi (Presaging Critical Residues in Protein interfaces) is a method that uses the Bayesian networks technique to unify evolutionary, structural, and energetic determinants into a common probabilistic framework. PCRPi was upgraded to PCRPi-W[12] to function as a web server. The users can upload a complex or enter a PDB code and select the type of Bayesian network architecture (expert or naïve) (Assi et al., 2010; Mora et al., 2010). HotPoint[13] is another hotspot prediction server that uses an empirical formula technique and simple architecture. Its prediction method is based on the contact potential of the interface residues and solvent accessibility developed by Tuncbag et al. (2009). The accuracy of this server is about 70%. The results are a table of interface residues in which the hotspots and their properties are highlighted (Tuncbag et al., 2009, 2010). Grosdidier and Fernández-Recio (2008) have developed an energy-based (Docking) tool with a normalized interface propensity technique. Higa and Tozzi (2009) have developed a tool based on structural and evolutionary methods with the SVM technique. Rajamani et al. (2004) has developed a tool based on sidechain ΔASA (accessible surface area) with the MD technique. HSPred[14] is an energy-based tool with an SVM (Residue specific) technique (Lise et al., 2009, 2011). MINERVA is a tool based on molecular interaction, structure, and sequence methods with decision tree and SVM techniques (Cho et al., 2009). KFC2[15] is a server based on various structural features and ASA methods with the SVM technique (Zhu and Mitchell, 2011). Guharoy and Chakrabarti (2009) have developed a tool based on the interface location and H-bonding methods with the simple algorithm technique.

PEPTIDE–PROTEIN DOCKING TOOLS

Molecular docking is a highly applicable method in the design and discovery of small-molecule drugs. This method has also undergone drastic progress in the prediction of PPIs. The prediction of peptide–protein interactions is the subject of similar attempts to develop more amenable peptide therapeutics (Diller et al., 2015; Ciemny et al., 2018). However, docking methods generally struggle with the issue of modeling the considerably more flexible and larger peptide molecules (London et al., 2013). However, peptide therapeutics have recently garnered a lot of attention, which has led to rapid advancements in peptide-protein docking-related technologies. These efforts have resulted in advances in drug design and discovery (Fosgerau and Hoffmann, 2015; Bruzzoni-Giovanelli et al., 2018; Ciemny et al., 2018). There are three main approaches for peptide-protein docking: global docking, local docking, and template-based docking. Different methods have varying degrees of prediction accuracy, often dictated by the amount of interaction information given as input (Ciemny et al., 2018). Template-based docking methods build a model of the complex using known structures, and it can be beneficial if the template is close to the investigated complex (Kundrotas et al., 2012; Lee et al., 2015; Lensink et al., 2017; Marcu et al., 2017; Pallara et al., 2017). Local docking methods look for a peptide-binding pose that is close to a user-defined binding site. Thus, the docking accuracy relies on the input information. The more precise the defined binding site, the better the results (Ciemny et al., 2018). Global docking methods conduct a collaborative scan for the pose and peptide-binding site. The most basic procedure for this approach is considering the protein and peptide input conformations to be rigid and conducting a comprehensive rigid-body docking. Predicting the peptide conformation based on a sequence given by the user is a more complicated approach for this method. Typically, their pipeline includes three phases; primarily, the input peptide conformations should be created

[9]http://foldxsuite.crg.eu/

[10]https://robetta.bakerlab.org/

[11]http://ftmap.bu.edu/serverhelp.php

[12]http://www.bioinsilico.org/PCRPi/

[13]http://prism.ccbb.ku.edu.tr/hotpoint/

[14]http://bioinf.cs.ucl.ac.uk/psipred/

[15]https://mitchell-web.ornl.gov/KFC_Server/index.php

by various strategies [e.g., utilizing monomeric protein structure fragments (Yan et al., 2016; Porter et al., 2017), threading the sequence onto a predefined set of template conformations (de Vries et al., 2017), or peptide folding simulation in solution (Ben-Shimon and Niv, 2015)]; then, the docking of rigid bodies should be implemented; ultimately, scoring and, or refinement of the models should be performed (Ciemny et al., 2018). At least three significant challenges lie ahead in the path of efficient peptide-protein docking. The first challenge is the prediction of significant conformational changes in the protein and peptide molecules (flexibility problem) upon docking. The second challenge is selecting the structure with the highest accuracy from a large number of produced models (scoring problem). The third challenge is integrating computational predictions and experimental findings into the peptide-protein docking scheme (integrative modeling) (Ciemny et al., 2018). **Table 7** includes features and descriptions of the main peptide-protein docking tools and servers that are currently available.

VIRTUAL SCREENING METHODS FOR PEPTIDE–PROTEIN INTERACTIONS

Virtual screening (VS) is a robust computational technique capable of searching huge libraries of small molecules and identifying the most suitable ones against a protein receptor. VS has emerged as a complementary technique of high-throughput screening (HTS). Nowadays, thanks to the advancements in VS, it has become an indispensable part of the drug discovery process, leading to enormous savings in cost and time. Recent studies have established that VS can help to develop inhibitors of PPIs.

Exploration of new macromolecular structures by NMR or x-ray crystallography methods, human genome sequencing, and rapid computational methods could improve VS searches. Although increasing the numbers of the unveiled structures of protein–ligand complexes has made VS more convenient, 3D structure prediction approaches could be employed where experimentally determined structures of proteins/peptides are not available (Slater and Kontoyianni, 2019).

There are several accessible public databases for known drugs, small molecules, and chemical compounds (natural or synthetic) which could be searched when implementing VS strategies: ChemDB[16], ChemBank[17], NCI Open Database[18], ChEMBL[19], PubChem[20], ZINK[21], ChemSpider[22], and DrugBank[23] (Lavecchia and Di Giovanni, 2013). There are also some commercial databases containing data derived from patents or literature, including ACD[24] and WOMBAT[25] (Lavecchia and Di Giovanni, 2013). There are two main categories of VS: ligand-based VS (LBVS) and structure-based VS (SBVS).

Ligand-Based VS

The LBVS approach relies on the extracted structural and bioactivity information from an enormous small-molecule library. Three-dimensional shape matching is one of the popular LBVS methods based on seeking molecules with a similar shape to that of the known active molecules. Utilizing pharmacophore models to find the intended ligand, quantitative structure–activity relationships (QSAR), and chemical similarity analysis (to look in a database of molecules against one or more active ligand structures) are additional LBVS methods.

Similarity analysis is one of the most common techniques of VS. In the similarity searching method, the closest molecules are identified for a known active reference structure. Nevertheless, this method is simply influenced by the users because the selection of accurate input molecules is a challenging issue. However, this is a fast VS method (Lavecchia and Di Giovanni, 2013; Wu et al., 2019).

Pharmacophore modeling is another method for LBVS. A pharmacophore is a set of crucial molecular properties involved in accurate molecular recognition and interactions of a ligand with a specific biological target. Since 3D models are necessary for docking, pharmacophores could serve as vital VS processes to explore novel ligands for receptors with unknown 3D structures. There are various pharmacophore-based VS case studies for peptides. For example, a study designing the pharmacophore model for secretin resulted in gaining novel angiotensin-converting enzyme (ACE) inhibitory peptides with the desired biological activity. Angiotensin-I-converting enzyme inhibitory peptides and Intestinal Peptide Transporter hPepT1 are some of the more successful examples of pharmacophore modeling in LBVS methods (Dong et al., 2011; Wang et al., 2011; Osmulski et al., 2020). However, pharmacophore modeling has some limitations, especially when working with peptides. Some of the snags present in peptide-based pharmacophore modeling are the lack of acceptable scoring metrics, lack of clear instructor pharmacophore query, improper binding affinity evaluation, and incorrect or inadequate conformational sampling. These limitations could lead to false-positive and false-negative results (Kaserer et al., 2015; Ciemny et al., 2018; Slater and Kontoyianni, 2019).

Quantitative structure–activity relationship is one of the most popular LBVS methods. This technique could involve the interplay between biological function, the potency of active molecules, and their structural/physicochemical features. QSAR-based methods need information such as the values of IC_{50} and the binding affinity (K_d). QSAR modeling is classified into 2D-QSAR and 3D-QSAR; 2D-based algorithms are faster but less precise in comparison with 3D-based algorithms. The solubility,

[16]http://cdb.ics.uci.edu
[17]http://chembank.broadinstitute.org
[18]http://cactus.nci.nih.gov/ncidb2.2/
[19]https://www.ebi.ac.uk/chembl/
[20]http://pubchem.ncbi.nlm.nih.gov
[21]http://zinc.docking.org
[22]http://www.chemspider.com
[23]http://www.drugbank.ca

[24]http://accelrys.com/products/databases/sourcing/avaible-chemicalsdirectory.html
[25]https://www.proofpoint.com/us/wombat-security-is-now-proofpoint

TABLE 7 | Peptide-protein docking tools and servers.

Tool or server	URL	Required input	Brief description	References
PIPERFlexPepDock	http://piperfpd.furmanlab.cs.huji.ac.il	N/A	(1) Global docking method, (2) Using Rosetta fragment picker for predicting peptide conformation, (3) Rigid-body docking by using PIPER (Kozakov et al., 2006), (4) scoring by using Rosetta energy function, (5) Rosetta FlexPep Dock for refinement (London et al., 2011)	Alam et al., 2017
ClusPro PeptiDock	https://peptidock.cluspro.org/	N/A	(1) Global docking method, (2) Prediction of peptide conformation based on motif, (3) Rigid-body docking by using PIPER[1], (4) Using structural clustering for scoring	Porter et al., 2017
CABS-dock	http://biocomp.chem.uw.edu.pl/CABSdock and as a standalone version	N/A	(1) Global docking method, (2) scoring based on clustering, (3) Receptor flexibility is typically limited to small backbone, which can be increased if needed	Kurcinski et al., 2015
pepATTRACT	http://bioserv.rpbs.univ-paris-diderot.fr/services/pepATTRACT/	N/A	(1) Global docking method, (2) use ATTRACTscore for scoring, (3) use iATTRACT for flexible refinement of models (Schindler et al., 2015), (4)both interacting residues of receptor and ligand are flexible	Ciemny et al., 2018
Surflex-Dock	Standalone version	Pc and B (binding site region mark by user)	(1) Local docking method, (2) Peptide conformations inside binding pockets are created using a rotamer library, (3) Receptor flexibility is restricted to the pocket of binding site	Jain, 2003
Gold	Standalone version	Pc and B(binding site region mark by user)	(1) Local docking method, (2) Monte-Carlo-based sampling of peptide conformations inside binding site pocket, (3) Flexibility in receptors is either restricted to side chains or is implicit (ensemble docking)	Verdonk et al., 2003
DINC 2.0	http://dinc.kavrakilab.org	Pc and B(binding site region mark by user)	(1) Local docking method, (2) The structure of the receptor remains rigid during docking, (3) for docking long peptides according to AutoDock4, the peptide is divided into increasing length segments.	Antunes et al., 2017
AutoDock Vina	Standalone version	Pc and B(binding site region mark by user)	(1) Local docking method, (2) Monte-Carlo-based sampling of peptide conformations inside binding site pocket, (3) Receptor flexibility is typically limited to side chains, which can be increased to backbone if needed	Rentzsch and Renard, 2015
PEP-FOLD 3	http://bioserv.rpbs.univ-paris-diderot.fr/services/PEP-FOLD3	PcB	(1) Local docking method, (2) sampling of peptide conformations according to Monte-Carlo, (3) clustering of resulting models based on RMSD	Lamiable et al., 2016
HADDOCK peptide docking	http://milou.science.uu.nl/services/HADDOCK2.2/haddock.php	PcB (binding site residues list by user)	(1) Local docking method, (2) Threading a peptide sequence into three peptide conformations results in the creation of peptide structures, (3) rigid-body docking of peptide inside the binding site pocket, (4) binding free energy used for scoring, (5) binding site residues and peptide are fully flexible	Trellet et al., 2013
PepCrawler	http://bioinfo3d.cs.tau.ac.il/PepCrawler/	PcB	(1) Local docking method, (2) peptide is fully flexible and Rapidly exploring Random Trees algorithm using for its docking, (3) use clustering for scoring, (4) the flexibility of Receptor restricted to sidechains	Donsky and Wolfson, 2011
Rosetta FlexPepDock	http://flexpepdock.furmanlab.cs.huji.ac.il and standalone version	PcB	(1) Local docking method, (2) optimization flexible peptide inside receptor pocket based on Monte Carlo, (3) Receptor flexibility is typically limited to side chains, which can be increased if needed, (4)Using Rosetta energy function for scoring	London et al., 2011
PepComposer	http://biocomputing.it/pepcomposer/webserver	B (does not require peptide sequence)	(1) Template-based docking method, (2) In the database of experimentally solved monomeric proteins, look for regions that are structurally close to the region of a predefined binding site	Obarska-Kosinska et al., 2016
GalaxyPepDock	http://galaxy.seoklab.org/pepdock and a standalone version	N/A	(1) Template-based docking method, (2) Look for templates that are identical in form and interaction, (3) energy-based optimization use for model building, (4)scoring is done according to energy	Lee et al., 2015

flexibility, ligand and protein conformations, and structures are not considered in both of the methods (Kanakaveti et al., 2020).

Structure-Based VS

The SBVS methods require knowledge of the 3D structures of proteins and not the biological function of known molecules. SBVS involves docking the candidate molecules with the protein target, followed by ranking the predicted binding affinity by scoring functions to detect potential lead candidates. In this approach, the 3D structure of the protein of interest should be available through x-ray crystallography, NMR, or homology modeling. Subsequently, docking could engage the small molecules as ligands of the receptor *via* computational algorithms; then, the top-ranked compounds could be selected for further experimental studies. Scoring of the ligands through different scoring functions (empirical, knowledge-based, and force field-based) is a critical step in SBVS. The flexibility of the target structure is another complicated aspect of SBVS, which could noticeably compromise the accuracy of the approach. In recent years, docking algorithms are seriously confronting this challenge by improving soft docking. MD simulation, which considers ligand flexibility and entropic effects, could also be combined with SBVS or LBVS to increase the information accuracy of the binding pose of candidate molecules and subsequently improve the drug development (Yan et al., 2019; Wang and Sun, 2020).

Combining Ligand-Based and Structure-Based Approaches

The drawbacks and limitations of traditional VS methods could be alleviated by combining LBVS and SBVS. This unified approach applies both structural similarity and ligand-based data. A researcher could select one of the LBVS, SBVS, or integrated approaches depending on the case study. One of the successful reports in recent years is the designing of the polo-box domain of polo-like kinase 1 (PLK1-PBD) inhibitor through a combined strategy of SBVS pharmacophore modeling and molecular-docking screening techniques (Ramezani et al., 2019; Yan et al., 2019). The study resulted in the discovery of a peptide as a potent candidate for further experimental investigation. Notwithstanding the successful results gained by the combined approach, critical improvements in the combination strategies are still needed. One of the fundamental limitations is the complicated procedure of the platform handling, so improving the performance of this process would bring new advancements soon (Wang and Sun, 2020).

OPTIMIZING INTERFERING EFFECTS OF PEPTIDES

The interfering effects of peptides could not be accessed accurately by biophysical techniques such as x-ray crystallography, NMR spectroscopy, and fluorescence spectroscopy. They have unique features such as high selectivity and immunogenicity (Bruzzoni-Giovanelli et al., 2018). Despite their advantageous features, they could exhibit limited cellular penetrability, low *in vivo* stability, low solubility, and low binding strength. However, various methods have been considered to improve these limitations. The peptides could be optimized by chemical, biophysical, and *in silico* methods (Bruzzoni-Giovanelli et al., 2018). *In silico* methods of peptide optimization seem appealing due to their computational nature, which have the advantages of low cost, less time consumption, and avoiding the ethical issues of empirical analyses. There are some modifications that can be made to the *in silico* methods which can improve the efficacy of interfering peptides.

One way to optimize the performance of interfering peptides is the utilization of peptide design tools. Peptide design tools predict the spatial and energy constraints applied to them and suggest the best folding. Two main peptide-designing approaches include the stochastical and deterministic methods. In the deterministic approach, a complete space sequence is searched to reach the sequence fold with the lowest formation energy. In contrast, the stochastical method searches for the sequence space heuristically, which includes MC and genetic algorithms. The structure of the interfering peptide is fixed by optimizing the rotation angles of the lateral chains and energy minimization is performed by tools such as Rosetta Design. This software also improves the network of hydrogen bonds and van der Waals interactions (Roy et al., 2017). It should be noted that the scaffold can be changed during the modification of amino acids. Most methods such as GRAFTER, FITSIT, Proda Match, and Scaffold selecting suitable peptide patterns require geometric constraints such as the coordinates of the pattern-representing atoms. The AUTO match tool exhibits the flexibility of backbone patterns. When a correct peptide pattern is chosen, side-chain amino acids need to be modified to improve their correctness. Side chain changes can be evaluated by various factors, such as determining the binding affinity and structural stability. Tools such as ORBIT are used to reform the side chain that can bind to the target molecule (Roy et al., 2017). PPIs have a crucial role in signal transduction processes. A rapid computational approach has been developed to predict energetically critical amino acid residues in PPIs. The input consists of a 3D structure of the protein–protein complex. The output is a list of "hot-spot" or amino acids side chains that are predicted to become unstable when mutated to alanine (Kortemme et al., 2004). *In silico* alanine scanning could be used to improve the efficacy of the interfering peptides.

Poor cell membrane permeability of interfering peptides is a significant hurdle. Therefore, improvement of membrane permeability or development of strategies that facilitate active intracellular uptake will be critical for successful peptide-based targeting of intracellular PPIs. Increased uptake could be achieved by the identification of unnecessary hydrophobic amino acids. These amino acids can be replaced by charged or polar residues while maintaining their native bioactivity. Recently, *in silico* methods have been applied to speed up this process (Lee et al., 2019). CcSOL Omics is software that is used for the prediction of proteome solubility and the identification of solvent motifs according to the given amino acid sequence. PROSO-II is another SVM-based tool that predicts the solubility of a peptide based on physicochemical properties

such as hydrophobicity, hydrophilicity, and features of secondary structure (Lee et al., 2019).

One of the main impediments ahead of clinical development of interfering peptides is their high sensitivity to proteases. Their half-life is highly reduced by proteolytic cleavage. The most common structural changes that increase protein stability are chemical changes. These optimizations include the acetylation of N-terminus and C-terminus ends of the peptide scaffold, the introduction of dextrorotary (D)-amino acids, and peptide scaffold cyclization (Sorolla et al., 2020). Engineering peptides by introducing D-amino acids instead of levorotatory (L) forms is an effective strategy to avoid proteolytic degradation by proteases. These D-amino acids could cause structural changes in the target peptides, which makes them unrecognizable by proteases. Recent studies have shown that interfering peptides containing D-amino acids have a longer half-life. Many therapeutic peptides containing unnatural amino acids have been approved by the FDA, such as degarelix for prostate cancer, semaglutide for type 2 diabetes, and carbetocin (an oxytocin analog containing methyl-tyrosine) for postpartum hemorrhage (Sorolla et al., 2020). Cyclization of peptides can increase their half-lives. This cyclization can be accomplished by different methods, such as the formation of a disulfide bond between cytosine, adding an amide bond between the C- and N-terminus (head to tail), and addition of amide bond between natural amino acid side chains (side chain cyclization). Click chemistry software is a widely used tool for designing cyclic peptides. PEP-Cyclizer is another software that is used to design head-to-tail cyclization. This software has other complementary features such as the ability to search for candidate sequences compatible with the cyclization of the peptide (a facility to assist medicinal chemists), the generation of 3D models of a cyclic peptide starting from the 3D structure of the un-cyclized peptide and the sequence of the cyclized peptide, and preliminary steps for the conformational stability analysis of other peptides, or peptide-receptor docking (Pierce et al., 2014).

PEPTIDE–PROTEIN BINDING ENERGY CALCULATION TOOLS

The value of determining the binding energy of protein–ligand interactions in docking studies is apparent in the field of drug design. Acquisition of sufficient knowledge at a molecular level leads to accurate simulation, a valuable tool for drug design purposes. Experimentally measuring an inhibition constant (Ki) of the enzyme or protein in the presence of both the inhibitor and the substrate can estimate the binding affinity. In theoretical calculations, evaluating the properties of the protein, ligand, and after that, the complex can estimate the free energy of the ligand. Theoretically calculated free energies of the binding are often compared with the free energy of the reaction by calculating the K_d. Molecular mechanic force fields, which play a vital role in the conformational flexibility studies, like AMBER, MMFF, CHARM, and OPLS, can calculate various interactions in non-bonded atoms (Vanommeslaeghe et al., 2014; Ciemny et al., 2018). There are several methods for calculating the binding energy, namely endpoint, pathway, and alchemical methods.

Endpoint Methods

Endpoint methods are fast; however, their accuracy is usually limited to rational ranking (with r2 starting from 0.4 to 0.9, with a median of ∼0.7). The main advantage of endpoint methods is the requirement of only the simulation of the bound and free states of the ligand compared with pathway methods, which demand the simulation of many intermediate states likewise. Molecular mechanics/generalized Born surface area (MM/GBSA) and molecular mechanics/Poisson–Boltzmann surface area (MM/PBSA) are two general similar endpoint methods employed in protein–ligand-free energy calculations (Wang et al., 2019). Changes in solvation free energy, molecular mechanical energy, and conformational entropy are utilized to calculate the free energy of binding (Hall et al., 2020).

Linear interaction energy (LIE) is another endpoint approach used to figure out binding affinities. LIE relies on the concept that the free energy of binding shows a linear dependency on the polar and non-polar variations in ligand-surrounding energies. The strategy involves calculating values for the protein–ligand binding free energy ΔG bind with conformational sampling. Efforts such as considering multiple binding poses and continuum electrostatics solvation have promoted the accuracy of the LIE method (Rifai et al., 2020).

Chemical Methods

Although physically non-realizable, there are feasible computational processes of moving a set of atoms in a system from one state to another. In such a situation, modeling by alchemical free energy calculations could be one of the helpful computational processes. In strategies based on alchemical modifications, shifting the ligand into non-interacting mock particles may offer the absolute free energies of binding. Further, calculating the difference of free energy between two ligands can test the relative free energies of binding (de Ruiter and Oostenbrink, 2011). Free energy perturbation (FEP), Bennet's acceptance ratio (BAR), and thermodynamic integration (TI) are typical samples of alchemical methods, in which the statistical mechanics provide the demanded data. Performing more extended simulations may yield way more accurate energy calculations (Ciemny et al., 2018).

In addition to established methods, some prefer using combinations of existing approaches or try novel strategies. RETI is a successful combination of TI and replica exchange (RE). TI is known as a powerful method used to calculate free energy differences. However, when several confirmations are involved, getting accurate outcomes becomes problematic. RETI can somewhat solve the problem by enhancing sampling efficiency. Enhanced sampling-one-step perturbation (ES-OS) and linear interaction energy/one-step perturbation (LIE/OS) are among other combined approaches. The aim of using the LIE/OS method is to enhance the accuracy of energy calculation. LIE calculates the charging atoms in the interaction cavity, while OS is applied to explain the contributions from cavity formation (de Ruiter and Oostenbrink, 2011).

Path Sampling

Path sampling approaches can meet the computational aspect of a process using the separation of timescales in biomolecular systems. Thus, it is advantageous when used in process of non-clear separation timescales. Path sampling methods compute functional transition rather than stable states, by physically removing the ligand from the protein and calculating the mean force along this path. Similarly, path sampling can be used efficiently for the conformational sampling of stable states fragmented by low barriers. Transition path sampling (TPS) and MC simulations are two approaches using a complete path. TPS is helpful for chemical or physical transitions of a system from one stable state to another state (such as protein folding or chemical reactions) that infrequently occur to be observed on a computer timescale (Chong et al., 2017).

There are some vital factors to be considered in using these methods, which might remarkably affect the accuracy and computational time of calculation. Deciding on the solvent, the simulation length, and ligand orientations, following the selection of relative or absolute free binding energies, is a critical step in the calculation process (de Beer, 2012).

Common Issues

Improving the accuracy and the speed of calculations simultaneously is the main aim of the methods described above; however, it seems challenging. As an example, factoring in solvent interactions will enhance the accuracy but also will increase the required computational time. Including explicit water molecules in the binding sites will increase the accuracy for specific systems. In explicit water simulations, grand canonical MC simulations (GCMC) can determine the fluctuation of the number of water molecules in the binding site. Paying attention to polarizability, accurate force field, and charge transfer is crucial in exact free energy calculations; their effects can be considered using quantum mechanics. Quantum mechanics can efficiently calculate electrostatic interaction energies. However, it would not be affordable in the study of massive molecules. Semi-empirical quantum methods are essential in computational chemistry for treating large molecules and studying electrostatic interactions in peptide-protein interactions. Semi-empirical approaches are generally based on the Hartree–Fock formalism with some more approximations and empirical data usage (de Beer, 2012; Rifai et al., 2020).

As mentioned above, a combination of the present methods has been recently developed to overcome the sampling problems and other shortcomings of the methods on their own, while strengthening their advantages. It is assumed that these combined methods would result in more accurate energy binding calculations, consequently having more reliable outcomes for application in drug design developments.

DISCUSSION

In silico methods are implanted into every corner of the biological analyses. The study of IPs capable of modulating the PPIs is no exception and neither are the extended *in silico* tools established to develop, analyze, and optimize the IPs. These methods are anticipated to grow and become more accurate by reiterating the cycles of prediction and empirical assessment of these predictions. More precise algorithms would be developed, including the parameters of new players discovered by empirical studies. The novel and more accurate *in silico* tools would design and optimize an almost unlimited number of IPs with a high affinity against extracellular or intracellular (CPPs) PPIs. These tools would also help develop pharmacokinetically stable, safe, and effective IPs to modulate the PPIs within the cellular membranes. Moreover, these tools would be employed to predict, exert, and analyze specific chemical modifications to improve the ADME properties of the IPs. They also would be harnessed to design multifunctional IPs and even remotely controlled PPI inhibitors. Moreover, available natural peptides, evolutionarily selected for high stability and specificity, would be employed by *in silico* tools for rational structure-based design of IPs harboring similar properties. The ever-growing need for more effective therapeutics would be the driving force for further growth of the *in silico* methods in IP development. Given the apparent advantages of the peptides over small molecule drugs, higher investment of the pharmaceutical industry into the development of IPs does not seem farfetched. *In silico* tools will play a pivotal role in the transition from small molecule-based modulators of PPIs to peptide-based modulators.

Modulation of PPIs using the IPs is one of the hot research topics of various scientific fields such as biochemistry, chemical biology, and pharmacology. Recent progress in developing *in silico* methods for the evaluation and identification of these IPs has hugely extended the field. Although some issues about the pharmacodynamics and pharmacokinetics of peptides remain to be addressed, many companies have already devoted themselves to peptide discovery, which resulted in numerous peptide drugs and homologous compounds on the market. *In silico* methods could offer a comprehensive and exciting portfolio of applications in IPs targeting the PPIs. The interest in these methods is reflected in the increasing number of algorithms, software, and related publications. These methods have a lot to offer toward resolving challenges like low membrane permeability, the tendency for aggregation, short half-life, fast elimination (if not stabilized), proteolytic degradation, specific targeting, toxicity, immunogenicity, and optimization of IPs. Each issue could be dealt with by using a combination of *in silico* tools developed based on the experimental results. Most of the peptide-related challenges require atomic-level structural information. The structural information about the peptides could be found in structural databases. The *in silico* methods could predict the structure of peptides lacking the previously resolved 3D structures. Given the 3D structure of an IP, its properties could be analyzed and optimized to circumvent functional limitations. These structures could also be employed to screen peptide libraries and find new targeting peptides. The efficacy of *in silico* tools highly depends on the accuracy of their algorithms. These algorithms are continuously revised considering the evidence obtained from experimental studies. Given their high potential to

unravel the questions about IP design and optimization, *in silico* tools would become an inevitable part of the development of IPs that modulate the PPIs.

AUTHOR CONTRIBUTIONS

SK, AJ, and MR contributed to the conception and design of the study. All authors contributed to the study data collection and data analysis, wrote the first draft of the manuscript, commented on previous versions of the manuscript, and read and approved the final manuscript.

ACKNOWLEDGMENTS

The authors wish to thank Shahid Rajaee Teacher Training University for supporting the conduct of this research.

REFERENCES

Abes, R., Arzumanov, A. A., Moulton, H. M., Abes, S., Ivanova, G. D., Iversen, P. L., et al. (2007). Cell-penetrating-peptide-based delivery of oligonucleotides: an overview. *Biochem. Soc. Trans.* 35(Pt 4), 775–779. doi: 10.1042/bst0350775

Agrawal, P., Bhagat, D., Mahalwal, M., Sharma, N., and Raghava, G. P. S. (2020). AntiCP 2.0: an updated model for predicting anticancer peptides. *bioRxiv [Preprint]* doi: 10.1101/2020.03.23.003780

Agrawal, P., Bhalla, S., Chaudhary, K., Kumar, R., Sharma, M., and Raghava, G. P. (2018). In silico approach for prediction of antifungal peptides. *Front. Microbiol.* 9:323. doi: 10.3389/fmicb.2018.00323

Agrawal, P., Bhalla, S., Usmani, S. S., Singh, S., Chaudhary, K., Raghava, G. P., et al. (2016). CPPsite 2.0: a repository of experimentally validated cell-penetrating peptides. *Nucleic Acids Res.* 44, D1098–D1103.

Aguilera-Mendoza, L., Marrero-Ponce, Y., Beltran, J. A., Tellez Ibarra, R., Guillen-Ramirez, H. A., and Brizuela, C. A. (2019). Graph-based data integration from bioactive peptide databases of pharmaceutical interest: toward an organized collection enabling visual network analysis. *Bioinformatics* 35, 4739–4747. doi: 10.1093/bioinformatics/btz260

Alam, N., Goldstein, O., Xia, B., Porter, K. A., Kozakov, D., and Schueler-Furman, O. (2017). High-resolution global peptide-protein docking using fragments-based PIPER-FlexPepDock. *PLoS Comput. Biol.* 13:e1005905. doi: 10.1371/journal.pcbi.1005905

Antosova, Z., Mackova, M., Kral, V., and Macek, T. (2009). Therapeutic application of peptides and proteins: parenteral forever? *Trends Biotechnol.* 27, 628–635. doi: 10.1016/j.tibtech.2009.07.009

Antunes, D. A., Moll, M., Devaurs, D., Jackson, K. R., Lizée, G., and Kavraki, L. E. (2017). DINC 2.0: a new protein–peptide docking webserver using an incremental approach. *Cancer Res.* 77, e55–e57.

Arkin, M. R., and Wells, J. A. (2004). Small-molecule inhibitors of protein–protein interactions: progressing towards the dream. *Nat. Rev. Drug Discov.* 3, 301–317. doi: 10.1038/nrd1343

Assi, S. A., Tanaka, T., Rabbitts, T. H., and Fernandez-Fuentes, N. (2010). PCRPi: presaging critical residues in protein interfaces, a new computational tool to chart hotspots in protein interfaces. *Nucleic Acids Res.* 38:e86. doi: 10.1093/nar/gkp1158

Bakail, M., and Ochsenbein, F. (2016). Targeting protein–protein interactions, a wide open field for drug design. *C. R. Chim.* 19, 19–27. doi: 10.1016/j.crci.2015.12.004

Beaufays, J., Lins, L., Thomas, A., and Brasseur, R. (2012). In silico predictions of 3D structures of linear and cyclic peptides with natural and non-proteinogenic residues. *J. Pept. Sci.* 18, 17–24. doi: 10.1002/psc.1410

Beerten, J., Van Durme, J., Gallardo, R., Capriotti, E., Serpell, L., Rousseau, F., et al. (2015). WALTZ-DB: a benchmark database of amyloidogenic hexapeptides. *Bioinformatics* 31, 1698–1700. doi: 10.1093/bioinformatics/btv027

Ben-Shimon, A., and Niv, M. Y. (2015). AnchorDock: blind and flexible anchor-driven peptide docking. *Structure* 23, 929–940. doi: 10.1016/j.str.2015.03.010

Blazer, L. L., and Neubig, R. R. (2009). Small molecule protein–protein interaction inhibitors as CNS therapeutic agents: current progress and future hurdles. *Neuropsychopharmacology* 34, 126–141. doi: 10.1038/npp.2008.151

Bogan, A. A., and Thorn, K. S. (1998). Anatomy of hotspots in protein interfaces. *J. Mol. Biol.* 280, 1–9. doi: 10.1006/jmbi.1998.1843

Bowie, J. U., Luthy, R., and Eisenberg, D. (1991). A method to identify protein sequences that fold into a known three-dimensional structure. *Science* 253, 164–170. doi: 10.1126/science.1853201

Bradley, P., Misura, K. M., and Baker, D. (2005). Toward high-resolution de novo structure prediction for small proteins. *Science* 309, 1868–1871. doi: 10.1126/science.1113801

Brenke, R., Kozakov, D., Chuang, G.-Y., Beglov, D., Hall, D., Landon, M. R., et al. (2009). Fragment-based identification of druggable 'hotspots' of proteins using Fourier domain correlation techniques. *Bioinformatics* 25, 621–627. doi: 10.1093/bioinformatics/btp036

Bruzzoni-Giovanelli, H., Alezra, V., Wolff, N., Dong, C.-Z., Tuffery, P., and Rebollo, A. (2018). Interfering peptides targeting protein–protein interactions: the next generation of drugs? *Drug Discov. Today* 23, 272–285. doi: 10.1016/j.drudis.2017.10.016

Burbach, J. P. H. (2010). Neuropeptides from concept to online database www.neuropeptides. nl. *Eur. J. Pharmacol.* 626, 27–48. doi: 10.1016/j.ejphar.2009.10.015

Bystroff, C., and Shao, Y. (2002). Fully automated ab initio protein structure prediction using I-SITES, HMMSTR and ROSETTA. *Bioinformatics* 18(Suppl._1), S54–S61.

Bystroff, C., Thorsson, V., and Baker, D. (2000). HMMSTR: a hidden Markov model for local sequence-structure correlations in proteins. *J. Mol. Biol.* 301, 173–190. doi: 10.1006/jmbi.2000.3837

Caffrey, D. R., Somaroo, S., Hughes, J. D., Mintseris, J., and Huang, E. S. (2004). Are protein–protein interfaces more conserved in sequence than the rest of the protein surface? *Protein Sci.* 13, 190–202. doi: 10.1110/ps.03323604

Casals, F., Idaghdour, Y., Hussin, J., and Awadalla, P. (2012). Next-generation sequencing approaches for genetic mapping of complex diseases. *J. Neuroimmunol.* 248, 10–22. doi: 10.1016/j.jneuroim.2011.12.017

Chen, H., and Zhou, H. X. (2005). Prediction of interface residues in protein–protein complexes by a consensus neural network method: test against NMR data. *Proteins* 61, 21–35. doi: 10.1002/prot.20514

Chen, W., Ding, H., Feng, P., Lin, H., and Chou, K.-C. (2016). iACP: a sequence-based tool for identifying anticancer peptides. *Oncotarget* 7:16895. doi: 10.18632/oncotarget.7815

Chen, X.-W., and Liu, M. (2005). Prediction of protein–protein interactions using random decision forest framework. *Bioinformatics* 21, 4394–4400. doi: 10.1093/bioinformatics/bti721

Cho, K.-I., Kim, D., and Lee, D. (2009). A feature-based approach to modeling protein–protein interaction hotspots. *Nucleic Acids Res.* 37, 2672–2687. doi: 10.1093/nar/gkp132

Chong, L. T., Saglam, A. S., and Zuckerman, D. M. (2017). Path-sampling strategies for simulating rare events in biomolecular systems. *Curr. Opin. Struct. Biol.* 43, 88–94. doi: 10.1016/j.sbi.2016.11.019

Ciemny, M., Kurcinski, M., Kamel, K., Kolinski, A., Alam, N., Schueler-Furman, O., et al. (2018). Protein–peptide docking: opportunities and challenges. *Drug Discov. Today* 23, 1530–1537. doi: 10.1016/j.drudis.2018.05.006

Clackson, T., Ultsch, M. H., Wells, J. A., and de Vos, A. M. (1998). Structural and functional analysis of the 1: 1 growth hormone: receptor complex reveals the molecular basis for receptor affinity. *J. Mol. Biol.* 277, 1111–1128. doi: 10.1006/jmbi.1998.1669

Clackson, T., and Wells, J. A. (1995). A hotspot of binding energy in a hormone-receptor interface. *Science* 267, 383–386. doi: 10.1126/science.7529940

Cunningham, A. D., Qvit, N., and Mochly-Rosen, D. (2017). Peptides and peptidomimetics as regulators of protein–protein interactions. *Curr. Opin. Struct. Biol.* 44, 59–66. doi: 10.1016/j.sbi.2016.12.009

Cunningham, B. C., and Wells, J. A. (1989). High-resolution epitope mapping of hGH-receptor interactions by alanine-scanning mutagenesis. *Science* 244, 1081–1085. doi: 10.1126/science.2471267

Das, D., Jaiswal, M., Khan, F. N., Ahamad, S., and Kumar, S. (2020). PlantPepDB: a manually curated plant peptide database. *Sci. Rep.* 10:2194.

de Beer, S. B. A. (2012). *Application of Free Energy Calculations for Drug Design*. De Boelelaan: Vrije Universiteit Amsterdem.

de Ruiter, A., and Oostenbrink, C. (2011). Free energy calculations of protein–ligand interactions. *Curr. Opin. Chem. Biol.* 15, 547–552. doi: 10.1016/j.cbpa.2011.05.021

de Vries, S. J., and Bonvin, A. M. (2008). How proteins get in touch: interface prediction in the study of biomolecular complexes. *Curr. Protein Pept. Sci.* 9, 394–406. doi: 10.2174/138920308785132712

de Vries, S. J., and Bonvin, A. M. (2011). CPORT: a consensus interface predictor and its performance in prediction-driven docking with HADDOCK. *PLoS One* 6:e17695. doi: 10.1371/journal.pone.0017695

de Vries, S. J., Rey, J., Schindler, C. E., Zacharias, M., and Tuffery, P. (2017). The pepATTRACT web server for blind, large-scale peptide–protein docking. *Nucleic Acids Res.* 45, W361–W364.

de Vries, S. J., van Dijk, A. D., and Bonvin, A. M. (2006). WHISCY: what information does surface conservation yield? Application to data-driven docking. *Proteins* 63, 479–489. doi: 10.1002/prot.20842

DeLano, W. L. (2002). Unraveling hotspots in binding interfaces: progress and challenges. *Curr. Opin. Struct. Biol.* 12, 14–20. doi: 10.1016/s0959-440x(02)00283-x

DeLano, W. L., Ultsch, M. H., and Wells, J. A. (2000). Convergent solutions to binding at a protein-protein interface. *Science* 287, 1279–1283. doi: 10.1126/science.287.5456.1279

Di Luca, M., Maccari, G., Maisetta, G., and Batoni, G. (2015). BaAMPs: the database of biofilm-active antimicrobial peptides. *Biofouling* 31, 193–199. doi: 10.1080/08927014.2015.1021340

Diller, D. J., Swanson, J., Bayden, A. S., Jarosinski, M., and Audie, J. (2015). Rational, computer-enabled peptide drug design: principles, methods, applications and future directions. *Future Med. Chem.* 7, 2173–2193. doi: 10.4155/fmc.15.142

Dong, M., Lam, P. C.-H., Pinon, D. I., Hosohata, K., Orry, A., Sexton, P. M., et al. (2011). Molecular basis of secretin docking to its intact receptor using multiple photolabile probes distributed throughout the pharmacophore. *J. Biol. Chem.* 286, 23888–23899. doi: 10.1074/jbc.m111.245969

Donsky, E., and Wolfson, H. J. (2011). PepCrawler: a fast RRT-based algorithm for high-resolution refinement and binding affinity estimation of peptide inhibitors. *Bioinformatics* 27, 2836–2842. doi: 10.1093/bioinformatics/btr498

Duarte, J. M., Srebniak, A., Schärer, M. A., and Capitani, G. (2012). Protein interface classification by evolutionary analysis. *BMC Bioinformatics* 13:334. doi: 10.1186/1471-2105-13-334

Ellert-Miklaszewska, A., Poleszak, K., and Kaminska, B. (2017). Short peptides interfering with signaling pathways as new therapeutic tools for cancer treatment. *Future Med Chem.* 9, 199–221. doi: 10.4155/fmc-2016-0189

Esmaielbeiki, R., Krawczyk, K., Knapp, B., Nebel, J.-C., and Deane, C. M. (2016). Progress and challenges in predicting protein interfaces. *Brief. Bioinform.* 17, 117–131. doi: 10.1093/bib/bbv027

Esmaielbeiki, R., and Nebel, J.-C. (2014). Scoring docking conformations using predicted protein interfaces. *BMC Bioinformatics* 15:171.

Etchebest, C., Benros, C., Hazout, S., and de Brevern, A. G. (2005). A structural alphabet for local protein structures: improved prediction methods. *Proteins* 59, 810–827. doi: 10.1002/prot.20458

Fischer, D., Elofsson, A., Rychlewski, L., Pazos, F., Valencia, A., Rost, B., et al. (2001). CAFASP2: the second critical assessment of fully automated structure prediction methods. *Proteins* 45, 171–183. doi: 10.1002/prot.10036

Fischer, T., Arunachalam, K., Bailey, D., Mangual, V., Bakhru, S., Russo, R., et al. (2003). The binding interface database (BID): a compilation of amino acid hotspots in protein interfaces. *Bioinformatics* 19, 1453–1454. doi: 10.1093/bioinformatics/btg163

Flissi, A., Ricart, E., Campart, C., Chevalier, M., Dufresne, Y., Michalik, J., et al. (2020). Norine: update of the nonribosomal peptide resource. *Nucleic Acids Res.* 48, D465–D469.

Fosgerau, K., and Hoffmann, T. (2015). Peptide therapeutics: current status and future directions. *Drug Discov. Today* 20, 122–128. doi: 10.1016/j.drudis.2014.10.003

Gao, Y., Wang, R., and Lai, L. (2004). Structure-based method for analyzing protein–protein interfaces. *J. Mol. Model.* 10, 44–54. doi: 10.1007/s00894-003-0168-3

Gautam, A., Chaudhary, K., Kumar, R., Sharma, A., Kapoor, P., Tyagi, A., et al. (2013). In silico approaches for designing highly effective cell penetrating peptides. *J. Transl. Med.* 11:74. doi: 10.1186/1479-5876-11-74

Gautam, A., Chaudhary, K., Singh, S., Joshi, A., Anand, P., Tuknait, A., et al. (2014). Hemolytik: a database of experimentally determined hemolytic and non-hemolytic peptides. *Nucleic Acids Res.* 42, D444–D449.

Gautam, A., Singh, H., Tyagi, A., Chaudhary, K., Kumar, R., Kapoor, P., et al. (2012). CPPsite: a curated database of cell penetrating peptides. *Database* 2012:bas015. doi: 10.1093/database/bas015

Gesell, J., Zasloff, M., and Opella, S. J. (1997). Two-dimensional 1H NMR experiments show that the 23-residue magainin antibiotic peptide is an α-helix in dodecylphosphocholine micelles, sodium dodecylsulfate micelles, and trifluoroethanol/water solution. *J. Biomol. NMR* 9, 127–135.

Gogoladze, G., Grigolava, M., Vishnepolsky, B., Chubinidze, M., Duroux, P., Lefranc, M.-P., et al. (2014). DBAASP: database of antimicrobial activity and structure of peptides. *FEMS Microbiol. Lett.* 357, 63–68. doi: 10.1111/1574-6968.12489

Gómez, E. A., Giraldo, P., and Orduz, S. (2017). InverPep: a database of invertebrate antimicrobial peptides. *J. Glob. Antimicrob. Resist.* 8, 13–17. doi: 10.1016/j.jgar.2016.10.003

Grishin, N. V., and Phillips, M. A. (1994). The subunit interfaces of oligomeric enzymes are conserved to a similar extent to the overall protein sequences. *Protein Sci.* 3, 2455–2458. doi: 10.1002/pro.5560031231

Grosdidier, S., and Fernández-Recio, J. (2008). Identification of hot-spot residues in protein-protein interactions by computational docking. *BMC Bioinformatics* 9:447. doi: 10.1186/1471-2105-9-447

Guerois, R., Nielsen, J. E., and Serrano, L. (2002). Predicting changes in the stability of proteins and protein complexes: a study of more than 1000 mutations. *J. Mol. Biol.* 320, 369–387. doi: 10.1016/S0022-2836(02)00442-4

Guharoy, M., and Chakrabarti, P. (2009). Empirical estimation of the energetic contribution of individual interface residues in structures of protein–protein complexes. *J. Comput. Aided Mol. Des.* 23, 645–654. doi: 10.1007/s10822-009-9282-3

Guidotti, G., Brambilla, L., and Rossi, D. (2017). Cell-penetrating peptides: from basic research to clinics. *Trends Pharmacol. Sci.* 38, 406–424. doi: 10.1016/j.tips.2017.01.003

Gupta, S., Kapoor, P., Chaudhary, K., Gautam, A., Kumar, R., Raghava, G. P., et al. (2013). In silico approach for predicting toxicity of peptides and proteins. *PLoS One* 8:e73957. doi: 10.1371/journal.pone.0073957

Gupta, S., Madhu, M. K., Sharma, A. K., and Sharma, V. K. (2016). ProInflam: a webserver for the prediction of proinflammatory antigenicity of peptides and proteins. *J. Transl. Med.* 14, 1–10.

Halabi, N., Rivoire, O., Leibler, S., and Ranganathan, R. (2009). Protein sectors: evolutionary units of three-dimensional structure. *Cell* 138, 774–786. doi: 10.1016/j.cell.2009.07.038

Hall, R., Dixon, T., and Dickson, A. (2020). On calculating free energy differences using ensembles of transition paths. *Front. Mol. Biosci.* 7:106. doi: 10.3389/fmolb.2020.00106

Hamer, R., Luo, Q., Armitage, J. P., Reinert, G., and Deane, C. M. (2010). i-Patch: interprotein contact prediction using local network information. *Proteins* 78, 2781–2797. doi: 10.1002/prot.22792

Hammami, R., Ben Hamida, J., Vergoten, G., and Fliss, I. (2009). PhytAMP: a database dedicated to antimicrobial plant peptides. *Nucleic Acids Res.* 37(Suppl._1), D963–D968.

Hammami, R., Zouhir, A., Le Lay, C., Hamida, J. B., and Fliss, I. (2010). BACTIBASE second release: a database and tool platform for bacteriocin characterization. *BMC Microbiol.* 10:22. doi: 10.1186/1471-2180-10-22

Hasan, M. M., Schaduangrat, N., Basith, S., Lee, G., Shoombuatong, W., and Manavalan, B. (2020). HLPpred-Fuse: improved and robust prediction of hemolytic peptide and its activity by fusing multiple feature representation. *Bioinformatics* 36, 3350–3356. doi: 10.1093/bioinformatics/btaa160

Heinig, M., and Frishman, D. (2004). STRIDE: a web server for secondary structure assignment from known atomic coordinates of proteins. *Nucleic Acids Res.* 32(Suppl._2), W500–W502.

Higa, R. H., and Tozzi, C. L. (2009). Prediction of binding hotspot residues by using structural and evolutionary parameters. *Genet. Mol. Biol.* 32, 626–633. doi: 10.1590/s1415-47572009000300029

Holton, T. A., Pollastri, G., Shields, D. C., and Mooney, C. (2013). CPPpred: prediction of cell penetrating peptides. *Bioinformatics* 29, 3094–3096. doi: 10.1093/bioinformatics/btt518

Hoofnagle, A. N., Resing, K. A., and Ahn, N. G. (2003). Protein analysis by hydrogen exchange mass spectrometry. *Annu. Rev. Biophys. Biomol. Struct.* 32, 1–25.

Hu, Z., Ma, B., Wolfson, H., and Nussinov, R. (2000). Conservation of polar residues as hotspots at protein interfaces. *Proteins* 39, 331–342. doi: 10.1002/(sici)1097-0134(20000601)39:4<331::aid-prot60>3.0.co;2-a

Hung, L.-H., Ngan, S.-C., Liu, T., and Samudrala, R. (2005). PROTINFO: new algorithms for enhanced protein structure predictions. *Nucleic Acids Res.* 33(Suppl._2), W77–W80.

Iwaniak, A., Minkiewicz, P., Darewicz, M., Sieniawski, K., and Starowicz, P. (2016). BIOPEP database of sensory peptides and amino acids. *Food Res. Int.* 85, 155–161. doi: 10.1016/j.foodres.2016.04.031

Jain, A. N. (2003). Surflex: fully automatic flexible molecular docking using a molecular similarity-based search engine. *J. Med. Chem.* 46, 499–511. doi: 10.1021/jm020406h

Janin, J., Henrick, K., Moult, J., Eyck, L. T., Sternberg, M. J., Vajda, S., et al. (2003). CAPRI: a critical assessment of predicted interactions. *Proteins* 52, 2–9. doi: 10.1002/prot.10381

Jhong, J.-H., Chi, Y.-H., Li, W.-C., Lin, T.-H., Huang, K.-Y., and Lee, T.-Y. (2019). dbAMP: an integrated resource for exploring antimicrobial peptides with functional activities and physicochemical properties on transcriptome and proteome data. *Nucleic Acids Res.* 47, D285–D297.

Jones, D. T., Taylort, W., and Thornton, J. M. (1992). A new approach to protein fold recognition. *Nature* 358, 86–89. doi: 10.1038/358086a0

Jordan, R. A., El-Manzalawy, Y., Dobbs, D., and Honavar, V. (2012). Predicting protein-protein interface residues using local surface structural similarity. *BMC Bioinformatics* 13:41. doi: 10.1186/1471-2105-13-41

Joseph, S., Karnik, S., Nilawe, P., Jayaraman, V. K., and Idicula-Thomas, S. (2012). ClassAMP: a prediction tool for classification of antimicrobial peptides. *IEEE/ACM Trans. Comput. Biol. Bioinform.* 9, 1535–1538. doi: 10.1109/tcbb.2012.89

Jouaux, E. M., Schmidtkunz, K., Müller, K. M., and Arndt, K. M. (2008). Targeting the c-Myc coiled coil with interfering peptides. *J. Pept. Sci.* 14, 1022–1031. doi: 10.1002/psc.1038

Kaas, Q., Yu, R., Jin, A.-H., Dutertre, S., and Craik, D. J. (2012). ConoServer: updated content, knowledge, and discovery tools in the conopeptide database. *Nucleic Acids Res.* 40, D325–D330.

Kanakaveti, V., Shanmugam, A., Ramakrishnan, C., Anoosha, P., Sakthivel, R., Rayala, S. K., et al. (2020). "Chapter Two - Computational approaches for identifying potential inhibitors on targeting protein interactions in drug discovery. *Adv. Protein Chem. Struct. Biol.* 121, 25–47. doi: 10.1016/bs.apcsb.2019.11.013

Kapoor, P., Singh, H., Gautam, A., Chaudhary, K., Kumar, R., and Raghava, G. P. (2012). TumorHoPe: a database of tumor homing peptides. *PLoS One* 7:e35187. doi: 10.1371/journal.pone.0035187

Kaserer, T., Beck, K. R., Akram, M., Odermatt, A., and Schuster, D. (2015). Pharmacophore models and pharmacophore-based virtual screening: concepts and applications exemplified on hydroxysteroid dehydrogenases. *Molecules* 20, 22799–22832. doi: 10.3390/molecules201219880

Kaspar, A. A., and Reichert, J. M. (2013). Future directions for peptide therapeutics development. *Drug Discov. Today* 18, 807–817. doi: 10.1016/j.drudis.2013.05.011

Kaur, H., Garg, A., and Raghava, G. P. S. (2007). PEPstr: a de novo method for tertiary structure prediction of small bioactive peptides. *Protein Pept. Lett.* 14, 626–631. doi: 10.2174/092986607781483859

Kenneth Morrow, J., and Zhang, S. (2012). Computational prediction of protein hotspot residues. *Curr. Pharm. Des.* 18, 1255–1265. doi: 10.2174/138161212799436412

Keskin, O., Ma, B., and Nussinov, R. (2005). Hot regions in protein–protein interactions: the organization and contribution of structurally conserved hotspot residues. *J. Mol. Biol.* 345, 1281–1294. doi: 10.1016/j.jmb.2004.10.077

Khalili, S., Rasaee, M. J., Mousavi, S. L., Amani, J., Jahangiri, A., and Borna, H. (2017). In silico prediction and in vitro verification of a novel multi-epitope antigen for HBV detection. *Mol. Genet. Microbiol. Virol.* 32, 230–240. doi: 10.3103/s0891416817040097

Khodashenas, S., Khalili, S., and Moghadam, M. F. (2019). A cell ELISA based method for exosome detection in diagnostic and therapeutic applications. *Biotechnol. Lett.* 41, 523–531. doi: 10.1007/s10529-019-02667-5

Kim, D. E., Chivian, D., and Baker, D. (2004). Protein structure prediction and analysis using the Robetta server. *Nucleic Acids Res.* 32(Suppl._2), W526–W531.

Kim, Y., Bark, S., Hook, V., and Bandeira, N. (2011). NeuroPedia: neuropeptide database and spectral library. *Bioinformatics* 27, 2772–2773. doi: 10.1093/bioinformatics/btr445

Kitchen, D. B., Decornez, H., Furr, J. R., and Bajorath, J. (2004). Docking and scoring in virtual screening for drug discovery: methods and applications. *Nat. Rev. Drug Discov.* 3, 935–949. doi: 10.1038/nrd1549

Kittichotirat, W., Guerquin, M., Bumgarner, R. E., and Samudrala, R. (2009). Protinfo PPC: a web server for atomic level prediction of protein complexes. *Nucleic Acids Res.* 37(Suppl._2), W519–W525.

Koboldt, D. C., Steinberg, K. M., Larson, D. E., Wilson, R. K., and Mardis, E. R. (2013). The next-generation sequencing revolution and its impact on genomics. *Cell* 155, 27–38. doi: 10.1016/j.cell.2013.09.006

Kortemme, T., Kim, D. E., and Baker, D. (2004). Computational alanine scanning of protein-protein interfaces. *Sci. STKE* 2004:l2.

Kouadio, J.-L. K., Horn, J. R., Pal, G., and Kossiakoff, A. A. (2005). Shotgun alanine scanning shows that growth hormone can bind productively to its receptor through a drastically minimized interface. *J. Biol. Chem.* 280, 25524–25532. doi: 10.1074/jbc.m502167200

Kozakov, D., Brenke, R., Comeau, S. R., and Vajda, S. (2006). PIPER: an FFT-based protein docking program with pairwise potentials. *Proteins* 65, 392–406. doi: 10.1002/prot.21117

Kozlowski, L. P., and Bujnicki, J. M. (2012). MetaDisorder: a meta-server for the prediction of intrinsic disorder in proteins. *BMC Bioinformatics* 13:111.

Kufareva, I., Budagyan, L., Raush, E., Totrov, M., and Abagyan, R. (2007). PIER: protein interface recognition for structural proteomics. *Proteins* 67, 400–417. doi: 10.1002/prot.21233

Kundrotas, P. J., Zhu, Z., Janin, J., and Vakser, I. A. (2012). Templates are available to model nearly all complexes of structurally characterized proteins. *Proc. Natl. Acad. Sci. U.S.A.* 109, 9438–9441. doi: 10.1073/pnas.1200678109

Kurcinski, M., Jamroz, M., Blaszczyk, M., Kolinski, A., and Kmiecik, S. (2015). CABS-dock web server for the flexible docking of peptides to proteins without prior knowledge of the binding site. *Nucleic Acids Res.* 43, W419–W424.

Laengsri, V., Nantasenamat, C., Schaduangrat, N., Nuchnoi, P., Prachayasittikul, V., and Shoombuatong, W. (2019). TargetAntiAngio: a sequence-based tool for the prediction and analysis of anti-angiogenic peptides. *Int. J. Mol. Sci.* 20, 2950. doi: 10.3390/ijms20122950

Lamiable, A., Thévenet, P., Rey, J., Vavrusa, M., Derreumaux, P., and Tufféry, P. (2016). PEP-FOLD3: faster de novo structure prediction for linear peptides in solution and in complex. *Nucleic Acids Res.* 44, W449–W454.

Lata, S., Mishra, N. K., and Raghava, G. P. (2010). AntiBP2: improved version of antibacterial peptide prediction. *BMC Bioinformatics* 11:S19.

Lavecchia, A., and Di Giovanni, C. (2013). Virtual screening strategies in drug discovery: a critical review. *Curr. Med. Chem.* 20, 2839–2860. doi: 10.2174/09298673113209990001

Lee, A. C.-L., Harris, J. L., Khanna, K. K., and Hong, J.-H. (2019). A comprehensive review on current advances in peptide drug development and design. *Int. J. Mol. Sci.* 20:2383. doi: 10.3390/ijms20102383

Lee, H., Heo, L., Lee, M. S., and Seok, C. (2015). GalaxyPepDock: a protein–peptide docking tool based on interaction similarity and energy optimization. *Nucleic Acids Res.* 43, W431–W435.

Lensink, M. F., Velankar, S., and Wodak, S. J. (2017). Modeling protein–protein and protein–peptide complexes: CAPRI 6th edition. *Proteins* 85, 359–377. doi: 10.1002/prot.25215

Li, R., Dowd, V., Stewart, D. J., Burton, S. J., and Lowe, C. R. (1998). Design, synthesis, and application of a protein A mimetic. *Nat. Biotechnol.* 16, 190–195. doi: 10.1038/nbt0298-190

Liang, S., Zhang, C., Liu, S., and Zhou, Y. (2006). Protein binding site prediction using an empirical scoring function. *Nucleic Acids Res.* 34, 3698–3707. doi: 10.1093/nar/gkl454

Lichtarge, O., Bourne, H. R., and Cohen, F. E. (1996). An evolutionary trace method defines binding surfaces common to protein families. *J. Mol. Biol.* 257, 342–358. doi: 10.1006/jmbi.1996.0167

Lise, S., Archambeau, C., Pontil, M., and Jones, D. T. (2009). Prediction of hotspot residues at protein-protein interfaces by combining machine learning and energy-based methods. *BMC Bioinformatics* 10:365. doi: 10.1186/1471-2105-10-365

Lise, S., Buchan, D., Pontil, M., and Jones, D. T. (2011). Predictions of hotspot residues at protein-protein interfaces using support vector machines. *PLoS One* 6:e16774. doi: 10.1371/journal.pone.0016774

Liu, F., Baggerman, G., Schoofs, L., and Wets, G. (2008). The construction of a bioactive peptide database in Metazoa. *J. Proteome Res.* 7, 4119–4131. doi: 10.1021/pr800037n

Livnah, O., Stura, E. A., Johnson, D. L., Middleton, S. A., Mulcahy, L. S., Wrighton, N. C., et al. (1996). Functional mimicry of a protein hormone by a peptide agonist: the EPO receptor complex at 2.8 Å. *Science* 273, 464–471. doi: 10.1126/science.273.5274.464

London, N., Raveh, B., Cohen, E., Fathi, G., and Schueler-Furman, O. (2011). Rosetta FlexPepDock web server—high resolution modeling of peptide–protein interactions. *Nucleic Acids Res.* 39(Suppl._2), W249–W253.

London, N., Raveh, B., and Schueler-Furman, O. (2013). Druggable protein–protein interactions–from hotspots to hot segments. *Curr. Opin. Chem. Biol.* 17, 952–959. doi: 10.1016/j.cbpa.2013.10.011

Louros, N., Konstantoulea, K., De Vleeschouwer, M., Ramakers, M., Schymkowitz, J., and Rousseau, F. (2020). WALTZ-DB 2.0: an updated database containing structural information of experimentally determined amyloid-forming peptides. *Nucleic Acids Res.* 48, D389–D393.

Lu, H., Zhou, Q., He, J., Jiang, Z., Peng, C., Tong, R., et al. (2020). Recent advances in the development of protein–protein interactions modulators: mechanisms and clinical trials. *Signal Transduct. Target. Ther.* 5, 1–23.

Luiz Folador, E., Fernandes de Oliveira Junior, A., Tiwari, S., Babar Jamal, S., Salgado Ferreira, R., Barh, D., et al. (2015). In silico protein-protein interactions: avoiding data and method biases over sensitivity and specificity. *Curr. Protein Pept. Sci.* 16, 689–700. doi: 10.2174/1389203716666150505235437

Manavalan, B., Basith, S., Shin, T. H., Choi, S., Kim, M. O., and Lee, G. (2017). MLACP: machine-learning-based prediction of anticancer peptides. *Oncotarget* 8:77121. doi: 10.18632/oncotarget.20365

Manavalan, B., Basith, S., Shin, T. H., Wei, L., and Lee, G. (2019a). AtbPpred: a robust sequence-based prediction of anti-tubercular peptides using extremely randomized trees. *Comput. Struct. Biotechnol. J.* 17, 972–981. doi: 10.1016/j.csbj.2019.06.024

Manavalan, B., Basith, S., Shin, T. H., Wei, L., and Lee, G. (2019b). mAHTPred: a sequence-based meta-predictor for improving the prediction of anti-hypertensive peptides using effective feature representation. *Bioinformatics* 35, 2757–2765. doi: 10.1093/bioinformatics/bty1047

Marcu, O., Dodson, E. J., Alam, N., Sperber, M., Kozakov, D., Lensink, M. F., et al. (2017). FlexPepDock lessons from CAPRI peptide–protein rounds and suggested new criteria for assessment of model quality and utility. *Proteins* 85, 445–462. doi: 10.1002/prot.25230

Mard-Soltani, M., Rasaee, M. J., Khalili, S., Sheikhi, A.-K., Hedayati, M., Ghaderi-Zefrehi, H., et al. (2018). The effect of differentially designed fusion proteins to elicit efficient anti-human thyroid stimulating hormone immune responses. *Iran. J. Allergy Asthma Immunol.* 17, 158–170.

Maupetit, J., Derreumaux, P., and Tuffery, P. (2009). PEP-FOLD: an online resource for de novo peptide structure prediction. *Nucleic Acids Res.* 37(Suppl._2), W498–W503.

Maupetit, J., Derreumaux, P., and Tufféry, P. (2010). A fast method for large-scale De Novo peptide and miniprotein structure prediction. *J. Comput. Chem.* 31, 726–738.

Meher, P. K., Sahu, T. K., Saini, V., and Rao, A. R. (2017). Predicting antimicrobial peptides with improved accuracy by incorporating the compositional, physico-chemical and structural features into Chou's general PseAAC. *Sci. Rep.* 7: 42362.

Mehta, D., Anand, P., Kumar, V., Joshi, A., Mathur, D., Singh, S., et al. (2014). ParaPep: a web resource for experimentally validated antiparasitic peptide sequences and their structures. *Database* 2014:bau051. doi: 10.1093/database/bau051

Mine, Y., Munir, H., Nakanishi, Y., and Sugiyama, D. (2016). Biomimetic peptides for the treatment of cancer. *Anticancer. Res.* 36, 3565–3570.

Minkiewicz, P., Dziuba, J., Iwaniak, A., Dziuba, M., and Darewicz, M. (2008). BIOPEP database and other programs for processing bioactive peptide sequences. *J. AOAC Int.* 91, 965–980. doi: 10.1093/jaoac/91.4.965

Minkiewicz, P., Iwaniak, A., and Darewicz, M. (2019). BIOPEP-UWM database of bioactive peptides: current opportunities. *Int. J. Mol. Sci.* 20:5978. doi: 10.3390/ijms20235978

Monge, A., Friesner, R. A., and Honig, B. (1994). An algorithm to generate low-resolution protein tertiary structures from knowledge of secondary structure. *Proc. Natl. Acad. Sci. U.S.A.* 91, 5027–5029. doi: 10.1073/pnas.91.11.5027

Mooney, C., Haslam, N. J., Pollastri, G., and Shields, D. C. (2012). Towards the improved discovery and design of functional peptides: common features of diverse classes permit generalized prediction of bioactivity. *PLoS One* 7:e45012. doi: 10.1371/journal.pone.0045012

Mora, J. S., Assi, S. A., and Fernandez-Fuentes, N. (2010). Presaging critical residues in protein interfaces-web server (PCRPi-W): a web server to chart hotspots in protein interfaces. *PLoS One* 5:e12352. doi: 10.1371/journal.pone.0012352

Moreira, I. S., Fernandes, P. A., and Ramos, M. J. (2007). hotspots—a review of the protein–protein interface determinant amino-acid residues. *Proteins* 68, 803–812. doi: 10.1002/prot.21396

Morrison, K. L., and Weiss, G. A. (2001). Combinatorial alanine-scanning. *Curr. Opin. Chem. Biol.* 5, 302–307. doi: 10.1016/s1367-5931(00)00206-4

Murakami, Y., and Mizuguchi, K. (2010). Applying the Naïve Bayes classifier with kernel density estimation to the prediction of protein–protein interaction sites. *Bioinformatics* 26, 1841–1848. doi: 10.1093/bioinformatics/btq302

Murakami, Y., Tripathi, L. P., Prathipati, P., and Mizuguchi, K. (2017). Network analysis and in silico prediction of protein–protein interactions with applications in drug discovery. *Curr. Opin. Struct. Biol.* 44, 134–142. doi: 10.1016/j.sbi.2017.02.005

Neuvirth, H., Raz, R., and Schreiber, G. (2004). ProMate: a structure based prediction program to identify the location of protein–protein binding sites. *J. Mol. Biol.* 338, 181–199. doi: 10.1016/j.jmb.2004.02.040

Nevola, L., and Giralt, E. (2015). Modulating protein–protein interactions: the potential of peptides. *Chem. Commun.* 51, 3302–3315. doi: 10.1039/c4cc08565e

Nielsen, S. D., Beverly, R. L., Qu, Y., and Dallas, D. C. (2017). Milk bioactive peptide database: a comprehensive database of milk protein-derived bioactive peptides and novel visualization. *Food Chem.* 232, 673–682. doi: 10.1016/j.foodchem.2017.04.056

Novković, M., Simunić, J., Bojović, V., Tossi, A., and Juretić, D. (2012). DADP: the database of anuran defense peptides. *Bioinformatics* 28, 1406–1407. doi: 10.1093/bioinformatics/bts141

Obarska-Kosinska, A., Iacoangeli, A., Lepore, R., and Tramontano, A. (2016). PepComposer: computational design of peptides binding to a given protein surface. *Nucleic Acids Res.* 44, W522–W528.

Osmulski, P. A., Karpowicz, P., Jankowska, E., Bohmann, J., Pickering, A. M., and Gaczyńska, M. (2020). New peptide-based pharmacophore activates 20S proteasome. *Molecules* 25:1439. doi: 10.3390/molecules25061439

Pallara, C., Jiménez-García, B., Romero, M., Moal, I. H., and Fernández-Recio, J. (2017). pyDock scoring for the new modeling challenges in docking: protein–peptide, homo-multimers, and domain–domain interactions. *Proteins* 85, 487–496. doi: 10.1002/prot.25184

Pierce, B. G., Wiehe, K., Hwang, H., Kim, B.-H., Vreven, T., and Weng, Z. (2014). ZDOCK server: interactive docking prediction of protein–protein complexes and symmetric multimers. *Bioinformatics* 30, 1771–1773. doi: 10.1093/bioinformatics/btu097

Pineda, S. S., Chaumeil, P.-A., Kunert, A., Kaas, Q., Thang, M. W., Le, L., et al. (2018). ArachnoServer 3.0: an online resource for automated discovery, analysis and annotation of spider toxins. *Bioinformatics* 34, 1074–1076. doi: 10.1093/bioinformatics/btx661

Pinzi, L., and Rastelli, G. (2019). Molecular docking: shifting paradigms in drug discovery. *Int. J. Mol. Sci.* 20:4331. doi: 10.3390/ijms20184331

Pirtskhalava, M., Amstrong, A. A., Grigolava, M., Chubinidze, M., Alimbarashvili, E., Vishnepolsky, B., et al. (2021). DBAASP v3: database of antimicrobial/cytotoxic activity and structure of peptides as a resource for development of new therapeutics. *Nucleic Acids Res.* 49, D288–D297.

Pirtskhalava, M., Gabrielian, A., Cruz, P., Griggs, H. L., Squires, R. B., Hurt, D. E., et al. (2016). DBAASP v. 2: an enhanced database of structure and antimicrobial/cytotoxic activity of natural and synthetic peptides. *Nucleic Acids Res.* 44, D1104–D1112.

Pleasant-Jenkins, D., Reese, C., Chinnakkannu, P., Kasiganesan, H., Tourkina, E., Hoffman, S., et al. (2017). Reversal of maladaptive fibrosis and compromised ventricular function in the pressure overloaded heart by a caveolin-1 surrogate peptide. *Lab. Invest.* 97, 370–382. doi: 10.1038/labinvest.2016.153

Porollo, A., and Meller, J. (2007). Prediction-based fingerprints of protein–protein interactions. *Proteins* 66, 630–645. doi: 10.1002/prot.21248

Porter, K. A., Desta, I., Kozakov, D., and Vajda, S. (2019). What method to use for protein–protein docking? *Curr. Opin. Struct. Biol.* 55, 1–7. doi: 10.1016/j.sbi.2018.12.010

Porter, K. A., Xia, B., Beglov, D., Bohnuud, T., Alam, N., Schueler-Furman, O., et al. (2017). ClusPro PeptiDock: efficient global docking of peptide recognition motifs using FFT. *Bioinformatics* 33, 3299–3301. doi: 10.1093/bioinformatics/btx216

Qin, S., and Zhou, H.-X. (2007). meta-PPISP: a meta web server for protein-protein interaction site prediction. *Bioinformatics* 23, 3386–3387. doi: 10.1093/bioinformatics/btm434

Qureshi, A., Kaur, G., and Kumar, M. (2017). AVC pred: an integrated web server for prediction and design of antiviral compounds. *Chem. Biol. Drug Des.* 89, 74–83. doi: 10.1111/cbdd.12834

Qureshi, A., Thakur, N., and Kumar, M. (2013). HIPdb: a database of experimentally validated HIV inhibiting peptides. *PLoS One* 8:e54908. doi: 10.1371/journal.pone.0054908

Qureshi, A., Thakur, N., Tandon, H., and Kumar, M. (2014). AVPdb: a database of experimentally validated antiviral peptides targeting medically important viruses. *Nucleic Acids Res.* 42, D1147–D1153.

Rahbar, M. R., Zarei, M., Jahangiri, A., Khalili, S., Nezafat, N., Negahdaripour, M., et al. (2019). Trimeric autotransporter adhesins in *Acinetobacter baumannii*, coincidental evolution at work. *Infect. Genet. Evol.* 71, 116–127. doi: 10.1016/j.meegid.2019.03.023

Rajamani, D., Thiel, S., Vajda, S., and Camacho, C. J. (2004). Anchor residues in protein–protein interactions. *Proc. Natl. Acad. Sci. U.S.A.* 101, 11287–11292. doi: 10.1073/pnas.0401942101

Ramezani, A., Zakeri, A., Mard-Soltani, M., Mohammadian, A., Hashemi, Z. S., Mohammadpour, H., et al. (2019). Structure based screening for inhibitory therapeutics of CTLA-4 unveiled new insights about biology of ACTH. *Int. J. Pept. Res. Ther.* 26, 1–11.

Ramos-Martín, F., Annaval, T., Buchoux, S., Sarazin, C., and D'amelio, N. (2019). ADAPTABLE: a comprehensive web platform of antimicrobial peptides tailored to the user's research. *Life Sci. Alliance* 2:e201900512. doi: 10.26508/lsa.201900512

Raveh, B., London, N., and Schueler-Furman, O. (2010). Sub-angstrom modeling of complexes between flexible peptides and globular proteins. *Proteins* 78, 2029–2040. doi: 10.1002/prot.22716

Raveh, B., London, N., Zimmerman, L., and Schueler-Furman, O. (2011). Rosetta FlexPepDock ab-initio: simultaneous folding, docking and refinement of peptides onto their receptors. *PLoS One* 6:e18934. doi: 10.1371/journal.pone.0018934

Rentzsch, R., and Renard, B. Y. (2015). Docking small peptides remains a great challenge: an assessment using AutoDock Vina. *Brief. Bioinform.* 16, 1045–1056. doi: 10.1093/bib/bbv008

Rifai, E. A., van Dijk, M., and Geerke, D. P. (2020). Recent developments in linear interaction energy based binding free energy calculations. *Front. Mol. Biosci.* 7:114. doi: 10.3389/fmolb.2020.00114

Roy, A., Nair, S., Sen, N., Soni, N., and Madhusudhan, M. J. M. (2017). In silico methods for design of biological therapeutics. *Methods* 131, 33–65. doi: 10.1016/j.ymeth.2017.09.008

Sali, A. (1995). Comparative protein modeling by satisfaction of spatial restraints. *Mol. Med. Today* 1, 270–277. doi: 10.1016/s1357-4310(95)91170-7

Sanchez, R., and Šali, A. (1997). Advances in comparative protein-structure modelling. *Curr. Opin. Struct. Biol.* 7, 206–214. doi: 10.1016/s0959-440x(97)80027-9

Schaduangrat, N., Nantasenamat, C., Prachayasittikul, V., and Shoombuatong, W. (2019a). ACPred: a computational tool for the prediction and analysis of anticancer peptides. *Molecules* 24:1973. doi: 10.3390/molecules24101973

Schaduangrat, N., Nantasenamat, C., Prachayasittikul, V., and Shoombuatong, W. (2019b). Meta-iAVP: a sequence-based meta-predictor for improving the prediction of antiviral peptides using effective feature representation. *Int. J. Mol. Sci.* 20:5743. doi: 10.3390/ijms20225743

Schindler, C. E., de Vries, S. J., and Zacharias, M. (2015). Fully blind peptide-protein docking with pepATTRACT. *Structure* 23, 1507–1515. doi: 10.1016/j.str.2015.05.021

Schreiber, G., and Fersht, A. R. (1995). Energetics of protein-protein interactions: analysis ofthe Barnase-Barstar interface by single mutations and double mutant cycles. *J. Mol. Biol.* 248, 478–486. doi: 10.1016/s0022-2836(95)80064-6

Schymkowitz, J., Borg, J., Stricher, F., Nys, R., Rousseau, F., and Serrano, L. (2005). The FoldX web server: an online force field. *Nucleic Acids Res.* 33(Suppl._2), W382–W388.

Seebah, S., Suresh, A., Zhuo, S., Choong, Y. H., Chua, H., Chuon, D., et al. (2007). Defensins knowledgebase: a manually curated database and information source focused on the defensins family of antimicrobial peptides. *Nucleic Acids Res.* 35(Suppl._1), D265–D268.

Sharma, A., Singla, D., Rashid, M., and Raghava, G. P. S. (2014). Designing of peptides with desired half-life in intestine-like environment. *BMC Bioinformatics* 15:282. doi: 10.1186/1471-2105-15-282

Shi, X.-D., Sun, K., Hu, R., Liu, X.-Y., Hu, Q.-M., Sun, X.-Y., et al. (2016). Blocking the interaction between EphB2 and ADDLs by a small peptide rescues impaired synaptic plasticity and memory deficits in a mouse model of Alzheimer's disease. *J. Neurosci.* 36, 11959–11973. doi: 10.1523/jneurosci.1327-16.2016

Shoemaker, B. A., and Panchenko, A. R. (2007). Deciphering protein–protein interactions. Part I. Experimental techniques and databases. *PLoS Comput Biol.* 3:e42. doi: 10.1371/journal.pcbi.0030042

Shoemaker, B. A., Zhang, D., Thangudu, R. R., Tyagi, M., Fong, J. H., Marchler-Bauer, A., et al. (2010). Inferred Biomolecular Interaction Server—a web server to analyze and predict protein interacting partners and binding sites. *Nucleic Acids Res.* 38(Suppl._1), D518–D524.

Sidhu, S. S., Lowman, H. B., Cunningham, B. C., and Wells, J. A. (2000). [21] Phage display for selection of novel binding peptides. *Methods Enzymol.* 328, 333–365.

Singh, S., Chaudhary, K., Dhanda, S. K., Bhalla, S., Usmani, S. S., Gautam, A., et al. (2016). SATPdb: a database of structurally annotated therapeutic peptides. *Nucleic Acids Res.* 44, D1119–D1126.

Skolnick, J., Fetrow, J. S., and Kolinski, A. (2000). Structural genomics and its importance for gene function analysis. *Nat. Biotechnol.* 18, 283–287. doi: 10.1038/73723

Slater, O., and Kontoyianni, M. (2019). The compromise of virtual screening and its impact on drug discovery. *Exp. Opin. Drug Discov.* 14, 619–637. doi: 10.1080/17460441.2019.1604677

Sorolla, A., Wang, E., Golden, E., Duffy, C., Henriques, S. T., Redfern, A. D., et al. (2020). Precision medicine by designer interference peptides: applications in oncology and molecular therapeutics. *Oncogene* 39, 1167–1184. doi: 10.1038/s41388-019-1056-3

Souza, F. R., Souza, L. M. P., and Pimentel, A. S. (2020). Recent open issues in coarse grained force fields. *J. Chem. Inf. Model.* 60, 5881–5884. doi: 10.1021/acs.jcim.0c01265

Stites, W. E. (1997). Protein- protein interactions: interface structure, binding thermodynamics, and mutational analysis. *Chem. Rev.* 97, 1233–1250. doi: 10.1021/cr960387h

Stone, T. A., and Deber, C. M. (2017). Therapeutic design of peptide modulators of protein-protein interactions in membranes. *Biochim. Biophys. Acta* 1859, 577–585. doi: 10.1016/j.bbamem.2016.08.013

Thakur, N., Qureshi, A., and Kumar, M. (2012). AVPpred: collection and prediction of highly effective antiviral peptides. *Nucleic Acids Res.* 40, W199–W204.

Thanos, C. D., DeLano, W. L., and Wells, J. A. (2006). Hot-spot mimicry of a cytokine receptor by a small molecule. *Proc. Natl. Acad. Sci. U.S.A.* 103, 15422–15427. doi: 10.1073/pnas.0607058103

Thevenet, P., Shen, Y., Maupetit, J., Guyon, F., Derreumaux, P., and Tuffery, P. (2012). PEP-FOLD: an updated de novo structure prediction server for both linear and disulfide bonded cyclic peptides. *Nucleic Acids Res.* 40, W288–W293.

Thomas, A., Deshayes, S., Decaffmeyer, M., Van Eyck, M. H., Charloteaux, B., and Brasseur, R. (2006). Prediction of peptide structure: how far are we? *Proteins* 65, 889–897. doi: 10.1002/prot.21151

Thomas, S., Karnik, S., Barai, R. S., Jayaraman, V. K., and Idicula-Thomas, S. (2010). CAMP: a useful resource for research on antimicrobial peptides. *Nucleic Acids Res.* 38(Suppl._1), D774–D780.

Thorn, K. S., and Bogan, A. A. (2001). ASEdb: a database of alanine mutations and their effects on the free energy of binding in protein interactions. *Bioinformatics* 17, 284–285. doi: 10.1093/bioinformatics/17.3.284

Tilley, J. W., Chen, L., Fry, D. C., Emerson, S. D., Powers, G. D., Biondi, D., et al. (1997). Identification of a small molecule inhibitor of the IL-2/IL-2Rα receptor interaction which binds to IL-2. *J. Am. Chem. Soc.* 119, 7589–7590. doi: 10.1021/ja970702x

Trabuco, L. G., Lise, S., Petsalaki, E., and Russell, R. B. (2012). PepSite: prediction of peptide-binding sites from protein surfaces. *Nucleic Acids Res.* 40, W423–W427.

Trellet, M., Melquiond, A. S., and Bonvin, A. M. (2013). A unified conformational selection and induced fit approach to protein-peptide docking. *PLoS One* 8:e58769. doi: 10.1371/journal.pone.0058769

Tuncbag, N., Gursoy, A., and Keskin, O. (2009). Identification of computational hotspots in protein interfaces: combining solvent accessibility and inter-residue potentials improves the accuracy. *Bioinformatics* 25, 1513–1520. doi: 10.1093/bioinformatics/btp240

Tuncbag, N., Keskin, O., and Gursoy, A. (2010). HotPoint: hotspot prediction server for protein interfaces. *Nucleic Acids Res.* 38(Suppl._2), W402–W406.

Tyagi, A., Tuknait, A., Anand, P., Gupta, S., Sharma, M., Mathur, D., et al. (2015). CancerPPD: a database of anticancer peptides and proteins. *Nucleic Acids Res.* 43, D837–D843.

Usmani, S. S., Bedi, G., Samuel, J. S., Singh, S., Kalra, S., Kumar, P., et al. (2017). THPdb: database of FDA-approved peptide and protein therapeutics. *PLoS One* 12:e0181748. doi: 10.1371/journal.pone.0181748

Usmani, S. S., Kumar, R., Kumar, V., Singh, S., and Raghava, G. P. (2018). AntiTbPdb: a knowledgebase of anti-tubercular peptides. *Database* 2018:bay025.

van Heel, A. J., de Jong, A., Song, C., Viel, J. H., Kok, J., and Kuipers, O. P. (2018). BAGEL4: a user-friendly web server to thoroughly mine RiPPs and bacteriocins. *Nucleic Acids Res.* 46, W278–W281.

Vanommeslaeghe, K., Guvench, O., and MacKerell, A. D. Jr. (2014). Molecular mechanics. *Curr. Pharm. Des.* 20, 3281–3292. doi: 10.2174/13816128113199990600

Verdonk, M. L., Cole, J. C., Hartshorn, M. J., Murray, C. W., and Taylor, R. D. (2003). Improved protein–ligand docking using GOLD. *Proteins* 52, 609–623. doi: 10.1002/prot.10465

Vishnepolsky, B., Zaalishvili, G., Karapetian, M., Gabrielian, A., Rosenthal, A., Hurt, D. E., et al. (2019a). "Development of the model of in silico design of AMPs active against Staphylococcus aureus 25923," in *Proceedings of the 5th International Electronic Conference on Medicinal Chemistry session ECMC-5*, (Basel: MDPI), doi: 10.3390/ECMC2019-06359

Vishnepolsky, B., Zaalishvili, G., Karapetian, M., Nasrashvili, T., Kuljanishvili, N., Gabrielian, A., et al. (2019b). De novo design and in vitro testing of antimicrobial peptides against Gram-negative bacteria. *Pharmaceuticals* 12:82. doi: 10.3390/ph12020082

Waghu, F. H., Barai, R. S., Gurung, P., and Idicula-Thomas, S. (2016). CAMPR3: a database on sequences, structures and signatures of antimicrobial peptides. *Nucleic Acids Res.* 44, D1094–D1097.

Waghu, F. H., Gopi, L., Barai, R. S., Ramteke, P., Nizami, B., and Idicula-Thomas, S. (2014). CAMP: collection of sequences and structures of antimicrobial peptides. *Nucleic Acids Res.* 42, D1154–D1158.

Wang, E., Sun, H., Wang, J., Wang, Z., Liu, H., Zhang, J. Z. H., et al. (2019). End-point binding free energy calculation with MM/PBSA and MM/GBSA: strategies and applications in drug design. *Chem. Rev.* 119, 9478–9508. doi: 10.1021/acs.chemrev.9b00055

Wang, G., Li, X., and Wang, Z. (2009). APD2: the updated antimicrobial peptide database and its application in peptide design. *Nucleic Acids Res.* 37(Suppl._1), D933–D937.

Wang, G., Li, X., and Wang, Z. (2016). APD3: the antimicrobial peptide database as a tool for research and education. *Nucleic Acids Res.* 44, D1087–D1093.

Wang, J., Yin, T., Xiao, X., He, D., Xue, Z., Jiang, X., et al. (2018). StraPep: a structure database of bioactive peptides. *Database* 2018:bay038.

Wang, Y., Wang, M., Yin, S., Jang, R., Wang, J., Xue, Z., et al. (2015). NeuroPep: a comprehensive resource of neuropeptides. *Database* 2015:bav038. doi: 10.1093/database/bav038

Wang, Z., and Sun, H. (2020). Combined strategies in structure-based virtual screening. *Phys. Chem. Chem. Phys.* 22, 3149–3159. doi: 10.1039/c9cp06303j

Wang, Z., and Wang, G. (2004). APD: the antimicrobial peptide database. *Nucleic Acids Res.* 32(Suppl._1), D590–D592.

Wang, Z., Zhang, S., Jin, H., Wang, W., Huo, J., Zhou, L., et al. (2011). Angiotensin-I-converting enzyme inhibitory peptides: chemical feature based pharmacophore generation. *Eur. J. Med. Chem.* 46, 3428–3433. doi: 10.1016/j.ejmech.2011.05.007

Wei, L., Xing, P., Su, R., Shi, G., Ma, Z. S., and Zou, Q. (2017). CPPred-RF: a sequence-based predictor for identifying cell-penetrating peptides and their uptake efficiency. *J. Proteome Res.* 16, 2044–2053. doi: 10.1021/acs.jproteome.7b00019

Wells, J. A. (1990). Additivity of mutational effects in proteins. *Biochemistry* 29, 8509–8517. doi: 10.1021/bi00489a001

Wells, J. A. (1991). "[18] Systematic mutational analyses of protein-protein interfaces. *Methods Enzymol.* 202, 390–411. doi: 10.1016/0076-6879(91)02020-a

Wells, J. A., and McClendon, C. L. (2007). Reaching for high-hanging fruit in drug discovery at protein–protein interfaces. *Nature* 450, 1001–1009. doi: 10.1038/nature06526

White, A. W., Westwell, A., and Brahemi, G. (2008). Protein-protein interactions as targets for small-molecule therapeutics in cancer. *Expert Rev. Mol. Med.* 10:e8.

Whitmore, L., and Wallace, B. (2004). The Peptaibol Database: a database for sequences and structures of naturally occurring peptaibols. *Nucleic Acids Res.* 32(Suppl._1), D593–D594.

Wrighton, N. C., Farrell, F. X., Chang, R., Kashyap, A. K., Barbone, F. P., Mulcahy, L. S., et al. (1996). Small peptides as potent mimetics of the protein hormone erythropoietin. *Science* 273, 458–463. doi: 10.1126/science.273.5274.458

Wu, K.-J., Lei, P.-M., Liu, H., Wu, C., Leung, C.-H., and Ma, D.-L. (2019). Mimicking strategy for protein-protein interaction inhibitor discovery by virtual screening. *Molecules* 24:4428. doi: 10.3390/molecules24244428

Wynendaele, E., Bronselaer, A., Nielandt, J., D'Hondt, M., Stalmans, S., Bracke, N., et al. (2012). Quorumpeps database: chemical space, microbial origin and functionality of quorum sensing peptides. *Nucleic Acids Res.* 41, D655–D659. doi: 10.1093/nar/gks1137

Wynendaele, E., Bronselaer, A., Nielandt, J., D'Hondt, M., Stalmans, S., Bracke, N., et al. (2013). Quorumpeps database: chemical space, microbial origin and functionality of quorum sensing peptides. *Nucleic Acids Res.* 41, D655–D659.

Xie, Z., Deng, X., and Shu, K. (2020). Prediction of protein-protein interaction sites using convolutional neural network and improved data sets. *Int. J. Mol. Sci.* 21:467. doi: 10.3390/ijms21020467

Yan, C., Xu, X., and Zou, X. (2016). Fully blind docking at the atomic level for protein-peptide complex structure prediction. *Structure* 24, 1842–1853. doi: 10.1016/j.str.2016.07.021

Yan, F., Liu, G., Chen, T., Fu, X., and Niu, M.-M. (2019). Structure-based virtual screening and biological evaluation of peptide inhibitors for polo-box domain. *Molecules* 25:107. doi: 10.3390/molecules25010107

Yan, J., Bhadra, P., Li, A., Sethiya, P., Qin, L., Tai, H. K., et al. (2020). Deep-AmPEP30: improve short antimicrobial peptides prediction with deep learning. *Mol. Ther. Nucleic Acids.* 20, 882–894. doi: 10.1016/j.omtn.2020.05.006

Yang, Z. R. (2008). Peptide bioinformatics: peptide classification using peptide machines. *Methods Mol. Biol.* 458, 159–183. doi: 10.1007/978-1-60327-101-1_9

Ye, G., Wu, H., Huang, J., Wang, W., Ge, K., Li, G., et al. (2020). LAMP2: a major update of the database linking antimicrobial peptides. *Database* 2020:baaa061.

Zemla, A. (2003). LGA: a method for finding 3D similarities in protein structures. *Nucleic Acids Res.* 31, 3370–3374. doi: 10.1093/nar/gkg571

Zhai, D., Chin, K., Wang, M., and Liu, F. (2014). Disruption of the nuclear p53-GAPDH complex protects against ischemia-induced neuronal damage. *Mol. Brain* 7:20. doi: 10.1186/1756-6606-7-20

Zhang, Q. C., Deng, L., Fisher, M., Guan, J., Honig, B., and Petrey, D. (2011). PredUs: a web server for predicting protein interfaces using structural neighbors. *Nucleic Acids Res.* 39(Suppl._2), W283–W287.

Zhu, X., and Mitchell, J. C. (2011). KFC2: a knowledge-based hotspot prediction method based on interface solvation, atomic density, and plasticity features. *Proteins* 79, 2671–2683. doi: 10.1002/prot.23094

Conflict of Interest: The authors declare that the research was conducted in the absence of any commercial or financial relationships that could be construed as a potential conflict of interest.

frontiers in Molecular Biosciences

REVIEW
published: 20 May 2021
doi: 10.3389/fmolb.2021.681617

Computational Modeling as a Tool to Investigate PPI: From Drug Design to Tissue Engineering

Juan J. Perez[1]*, *Roman A. Perez*[2] *and Alberto Perez*[3]

[1]Department of Chemical Engineering, Universitat Politecnica de Catalunya, Barcelona, Spain, [2]Bioengineering Institute of Technology, Universitat Internacional de Catalunya, Sant Cugat, Spain, [3]The Quantum Theory Project, Department of Chemistry, University of Florida, Gainesville, FL, United States

Protein-protein interactions (PPIs) mediate a large number of important regulatory pathways. Their modulation represents an important strategy for discovering novel therapeutic agents. However, the features of PPI binding surfaces make the use of structure-based drug discovery methods very challenging. Among the diverse approaches used in the literature to tackle the problem, linear peptides have demonstrated to be a suitable methodology to discover PPI disruptors. Unfortunately, the poor pharmacokinetic properties of linear peptides prevent their direct use as drugs. However, they can be used as models to design enzyme resistant analogs including, cyclic peptides, peptide surrogates or peptidomimetics. Small molecules have a narrower set of targets they can bind to, but the screening technology based on virtual docking is robust and well tested, adding to the computational tools used to disrupt PPI. We review computational approaches used to understand and modulate PPI and highlight applications in a few case studies involved in physiological processes such as cell growth, apoptosis and intercellular communication.

Keywords: protein-protein interactions, linear peptide motifs, computational methods, epitopes, tissue engineering, p53, Bcl-2

OPEN ACCESS

Edited by:
Laura Belvisi,
University of Milan, Italy

Reviewed by:
Sebastian Kmiecik,
University of Warsaw, Poland
Helen Mott,
University of Cambridge,
United Kingdom

***Correspondence:**
Juan J. Perez
juan.jesus.perez@upc.edu

Specialty section:
This article was submitted to Molecular Recognition, a section of the journal Frontiers in Molecular Biosciences

Received: *17 March 2021*
Accepted: *05 May 2021*
Published: *20 May 2021*

Citation:
Perez JJ, Perez RA and Perez A (2021) Computational Modeling as a Tool to Investigate PPI: From Drug Design to Tissue Engineering. Front. Mol. Biosci. 8:681617. doi: 10.3389/fmolb.2021.681617

INTRODUCTION

Most proteins mediate complicated metabolic and signaling pathways through interaction with other proteins, either in the form of dimers or as components of larger complexes (Hunter, 2000; Stelzl et al., 2005). Some of these interactions are transient, while others are more permanent. It is estimated that there are approximately 650,000 types of specific protein-protein interactions (PPI) in a human cell (Stumpf et al., 2008) and as much as 40% of these are mediated by short peptide linear binding motifs (London et al., 2013). Actually, protein domains involved in PPIs often bind multiple peptides that share linear motifs—common sequence patterns—like for example, the canonical SH3 domain-binding PxxP motif (Mayer, 2001). These motifs are often embedded within locally unstructured protein regions but can also bind their partners as short, isolated peptides acting as PPIs inhibitors.

Mapping PPIs is key to understand a wide range of physiological processes such as cell growth, apoptosis and intercellular communication. In turn, anomalies in protein interaction networks including the concentration of a specific protein in the cell are associated with diseases such as cancer, infectious diseases, and neurodegenerative diseases (Gonzalez and Kann, 2012). Accordingly, a detailed understanding of the human interactome--the complex network of PPIs—(Luck et al., 2020) offers novel opportunities for therapeutical intervention (Milroy et al., 2014).

Designing different kinds of PPIs modulators, including inhibitors that arrest signaling by disrupting a specific PPI or enhancers that restore signaling through facilitation of a specific PPI is now a major goal in controlling cell processes and pathways. In addition, allosteric binders can provide a different type of PPI modulation, acting through the selective perturbation of a protein interaction with specific partners and modulating a signaling pathway accordingly (Cesa et al., 2015). Indeed, this procedure opens the possibility of designing two different disruptors acting on the same target that produce different cellular responses due to the way they alter local PPI networks. Conceptually, designing PPI disruptors is simpler than designing enhancers, since the latter require finding a short linker that brings the two proteins in close contact to each other, whereas the former require finding molecules that bind to any site of any of the two proteins to prevent their association.

Designing modulators of PPIs is challenging compared to ligands targeting enzymes or GPCRs, due to the specific features of protein-protein interfaces including a large and flat interfacial area (~1500–3000 $Å^2$), lacking in grooves or binding pockets (Wells and McClendon, 2007). Moreover, the PPI binding free energy is characterized by a large buried hydrophobic surface area, suggesting a large entropic contribution—although electrostatic complementarity of interacting protein surfaces is also important in PPIs. Consequently, the binding free energy is not correlated to the PPI surface area buried. For example, the complex of the tumor suppressor p53 protein to its negative regulator MDM2 described below is an example of a small contact surface area and high affinity (Borcherds et al., 2014), while the complex of the Bcl2-associated athanogene (Bag) and an eukaryotic chaperone 70-kDa heat shock protein (Hsp70) exhibits a high surface area, but a small binding free energy (Sondermann et al., 2001). Interestingly, PPI surfaces exhibit a reduced number of key contributors or "hot spots" to the binding free energy (<2 kcal/mol) that are usually found at the center of the interface. Tryptophan, arginine and tyrosine are the most frequent residues identified as "hot spots", whereas other residues such as valine, lysine or serine rarely participate (Hu et al., 2000). The occurrence of key residues in PPIs was demonstrated for the first time in the seminal study of the complex of the human growth hormone (hGH) and the extracellular domain of its receptor (gGHbd) (Clackson and Wells, 1995). In order to understand the contribution of each residue to the PPI, the authors produced all the possible gGHbd mutants generated by substitution of each individual residue involved in the PPI surface area by alanine. The process permitted to show that 8 out of 31 side chains involved in the PPI surface area contributed about 85% to the binding free energy of the complex. Alanine scanning technique is currently carried out *in vivo* using phage display technology in a combinatorial fashion (Morrison and Weiss, 2001) and computational strategies to perform alanine scanning have also been developed (Kortemme et al., 2004).

Diverse kinds of molecules from small molecules to antibodies have been used in the past as PPI disruptors (Gordo and Giralt, 2009). Among them, peptides have emerged as privileged molecules (Nevola and Giralt, 2015; Bruzzoni-Giovanelli et al., 2018). Analysis of protein complexes show that a large number of structures involve short linear peptide binding motifs and a globular protein domain. Interestingly, these peptide segments are responsible for most of the binding free energy (Petsalaki and Russell, 2008). Peptides are flexible and can adapt themselves to large surfaces, can be easily optimized and are safe and well tolerated. However, peptides exhibit limitations as drugs including the means of administration, poor pharmacokinetic profile and bioavailability. Despite their drawbacks to be used as drugs, peptides can be modified to produce peptidomimetics and peptide surrogates including cyclic peptides with an improved ADME profile. Peptidomimetics refers to small molecules that mimic key stereochemical features of the bioactive conformation of a target peptide (Perez et al., 2002; Akram et al., 2014; Perez, 2018; Santini and Zacharias, 2020; Tomasella et al., 2021). Designing peptidomimetics requires knowledge of key residues involved in peptide-protein interactions and structural features of the bioactive conformation. When the 3D structure of the complex is available, the process is simpler, however most of the times the bioactive conformation needs to be assessed using a combination of biophysical and computational methods together with the synthesis and biological evaluation of the molecules designed. In this case the roadmap normally followed for designing peptidomimetics is shown in **Figure 1**.

Below we describe the use of computational methods in conjunction of other biophysical and medicinal chemistry techniques to help to understand the features of peptide ligands, necessary to design PPI disruptors peptidomimetics and peptide surrogates and describe a few examples in drug discovery and tissue engineering.

STRUCTURAL FEATURES OF PROTEIN-PEPTIDE INTERACTIONS

The increased awareness on the role of peptide epitopes for mediating PPI has evidenced the need for a deeper structural understanding. Complexes are underrepresented in the PDB with respect to their biological prevalence, and experimental techniques often require expensive approaches (e.g., isotope labeling in NMR) to characterize peptide-protein interactions. Computational tools are a promising approach to bridge the gap. The goal of computational methods is to predict where and how a peptide would bind a protein receptor, distinguish which peptide sequences might be better binders, and help in the design process. Improvements in computational tools continue to push our ability to gain structural insights applicable to design principles.

Curated peptide-protein databases such as pepBDB (Wen et al., 2019), peptiDB (London et al., 2010) or pepBind (Das et al., 2013) compile a list of known protein-peptide systems found in the Protein Data Bank (PDB) (Berman et al., 2000). These curated databases are useful for the training, classification and understanding of peptide-protein interactions. Analyzing these databases helps to classify the types of interaction according to peptide structure, binding interface or degree of challenge for computational methods amongst other metrics. For example, Arkin and co-workers classified three types of peptide-protein binding (Arkin et al., 2014) according to the primary, secondary or tertiary structure they adopt. The primary structure binding motif is represented by short linear peptides such as those present in interactions between the extracellular matrix and

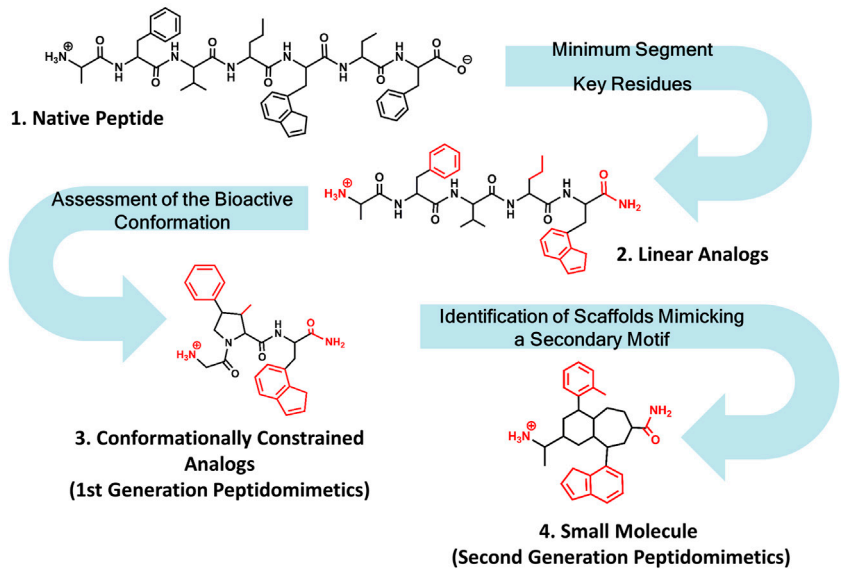

FIGURE 1 | Roadmap for peptidomimetics design. Starting from the native peptide (1), first step regards establishing the shortest peptide fragment with activity, as well as identification of key residues involved in recognition (in red) (2). Next, using information about the secondary structure of the peptide in its bound conformation, proceed to design conformationally constrained analogs mimicking the bioactive conformation (3). These analogs represent the first generation peptidomimetics. Finally, identification of small molecule scaffolds that permit a correct spatial arrangement of relevant chemical groups (identified in step 2) to yield second generation peptidomimetics (4).

membrane bound integrins (Ruoslahti, 1996). Secondary structure motifs involve the peptide adopting a determined secondary structure (e.g., alpha helix or beta strand) such as in the p53-MDM2 interaction (Kussie et al., 1996) or the BH3-Bcl-2 interaction (Adams and Cory, 1998), whereas tertiary structure represents discontinuous binding sites such as the XIAP-Smac interaction (Wu et al., 2000). A different classification for peptide-protein interactions is by looking at the protein-protein interface they are posed to inhibit (Yan et al., 2008). Peptides binding deep cavities are typically easier to model than those that interact with extended flat surfaces. Finally, one of the more challenging aspects is the degree of plasticity in the binding mode. This includes the conformational changes of the protein receptor as well as the ability to accommodate multiple binding conformations. This is especially characteristic of protein interaction hubs such as those involved in gene regulation (Aiyer et al., 2021). Many peptides are intrinsically disordered and fold upon binding, hence optimization of peptide design will often try to maximize interactions in the complex as well as the propensity of the peptide to adopt bound structures (e.g. through chemical staples or cyclization). Peptidomimetics are often a solution in which the peptide interactions are closely maintained while designing a molecule with a lower number of degrees of conformational freedom.

COMPUTATIONAL METHODS USED TO STUDY PROTEIN-PEPTIDE INTERACTIONS

Approaches such as docking and free energy perturbation are now routinely used in the drug discovery process for small molecules. Docking methodologies explore libraries of millions of virtual compounds in search for small molecule scaffolds or for drug repurposing efforts (Kitchen et al., 2004). Meanwhile, free energy perturbation methods are now able to calculate relative (and absolute) binding free energies with errors comparable to experiments (Wang et al., 2015). Despite the successes, they have well known limitations regarding the nature of the ligands (e.g., flexibility or charge) as well as the structural rearrangements needed in the protein receptor, which become important for peptide-protein systems.

Since 2001, the CAPRI (Critical Assessment of Predicted Interactions) (Janin et al., 2003) has been instrumental in assessing the developments in methods that predict macromolecular assemblies as well as scoring functions that can identify the best predictions. The focus has been in interactions between a protein and other proteins, nucleic acids and peptides–with an emphasis on protein-protein interactions. CAPRI is a blind prediction effort in the spirit of CASP (Critical Assessment of Structure Prediction) (Moult et al., 1995): research groups from around the world use their methods to predict atomic resolution 3D structures for targets provided by CAPRI, and to predict the ranking of models based on scoring functions. The event operates with strict time deadlines for each target. At the end of the event, assessors rank the predictions comparing them to the experimental structure (which is unknown to the community at the time of the predictions). Assessors are also blind to which group performed each prediction (double-blind experiment). These methods perform well for easy targets in which there are small changes in the proteins between their free and bound form.

Performance decreases for both scoring and prediction methods for the "hard" targets in which binding requires conformational changes in the proteins with respect to their free form (Lensink et al., 2019).

The above limitations become relevant for the study of peptide-protein systems. Many peptides are intrinsically disordered in their free form, becoming structured during the binding process. Predicting bound conformations requires tackling this conformational flexibility and estimating the entropic contribution of adopting bound conformations to the free energy. Knowing the bound conformation of a protein-peptide system does not imply that other peptide sequences can adopt the same bound conformation. This binding plasticity is best exemplified by: 1) receptors that bind different peptide sequences in different conformations (Aiyer et al., 2021) and 2) peptide sequences that can adopt different structures when binding different receptors (Huart and Hupp, 2013). This amount of binding plasticity is a challenge for predicting peptide-protein interactions and for computing binding affinities.

Amongst the difficulties in predicting bound conformations for protein-ligand interactions is the mechanisms by which binding takes places. It is now widely accepted that binding happens through a combination of two main binding mechanisms, traditionally described as induced fit and conformational selection. The mechanism behind induced fit is that a ligand will bind in the active site and the protein/ligand system will undergo a conformational transition toward the bound conformation. In the conformational selection mechanism, the protein and ligand each have an ensemble of possible conformations available to them—and binding occurs through a specific conformation. Each particular system under study will have a different contribution from each mechanism. Thus, how much a system changes from the unbound/bound conformation is often used as a measure of the difficulty in predicting binding. The fly casting mechanism (Shoemaker et al., 2000; Sugase et al., 2007) has been coined to understand how intrinsically disordered domains can accelerate molecular recognition. This binding mechanism is often exhibited in peptide epitopes involved in PPIs. The resulting peptides are often intrinsically disordered as described in the above paragraph, resulting in a more challenging scenario than in small molecules, where now both the protein and peptide molecules can change conformations significantly from their free form.

Docking-Based Approaches

An array of docking methodologies have emerged in the last few years, in response to a growing pharmacological interest for peptide-based drugs. Excellent reviews on such methods have been published (Ciemny et al., 2016; Porter et al., 2019; Aderinwale et al., 2020), along with studies providing benchmark sets for assessing current and future methods. Here we provide an overview of the general principles behind these approaches as well as efforts from the simulation community in predicting protein-peptide interactions.

Docking methods operate in different search modes depending on the known information about the system of interest. The ultimate goal is to recover the binding site and binding mode for the protein-peptide conformation. This problem can be broadly divided in two parts: the search problem and the scoring problem. The search problem is related to exploring the relative peptide-protein relative position and orientation, as well as the internal conformation of the protein and peptide. The scoring stage aims to identify the correctly bound structures amongst all predictions based on a function that relates docking structures to a score. Assessment of success is done on the top scoring poses.

For computational efficiency, docking methods reduce the search space in several ways, depending on the known information about the system. In a global search strategy, the peptide explores binding at all possible sites along the protein-receptor surface (Pierce et al., 2011; Kurcinski et al., 2015; Alam et al., 2017; de Vries et al., 2017; Porter et al., 2017; Xu et al., 2018; Zhou et al., 2018). Whereas in a local search approach, the binding region is limited based on prior knowledge, resulting in a more directed search (Jain, 2007; Antes 2010; Donsky and Wolfson, 2011; London et al., 2011; Trellet et al., 2013; Rentzsch and Renard, 2015; Lamiable et al., 2016; Antunes et al., 2017; Zhang and Sanner, 2019). Finally, template-based approaches forego this search by building flexibility on top of models extracted from structural databases based on protein and peptide alignments (Lee et al., 2015; Obarska-Kosinska et al., 2016).

The methods can be further divided based on how much conformational freedom is allowed for the protein receptor and the peptide. The protein receptor flexibility is a common problem to protein-protein and protein-small molecule docking (Andrusier et al., 2008; B-Rao et al., 2009). Approaches to model protein flexibility include the use of soft potentials (Fernández et al., 2002; Ferrari et al., 2004), explore rotameric states (Leach, 1994), using different protein receptor structures (Amaro et al., 2018; Falcon et al., 2019) or refining with molecular dynamics (Alonso et al., 2006). The challenges in modeling peptides arises from: 1) peptides can have different conformations in their free/bound states; 2) the same peptide sequence might bind different proteins in different conformations (Huart and Hupp, 2013), and 3) different peptide sequences can bind the same receptor in different conformations (Aiyer et al., 2021). Most docking methods use a flexible strategy for the peptide conformation. Rather than exhaustively sampling all possible conformations two approaches are typically taken: 1) based on sequence, and 2) based on representative peptide conformations. In the first approach the peptide sequence is used to either query the pdb for possible conformations of the peptide fragment (e.g., in proteins that contain that sequence) or predict secondary structure (Yan et al., 2016). The second approach uses several initial conformations generally adopted by peptides during binding (e.g., helix or extended) (see Weng et al., 2020).

Scoring functions have the task of identifying which poses are likely to be biologically relevant. Ideally these functions should reflect the underscoring binding affinities of different poses and compounds (Li et al., 2021). Their use dates back to the early days of docking methods to understand protein complexes (Kuntz et al., 1982). Scoring functions are typically divided in four types: 1) empirical fits, 2) knowledge based, 3) machine learning, and 4)

first principles (Li et al., 2019; Li et al., 2021). One of the challenges in the adequate development of scoring functions is the ability to generate poses that include both good binders and bad binders. These has led to the development of decoy sets (Graves et al., 2005; Stein et al., 2021), often used as training sets for new functions. How these decoy sets are generated influences the corresponding scoring functions, often resulting in biases. Recent efforts aim at detecting and overcoming such biases (Morrone et al., 2020). Scoring functions that work for protein-protein or protein-small molecule systems are not always transferable to protein-peptide systems, resulting in the development of several specific peptide-protein scoring functions (Raveh et al., 2011; Kurcinski et al., 2015; Spiliotopoulos et al., 2016; Tao et al., 2020).

Despite the importance of blind studies (Lensink et al., 2007), there have been few protein-peptide targets in CAPRI in recent years (Weng et al., 2020). Benchmarking studies (Agrawal et al., 2019; Santos et al., 2020; Weng et al., 2020) and peptide protein datasets (London et al., 2010; Hauser and Windshügel, 2016) provide the community with the tools needed to improve docking and scoring methodologies. These benchmarks are typically divided into easy/medium/hard categories according to the conformational changes that the peptide has to undergo to bind (Trellet et al., 2013; Weng et al., 2020). A recent benchmark study using 14 different docking programs (Weng et al., 2020) shows that despite improvements in peptide-protein docking, predicting binding modes when large conformational changes are involved remains challenging.

Free Energy-Based Approaches

We refer in this category to methods that produce ensembles obeying detailed balance, and using statistical mechanics to infer representative structures and free energies. Sampling is generally achieved through Monte Carlo (Metropolis et al., 1953; Hansmann and Okamoto, 1999) or Molecular Dynamics (MD) (McCammon et al., 1977) approaches using a force field to represent atomic interactions and capture the entropic contribution in the ensembles. In these approaches, a single point structure evaluation of the potential (given a force field) is not relevant to identify low free energy states—whereas scoring functions in docking or knowledge-based potentials are intended to evaluate single structures. Through the sampling of the free energy landscape these methods capture kinetics, mechanisms of action and binding affinities. The challenge in these methodologies is to sample timescales relevant to binding events. Simulations now routinely sample the microsecond timescale, but binding events typically require reaching the millisecond timescale. Despite improvements using specialized hardware (Pan et al., 2017), using brute force MD for binding remains computationally unfeasible. A common strategy is to use MD based approaches as the last stage of docking pipelines, leading to refined models. Recently, improvements in advanced sampling techniques and computer efficiency are opening new opportunities to study peptide-protein binding.

Free energy perturbation (FEP) methods are the golden standard for characterizing binding free energies of small molecules (relative or absolute) (Wang et al., 2015). FEP requires knowledge of the bound state and uses a path independent approach, generally combining alchemical transformations and restraints to evaluate the binding free energy change. These methods suffer when there are large changes in the scaffold of the molecule, the overall charge or when multiple binding modes have to be included (Gill et al., 2018; Ruiter and Oostenbrink, 2020; Wallraven et al., 2020). Thus, the successes of FEP for small molecules are not yet generally transferable to protein-protein or protein-peptide systems. Advanced sampling strategies are opening possibilities to study the peptide binding process and extract binding affinities, albeit at a greater computational expense.

Although there are many advanced sampling techniques, for the purpose of peptide binding we distinguish between those that capture kinetics and mechanisms of action and those that identify states and binding free energies. Advances in frameworks that combine multiple unbiased MD trajectories to recover kinetic and mechanistic properties such as Markov State Models (Noé et al., 2009; Bowman et al., 2010), weighted ensemble methods (Huber and Kim, 1996; Zhang et al., 2010) and milestoning (Faradjian and Elber, 2004; Votapka and Amaro, 2015) have been used to study several peptide-protein systems (Giorgino et al., 2012; Zwier et al., 2016; Paul et al., 2017; Zhou et al., 2017). These methods can be used to estimate on and off-rates, with off-rates being significantly harder to obtain due to the long timescales needed to observe unbinding events.

A second class of advanced sampling strategies combines known information (e.g., from experiments) and generalized ensemble methodologies (Sugita and Okamoto, 1999; Fukunishi et al., 2002) to identify bound conformations (Morrone et al., 2017a; Morrone et al., 2017b; Lang and Perez, 2021). These approaches are also used to obtain qualitative relative binding affinities from competitive binding simulations (Morrone et al., 2017a; Morrone et al., 2017b).

There are yet few instances of using these methodologies as well as progress towards more quantitative methodologies. For example, in frameworks that use multiple unbiased trajectories questions like how many simulations to start from each state, how to reweight them or how to visualize them in a space that allows interpretation of the ensembles is an area of active development.

From Bound Conformations to Sequence Design

A final strategy used by the community is to identify mutations to a peptide sequence that will favor interaction with the protein through the use of fast approaches that rely on statistical or empirical potentials (Takano et al., 1999; Guerois et al., 2002) described in the docking section. Here, we typically have knowledge of a protein-protein interaction and the related structure, and use the binding epitope as a structural template. These methods are then used to mutate each residue in the peptide into different amino acids, using a fast scoring function to predict those mutations that lead to greater affinity (Delgado et al., 2019; Torres et al., 2019).

In what follows, we describe three specific examples of PPIs involved in diverse physiological process including cell growth, apoptosis or intercellular communication, together with a

summarized description of the advances carried out for the development of peptide analogs, surrogates or peptidomimetics.

THE p53-MDM2/X INTERACTION

P53 has been named the "guardian of the genome" for its tumor-suppressor activity. It is a protein interaction hub, predicted to be involved in over a thousand PPIs (Tan et al., 2019) through its different functional domains (May and May, 1999). In this section we will focus on the interaction between the p53 transactivation domain and the MDM2 protein (or its homologous MDMX) which marks p53 for degradation. Inhibition of the p53-MDM2/X interaction has been an important cancer target, since it liberates p53 to carry its tumor-suppressor activity. Despite the homology between MDM2 and MDMX, developing dual inhibitor drugs remains an active field of research, with several candidates in clinical trials.

The p53-MDM2 interaction involves a short intrinsically disordered epitope from the terminal transactivation domain of p53 binding as a helix to the N-terminal domain of MDM2 (Kussie et al., 1996). MDM2 has a deep hydrophobic cavity which anchors three residues from p53 (Phe^{19}, Trp^{23} and Leu^{26}; see PDB id 1YCR, see **Figure 2**), (Kussie et al., 1996). MDMX shares an 80% homology in the binding site with MDM2, resulting in p53 binding along the same binding mode (PDB id 3DAB) (Hu et al., 2006; Popowicz et al., 2008). Despite their similarity, MDMX presents a shallower binding site, which poses difficulties for developing binding inhibitors. Computational approaches have played a role in both the rational design of small molecules (Bowman et al., 2007) and peptides as potential drugs (Tan et al., 2016).

Studies based on MD and docking have tried to characterize the details of the p53-MDM2 interaction. Studies using MSM approaches are now yielding on-rates for p53-MDM2 close to experiment, while the off-rates remain challenging to estimate directly (Zwier et al., 2016; Zhou et al., 2017). These studies are also providing information about the binding mechanisms, predicting the helicity needed for a peptide to switch from an induced fit binding paradigm to one in which conformational selection dominates (Zhou et al., 2017). Some studies are also using the longer MDM2 construct, which includes a "lid" region that effectively reduces the amount of time the binding site is accessible for p53 binding. Molecular dynamics approaches yield detailed information on the effect of the lid disordered region on the binding energy surface of MDM2 and compares it to the case of p53 and several other small molecule drugs (Bueren-Calabuig and Michael, 2015). Recent flexible docking simulations of the p53 peptide starting from unbound conformations and including the disordered tails in MDM2 reported the best scoring structure to be 3.74 Å from the experimentally bound structure (Ciemny et al., 2018).

The small molecule drug Nutlin-3a (**1** in **Figure 3**) and its derivative, idasanutlin (**2** in **Figure 3**) now in pPhase III trial for relapsed/refractory acute myeloid leukemia were developed for its ability to bind an inhibit MDM2 (Vassilev et al., 2004; Vassilev, 2005; Ding et al., 2013). However, this family of compounds are not efficient against MDMX (Hu et al., 2006; Joseph et al., 2010)—similar trends have been observed in other compounds like AMG-232 (**3** in **Figure 3**), where binding to MDMX has significantly lower affinity than for MDM2. Furthermore, small molecules inhibitors of MDMX have not been successful in culture cells (Reed et al., 2010). Small molecule designs have tried to mimic the three hydrophobic residues found in the p53 binding epitope as a template for efficient inhibitor design (Gonzalez-Lopez de Turiso et al., 2013; Furet et al., 2016; Burgess et al., 2016) while reducing their toxicity. Several such designs are currently undergoing clinical trials (Burgess et al., 2016).

A different strategy for dual inhibition identifies peptide sequences based on the known binding motif. As a result, several linear peptides designs (Pazgier et al., 2009; Phan et al., 2010) with greater affinity than the original p53 peptide have been found. Peptide designs conserve the three hydrophobic residues that anchor in MDM2/X and make longer helices. Brownian Dynamics was used to investigate differences in binding kinetics for several peptide sequences (ElSawy et al., 2016). Despite the greater binding affinity to MDM2 and MDMX as mentioned above, linear peptides exhibited a poor ADME profile: they are easily degraded and hampered to cross barriers, limiting their use

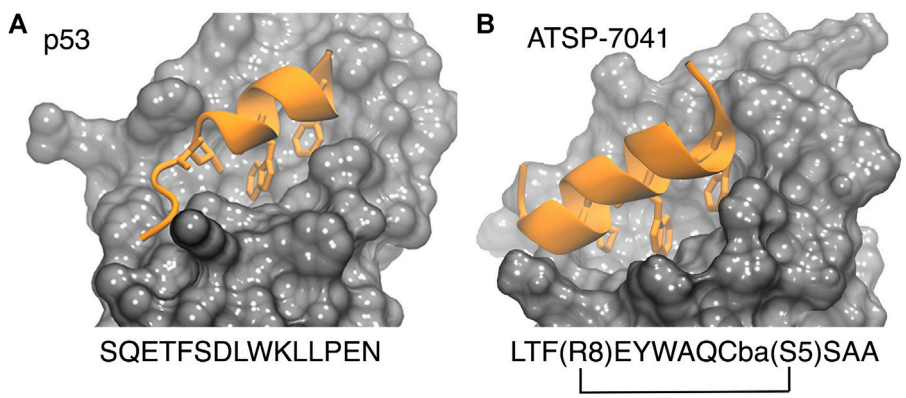

FIGURE 2 | P53 (**left**, PDB 1ycr) and a stapled peptide (**right**, MELD prediction) binding MDM2. Three anchoring hydrophobic residues in the peptide as shown as sticks (orange). The cartoon representation shows the extended helix for the ATSP7041 stapled peptide.

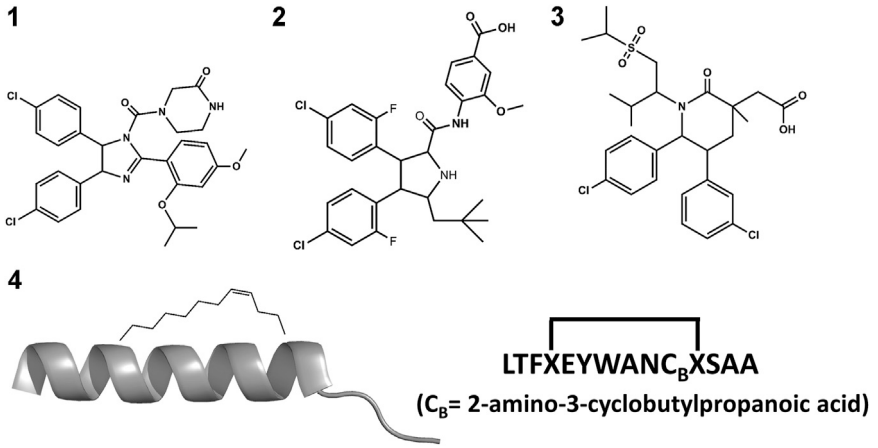

FIGURE 3 | Chemical structures of nutlin-3a (1); idasanutlin (2); AMG-232 (3) and ATSP-7041 (4).

as drugs. They are however great starting points for peptidomimetic design. A different strategy uses non-standard amino acid backbones (Sang et al., 2020) to increase resistance to degradation while keeping the side-chains that allow strong interactions with the protein receptors. Several such peptides have advanced to clinical trials (Carvajal et al., 2018; Jiang and Zawacka-Pankau, 2020).

Stapled peptides represent an interesting alternative to overcome some limitations of linear peptides by easily crossing barriers, being resistant to degradation and adopting stable helical conformations that favor binding (Bernal et al., 2007; Chang et al., 2013; Meric-Bernstam et al., 2017), leading to strong inhibitors. Tan and co-workers introduced the need for rational design to incorporate chemical staples by maintaining enthalpic interactions while reducing entropic costs (Tan et al., 2016). Our work on this field has centered on identifying bound conformations through integrative modeling approaches based on molecular dynamics simulations (Morrone et al., 2017a; Morrone et al., 2017b; Lang and Perez, 2021). We have been able to predict the binding of several linear and cyclic peptides as well as qualitative relative binding free energies (Morrone et al., 2017b). We identify different binding mechanisms for different peptides (Lang and Perez, 2021): p53 which is intrinsically disordered binds in a disordered state and then folds in the active site, whereas ATSP-7041 (**4** in **Figure 3**) is a stapled peptide that binds as a helix. In the latter case, an incorrect orientation of the side chains requires partial unbinding and rebinding of the stapled inhibitor. Due to long residence times, even partial unbinding can be a slow step in simulations, leading to slow convergence. A linear peptide (pdiq) with strong helical propensities is shown to be able to rearrange its side chains by partially unfolding in the active site. Thus, pdiq avoids the slow unbinding step.

THE BH3-BCL-2 INTERACTION

Apoptosis is an evolutionarily conserved, regulated form of cell death involved in tissue homeostasis, embryonic development and immunity (Elmore, 2007). Apoptosis dysregulation has a major impact in disease, since an excessive response can lead to neurodegeneration or an increased ischemic risk, whereas a defective response plays a major role in tumor development and autoimmune diseases (Favaloro et al., 2012). The intrinsic apoptotic pathway (physiologically dominant and not mediated by a death receptor) is regulated through a complicated PPI network involving the B-cell lymphoma-2 (Bcl-2) family of proteins. With some of the members exhibiting pro-apoptotic activity and others pro-survival profiles, the apoptotic process is initiated by the interaction of pro-apoptotic and pro-survival members regulating mitochondrial outer membrane permeability, a crucial step in apoptosis (Chipuk et al., 2010; Czabotar et al., 2014). The interplay of the members of this family of proteins represents a good example illustrating how a short linear peptide motif is key to regulate a complex network of PPIs.

More than 20 members of the Bcl-2 protein family have been characterized so far. Sequence analysis indicates that they share one or more specific conserved regions known as Bcl-2 homology (BH) domains that are necessary for function, since their deletion via molecular cloning affects survival/apoptosis rates. Pro-survival members such as Bcl-2, Bcl-xL, Bcl-w, Mcl-1, Bfl1/A1 and Bcl-B are characterized for exhibiting four homology domains (BH1-BH4) together with a transmembrane domain. On the other hand, pro-apoptotic members can be classified into two subgroups: the multi-BH domain proteins including the pro-apoptotic effectors Bax and Bak with four BH domains (BH1-BH4) together to a transmembrane domain and the BH3-only proteins such as Bim, Bid, Puma, Bad, Bik, Bmf, Hrk and Noxa that share little sequence homology, apart from the BH3-domain (Chittenden, 2002). Some of the BH3-only proteins like Bim, Bid and to a lesser extend Puma are direct activators of the pro-apoptotic effector proteins, whereas the rest are sensitizers that indirectly activate Bak and Bax by binding to pro-survival proteins and liberating BH3-only activators (Singh et al., 2019) (**Figure 4**).

Despite the progress made in the last years, the mechanism of apoptosis regulation by the Bcl-2 family of proteins is not completely understood (Ichim and Tait, 2016). It is well established that the relative amounts of pro-apoptotic and pro-survival proteins in a cell, together with the capability of these proteins to form heterodimers, determine cell susceptibility to undergo apoptosis (Oltvai et al., 1993). Moreover, it is well established that pro-survival proteins inhibit apoptosis by directly binding to and sequestering their pro-apoptotic counterparts. This hypothesis was demonstrated when the BH3 domain of pro-apoptotic proteins showed capability to induce apoptosis in cell-free systems and HeLa cells (Holinger et al., 1999; Wang et al., 2000). Thus, under normal conditions in healthy cells, pro-survival Bcl-2 proteins sequester pro-apoptotic effectors as well as BH3-only proteins, preventing apoptosis. However, upon cytotoxic stress, the overwhelming number of BH3-only proteins produced activate pro-apoptotic effectors either by direct binding or through the liberation of restrained pro-apoptotic effectors by binding to pro-survival Bcl-2 proteins. This process originates the accumulation and activation of pro-apoptotic effectors with their subsequent oligomerization at the mitochondrial outer membrane, inducing its permeability (Chipuk et al., 2010; Singh et al., 2019). Moreover, the variable affinities exhibited by the diverse members of family for each other and their modulation when proteins are embedded in a membrane are also relevant. Consequently, BH3 domain peptide analogs and surrogates have been long considered appealing molecules for therapeutical intervention (Goldsmith et al., 2006), especially in cancer, since downregulation of apoptosis is considered a key step for the initiation and maintenance of the disease (Hanahan and Weinberg, 2000; Hanahan and Weinberg, 2011).

Structural studies on diverse members of the Bcl-2 family have provided a wealth of information, being key to understand the molecular mechanisms by which the intrinsic apoptosis pathway is regulated. The 3D structure of the human Bcl-xL in its apo form, solved by NMR spectroscopy and X-ray crystallography was the first one available (Muchmore et al., 1996). It consists of eight alpha helices (α1-α8) that are connected to the BH domains. Specifically, the BH2 spans along helix α8, the BH3 along helix α2 and the BH4 along helix α1. In contrast, the BH1 spans partially along helices α4 and α5 together to the loop connecting them (**Figure 5A**). In addition, the protein also has a C-terminal segment that serves as an anchor to the membrane, needed to be removed to conduct structural studies. A major feature of the structure is the large hydrophobic groove formed by the BH1-BH3 domains that corresponds to the interaction site of the BH3 domain of its counterpart family members, as shown in diverse crystallographic structures. The structures of the rest of the pro-survival members of the Bcl-2 family in their apo form exhibit the same topology (Petros et al., 2001; Hinds et al., 2003; Day et al., 2005; Harvey et al., 2018). Interestingly, the structures of the pro-apoptotic effectors Bak and Bax also exhibit the same topology, despite their diametrically opposing functions (Suzuki et al., 2000; Moldoveanu et al., 2006). In contrast, except for Bid that also exhibits a similar structure (Chou et al., 1999), most BH3-only proteins are intrinsically disordered (Hinds et al., 2007).

There are currently no heterodimer structures available involving Bcl-2 family members. However, several structures of pro-survival Bcl-2 members bound to BH3, the linear peptide motif involved in pro-survival-pro-apoptotic PPIs are

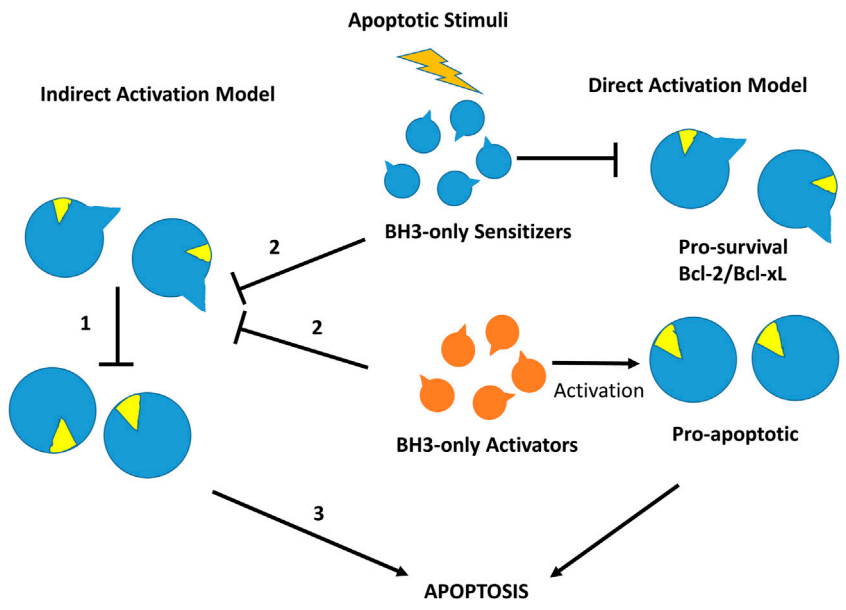

FIGURE 4 | Direct and indirect mechanism models for Bax or Bak activation in the intrinsic cell death pathway. In the indirect activation model **(left)**, in the resting state effectors Bax and Bak are inhibited directly by pro-survival members (1). After an apoptotic stimulus, BH3-only proteins bind to pro-survival proteins releasing pre-activated Bak and Bax (2) to initiate the apoptosis process (3). In the direct activation model **(right)**, after an apoptotic stimulus BH3-only activators activate Bak/Bax, whereas BH3-sensitizers inhibit pro-survival Bcl-2 members, initiating the apoptotic process.

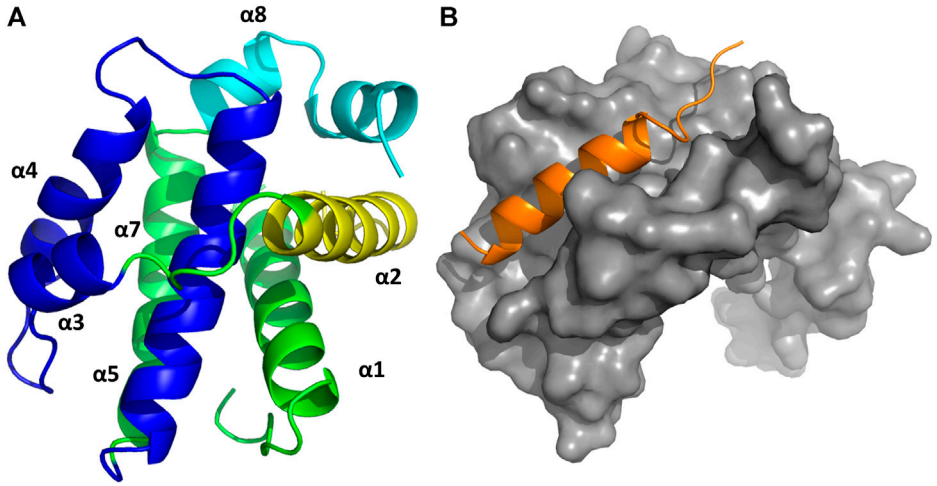

FIGURE 5 | (A) 3D structure of Bcl-xL (PDB ID: 1MAZ) with the diverse elements of secondary structure labeled. The BH domains are color-coded: BH1 navy blue; BH2 cyan; BH3 yellow; BH4 dark green. **(B)** 3D structure of the complex Bcl-xL/BH3-Bak (in orange) (PDB ID:5FMK).

available. The complex Bcl-xL-Bak BH3 domain was the first three dimensional structure solved of any Bcl-2 protein complex (**Figure 5B**) (Sattler et al., 1997). The structure shows the BH3 domain in a helical structure bound to a hydrophobic groove with four hydrophobic residues projecting their side chains into the cleft and with the Asp^{83} residue displaying an electrostatic interaction with Arg^{139} in Bcl-xL. Subsequently, several structures of BH3 domains bound to diverse pro-survival Bcl-2 members were reported in the literature, all of them exhibiting the same general features found in the Bcl-xL-Bak BH3 complex (Petros et al., 2004). Sequence alignment of the diverse BH3 domains shows they display the consensus sequence $\Phi_1\Sigma XX\Phi_2XX\Phi_3\Sigma DZ\Phi_4\Gamma$, where Φ_n represents a hydrophobic residue, Σ is a residue with a short side chain, Z an acidic residue, Γ is a hydrophilic residue and X represents any residue (Chen et al., 2005; Day et al., 2008; Lomonosova and Chinnadurai, 2008). The Φ_2 residue is a leucine in all pro-apoptotic BH3-only members whereas Ile, Leu, Val, Met or an aromatic residue are frequently found for the rest Φ_n. The pattern Φ_n display guarantees their alienation on the same face of a helical structure. These four residues together with the conserved aspartic acid are the residues responsible for binding the hot spots at the hydrophobic binding cleft consisting of four hydrophobic pockets (P1-P4) together with a conserved arginine. As mentioned above, the pro-apoptotic BH3 domains bind the pro-survival proteins with different affinities. Thus, Bim and Puma have comparable affinity for all pro-survival proteins. Bad and Bmf preferently bind Bcl-2, Bcl-xL and Bcl-w, whereas Noxa bind only Mcl-1 and Bfl1/A1 and Bid, Bik and Hrk bind Bcl-xL, Bcl-1 and Bfl1/A1 (Chen et al., 2005). This differential profile is due to differences in their sequence, since mutations can reverse binding preferences (Campbell et al., 2015). Numerous structural and computational studies have been performed to understand the nature of the binding preferences between BH3 peptides the diverse members of the Bcl-2 family, providing a deeper insight into the nature of these interactions key to design BH3 peptide surrogates and peptidomimetics (Lama and Sankararamakrishnan, 2011; Ivanov et al., 2016; Zhang et al., 2018; Vila-Julià et al., 2020). This knowledge is specially relevant for designing selective BH3 analogs (Denis et al., 2020; Reddy et al., 2020).

In order to design drugs with BH3 functionality, peptide analogs and surrogates are expected to be more resistant to proteolytic enzymes and can also be designed to exhibit higher populations of the bioactive conformation in solution compared to the original linear peptides. Diverse strategies have been used for the discovery of potent peptide surrogates of the BH3 domain (Orzáez et al., 2009). As a general strategy, increased resistance to proteolytic enzymes can be carried out by replacing peptide bonds by isosteres or using a holistic approach, constructing retro-inverso analogs or peptoids (Perez et al., 2002; Akram et al., 2014; Perez, 2018). The design of α/β peptide surrogates of BH3 with sequences alternating α and β amino acids have been successfully designed (Horne et al., 2008). Interestingly, the α/β alternating pattern can modify the pharmacodynamic profile of the analogs changing their affinity or moreover, their selectivity for the different pro-survival proteins (Boersma et al., 2012).

Experimental studies as well as computational studies reveal that BH3 peptides do not exhibit a helical structure in solution (Petros et al., 2000; Perez et al., 2016). In order to avoid negative configurational entropy effects, the affinity of the analogs can be increased by designing analogs that enhance the bioactive conformation population in solution by embedding helix enhancer residues in the sequence (Delgado-Soler et al., 2013). An alternative approach focused on constraining the helical structure of the analogs in solution. Early attempts to stabilize the Bak BH3 peptide used lactam cross-links side chain-to-side chain at positions i and i+4 (**5** in **Figure 6**). Unfortunately, although the peptides exhibit helical structure, none of these analogs showed any binding to Bcl-2 due to a steric hindrance with the receptor (Yang et al., 2004). In contrast, the hydrocarbon

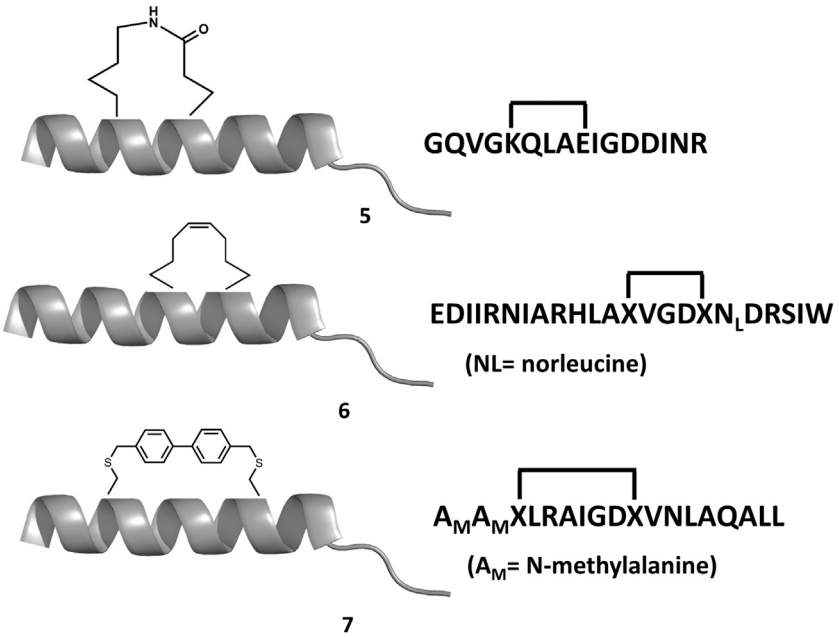

FIGURE 6 | Chemical structures of diverse stapled analogs of the BH3 domain.

stapling approach demonstrated to be a successful approach. In this case, macrocyclization between specific residues of the helix occurs via a ring-closing metathesis reaction using α,α-di-substituted amino acids with olefin tethers as building blocks. This procedure was successfully used to stabilize the Bid BH3 peptide (**6** in **Figure 6**), proving to be helical, protease-resistant, and cell-permeable molecules that bound with increased affinity to multidomain Bcl-2 member pockets (Walensky et al., 2004). However, not every stapled BH3 helix exhibits improved bioactivity, which requires the synthesis and testing of a set of modified peptides to identify suitable candidates. Other types of staples have also been used. For example, bisaryl cross-linkers have been used recently to reinforce peptide helices containing two cysteines at positions i and i+7. This approach has been used for the stabilization of the Noxa BH3 peptide (**7** in **Figure 6**), showing a potent cell-killing activity in Mcl-1-overexpressing cancer cells (Muppidi et al., 2012). After an optimization process, the final molecule exhibits increased helicity in regard to the native peptide and an improved pharmacokinetic profile including cell permeability and proteolytic stability.

A different strategy focuses on finding small-molecule mimics of the BH3 domains (Roy et al., 2014; Yap et al., 2017). Despite a-helix mimics have been reported (Yap et al., 2017), most of the BH3 mimetics have been discovered from an optimization process that started with a hit identified by high throughput screening, followed a hit-to-lead structure-based optimization process helped with biophysical techniques and computational methods. Hits identified from natural products libraries include antimycin A3 (Tzung et al., 2001), gossypol and purpurogallin (Kitada et al., 2003), epigallocatechin gallate and theaflavinin or the alkaloid prodigiosin (Chang et al., 2011). On the other hand, hits found in commercial libraries include BH3I-1 and BH3I-2 (Degterev et al., 2001). Gossypol was used as starting structure to discover interesting Bcl-2 inhibitors (Becattini et al., 2004) like sabutoclax (**8** in **Figure 7**) (Wei et al., 2010) or TW-37 (**9** in **Figure 7**) (Wang et al., 2006). Similarly, prodigiosin was used as starting molecule to discover obatoclax (**10** in **Figure 7**), an inhibitor of pro-survival members of the Bcl-2 family that antagonize Bax or Bak, causing cytotoxicity. The compound has gone through several clinical II studies for the treatment of patients with solid tumors and hematopoietic malignancies (Shoemaker et al., 2006). On the other hand, optimization of BH3I-1 led to the discovery of WL-276 (**11** in **Figure 7**) (Wang et al., 2008) with a similar inhibitory activity against Bcl-2 and enhanced inhibitory activity against Bcl-X_L as compared with gossypol. In contrast, WL-276 effectively induces apoptosis in PC-3 cells at low micromolar concentrations. Similarly, the compound WEHI-539 (**12** in **Figure 7**) was optimized from a hit identified in high throughput screening following a structure-guided approach. The compound exhibits high affinity and selectivity for BCL-X_L and potently kills cells by selectively antagonizing its pro-survival activity (Lessene et al., 2013).

A NMR spectroscopy based fragment screening approach coupled with computational studies was also used to discover other small-molecule inhibitors of Bcl-2. Specifically, these studies led to the discovery of ABT- 737 (**13** in **Figure 8**) (Oltersdof et al., 2005), a potent small-molecule inhibitor of Bcl-2, Bcl-xL, and Bcl-w. Although the compound is not orally available, it exhibits an acceptable pharmacokinetic profile when administered intraperitoneally. The crystallographic structure of the complex with Bcl-x_L (Lee et al., 2007) shows ABT-737 sitting on the hydrophobic BH3 binding cleft as expected from its design (**Figure 9**). Further optimization of the molecule led to the discovery of the orally bioavailable Navitoclax (ABT-263) (**14**

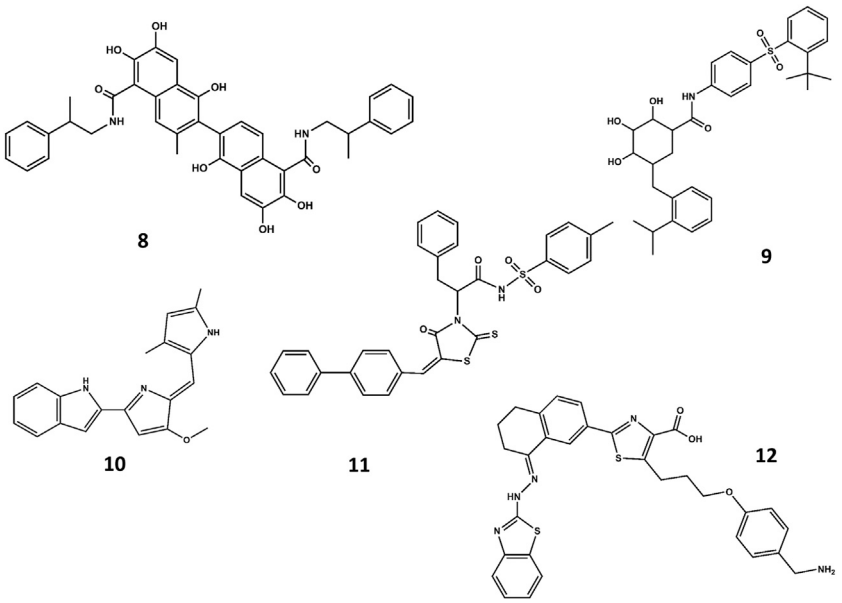

FIGURE 7 | Chemical structures of diverse small molecule mimics of the BH3 domain. Sabutoclax (**8**); TW-37 (**9**); obatoclax (**10**); WL-276 (**11**); WEHI-539 (**12**).

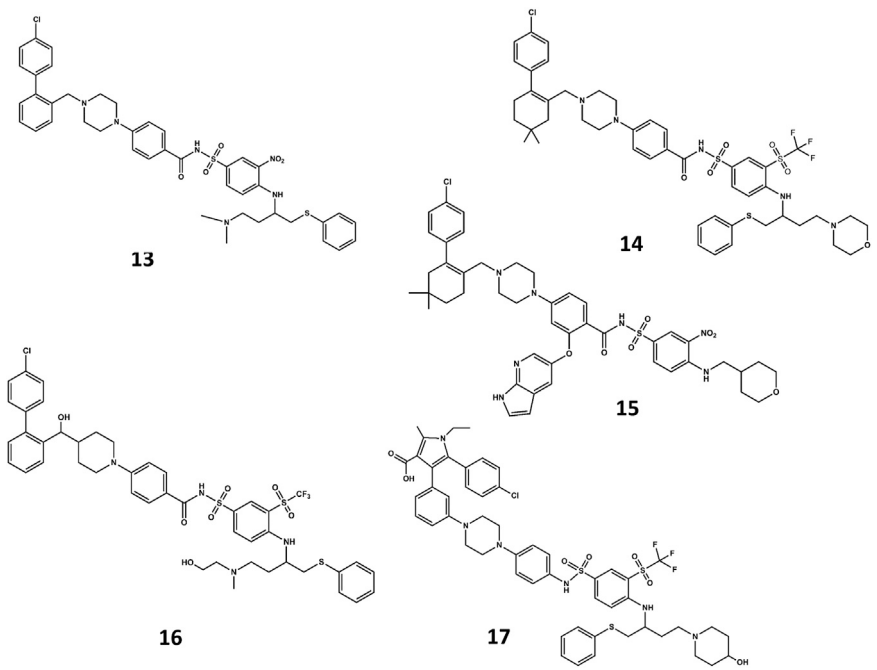

FIGURE 8 | Chemical structures of diverse small molecule mimics of the BH3 domain. ABT-737 (**13**); Navitoclax (ABT-263) (**14**); venetoclax (ABT-199) (**15**); BM-975 (**16**); AZD4320 (**17**).

in **Figure 8**) (Tse et al., 2008). Both compounds are peptidomimetics of the Bad-BH3 domain, so they are potent binders of Bcl-2, Bcl-xL and Bcl-w, but not to Mcl-1 or Bfl1/A1, exhibiting a demonstrated antitumor activity *in vitro* and *in vivo*. While clinical responses with navitoclax were promising, mechanistic dose-limiting thrombocytopoenia was observed in patients under treatment due to Bcl-xL inhibition in platelets. Further studies were undertaken to remove the undesired side effects, leading in the discovery of venetoclax (ABT-199) (**15** in **Figure 8**) (Pan et al., 2014), a highly selective Bcl-2 inhibitor that

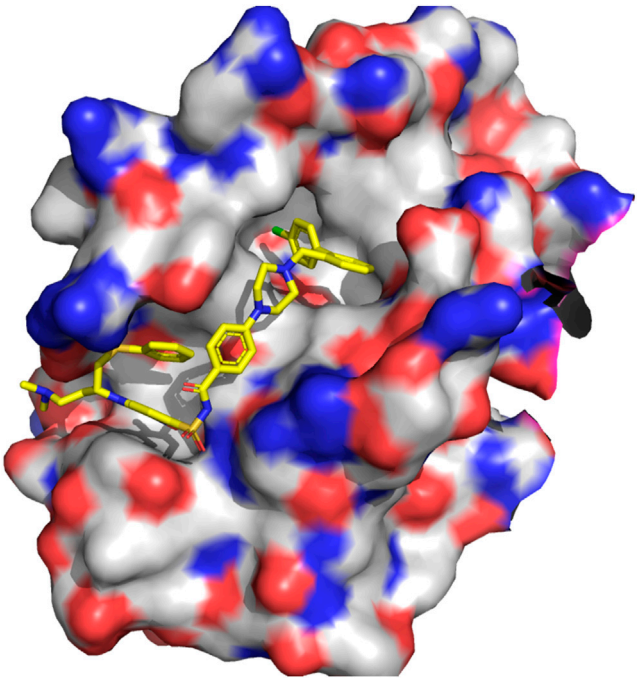

FIGURE 9 | 3D structure of the complex Bcl-xL/ABT-737 (PDB ID: 5MFK).

was approved by the US FDA in April 2016 as a second-line treatment for chronic lymphocytic leukemia. Inspired by ABT-737, a series of inhibitors with a 4,5-diphenyl-1H-pyrrole-3-carboxylic acid as core structure have been developed. Among them, compound BM-957 (**16** in **Figure 8**) that binds to Bcl-2 and Bcl-xL with high affinity and shows potent activity in cell growth inhibition in small-cell lung cancer cell lines like the H1147 and H146 (Chen et al., 2012). Also inspired by ABT-737 and following a structure based process, AZD4320 (**17** in **Figure 8**) was recently developed (Balachander et al., 2020). This is a dual inhibitor of Bcl-2 and Bcl-xL that minimizes Bcl-xL–mediated thrombocytopenia. The compound has been used satisfactorily to design AZD0466, a drug-dendrimer conjugate, where AZD4320 is chemically conjugated to a PEGylated poly-lysine dendrimer (Patterson et al., 2021).

INTEGRINS AND TISSUE ENGINEERING

Integrins orchestrate cell–cell and cell–extracellular matrix adhesive interactions from embryonic development to mature tissue function involving PPIs with other proteins located in the extracellular matrix (ECM) of tissues (Barczyk et al., 2010). The ECM refers to different molecules that are secreted by cells, mainly polysaccharides, small molecules and proteins, that serve as matrix that provide structural and biochemical support to the surrounding cells (Frantz et al., 2010). Such interactions occur naturally in native tissues and can be altered in the presence of injuries or damaged tissues. In this context, and in order to allow tissue regeneration, the discipline of tissue engineering has emerged in order to guide cells, tissues and ultimately, organs, to recover their function (Langer and Vacanti, 1993). However, integrins not only play an important role in regulating cell adhesion, but also function as integral transmembrane signaling molecules in the regulation of cellular behavior such as organization of the intracellular cytoskeleton, regulation of the cell cycle or movement of new receptors to the cell membrane (Giancotti and Ruoslahti, 1999; Kadry and Calderwood, 2020). They are also involved in blood coagulation and in pathophysiological processes such as tumor growth, metastasis, or angiogenesis. Specific functions of integrins have been exploited for therapeutical intervention. Thus, diverse PPIs disruptors have been designed for the treatment of thrombosis, stroke and myocardial ischemia (Scarborough and Gretler, 2000) or for the treatment of cancer and osteoporosis (Auzzas et al., 2010). On the other hand, knowledge of the nature of the PPIs involved with the ECM can be used to mimic integrin ligands in tissue engineering.

Integrins are heterodimers integral transmembrane proteins composed of α and β subunits that modulate the association between the extracellular matrix and the cytoskeleton. More than twenty different α/β heterodimeric integrins have been recognized, resulting from the combination of eighteen α and eight β subunits (Hynes 2002; Barczyk et al., 2010). The most widely studied members of this subgroup have in common a β3 subunit. Specifically, the platelet receptor αIIbβ3 that binds fibrinogen, involved in the blood coagulation process and, the fibronectin receptor αvβ3 that binds a wide variety of ligands and is up-regulated in many solid tumors contributing to the mechanisms involved in tumor growth and metastatic dissemination. Integrins signaling is initiated by binding to different proteins in the ECM including fibronectin, laminin, vitronectin, collagen or cell-surface receptors such as intercellular adhesion molecule-1 (ICAM-1) and vascular cell-adhesion molecule-1 (VCAM-1).

Integrins and ECM proteins PPIs occur via short peptide linear binding motifs (Ruoslahti, 1996). One of these motifs is the sequence Arg-Gly-Asp (RGD), common to a subgroup of eight integrins that was the object of study for designing inhibitors of platelet aggregation. The RGD motif is not a potent inhibitor of αIIbβ3 in platelet aggregation assays. However, extension with an amino acid at the C-terminal significantly enhances the inhibitory activity of these peptides (Pierschbacher and Ruoslahti, 1984). Subsequent studies by means of NMR conformational analysis and molecular dynamics simulations led to the design of cyclic peptides embedding the RGD sequence. These studies demonstrated that analog selectivity for different integrins was associated with the conformation the RGD segment attains. Specifically, the distance between the basic arginine side chain and the acid aspartic side chain controlled by the conformation of the macrocycle. In the αIIbβ3 selective pentacyclic peptides the peptide adopts a conformation with a β-turn centered on Gly together with a distorted type II′ β-turn involving the two other residues at the i+1 and i+2 positions, respectively (Müller et al., 1994). On the other hand, pentacyclic peptides selective for the αvβ3 receptor exhibit a reverse β-turn centered on the Asp residue and a distorted type II′-β turn with Gly and Asp at the i+1 and i+2 positions, respectively. In the case of the hexacyclic peptides, selectivity could be shifted from αIIbβ3 to αvβ3 by forcing the conformation attained by the peptide from a type II′

to a type I β-turn conformation. This forces the arginine side chain either to adopt a pseudoequatorial orientation or to be raised above the plane of the backbone in a pseudoaxial orientation, respectively (Bach et al., 1996). These studies led to the discovery of selective antagonists of the αIIbβ3 and αvβ3 receptors (Andronati et al., 2004; Auzzas et al., 2010) including the commercially available cyclic heptapeptide eptifibatide, a potent αIIbβ3 selective antagonist (Scarborough et al., 1993), and the cyclic pentapeptide cilengitide, a potent αvβ3 selective antagonist (Dechantsreiter et al., 1999).

The concept of tissue engineering aims at stimulating the regeneration of a damaged tissue (Perez et al., 2015). For this purpose, the combination of three main elements is essential in order to provide the appropriate signaling to induce the desired effect (Perez et al., 2013). The three key elements are: scaffolds, short linear peptide motifs and cells. The aim of these three main components is to mimic to the maximum extent the situation that takes place in natural tissue healing (Perez et al., 2015). In this sense, the scaffold serves as a matrix that presents similar characteristics to the natural extracellular matrix of tissues. The scaffold can be loaded with molecules involved in the regeneration of the tissues, which depending on the tissues, can involve growth factors, cytokines or drugs (Garg et al., 2012). Finally, these constructs will allow the attachment, proliferation and differentiation of cells that will ultimately, once implanted in the site of defect, guide the surrounding tissues to induce new tissue formation. Among the three different elements, scaffolds play a pivotal role in providing the appropriate cues to allow the interplay between cells and tissue with the scaffolds itself (Perez et al., 2013).

Scaffolds can be composed of different types of materials, which can be from polymeric origin, ceramics or metallic (O'Brien, 2011). The selection of the materials will mainly depend on the targeted tissue to be regenerated, using soft materials (polymers) for soft tissues such as neuronal tissues and cartilage, and stiff materials (ceramics and metals) for hard tissues, mainly bone (Engler et al., 2006). In all cases, these scaffolds need to mimic to some extent the ECM. In order to replicate the attachment of cells onto the ECM, synthetic materials need to provide similar ECM cues to allow the protein-protein interaction that will eventually lead to cell attachment and guide cells into the regeneration processes (Perez et al., 2013). Hence, the scaffolds, if properly selected, can act as mediator and guidance for the regeneration of tissues. For this purpose, the scaffolds themselves can be composed of natural proteins which possess cell recognition sites (epitopes) that will allow the interaction with cells, or they can be designed as a non-protein origin (Dhandayuthapani et al., 2011). In the latter case, it is essential to provide within the scaffolds certain cues to allow cell-material interaction (Tallawi et al., 2015). For this purpose, several domains can be covalently attached on the surface of the materials, such as proteins, peptides, drugs or growth factors to name a few. Generally speaking, proteins present certain cell instructive domains that will allow the recognition by cells and allow interaction. Nevertheless, the presence of proteins within the body can induce non-desired effects such as an acute immune response. Furthermore, as proteins are big molecules, their epitopes need to be properly exposed for cells to interact, otherwise their positive effect can be neglected. Taking this into account, peptides have appeared as domains that can be used as well, allowing only using the specific amino acid sequence that is active for cell adhesion or cell guidance with the added value that will prevent from any immune response and will be easily allocated in the proper manner to allow cell interaction (Perez et al., 2013; Tallawi et al., 2015; Klimek and Ginalska, 2020).

Regarding the short linear peptide motifs, there have been a number of epitopes discovered to have relevant properties in specific cell functionalities. The most widely known amino acid sequence is RGD (Arg-Gly-Asp), which is an amino acid sequence found in several ECM proteins, such as collagen, laminin, fibronectin or vitronectin, mainly having key role in cell adhesion (Jeschke et al., 2002; Petrie et al., 2008; Von Der Mark et al., 2010). Several peptides possess similar potential to allow cell adhesion, such as PHSRN and YIGSR (Fittkau et al., 2005). There are other amino acid sequences with different potential and with more specific targets. For instance, IKVAV, which is an epitope from the α-1 laminin chain, enhances cell growth, neuronal differentiation and nerve regeneration (Patel et al., 2019). In a similar way, KLPGWSG induces as well neuronal differentiation (Caprini et al., 2013). While these peptides are related with ECM proteins, other peptides have mimicked specific growth factors, such as bone morphogenetic protein, vascular endothelial growth factors or brain derived neurotrophic factors. These growth factors are molecules that are released from cells into the ECM and have great therapeutic potential. In this sense, peptide such as KPSS, KLT and RGI are able to regulate bone regeneration, angiogenesis and nerve regeneration respectively (Ding et al., 2020).

Despite general knowledge on how certain epitopes are able to guide cell behavior, there are still undiscovered number of epitopes that could provide similar potential to those already known. While these epitopes could be empirically and experimentally discovered, this would be both time consuming and not cost-effective. For this reason, computational strategies open a window of unlimited epitope discovery that will more finally tune tissue guidance. Up to now, sequences are not taken into account as cell specific, or in other words, as integrins specific, since not all cells present that same cell membrane integrins. Discovering among the selective interactions of certain integrins with specific peptides may be of great potential.

OPPORTUNITIES FOR COMPUTATIONAL APPROACHES IN TISSUE ENGINEERING

A straightforward application of the principles described in the cases of p53 and bcl2 into tissue engineering is the identification of naturally occuring binding modes and interactions between ECM elments and integrins. This knowledge can lead to the identification of functional peptide motifs that have not currently been identified and the design of new chemical molecules that bind certain integrins specifically. As an example, the RGD motif has been characterized using computational and experimental tools due to its ability to bind different integrin types. However, the interplay of internal structure of the motif and binding mode give rise to nuances in the binding and recognition (Dechantsreiter et al., 1999; Kapp et al., 2017). Thus, the presence of an RGD motif inside a particular scaffold might force conformations of the motif that are only recognized by a subset of

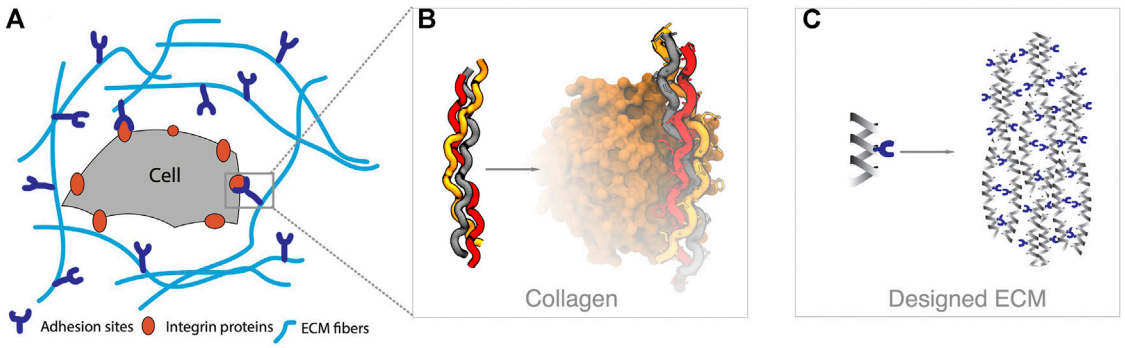

FIGURE 10 | Tissue engineering overview. **(A)** The surface of a cell is covered with different types of integrin proteins, which recognize molecular queues in the extracellular matrix (ECM) environment. **(B)** The ECM is composed of diverse biological components, such as collagen fibers, which can interact with integrins through specific amino acid sequences (e.g., GFOGER in the example, pdbid 1dzi). **(C)** The goal in tissue engineering is to design materials, such as self-assembling peptides that provide an ECM scaffold and chemical queues that can trigger cellular behavior.

integins. A hybrid computational and experimental approach used metadynamics based sampling to design a small molecule antagonist (RUC-1) that is specific to only one type of integrin (Zhu et al., 2010). The native RGD antagonist binds different integrins and induces a conformational change between a closed and an open state; whereas the RUC-1 antagonist binds only in the αIIbβ3 integrin without inducing a change between the closed and open state (Zhu et al., 2010). Other computational approaches target membrane proteins like integrins by optimizing the sequence of the peptide epitope that binds the membrane receptors (Yin et al., 2007; Shandler et al., 2011).

A second area of interest is in the development of material that self-assembles to provide a scaffold for cells. A common strategy is to use self-assembling peptides that can from hydrogels on injection into a patient–thus localizing to a specific region in the body (Wade et al., 2012; Loo et al., 2015). There are several approaches to achieve molecular self-assembly which have been previously described experimentally (Loo et al., 2015), many of which rely on peptide sequences. These self-assembling peptides should have a sequence capable of self-assembling, while at the same time carrying a sequence motif that is accessible and recognizable by integrins, to dictate their behavior (see **Figure 10**). This is a chance for computational approaches to carry out systematic analysis of optimal sequence design to achieve specific mechanical properties (e.g., mechanical stiffness), and rational optimization for active and accessible conformations of the integrin-binding motifs. Smadbeck and co-workers designed short peptide motifs that were able to self-assemble and did a posterior characterization using experimental approaches (Smadbeck et al., 2014), a second strategy is based on using proteins that fold into stable structures and then self-assemble (Chen et al., 2019). Despite these successes in computational design, many hybrid approaches rely on an experimental design followed by computational characterization, typically with molecular dynamics (Cormier et al., 2013; Leonard et al., 2013). The accumulated knowledge on peptides secondary structure propensities (Jones, 1999; Moreau et al., 2009; Best et al., 2012), protein structure and assembly prediction (Lensink et al., 2007; Moult et al., 1995) and design principles (Simons et al., 1999; Delgado et al., 2019) can provide useful insights in this area of research.

CONCLUSION

Computational and modeling approaches have long been involved in rational drug discovery. As the methods have matured, new opportunities emerge to model other types of molecules that can be beneficial as drugs, such as peptides. The challenges for computational methods continue to be related to sampling, scoring and the nature of the system under study. In systems where the protein receptor and ligand are rigid, predicting bound conformations is less challenging, and the quality of the scoring function dictates the accuracy of the predictions. As the systems become more flexible (both protein and ligand) requiring large conformational transitions and ability to bind through several possible binding modes, the interplay between sampling and scoring becomes more relevant to account not only for direct interactions but the ability to adopt bound conformations. General strategies for design include maximizing peptide interactions in the bound conformation and deriving peptidomimetic or small molecule solutions that maintain the interaction profile while reducing the internal flexibility of the ligand. We have highlighted opportunities to apply these methods to the field of tissue engineering, where recent advances in structure prediction can play a big role.

AUTHOR CONTRIBUTIONS

All authors listed have made a substantial, direct, and intellectual contribution to the work and approved it for publication.

FUNDING

JJP likes to thank the Government of Catalonia (2017 SGR 163) and the Instituto de Salud Carlos III (COV20/00052) for financial support. AP is thankful for a seed grant from the University of Florida Informatics Institute (00130138). RAP is thankful for the

funds provided by the Government of Catalonia (2017 SGR 708), the Spanish Ministry of Science and Innovation (Ramón y Cajal fellowship (RYC2018-025977-I) and project RTI2018-096088-J-100 (MINECO/FEDER).

REFERENCES

Adams, J. M., and Cory, S. (1998). The Bcl-2 Protein Family: Arbiters of Cell Survival. *Science* 281, 1322–1326. doi:10.1126/science.281.5381.1322

Aderinwale, T., Christoffer, C. W., Sarkar, D., Alnabati, E., and Kihara, D. (2020). Computational Structure Modeling for Diverse Categories of Macromolecular Interactions. *Curr. Opin. Struct. Biol.* 64, 1–8. doi:10.1016/j.sbi.2020.05.017

Agrawal, P., Singh, H., Srivastava, H. K., Singh, S., Kishore, G., and Raghava, G. P. S. (2019). Benchmarking of Different Molecular Docking Methods for Protein-Peptide Docking. *BMC Bioinformatics* 19, 426. doi:10.1186/s12859-018-2449-y

Aiyer, S., Swapna, G. V. T., Ma, L. C., Liu, G., Hao, J., Chalmers, G., et al. (2021). A Common Binding Motif in the ET Domain of BRD3 Forms Polymorphic Structural Interfaces with Host and Viral Proteins. *Struct. S0969-* 2126, 00010–00011. doi:10.1016/j.str.2021.01.010

Akram, O. N., DeGraff, D. J., Sheehan, J. H., Tilley, W. D., Matusik, R. J., Ahn, J.-M., et al. (2014). Tailoring Peptidomimetics for Targeting Protein-Protein Interactions. *Mol. Cancer Res.* 12, 967–978. doi:10.1158/1541-7786.mcr-13-0611

Alam, N., Goldstein, O., Xia, B., Porter, K. A., Kozakov, D., and Schueler-Furman, O. (2017). High-resolution Global Peptide-Protein Docking Using Fragments-Based PIPER-FlexPepDock. *Plos Comput. Biol.* 13, e1005905. doi:10.1371/journal.pcbi.1005905

Alonso, H., Bliznyuk, A. A., and Gready, J. E. (2006). Combining Docking and Molecular Dynamic Simulations in Drug Design. *Med. Res. Rev.* 26, 531–568. doi:10.1002/med.20067

Amaro, R. E., Baudry, J., Baudry, J., Chodera, J., Demir, Ö., McCammon, J. A., et al. (2018). Ensemble Docking in Drug Discovery. *Biophysical J.* 114, 2271–2278. doi:10.1016/j.bpj.2018.02.038

Andronati, S. A., Karaseva, T. L., and Krysko, A. A. (2004). Peptidomimetics - Antagonists of the Fibrinogen Receptors: Molecular Design, Structures, Properties and Therapeutic Applications. *Curr. Med. Chem.* 11, 1183–1211. doi:10.2174/0929867043365314

Andrusier, N., Mashiach, E., Nussinov, R., and Wolfson, H. J. (2008). Principles of Flexible Protein-Protein Docking. *Proteins* 73, 271–289. doi:10.1002/prot.22170

Antes, I. (2010). DynaDock: A New Molecular Dynamics-Based Algorithm for Protein-Peptide Docking Including Receptor Flexibility. *Proteins* 78, 1084–1104. doi:10.1002/prot.22629

Antunes, D. A., Moll, M., Devaurs, D., Jackson, K. R., Lizée, G., and Kavraki, L. E. (2017). DINC 2.0: A New Protein–Peptide Docking Webserver Using an Incremental Approach. *Cancer Res.* 77, e55–e57. doi:10.1158/0008-5472.can-17-0511

Arkin, M. R., Tang, Y., and Wells, J. A. (2014). Small-Molecule Inhibitors of Protein-Protein Interactions: Progressing toward the Reality. *Chem. Biol.* 21, 1102–1114. doi:10.1016/j.chembiol.2014.09.001

Auzzas, L., Zanardi, F., Battistini, L., Burreddu, P., Carta, P., Rassu, G., et al. (2010). Targeting αvβ3 Integrin: Design and Applications of Mono- and Multifunctional RGD-Based Peptides and Semipeptides. *Cmc* 17, 1255–1299. doi:10.2174/092986710790936301

Bach, A. C., Espina, J. R., Jackson, S. A., Stouten, P. F. W., Duke, J. L., Mousa, S. A., et al. (1996). Type II' to Type I β-Turn Swap Changes Specificity for Integrins. *J. Am. Chem. Soc.* 118, 293–294. doi:10.1021/ja953163+

Balachander, S. B., Criscione, S. W., Byth, K. F., Cidado, J., Adam, A., Lewis, P., et al. (2020). AZD4320, A Dual Inhibitor of Bcl-2 and Bcl-xL, Induces Tumor Regression in Hematologic Cancer Models without Dose-Limiting Thrombocytopenia. *Clin. Cancer Res.* 26, 6535–6549. doi:10.1158/1078-0432.ccr-20-0863

Barczyk, M., Carracedo, S., and Gullberg, D. (2010). Integrins. *Cell Tissue Res* 339, 269–280. doi:10.1007/s00441-009-0834-6

Becattini, B., Kitada, S., Leone, M., Monosov, E., Chandler, S., Zhai, D., et al. (2004). Rational Design and Real Time, In-Cell Detection of the Proapoptotic Activity of a Novel Compound Targeting Bcl-XL. *Chem. Biol.* 11, 389–395. doi:10.1016/j.chembiol.2004.02.020

Berman, H. M., Battistuz, T., Bhat, T. N., Bluhm, W. F., Bourne, P. E., Burkhardt, K., et al. (2000). The Protein Data Bank. *Nucl. Acids Res.* 28, 235–242. doi:10.1093/nar/28.1.235

Bernal, F., Tyler, A. F., Korsmeyer, S. J., Walensky, L. D., and Verdine, G. L. (2007). Reactivation of the P53 Tumor Suppressor Pathway by a Stapled P53 Peptide. *J. Am. Chem. Soc.* 129, 2456–2457. doi:10.1021/ja0693587

Best, R. B., de Sancho, D., and Mittal, J. (2012). Residue-Specific α-Helix Propensities from Molecular Simulation. *Biophysical J.* 102, 1462–1467. doi:10.1016/j.bpj.2012.02.024

Boersma, M. D., Haase, H. S., Peterson-Kaufman, K. J., Lee, E. F., Clarke, O. B., Colman, P. M., et al. (2012). Evaluation of Diverse α/β-Backbone Patterns for Functional α-Helix Mimicry: Analogues of the Bim BH3 Domain. *J. Am. Chem. Soc.* 134, 315–323. doi:10.1021/ja207148m

Borcherds, W., Theillet, F.-X., Katzer, A., Finzel, A., Mishall, K. M., Powell, A. T., et al. (2014). Disorder and Residual Helicity Alter P53-Mdm2 Binding Affinity and Signaling in Cells. *Nat. Chem. Biol.* 10, 1000–1002. doi:10.1038/nchembio.1668

Bowman, A. L., Nikolovska-Coleska, Z., Zhong, H., Wang, S., and Carlson, H. A. (2007). Small Molecule Inhibitors of the MDM2-P53 Interaction Discovered by Ensemble-Based Receptor Models. *J. Am. Chem. Soc.* 129, 12809–12814. doi:10.1021/ja073687x

Bowman, G. R., Ensign, D. L., and Pande, V. S. (2010). Enhanced Modeling via Network Theory: Adaptive Sampling of Markov State Models. *J. Chem. Theor. Comput.* 6, 787–794. doi:10.1021/ct900620b

B-Rao, C., Subramanian, J., and Sharma, S. D. (2009). Managing Protein Flexibility in Docking and its Applications. *Drug Discov. TodayToday* 14, 394–400. doi:10.1016/j.drudis.2009.01.003

Bruzzoni-Giovanelli, H., Alezra, V., Wolff, N., Dong, C.-Z., Tuffery, P., and Rebollo, A. (2018). Interfering Peptides Targeting Protein-Protein Interactions: the Next Generation of Drugs?. *Drug Discov. Today* 23, 272–285. doi:10.1016/j.drudis.2017.10.016

Bueren-Calabuig, J. A., and Michel, J. (2015). Elucidation of Ligand-dependent Modulation of Disorder-Order Transitions in the Oncoprotein MDM2. *Plos Comput. Biol.* 11, e1004282. doi:10.1371/journal.pcbi.1004282

Burgess, A., Chia, K. M., Haupt, S., Thomas, D., Haupt, Y., and Lim, E. (2016). Clinical Overview of MDM2/X-Targeted Therapies. *Front. Oncol* 6, 7. doi:10.3389/fonc.2016.00007

Campbell, S. T., Carlson, K. J., Buchholz, C. J., Helmers, M. R., and Ghosh, I. (2015). Mapping the BH3 Binding Interface of Bcl-xL, Bcl-2, and Mcl-1 Using Split-Luciferase Reassembly. *Biochemistry* 54, 2632–2643. doi:10.1021/bi501505y

Caprini, A., Silva, D., Zanoni, I., Cunha, C., Volontè, C., Vescovi, A., et al. (2013). A Novel Bioactive Peptide: Assessing its Activity over Murine Neural Stem Cells and its Potential for Neural Tissue Engineering. *New Biotechnol.* 30, 552–562. doi:10.1016/j.nbt.2013.03.005

Carvajal, L. A., Neriah, D. B., Senecal, A., Benard, L., Thiruthuvanathan, V., Yatsenko, T., et al. (2018). Dual Inhibition of MDMX and MDM2 as a Therapeutic Strategy in Leukemia. *Sci. Transl. Med.* 10, eaao3003. doi:10.1126/scitranslmed.aao3003

Cesa, L. C., Mapp, A. K., and Gestwicki, J. E. (2015). Direct and Propagated Effects of Small Molecules on Protein-Protein Interaction Networks. *Front. Bioeng. Biotechnol.* 3, 119. doi:10.3389/fbioe.2015.00119

Chang, C.-C., Chen, W.-C., Ho, T.-F., Wu, H.-S., and Wei, Y.-H. (2011). Development of Natural Anti-tumor Drugs by Microorganisms. *J. Biosci. Bioeng.* 111, 501–511. doi:10.1016/j.jbiosc.2010.12.026

Chang, Y. S., Graves, B., Guerlavais, V., Tovar, C., Packman, K., To, K.-H., et al. (2013). Stapled α–helical Peptide Drug Development: A Potent Dual Inhibitor of MDM2 and MDMX for P53-dependent Cancer Therapy. *Proc. Natl. Acad. Sci. USA* 110, E3445–E3454. doi:10.1073/pnas.1303002110

Chen, L., Willis, S. N., Wei, A., Smith, B. J., Fletcher, J. I., Hinds, M. G., et al. (2005). Differential Targeting of Prosurvival Bcl-2 Proteins by Their BH3-Only Ligands Allows Complementary Apoptotic Function. *Mol. Cel* 17, 393–403. doi:10.1016/j.molcel.2004.12.030

Chen, J., Zhou, H., Aguilar, A., Liu, L., Bai, L., McEachern, D., et al. (2012). Structure-Based Discovery of BM-957 as a Potent Small-Molecule Inhibitor of Bcl-2 and Bcl-xL Capable of Achieving Complete Tumor Regression. *J. Med. Chem.*, 55, 8502–8514.doi:10.1021/jm3010306

Chen, Z., Johnson, M. C., Chen, J., Bick, M. J., Boyken, S. E., Lin, B., et al. (2019). Self-Assembling 2D Arrays with De Novo Protein Building Blocks. *J. Am. Chem. Soc.* 141, 8891–8895. doi:10.1021/jacs.9b01978

Chipuk, J. E., Moldoveanu, T., Llambi, F., Parsons, M. J., and Green, D. R. (2010). The Bcl-2 Family Reunion. *Mol. Cel* 37, 299–310. doi:10.1016/j.molcel.2010.01.025

Chittenden, T. (2002). BH3 Domains: Intracellular Death-Ligands Critical for Initiating Apoptosis. *Cancer Cell* 2, 165–166. doi:10.1016/s1535-6108(02)00128-9

Chou, J. J., Li, H., Salvesen, G. S., Yuan, J., and Wagner, G. (1999). Solution Structure of Bid, an Intracellular Amplifier of Apoptotic Signaling. *Cell* 96, 615–624. doi:10.1016/s0092-8674(00)80572-3

Ciemny, M. P., Debinski, A., Paczkowska, M., Kolinski, A., Kurcinski, M., and Kmiecik, S. (2016). Protein-peptide Molecular Docking with Large-Scale Conformational Changes: the P53-MDM2 Interaction. *Sci. Rep.* 6, 37532. doi:10.1038/srep37532

Ciemny, M., Kurcinski, M., Kurcinski, M., Kamel, K., Kolinski, A., Alam, N., et al. (2018). Protein-peptide Docking: Opportunities and Challenges. *Drug Discov. Today* 23, 1530–1537. doi:10.1016/j.drudis.2018.05.006

Clackson, T., and Wells, J. (1995). A Hot Spot of Binding Energy in a Hormone-Receptor Interface. *Science* 267, 383–386. doi:10.1126/science.7529940

Cormier, A. R., Pang, X., Zimmerman, M. I., Zhou, H.-X., and Paravastu, A. K. (2013). Molecular Structure of RADA16-I Designer Self-Assembling Peptide Nanofibers. *ACS Nano* 7, 7562–7572. doi:10.1021/nn401562f

Czabotar, P. E., Lessene, G., Strasser, A., and Adams, J. M. (2014). Control of Apoptosis by the Bcl-2 Protein Family: Implications for Physiology and Therapy. *Nat. Rev. Mol. Cel Biol.* 15, 49–63. doi:10.1038/nrm3722

Das, A. A., Sharma, O. P., Kumar, M. S., Krishna, R., and Mathur, P. P. (2013). PepBind: A Comprehensive Database and Computational Tool for Analysis of Protein-Peptide Interactions. *Genomics, Proteomics & Bioinformatics* 11, 241–246. doi:10.1016/j.gpb.2013.03.002

Day, C. L., Chen, L., Richardson, S. J., Harrison, P. J., Huang, D. C. S., and Hinds, M. G. (2005). Solution Structure of Prosurvival Mcl-1 and Characterization of its Binding by Proapoptotic Bh3-Only Ligands. *J. Biol. Chem.* 280, 4738–4744. doi:10.1074/jbc.m411434200

Day, C. L., Smits, C., Fan, F. C., Lee, E. F., Fairlie, W. D., and Hinds, M. G. (2008). Structure of the BH3 Domains from the P53-Inducible BH3-Only Proteins Noxa and Puma in Complex with Mcl-1. *J. Mol. Biol.* 380, 958–971. doi:10.1016/j.jmb.2008.05.071

de Vries, S. J., Rey, J., Schindler, C. E. M., Zacharias, M., and Tuffery, P. (2017). The pepATTRACT Web Server for Blind, Large-Scale Peptide-Protein Docking. *Nucleic Acids Res.* 45, W361–W364. doi:10.1093/nar/gkx335

Dechantsreiter, M. A., Planker, E., Mathä, B., Lohof, E., Hölzemann, G., Jonczyk, A., et al. (1999). N-methylated Cyclic RGD Peptides as Highly Active and Selective αVβ3Integrin Antagonists. *J. Med. Chem.* 42, 3033–3040. doi:10.1021/jm970832g

Degterev, A., Lugovskoy, A., Cardone, M., Mulley, B., Wagner, G., Mitchison, T., et al. (2001). Identification of Small-Molecule Inhibitors of Interaction between the BH3 Domain and Bcl-xL. *Nat. Cel. Biol.* 3, 173–182. doi:10.1038/35055085

Delgado, J., Radusky, L. G., Cianferoni, D., and Serrano, L. (2019). FoldX 5.0: Working with RNA, Small Molecules and a New Graphical Interface. *Bioinformatics* 35, 4168–4169. doi:10.1093/bioinformatics/btz184

Delgado-Soler, L., del Mar Orzaez, M., and Rubio-Martinez, J. (2013). Structure-based Approach to the Design of BakBH3 Mimetic Peptides with Increased Helical Propensity. *J. Mol. Model.*, 19, 4305–4318.doi:10.1007/s00894-013-1944-3

Denis, C., Sopková-de Oliveira Santos, J., Bureau, R., and Voisin-Chiret, A. S. (2020). Hot-Spots of Mcl-1 Protein. *J. Med. Chem.* 63, 928–943. doi:10.1021/acs.jmedchem.9b00983

Dhandayuthapani, B., Yoshida, Y., Maekawa, T., and Kumar, D. S. (2011). Polymeric Scaffolds in Tissue Engineering Application: A Review. *Int. J. Polym. Sci.*, 2011, 290602. doi:10.1155/2011/290602

Ding, Q., Zhang, Z., Liu, J.-J., Jiang, N., Zhang, J., Ross, T. M., et al. (2013). Discovery of RG7388, a Potent and Selective P53-MDM2 Inhibitor in Clinical Development. *J. Med. Chem.* 56, 5979–5983. doi:10.1021/jm400487c

Ding, X., Zhao, H., Li, Y., Lee, A. L., Li, Z., Fu, M., et al. (2020). Synthetic Peptide Hydrogels as 3D Scaffolds for Tissue Engineering. *Adv. Drug Deliv. Rev.* 160, 78–104. doi:10.1016/j.addr.2020.10.005

Donsky, E., and Wolfson, H. J. (2011). PepCrawler: a Fast RRT-Based Algorithm for High-Resolution Refinement and Binding Affinity Estimation of Peptide Inhibitors. *Bioinformatics* 27, 2836–2842. doi:10.1093/bioinformatics/btr498

Elmore, S. (2007). Apoptosis: A Review of Programmed Cell Death. *Toxicol. Pathol.* 35, 495–516. doi:10.1080/01926230701320337

ElSawy, K. M., Lane, D. P., Verma, C. S., and Caves, L. S. D. (2016). Recognition Dynamics of P53 and MDM2: Implications for Peptide Design. *J. Phys. Chem. B* 120, 320–328. doi:10.1021/acs.jpcb.5b11162

Engler, A. J., Sen, S., Sweeney, H. L., and Discher, D. E. (2006). Matrix Elasticity Directs Stem Cell Lineage Specification. *Cell* 126, 677–689. doi:10.1016/j.cell.2006.06.044

Evangelista Falcon, W., Ellingson, S. R., Smith, J. C., and Baudry, J. (2019). Ensemble Docking in Drug Discovery: How Many Protein Configurations from Molecular Dynamics Simulations Are Needed to Reproduce Known Ligand Binding?. *J. Phys. Chem. B* 123, 5189–5195. doi:10.1021/acs.jpcb.8b11491

Faradjian, A. K., and Elber, R. (2004). Computing Time Scales from Reaction Coordinates by Milestoning. *J. Chem. Phys.* 120, 10880–10889. doi:10.1063/1.1738640

Favaloro, B., Allocati, N., Graziano, V., Di Ilio, C., and De Laurenzi, V. (2012). Role of Apoptosis in Disease. *Aging* 4, 330–349. doi:10.18632/aging.100459

Fernández, R. J., Totrov, M., and Abagyan, R. (2002). Soft Protein–Protein Docking in Internal Coordinates. *Protein Sci.* 11, 280–291.

Ferrari, A. M., Wei, B. Q., Costantino, L., and Shoichet, B. K. (2004). Soft Docking and Multiple Receptor Conformations in Virtual Screening. *J. Med. Chem.* 47, 5076–5084. doi:10.1021/jm049756p

Fittkau, M. H., Zilla, P., Bezuidenhout, D., Lutolf, M. P., Human, P., Hubbell, J. A., et al. (2005). The Selective Modulation of Endothelial Cell Mobility on RGD Peptide Containing Surfaces by YIGSR Peptides. *Biomaterials* 26, 167–174. doi:10.1016/j.biomaterials.2004.02.012

Frantz, C., Stewart, K. M., and Weaver, V. M. (2010). The Extracellular Matrix at a Glance. *J. Cel Sci.* 123, 4195–4200. doi:10.1242/jcs.023820

Fukunishi, H., Watanabe, O., and Takada, S. (2002). On the Hamiltonian Replica Exchange Method for Efficient Sampling of Biomolecular Systems: Application to Protein Structure Prediction. *J. Chem. Phys.* 116, 9058–9067. doi:10.1063/1.1472510

Furet, P., Masuya, K., Kallen, J., Stachyra-Valat, T., Ruetz, S., Guagnano, V., et al. (2016). Discovery of a Novel Class of Highly Potent Inhibitors of the P53-MDM2 Interaction by Structure-Based Design Starting from a Conformational Argument. *Bioorg. Med. Chem. Lett.* 26, 4837–4841. doi:10.1016/j.bmcl.2016.08.010

Garg, T., Singh, O., Arora, S., and Murthy, R. S. R. (2012). Scaffold: A Novel Carrier for Cell and Drug Delivery. *Crit. Rev. Ther. Drug Carrier Syst.* 29, 1–63. doi:10.1615/critrevtherdrugcarriersyst.v29.i1.10

Giancotti, F. G., and Ruoslahti, E. (1999). Integrin Signaling. *Science* 285, 1028–1033. doi:10.1126/science.285.5430.1028

Gill, S. C., Lim, N. M., Grinaway, P. B., Rustenburg, A. S., Fass, J., Ross, G. A., et al. (2018). Binding Modes of Ligands Using Enhanced Sampling (BLUES): Rapid Decorrelation of Ligand Binding Modes via Nonequilibrium Candidate Monte Carlo. *J. Phys. Chem. B* 122, 5579–5598. doi:10.1021/acs.jpcb.7b11820

Giorgino, T., Buch, I., and De Fabritiis, G. (2012). Visualizing the Induced Binding of SH2-Phosphopeptide. *J. Chem. Theor. Comput.* 8, 1171–1175. doi:10.1021/ct300003f

Goldsmith, K. C., Liu, X., Dam, V., Morgan, B. T., Shabbout, M., Cnaan, A., et al. (2006). BH3 Peptidomimetics Potently Activate Apoptosis and Demonstrate Single Agent Efficacy in Neuroblastoma. *Oncogene* 25, 4525–4533. doi:10.1038/sj.onc.1209489

Gonzalez, M. W., and Kann, M. G. (2012). Chapter 4: Protein Interactions and Disease. *Plos Comput. Biol.* 8, e1002819. doi:10.1371/journal.pcbi.1002819

Gonzalez-Lopez de Turiso, F., Sun, D., Rew, Y., Bartberger, M. D., Beck, H. P., Canon, J., et al. (2013). Rational Design and Binding Mode Duality of MDM2-P53 Inhibitors. *J. Med. Chem.* 56, 4053–4070. doi:10.1021/jm400293z

Gordo, S., and Giralt, E. (2009). Knitting and Untying the Protein Network: Modulation of Protein Ensembles as a Therapeutic Strategy. *Protein Sci.* 18, 481–493. doi:10.1002/pro.43

Graves, A. P., Brenk, R., and Shoichet, B. K. (2005). Decoys for Docking. *J. Med. Chem.* 48, 3714–3728. doi:10.1021/jm0491187

Guerois, R., Nielsen, J. E., and Serrano, L. (2002). Predicting Changes in the Stability of Proteins and Protein Complexes: A Study of More Than 1000 Mutations. *J. Mol. Biol.* 320, 369–387. doi:10.1016/s0022-2836(02)00442-4

Hanahan, D., and Weinberg, R. A. (2000). The Hallmarks of Cancer. *Cell* 100, 57–70. doi:10.1016/s0092-8674(00)81683-9

Hanahan, D., and Weinberg, R. A. (2011). Hallmarks of Cancer: the Next Generation. *Cell* 144, 646–674. doi:10.1016/j.cell.2011.02.013

Hansmann, U. H. E., and Okamoto, Y. (1999). New Monte Carlo Algorithms for Protein Folding. *Curr. Opin. Struct. Biol.* 9, 177–183. doi:10.1016/s0959-440x(99)80025-6

Harvey, E. P., Seo, H.-S., Guerra, R. M., Bird, G. H., Dhe-Paganon, S., and Walensky, L. D. (2018). Crystal Structures of Anti-apoptotic BFL-1 and its Complex with a Covalent Stapled Peptide Inhibitor. *Structure* 26, 153–160. doi:10.1016/j.str.2017.11.016

Hauser, A. S., and Windshügel, B. (2016). LEADS-PEP: A Benchmark Data Set for Assessment of Peptide Docking Performance. *J. Chem. Inf. Model.* 56, 188–200. doi:10.1021/acs.jcim.5b00234

Hinds, M. G., Lackmann, M., Skea, G. L., Harrison, P. J., Huang, D. C., and Day, C. L. (2003). The Structure of Bcl-W Reveals a Role for the C-Terminal Residues in Modulating Biological Activity. *EMBO J.* 22, 1497–1507. doi:10.1093/emboj/cdg144

Hinds, M. G., Smits, C., Fredericks-Short, R., Risk, J. M., Bailey, M., Huang, D. C. S., et al. (2007). Bim, Bad and Bmf: Intrinsically Unstructured Bh3-Only Proteins that Undergo a Localized Conformational Change upon Binding to Prosurvival Bcl-2 Targets. *Cell Death Differ* 14, 128–136. doi:10.1038/sj.cdd.4401934

Holinger, E. P., Chittenden, T., and Lutz, R. J. (1999). Bak BH3 Peptides Antagonize Bcl-xL Function and Induce Apoptosis through Cytochrome C-independent Activation of Caspases. *J. Biol. Chem.* 274, 13298–13304. doi:10.1074/jbc.274.19.13298

Horne, W. S., Boersma, M. D., Windsor, M. A., and Gellman, S. H. (2008). Sequence-Based Design of α/β-Peptide Foldamers that Mimic BH3 Domains. *Angew. Chem. Int. Ed.* 47, 2853–2856. doi:10.1002/anie.200705315

Hu, Z., Ma, B., Wolfson, H., and Nussinov, R. (2000). Conservation of Polar Residues as Hot Spots at Protein Interfaces. *Proteins* 39, 331–342. doi:10.1002/(sici)1097-0134(20000601)39:4<331::aid-prot60>3.0.co;2-a

Hu, B., Gilkes, D. M., Farooqi, B., Sebti, S. M., and Chen, J. (2006). MDMX Overexpression Prevents P53 Activation by the MDM2 Inhibitor Nutlin. *J. Biol. Chem.* 281, 33030–33035. doi:10.1074/jbc.c600147200

Huart, A. S., and Hupp, T. R. (2013). Evolution of Conformational Disorder & Diversity of the P53 Interactome. *Biodiscov* 8, e8952.

Huber, G. A., and Kim, S. (1996). Weighted-ensemble Brownian Dynamics Simulations for Protein Association Reactions. *Biophysical J.* 70, 97–110. doi:10.1016/s0006-3495(96)79552-8

Hunter, T. (2000). Signaling-2000 and beyond. *Cell* 100, 113–127. doi:10.1016/s0092-8674(00)81688-8

Hynes, R. O. (2002). Integrins: bidirectional, allosteric signaling machines. *Cell* 110, 673–687. doi:10.1016/s0092-8674(02)00971-6

Ichim, G., and Tait, S. W. G. (2016). A Fate Worse Than Death: Apoptosis as an Oncogenic Process. *Nat. Rev. Cancer* 16, 539–548. doi:10.1038/nrc.2016.58

Ivanov, S. M., Huber, R. G., Warwicker, J., and Bond, P. J. (2016). Energetics and Dynamics across the Bcl-2-Regulated Apoptotic Pathway Reveal Distinct Evolutionary Determinants of Specificity and Affinity. *Structure* 24, 2024–2033. doi:10.1016/j.str.2016.09.006

Jain, A. N. (2007). Surflex-Dock 2.1: Robust Performance from Ligand Energetic Modeling, Ring Flexibility, and Knowledge-Based Search. *J. Comput. Aided Mol. Des.* 21, 281–306. doi:10.1007/s10822-007-9114-2

Janin, J. l., Henrick, K., Moult, J., Eyck, L. T., Sternberg, M. J. E., Vajda, S., et al. (2003). CAPRI: A Critical Assessment of PRedicted Interactions. *Proteins* 52, 2–9. doi:10.1002/prot.10381

Jeschke, B., Meyer, J., Jonczyk, A., Kessler, H., Adamietz, P., Meenen, N. M., et al. (2002). RGD-peptides for Tissue Engineering of Articular Cartilage. *Biomaterials* 23, 3455–3463. doi:10.1016/s0142-9612(02)00052-2

Jiang, L., and Zawacka-Pankau, J. (2020). The p53/MDM2/MDMX-Targeted Therapies—A Clinical Synopsis. *Cell. Death Dis.* 11, 237. doi:10.1038/s41419-020-2445-9

Jones, D. T. (1999). Protein Secondary Structure Prediction Based on Position-specific Scoring Matrices. 1 Edited by G. Von Heijne. *J. Mol. Biol.* 292, 195–202. doi:10.1006/jmbi.1999.3091

Joseph, T. L., Madhumalar, A., Brown, C. J., Lane, D. P., and Verma, C. S. (2010). Differential Binding of P53 and Nutlin to MDM2 and MDMX: Computational Studies. *Cell Cycle* 9, 1167–1181. doi:10.4161/cc.9.6.11067

Kadry, Y. A., and Calderwood, D. A. (2020). Chapter 22: Structural and Signaling Functions of Integrins. *Biochim. Biophys. Acta (Bba) - Biomembranes* 1862, 183206. doi:10.1016/j.bbamem.2020.183206

Kapp, T. G., Rechenmacher, F., Neubauer, S., Maltsev, O. V., Cavalcanti-Adam, E. A., Zarka, R., et al. (2017). A Comprehensive Evaluation of the Activity and Selectivity Profile of Ligands for RGD-Binding Integrins. *Sci. Rep.* 7, 39805. doi:10.1038/srep39805

Kitada, S., Leone, M., Sareth, S., Zhai, D., Reed, J. C., and Pellecchia, M. (2003). Discovery, Characterization, and Structure−Activity Relationships Studies of Proapoptotic Polyphenols Targeting B-Cell Lymphocyte/Leukemia-2 Proteins. *J. Med. Chem.* 46, 4259–4264. doi:10.1021/jm030190z

Kitchen, D. B., Decornez, H., Furr, J. R., and Bajorath, J. (2004). Docking and Scoring in Virtual Screening for Drug Discovery: Methods and Applications. *Nat. Rev. Drug Discov.* 3, 935–949. doi:10.1038/nrd1549

Klimek, K., and Ginalska, G. (2020). Proteins and Peptides as Important Modifiers of the Polymer Scaffolds for Tissue Engineering Applications-A Review. *Polymers* 12, 844. doi:10.3390/polym12040844

Kortemme, T., Kim, D. E., and Baker, D. (2004). Computational Alanine Scanning of Protein-Protein Interfaces. *Sci. Signaling* 2004 (219), pl2. doi:10.1126/stke.2192004pl2

Kuntz, I. D., Blaney, J. M., Oatley, S. J., Langridge, R., and Ferrin, T. E. (1982). A Geometric Approach to Macromolecule-Ligand Interactions. *J. Mol. Biol.* 161, 269–288. doi:10.1016/0022-2836(82)90153-x

Kurcinski, M., Jamroz, M., Blaszczyk, M., Kolinski, A., and Kmiecik, S. (2015). CABS-dock Web Server for the Flexible Docking of Peptides to Proteins without Prior Knowledge of the Binding Site. *Nucleic Acids Res.* 43, W419–W424. doi:10.1093/nar/gkv456

Kussie, P. H., Gorina, S., Marechal, V., Elenbaas, B., Moreau, J., Levine, A. J., et al. (1996). Structure of the MDM2 Oncoprotein Bound to the P53 Tumor Suppressor Transactivation Domain. *Science* 274, 948–953. doi:10.1126/science.274.5289.948

Lama, D., and Sankararamakrishnan, R. (2011). Molecular Dynamics Simulations of Pro-apoptotic BH3 Peptide Helices in Aqueous Medium: Relationship between Helix Stability and Their Binding Affinities to the Anti-apoptotic Protein Bcl-XL. *J. Comput. Aided Mol. Des.* 25, 413–426. doi:10.1007/s10822-011-9428-y

Lamiable, A., Thévenet, P., Thévenet, P., Rey, J., Vavrusa, M., Derreumaux, P., et al. (2016). PEP-FOLD3: Fasterde Novostructure Prediction for Linear Peptides in Solution and in Complex. *Nucleic Acids Res.* 44, W449–W454. doi:10.1093/nar/gkw329

Lang, L., and Perez, A. (2021). Binding Ensembles of P53-MDM2 Peptide Inhibitors by Combining Bayesian Inference and Atomistic Simulations. *Molecules* 26, 198. doi:10.3390/molecules26010198

Langer, R., and Vacanti, J. (1993). Tissue Engineering. *Science* 260, 920–926. doi:10.1126/science.8493529

Leach, A. R. (1994). Ligand Docking to Proteins with Discrete Side-Chain Flexibility. *J. Mol. Biol.* 235, 345–356. doi:10.1016/s0022-2836(05)80038-5

Lee, E. F., Czabotar, P. E., Smith, B. J., Deshayes, K., Zobel, K., Colman, P. M., et al. (2007). Crystal Structure of ABT-737 Complexed with Bcl-xL: Implications for Selectivity of Antagonists of the Bcl-2 Family. *Cel Death Differ* 14, 1711–1713. doi:10.1038/sj.cdd.4402178

Lee, H., Heo, L., Lee, M. S., and Seok, C. (2015). GalaxyPepDock: a Protein-Peptide Docking Tool Based on Interaction Similarity and Energy Optimization. *Nucleic Acids Res.* 43, W431–W435. doi:10.1093/nar/gkv495

Lensink, M. F., Méndez, R., and Wodak, S. J. (2007). Docking and Scoring Protein Complexes: CAPRI 3rd Edition. *Proteins* 69, 704–718. doi:10.1002/prot.21804

Lensink, M. F., Brysbaert, G., Nadzirin, N., Velankar, S., Chaleil, R. A. G., Gerguri, T., et al. (2019). Blind Prediction of Homo-And Hetero-Protein Complexes: The CASP13-CAPRI Experiment. *Proteins* 87, 1200–1221. doi:10.1002/prot.25838

Leonard, S. R., Cormier, A. R., Pang, X., Zimmerman, M. I., Zhou, H.-X., and Paravastu, A. K. (2013). Solid-State NMR Evidence for β-Hairpin Structure

within MAX8 Designer Peptide Nanofibers. *Biophysical J.* 105, 222–230. doi:10.1016/j.bpj.2013.05.047

Lessene, G., Czabotar, P. E., Sleebs, B. E., Zobel, K., Lowes, K. N., Adams, J. M., et al. (2013). Structure-guided Design of a Selective BCL-XL Inhibitor. *Nat. Chem. Biol.* 9, 390–397. doi:10.1038/nchembio.1246

Li, J., Fu, A., and Zhang, L. (2019). An Overview of Scoring Functions Used for Protein-Ligand Interactions in Molecular Docking. *Interdiscip. Sci. Comput. Life Sci.* 11, 320–328. doi:10.1007/s12539-019-00327-w

Li, H., Sze, K. H., Lu, G., and Ballester, P. J. (2021). Machine-learning Scoring Functions for Structure-Based Virtual Screening. *Wires Comput. Mol. Sci.* 11, e1478. doi:10.1002/wcms.1478

Lomonosova, E., and Chinnadurai, G. (2008). BH3-only Proteins in Apoptosis and beyond: an Overview. *Oncogene* 27 (Suppl. 1), S2–S19. doi:10.1038/onc.2009.39

London, N., Movshovitz-Attias, D., and Schueler-Furman, O. (2010). The Structural Basis of Peptide-Protein Binding Strategies. *Structure* 18, 188–199. doi:10.1016/j.str.2009.11.012

London, N., Raveh, B., Cohen, E., Fathi, G., and Schueler-Furman, O. (2011). Rosetta FlexPepDock Web Server-High Resolution Modeling of Peptide-Protein Interactions. *Nucl. Acids Res.* 39, W249–W253. doi:10.1093/nar/gkr431

London, N., Raveh, B., and Schueler-Furman, O. (2013). Druggable Protein-Protein Interactions - from Hot Spots to Hot Segments. *Curr. Opin. Chem. Biol.* 17, 952–959. doi:10.1016/j.cbpa.2013.10.011

Loo, Y., Goktas, M., Tekinay, A. B., Guler, M. O., Hauser, C. A. E., and Mitraki, A. (2015). Self-Assembled Proteins and Peptides as Scaffolds for Tissue Regeneration. *Adv. Healthc. Mater.* 4, 2557–2586. doi:10.1002/adhm.201500402

Luck, K., Kim, D.-K., Lambourne, L., Spirohn, K., Begg, B. E., Bian, W., et al. (2020). A Reference Map of the Human Binary Protein Interactome. *Nature* 580, 402–408. doi:10.1038/s41586-020-2188-x

May, P., and May, E. (1999). Twenty Years of P53 Research: Structural and Functional Aspects of the P53 Protein. *Oncogene* 18, 7621–7636. doi:10.1038/sj.onc.1203285

Mayer, B. J. (2001). SH3 Domains: Complexity in Moderation. *J. Cel Sci.* 114, 1253–1263. doi:10.1242/jcs.114.7.1253

McCammon, J. A., Gelin, B. R., and Karplus, M. (1977). Dynamics of Folded Proteins. *Nature* 267, 585–590. doi:10.1038/267585a0

Meric-Bernstam, F., Saleh, M. N., Infante, J. R., Goel, S., Falchook, G. S., Shapiro, G., et al. (2017). Phase I Trial of a Novel Stapled Peptide ALRN-6924 Disrupting MDMX- and MDM2-Mediated Inhibition of WT P53 in Patients with Solid Tumors and Lymphomas. *Jco* 35, 2505. doi:10.1200/jco.2017.35.15_suppl.2505

Metropolis, N., Rosenbluth, A. W., Rosenbluth, M. N., Teller, A. H., and Teller, E. (1953). Equation of State Calculations by Fast Computing Machines. *J. Chem. Phys.* 21, 1087–1092. doi:10.1063/1.1699114

Milroy, L.-G., Grossmann, T. N., Hennig, S., Brunsveld, L., and Ottmann, C. (2014). Modulators of Protein-Protein Interactions. *Chem. Rev.* 114, 4695–4748. doi:10.1021/cr400698c

Moldoveanu, T., Liu, Q., Tocilj, A., Watson, M., Shore, G., and Gehring, K. (2006). The X-Ray Structure of a Bak Homodimer Reveals an Inhibitory Zinc Binding Site. *Mol. Cel* 24, 677–688. doi:10.1016/j.molcel.2006.10.014

Moreau, R. J., Schubert, C. R., Nasr, K. A., Török, M., Miller, J. S., Kennedy, R. J., et al. (2009). Context-independent, Temperature-dependent Helical Propensities for Amino Acid Residues. *J. Am. Chem. Soc.* 131, 13107–13116. doi:10.1021/ja904271k

Morrison, K. L., and Weiss, G. A. (2001). Combinatorial Alanine-Scanning. *Curr. Opin. Chem. Biol.* 5, 302–307. doi:10.1016/s1367-5931(00)00206-4

Morrone, J. A., Perez, A., Deng, Q., Ha, S. N., Holloway, M. K., Sawyer, T. K., et al. (2017a). Molecular Simulations Identify Binding Poses and Approximate Affinities of Stapled α-Helical Peptides to MDM2 and MDMX. *J. Chem. Theor. Comput.* 13, 863–869. doi:10.1021/acs.jctc.6b00978

Morrone, J. A., Perez, A., MacCallum, J., and Dill, K. A. (2017b). Computed Binding of Peptides to Proteins with MELD-Accelerated Molecular Dynamics. *J. Chem. Theor. Comput.* 13, 870–876. doi:10.1021/acs.jctc.6b00977

Morrone, J. A., Weber, J. K., Huynh, T., Luo, H., and Cornell, W. D. (2020). Combining Docking Pose Rank and Structure with Deep Learning Improves Protein-Ligand Binding Mode Prediction over a Baseline Docking Approach. *J. Chem. Inf. Model.* 60, 4170–4179. doi:10.1021/acs.jcim.9b00927

Moult, J., Pedersen, J. T., Judson, R., and Fidelis, K. (1995). A Large-Scale Experiment to Assess Protein Structure Prediction Methods. *Proteins Struct. Funct. Bioinform.* 23, ii–v. doi:10.1002/prot.340230303

Müller, G., Gurrath, M., and Kessler, H. (1994). Pharmacophore Refinement of gpIIb/IIIa Antagonists Based on Comparative Studies of Antiadhesive Cyclic and Acyclic RGD Peptides. *J. Comp. Aided Mol. Des.* 8, 709–730.

Muchmore, S. W., Sattler, M., Liang, H., Meadows, R. P., Harlan, J. E., Yoon, H. S., et al. (1996). X-ray and Nmr Structure of Human Bcl-Xl, an Inhibitor of Programmed Cell Death. *Nature* 381, 335–341. doi:10.1038/381335a0

Muppidi, A., Doi, K., Edwardraja, S., Drake, E. J., Gulick, A. M., Wang, H.-G., et al. (2012). Rational Design of Proteolytically Stable, Cell-Permeable Peptide-Based Selective Mcl-1 Inhibitors. *J. Am. Chem. Soc.*, 134, 14734–14737.doi:10.1021/ja306864v

Nevola, L., and Giralt, E. (2015). Modulating Protein-Protein Interactions: the Potential of Peptides. *Chem. Commun.* 51, 3302–3315. doi:10.1039/c4cc08565e

Noé, F., Schuette, C., Vanden-Eijnden, E., Reich, L., and Weikl, T. R. (2009). Constructing the Equilibrium Ensemble of Folding Pathways from Short Off-Equilibrium Simulations. *Proc. Natl. Acad. Sci.* 106, 19011–6. doi:10.1073/pnas.0905466106

O'Brien, F. J. (2011). Biomaterials & Scaffolds for Tissue Engineering. *Mater. Today* 14, 88–95. doi:10.1016/S1369-7021(11)70058-X

Obarska-Kosinska, A., Iacoangeli, A., Lepore, R., and Tramontano, A. (2016). PepComposer: Computational Design of Peptides Binding to a Given Protein Surface. *Nucleic Acids Res.* 44, W522–W528. doi:10.1093/nar/gkw366

Oltersdorf, T., Elmore, S. W., Shoemaker, A. R., Armstrong, R. C., Augeri, D. J., Belli, B. A., et al. (2005). An Inhibitor of Bcl-2 Family Proteins Induces Regression of Solid Tumours. *Nature* 435, 677–681. doi:10.1038/nature03579

Oltvai, Z. N., Milliman, C. L., and Korsmeyer, S. J. (1993). Bcl-2 Heterodimerizes In Vivo with a Conserved Homolog, Bax, that Accelerates Programmed Cell Death. *Cell* 74, 609–619. doi:10.1016/0092-8674(93)90509-o

Orzáez, M., Gortat, A., Mondragón, L., and Pérez-Payá, E. (2009). Peptides and Peptide Mimics as Modulators of Apoptotic Pathways. *ChemMedChem* 4, 146–160. doi:10.1002/cmdc.200800246

Pan, R., Hogdal, L. J., Benito, J. M., Bucci, D., Han, L., Borthakur, G., et al. (2014). Selective BCL-2 Inhibition by ABT-199 Causes On-Target Cell Death in Acute Myeloid Leukemia. *Cancer Discov.* 4, 362–375. doi:10.1158/2159-8290.cd-13-0609

Pan, A. C., Xu, H., Palpant, T., and Shaw, D. E. (2017). Quantitative Characterization of the Binding and Unbinding of Millimolar Drug Fragments with Molecular Dynamics Simulations. *J. Chem. Theor. Comput.* 13, 3372–3377. doi:10.1021/acs.jctc.7b00172

Patel, R., Santhosh, M., Dash, J. K., Karpoormath, R., Jha, A., Kwak, J., et al. (2019). Ile-Lys-Val-ala-Val (IKVAV) Peptide for Neuronal Tissue Engineering. *Polym. Adv. Technoladv. Technol.* 30, 4–12. doi:10.1002/pat.4442

Patterson, C. M., Balachander, S. B., Grant, I., Pop-Damkov, P., Kelly, B., McCoull, W., et al. (2021). Design and Optimisation of Dendrimer-Conjugated, Bcl-2/x_L Inhibitor, AZD0466, with Improved Therapeutic Index for Cancer Therapy. *Comm. Biol.* 4, 112. doi:10.1038/s42003-020-01631-8

Paul, F., Wehmeyer, C., Abualrous, E. T., Wu, H., Crabtree, M. D., Schöneberg, J., et al. (2017). Protein-peptide Association Kinetics beyond the Seconds Timescale from Atomistic Simulations. *Nat. Commun.* 8, 1095. doi:10.1038/s41467-017-01163-6

Pazgier, M., Liu, M., Zou, G., Yuan, W., Li, C., Li, C., et al. (2009). Structural Basis for High-Affinity Peptide Inhibition of P53 Interactions with MDM2 and MDMX. *Proc. Natl. Acad. Sci.* 106, 4665–4670. doi:10.1073/pnas.0900947106

Perez, J., Corcho, F., and Llorens, O. (2002). Molecular Modeling in the Design of Peptidomimetics and Peptide Surrogates. *Cmc* 9, 2209–2229. doi:10.2174/0929867023368683

Pérez, R. A., Won, J.-E., Knowles, J. C., and Kim, H.-W. (2013). Naturally and Synthetic Smart Composite Biomaterials for Tissue Regeneration. *Adv. Drug Deliv. Rev.* 65, 471–496. doi:10.1016/j.addr.2012.03.009

Perez, R. A., Seo, S.-J., Won, J.-E., Lee, E.-J., Jang, J.-H., Knowles, J. C., et al. (2015). Therapeutically Relevant Aspects in Bone Repair and Regeneration. *Mater. Today* 18, 573–589. doi:10.1016/j.mattod.2015.06.011

Perez, J. J., Tomas, M. S., and Rubio-Martinez, J. (2016). Assessment of the Sampling Performance of Multiple-Copy Dynamics versus a Unique Trajectory. *J. Chem. Inf. Model.* 56, 1950–1962. doi:10.1021/acs.jcim.6b00347

Perez, J. J. (2018). Designing Peptidomimetics. *Ctmc* 18, 566–590. doi:10.2174/1568026618666180522075258

Petrie, T. A., Raynor, J. E., Reyes, C. D., Burns, K. L., Collard, D. M., and García, A. J. (2008). The Effect of Integrin-specific Bioactive Coatings on Tissue Healing

and Implant Osseointegration. *Biomaterials* 29, 2849–2857. doi:10.1016/j.biomaterials.2008.03.036

Petros, A. M., Nettesheim, D. G., Wang, Y., Olejniczak, E. T., Meadows, R. P., Mack, J., et al. (2000). Rationale for Bcl-xL/Bad Peptide Complex Formation from Structure, Mutagenesis, and Biophysical Studies. *Protein Sci.*, 9, 2528–2534.doi:10.1017/s096183680000331x

Petros, A. M., Medek, A., Nettesheim, D. G., Kim, D. H., Yoon, H. S., Swift, K., et al. (2001). Solution Structure of the Antiapoptotic Protein Bcl-2. *Proc. Natl. Acad. Sci.* 98, 3012–3017. doi:10.1073/pnas.041619798

Petros, A. M., Olejniczak, E. T., and Fesik, S. W. (2004) Structural Biology of the Bcl-2 Family of Proteins. *Biochim. Biophys. Acta (Bba) - Mol. Cel Res.*, 1644, 83–94. doi:10.1016/j.bbamcr.2003.08.012

Petsalaki, E., and Russell, R. B. (2008). Peptide-mediated Interactions in Biological Systems: New Discoveries and Applications. *Curr. Opin. Biotechnol.* 19, 344–350. doi:10.1016/j.copbio.2008.06.004

Phan, J., Li, Z., Kasprzak, A., Li, B., Sebti, S., Guida, W., et al. (2010). Structure-based Design of High Affinity Peptides Inhibiting the Interaction of P53 with MDM2 and MDMX. *J. Biol. Chem.* 285, 2174–2183. doi:10.1074/jbc.m109.073056

Pierce, B. G., Hourai, Y., and Weng, Z. (2011). Accelerating Protein Docking in ZDOCK Using an Advanced 3D Convolution Library. *Plos One* 6, e24657. doi:10.1371/journal.pone.0024657

Pierschbacher, M. D., and Ruoslahti, E. (1984). Variants of the Cell Recognition Site of Fibronectin that Retain Attachment-Promoting Activity. *Proc. Natl. Acad. Sci.* 81, 5985–5988. doi:10.1073/pnas.81.19.5985

Popowicz, G., Czarna, A., and Holak, T. (2008). Structure of the Human Mdmx Protein Bound to the P53 Tumor Suppressor Transactivation Domain. *Cell Cycle* 7, 2441–2443. doi:10.4161/cc.6365

Porter, K. A., Xia, B., Beglov, D., Bohnuud, T., Alam, N., Schueler-Furman, O., et al. (2017). ClusPro PeptiDock: Efficient Global Docking of Peptide Recognition Motifs Using FFT. *Bioinformatics* 33, 3299–3301. doi:10.1093/bioinformatics/btx216

Porter, K. A., Desta, I., Kozakov, D., and Vajda, S. (2019). What Method to Use for Protein-Protein Docking?. *Curr. Opin. Struct. Biol.* 55, 1–7. doi:10.1016/j.sbi.2018.12.010

Raveh, B., London, N., Zimmerman, L., and Schueler-Furman, O. (2011). Rosetta FlexPepDock Ab-Initio: Simultaneous Folding, Docking and Refinement of Peptides onto Their Receptors. *Plos One* 6, e18934. doi:10.1371/journal.pone.0018934

Reddy, C. N., Manzar, N., Ateeq, B., and Sankararamakrishnan, R. (2020). Computational Design of BH3-Mimetic Peptide Inhibitors that Can Bind Specifically to Mcl-1 or Bcl-XL: Role of Non-hot Spot Residues. *Biochemistry* 59, 4379–4394. doi:10.1021/acs.biochem.0c00661

Reed, D., Shen, Y., Shelat, A. A., Arnold, L. A., Ferreira, A. M., Zhu, F., et al. (2010). Identification and Characterization of the First Small Molecule Inhibitor of MDMX*. *J. Biol. Chem.* 285, 10786–10796. doi:10.1074/jbc.m109.056747

Rentzsch, R., and Renard, B. Y. (2015). Docking Small Peptides Remains a Great Challenge: an Assessment Using AutoDock Vina. *Brief. Bioinform.* 16, 1045–1056. doi:10.1093/bib/bbv008

Roy, M. J., Vom, A., Czabotar, P. E., and Lessene, G. (2014). Cell Death and the Mitochondria: Therapeutic Targeting of the BCL-2 Family-Driven Pathway. *Br. J. Pharmacol.* 171, 1973–1987. doi:10.1111/bph.12431

Ruiter, A. de., and Oostenbrink, C. (2020). Advances in the Calculation of Binding Free Energies. *Curr. Opin. Struc. Biol.* 61, 207–212.

Ruoslahti, E. (1996). RGD and Other Recognition Sequences for Integrins. *Annu. Rev. Cel Dev. Biol.* 12, 697–715. doi:10.1146/annurev.cellbio.12.1.697

Sang, P., Shi, Y., Lu, J., Chen, L., Yang, L., Borcherds, W., et al. (2020). α-Helix-Mimicking Sulfono-γ-AApeptide Inhibitors for P53-MDM2/MDMX Protein-Protein Interactions. *J. Med. Chem.* 63, 975–986. doi:10.1021/acs.jmedchem.9b00993

Santini, B. L., and Zacharias, M. (2020). Rapid In Silico Design of Potential Cyclic Peptide Binders Targeting Protein-Protein Interfaces. *Front. Chem.* 8, 573259. doi:10.3389/fchem.2020.573259

Santos, K. B., Guedes, I. A., Karl, A. L. M., and Dardenne, L. E. (2020). Highly Flexible Ligand Docking: Benchmarking of the DockThor Program on the LEADS-PEP Protein-Peptide Data Set. *J. Chem. Inf. Model.* 60, 667–683. doi:10.1021/acs.jcim.9b00905

Sattler, M., Liang, H., Nettesheim, D., Meadows, R. P., Harlan, J. E., Eberstadt, M., et al. (1997). Structure of Bcl-Xl-Bak Peptide Complex: Recognition between Regulators of Apoptosis. *Science* 275, 983–986. doi:10.1126/science.275.5302.983

Scarborough, R. M., and Gretler, D. D. (2000). Platelet Glycoprotein IIb-IIIa Antagonists as Prototypical Integrin Blockers: Novel Parenteral and Potential Oral Antithrombotic Agents. *J. Med. Chem.* 43, 3453–3473. doi:10.1021/jm000022w

Scarborough, R. M., Naughton, M. A., Teng, W., Rose, J. W., Phillips, D. R., Nannizzi, L., et al. (1993). Design of Potent and Specific Integrin Antagonists. Peptide Antagonists with High Specificity for Glycoprotein IIb-IIIa. *J. Biol. Chem.* 268, 1066–1073. doi:10.1016/s0021-9258(18)54042-4

Shandler, S. J., Korendovych, I. V., Moore, D. T., Smith-Dupont, K. B., Streu, C. N., Litvinov, R. I., et al. (2011). Computational Design of a β-Peptide that Targets Transmembrane Helices. *J. Am. Chem. Soc.* 133, 12378–12381. doi:10.1021/ja204215f

Shoemaker, B. A., Portman, J. J., and Wolynes, P. G. (2000). Speeding Molecular Recognition by Using the Folding Funnel: The Fly-Casting Mechanism. *Proc. Natl. Acad. Sci.* 97, 8868–8873. doi:10.1073/pnas.160259697

Shoemaker, A. R., Oleksijew, A., Bauch, J., Belli, B. A., Borre, T., Bruncko, M., et al. (2006). A Small-Molecule Inhibitor of Bcl-XL Potentiates the Activity of Cytotoxic Drugs In Vitro and In Vivo. *Cancer Res.* 66, 8731–8739. doi:10.1158/0008-5472.can-06-0367

Simons, K. T., Bonneau, R., Ruczinski, I., and Baker, D. (1999). Ab Initio protein Structure Prediction of CASP III Targets Using ROSETTA. *Proteins* 37 (Suppl. 3), 171–176. doi:10.1002/(sici)1097-0134(1999)37:3+<171::aid-prot21>3.0.co;2-z

Singh, R., Letai, A., and Sarosiek, K. (2019). Regulation of Apoptosis in Health and Disease: the Balancing Act of Bcl-2 Family Proteins. *Nat. Rev. Mol. Cel Biol.* 20, 175–193. doi:10.1038/s41580-018-0089-8

Smadbeck, J., Chan, K. H., Khoury, G. A., Xue, B., Robinson, R. C., Hauser, C. A., et al. (2014). De Novo design and Experimental Characterization of Ultrashort Self-Associating Peptides. *Plos Comput. Biol.* 10, e1003718. doi:10.1371/journal.pcbi.1003718

Sondermann, H., Scheufler, C., Schneider, C., Hohfeld, J., Hartl, F. U., and Moarefi, I. (2001). Structure of a Bag/Hsc70 Complex: Convergent Functional Evolution of Hsp70 Nucleotide Exchange Factors. *Science* 291, 1553–1557. doi:10.1126/science.1057268

Spiliotopoulos, D., Kastritis, P. L., Melquiond, A. S., Bonvin, A. M., Musco, G., Rocchia, W., et al. (2016). dMM-PBSA: A New HADDOCK Scoring Function for Protein-Peptide Docking. *Front. Mol. Biosci.* 3, 46. doi:10.3389/fmolb.2016.00046

Stein, R. M., Yang, Y., Balius, T. E., O'Meara, M. J., Lyu, J., Young, J., et al. (2021). Property-Unmatched Decoys in Docking Benchmarks. *J. Chem. Inf. Model.* 61, 699–714. doi:10.1021/acs.jcim.0c00598

Stelzl, U., Worm, U., Lalowski, M., Haenig, C., Brembeck, F. H., Goehler, H., et al. (2005). A Human Protein-Protein Interaction Network: a Resource for Annotating the Proteome. *Cell* 122, 957–968. doi:10.1016/j.cell.2005.08.029

Stumpf, M. P. H., Thorne, T., de Silva, E., Stewart, R., An, H. J., Lappe, M., et al. (2008). Estimating the Size of the Human Interactome. *Proc. Natl. Acad. Sci.* 105, 6959–6964. doi:10.1073/pnas.0708078105

Sugase, K., Dyson, H. J., and Wright, P. E. (2007). Mechanism of Coupled Folding and Binding of an Intrinsically Disordered Protein. *Nature* 447, 1021–1025. doi:10.1038/nature05858

Sugita, Y., and Okamoto, Y. (1999). Replica-exchange Molecular Dynamics Method for Protein Folding. *Chem. Phys. Lett.* 314, 141–151. doi:10.1016/s0009-2614(99)01123-9

Suzuki, M., Youle, R. J., and Tjandra, N. (2000). Structure of Bax. *Cell* 103, 645–654. doi:10.1016/s0092-8674(00)00167-7

Takano, K., Ota, M., Ogasahara, K., Yamagata, Y., Nishikawa, K., and Yutani, K. (1999). Experimental Verification of the 'stability Profile of Mutant Protein' (SPMP) Data Using Mutant Human Lysozymes. *Protein Eng.* 12, 663–672. doi:10.1093/protein/12.8.663

Tallawi, M., Rosellini, E., Barbani, N., Cascone, M. G., Rai, R., Saint-Pierre, G., et al. (2015). Strategies for the Chemical and Biological Functionalization of Scaffolds for Cardiac Tissue Engineering: A Review. *J. R. Soc. Interf.* 12, 20150254. doi:10.1098/rsif.2015.0254

Tan, Y. S., Lane, D. P., and Verma, C. S. (2016). Stapled Peptide Design: Principles and Roles of Computation. *Drug Discov. Today* 21, 1642–1653. doi:10.1016/j.drudis.2016.06.012

Tan, Y. S., Mhoumadi, Y., and Verma, C. S. (2019). Roles of Computational Modelling in Understanding P53 Structure, Biology, and its Therapeutic Targeting. *J. Mol. Cel. Biol.* 11, 306–316. doi:10.1093/jmcb/mjz009

Tao, H., Zhang, Y., and Huang, S.-Y. (2020). Improving Protein-Peptide Docking Results via Pose-Clustering and Rescoring with a Combined Knowledge-Based and MM-GBSA Scoring Function. *J. Chem. Inf. Model.* 60, 2377–2387. doi:10.1021/acs.jcim.0c00058

Tomasella, C., Floris, M., Guccione, S., Pappalardo, M., and Basile, L. (2021). Peptidomimetics In Silico. *Mol. Inform.* 40, e2000087. doi:10.1002/minf.202000087

Torres, M. D. T., Sothiselvam, S., Lu, T. K., and de la Fuente-Nunez, C. (2019). Peptide Design Principles for Antimicrobial Applications. *J. Mol. Biol.* 431, 3547–3567. doi:10.1016/j.jmb.2018.12.015

Trellet, M., Melquiond, A. S. J., and Bonvin, A. M. J. J. (2013). A Unified Conformational Selection and Induced Fit Approach to Protein-Peptide Docking. *Plos One* 8, e58769. doi:10.1371/journal.pone.0058769

Tse, C., Shoemaker, A. R., Adickes, J., Anderson, M. G., Chen, J., Jin, S., et al. (2008). ABT-263: A Potent and Orally Bioavailable Bcl-2 Family Inhibitor. *Cancer Res.* 68, 3421–3428. doi:10.1158/0008-5472.can-07-5836

Tzung, S.-P., Kim, K. M., Basañez, G., Giedt, C. D., Simon, J., Zimmerberg, J., et al. (2001). Antimycin A Mimics a Cell-Death-Inducing Bcl-2 Homology Domain 3. *Nat. Cel. Biol.* 3, 183–191. doi:10.1038/35055095

Vassilev, L. T., Vu, B. T., Graves, B., Carvajal, D., Podlaski, F., Filipovic, Z., et al. (2004). *In Vivo* Activation of the P53 Pathway by Small-Molecule Antagonists of MDM2. *Science* 303, 844–848. doi:10.1126/science.1092472

Vassilev, L. T. (2005). p53 Activation by Small Molecules: Application in Oncology. *J. Med. Chem.* 48, 4491–4499. doi:10.1021/jm058174k

Vila-Julià, G., Granadino-Roldán, J. M., Perez, J. J., and Rubio-Martinez, J. (2020). Molecular Determinants for the Activation/Inhibition of Bak Protein by BH3 Peptides. *J. Chem. Inf. Model.* 60, 1632–1643. doi:10.1021/acs.jcim.9b01047

Von Der Mark, K., Park, J., Bauer, S., and Schmuki, P. (2010). Nanoscale Engineering of Biomimetic Surfaces: Cues from the Extracellular Matrix. *Cel Tissue Res* 339, 131–153. doi:10.1007/s00441-009-0896-5

Votapka, L. W., and Amaro, R. E. (2015). Multiscale Estimation of Binding Kinetics Using Brownian Dynamics, Molecular Dynamics and Milestoning. *Plos Comput. Biol.* 11, e1004381. doi:10.1371/journal.pcbi.1004381

Wade, R. J., and Burdick, J. A. (2012). Engineering ECM signals into biomaterials. *Mater. Today* 15, 454–459. doi:10.1016/s1369-7021(12)70197-9

Walensky, L. D., Kung, A. L., Escher, I., Malia, T. J., Barbuto, S., Wright, R., et al. (2004). Activation of Apoptosis In Vivo by a Hydrocarbon-Stapled BH3 Helix. *Science* 305, 1466–1470. doi:10.1126/science.1099191

Wallraven, K., Holmelin, F. L., Glas, A., Hennig, S., Frolov, A. I., Grossmann, T. N., et al. (2020). Adapting Free Energy Perturbation Simulations for Large Macrocyclic Ligands: How to Dissect Contributions from Direct Binding and Free Ligand Flexibility. *Chem. Sci.* 11, 2269–2276. doi:10.1039/c9sc04705k

Wang, J. L., Zhang, Z. J., Choksi, S., Shan, S., Lu, Z., Croce, C. M., et al. (2000). Cell Permeable Bcl-2 Binding Peptides: a Chemical Approach to Apoptosis Induction in Tumor Cells. *Cancer Res.* 60, 1498–1502.

Wang, G., Nikolovska-Coleska, Z., Yang, C.-Y., Wang, R., Tang, G., Guo, J., et al. (2006). Structure-Based Design of Potent Small-Molecule Inhibitors of Anti-apoptotic Bcl-2 Proteins. *J. Med. Chem.* 49, 6139–6142. doi:10.1021/jm060460o

Wang, L., Sloper, D. T., Addo, S. N., Tian, D., Slaton, J. W., and Xing, C. (2008). WL-276, an Antagonist against Bcl-2 Proteins, Overcomes Drug Resistance and Suppresses Prostate Tumor Growth. *Cancer Res.* 68, 4377–4383. doi:10.1158/0008-5472.can-07-6590

Wang, L., Wu, Y., Deng, Y., Kim, B., Pierce, L., Krilov, G., et al. (2015). Accurate and Reliable Prediction of Relative Ligand Binding Potency in Prospective Drug Discovery by Way of a Modern Free-Energy Calculation Protocol and Force Field. *J. Am. Chem. Soc.* 137, 2695–2703. doi:10.1021/ja512751q

Wei, J., Stebbins, J. L., Kitada, S., Dash, R., Placzek, W., Rega, M. F., et al. (2010). BI-97C1, an Optically Pure Apogossypol Derivative as Pan-Active Inhibitor of Antiapoptotic B-Cell Lymphoma/leukemia-2 (Bcl-2) Family Proteins. *J. Med. Chem.* 53, 4166–4176. doi:10.1021/jm1001265

Wells, J. A., and McClendon, C. L. (2007). Reaching for High-Hanging Fruit in Drug Discovery at Protein-Protein Interfaces. *Nature* 450, 1001–1009. doi:10.1038/nature06526

Wen, Z., He, J., Tao, H., and Huang, S.-Y. (2019). PepBDB: a Comprehensive Structural Database of Biological Peptide-Protein Interactions. *Bioinformatics* 35, 175–177. doi:10.1093/bioinformatics/bty579

Weng, G., Gao, J., Wang, Z., Wang, E., Hu, X., Yao, X., et al. (2020). Comprehensive Evaluation of Fourteen Docking Programs on Protein-Peptide Complexes. *J. Chem. Theor. Comput.* 16, 3959–3969. doi:10.1021/acs.jctc.9b01208

Wu, G., Chai, J., Suber, T. L., Wu, J.-W., Du, C., Wang, X., et al. (2000). Structural Basis of IAP Recognition by Smac/DIABLO. *Nature* 408, 1008–1012. doi:10.1038/35050012

Xu, X., Yan, C., and Zou, X. (2018). MDockPeP: An Ab-Initio Protein-Peptide Docking Server. *J. Comput. Chem.* 39, 2409–2413. doi:10.1002/jcc.25555

Yan, C., Wu, F., Jernigan, R. L., Dobbs, D., and Honavar, V. (2008). Characterization of Protein-Protein Interfaces. *Protein J.* 27, 59–70. doi:10.1007/s10930-007-9108-x

Yan, C., Xu, X., and Zou, X. (2016). Fully Blind Docking at the Atomic Level for Protein-Peptide Complex Structure Prediction. *Structure* 24, 1842–1853. doi:10.1016/j.str.2016.07.021

Yang, B., Liu, D., and Huang, Z. (2004). Synthesis and Helical Structure of Lactam Bridged BH3 Peptides Derived from Pro-apoptotic Bcl-2 Family Proteins. *Bioorg. Med. Chem. Lett.* 14, 1403–1406. doi:10.1016/j.bmcl.2003.09.101

Yap, J. L., Chen, L., Lanning, M. E., and Fletcher, S. (2017). Expanding the Cancer Arsenal with Targeted Therapies: Disarmament of the Antiapoptotic Bcl-2 Proteins by Small Molecules. *J. Med. Chem.* 60, 821–838. doi:10.1021/acs.jmedchem.5b01888

Yin, H., Slusky, J. S., Berger, B. W., Walters, R. S., Vilaire, G., Litvinov, R. I., et al. (2007). Computational Design of Peptides that Target Transmembrane Helices. *Science* 315, 1817–1822. doi:10.1126/science.1136782

Zhang, Y., and Sanner, M. F. (2019). AutoDock CrankPep: Combining Folding and Docking to Predict Protein-Peptide Complexes. *Bioinformatics* 35, 5121–5127. doi:10.1093/bioinformatics/btz459

Zhang, B. W., Jasnow, D., and Zuckerman, D. M. (2010). The "Weighted Ensemble" Path Sampling Method Is Statistically Exact for a Broad Class of Stochastic Processes and Binning Procedures. *J. Chem. Phys.* 132, 054107. doi:10.1063/1.3306345

Zhang, D., Liu, H., and Cui, J. (2018). Binding of Anti-apoptotic Bcl-2 with Different BH3 Peptides: A Molecular Dynamics Study. *Chem. Phys. Lett.* 691, 103–109. doi:10.1016/j.cplett.2017.10.030

Zhou, G., Pantelopulos, G. A., Mukherjee, S., and Voelz, V. A. (2017). Bridging Microscopic and Macroscopic Mechanisms of P53-MDM2 Binding with Kinetic Network Models. *Biophysical J.* 113, 785–793. doi:10.1016/j.bpj.2017.07.009

Zhou, P., Jin, B., Li, H., and Huang, S.-Y. (2018). HPEPDOCK: a Web Server for Blind Peptide-Protein Docking Based on a Hierarchical Algorithm. *Nucleic Acids Res.* 46, W443–W450. doi:10.1093/nar/gky357

Zhu, J., Zhu, J., Negri, A., Provasi, D., Filizola, M., Coller, B. S., et al. (2010). Closed Headpiece of Integrin αIIbβ3 and its Complex with an αIIbβ3-specific Antagonist that Does Not Induce Opening. *Blood* 116, 5050–5059. doi:10.1182/blood-2010-04-281154

Zwier, M. C., Pratt, A. J., Adelman, J. L., Kaus, J. W., Zuckerman, D. M., and Chong, L. T. (2016). Efficient Atomistic Simulation of Pathways and Calculation of Rate Constants for a Protein-Peptide Binding Process: Application to the MDM2 Protein and an Intrinsically Disordered P53 Peptide. *J. Phys. Chem. Lett.* 7, 3440–3445. doi:10.1021/acs.jpclett.6b01502

Conflict of Interest: The authors declare that the research was conducted in the absence of any commercial or financial relationships that could be construed as a potential conflict of interest.

frontiers in Molecular Biosciences

REVIEW
published: 14 June 2021
doi: 10.3389/fmolb.2021.697586

Therapeutic Peptides Targeting PPI in Clinical Development: Overview, Mechanism of Action and Perspectives

Walter Cabri, Paolo Cantelmi, Dario Corbisiero, Tommaso Fantoni, Lucia Ferrazzano, Giulia Martelli, Alexia Mattellone and Alessandra Tolomelli**

Department of Chemistry "Giacomo Ciamician", Alma Mater Studiorum University of Bologna, Bologna, Italy

Targeting protein-protein interactions (PPIs) has been recently recognized as an emerging therapeutic approach for several diseases. Up today, more than half a million PPI dysregulations have been found to be involved in pathological events. The dynamic nature of these processes and the involvement of large protein surfaces discouraged anyway the scientific community in considering them promising therapeutic targets. More recently peptide drugs received renewed attention since drug discovery has offered a broad range of structural diverse sequences, moving from traditionally endogenous peptides to sequences possessing improved pharmaceutical profiles. About 70 peptides are currently on the marked but several others are in clinical development. In this review we want to report the update on these novel APIs, focusing our attention on the molecules in clinical development, representing the direct consequence of the drug discovery process of the last 10 years. The comprehensive collection will be classified in function of the structural characteristics (native, analogous, heterologous) and on the basis of the therapeutic targets. The mechanism of interference on PPI will also be reported to offer useful information for novel peptide design.

Keywords: therapeutics, clinical trials, PPI, peptides, pharmacokinetic, GLP-1, cancer, SPPS

OPEN ACCESS

Edited by:
M. Angeles Jimenez, Instituto de Química Física Rocasolano (IQFR), Spain

Reviewed by:
Alemayehu A. Gorfe, University of Texas Health Science Center at Houston, United States
Efstratios Stratikos, National and Kapodistrian University of Athens, Greece

****Correspondence:***
Alessandra Tolomelli
alessandra.tolomelli@unibo.it
Walter Cabri
walter.cabri@unibo.it

Specialty section:
This article was submitted to Molecular Recognition, a section of the journal Frontiers in Molecular Biosciences

Received: *19 April 2021*
Accepted: *01 June 2021*
Published: *14 June 2021*

Citation:
Cabri W, Cantelmi P, Corbisiero D, Fantoni T, Ferrazzano L, Martelli G, Mattellone A and Tolomelli A (2021) Therapeutic Peptides Targeting PPI in Clinical Development: Overview, Mechanism of Action and Perspectives. Front. Mol. Biosci. 8:697586. doi: 10.3389/fmolb.2021.697586

INTRODUCTION

In the progression of many pathological states, protein–protein interactions (PPIs) play the fundamental role of mediators of signal transmission and for this reason they represent optimal targets for drug discovery.

The size of the human interactome, the complex network of protein interactions, has been estimated to involve about 650,000 relevant contacts (Stumpf et al., 2008) that regulate all biological events and are responsible, when dysregulated, of a great number of pathological diseases. The dynamic nature of PPI and the large contact area that is often required between the partners (approximately 1,000–4,000 Å) have discouraged in the past to consider them as interesting targets. Small molecule drugs indeed are able to inhibit only interactions involving a binding area from 300 to 1,000 Å (Jones and Thornton, 1996) and PPI often lack of definite pockets. Usually protein association occurs between hydrophobic regions called "hot spots", rich in amino acids that are able to form hydrogen bonds and π-interactions, and only a small number of crucial residues within the complete area are involved in determining binding affinity and specificity. Many hot spots core regions are associated with the presence of α-helix, β-sheet and β-turn protein secondary structure

motifs and peptidomimetics targeting PPI have been tailored in the past years to mimic these ordered structures (Robertson and Spring, 2018; Mabonga and Kappo, 2020).

In this scenario, peptides have been discarded as potential lead compounds because they were affected by several issues, namely the random conformations of short sequences, the difficulties in synthesis and purification of longer ones and the sensitivity to endopeptidases, determining generally half-lives of few minutes (Fozgerau and Hoffmann, 2015). Moreover, susceptibility to proteolytic degradation made oral administration a challenge. The development of reliable techniques for peptide synthesis and purification gave access to pharmaceutical grade peptides, even with a high number of amino acids. In addition, molecular design can easily overcome the above-mentioned limits, thanks to the incorporation of non-native amino acids, the introduction of lipophilic side chains or cyclic sequences. For this reason, in the last two decades peptides have found renewed attention (Lau and Dunn, 2018) and up today about 70 therapeutic peptides have been approved and launched on the market. Among the reasons behind the development of new chemical entities (NCEs) in the polypeptide segment there is the commercial and therapeutic success of GLP-1 analogues, Liraglutide and Semaglutide, for the treatment of type 2 diabetes and obesity, that exceeded 7.6 B$ sales in 2020 (Novo Nordisk 2020 annual report, February 3, 2021). The 13 h half-life of liraglutide (Neumiller and Campbell, 2009) and the 7 days half-life of semaglutide (Hall et al., 2018), which is also orally available, have been at the basis of the success of these medicines. Several market studies forecasted a consistent global growth and success of the peptide segment, from 29 B$ sales in 2019 to 48 B$ in 2025 (excluding insulin), with an annual 10% increase (Mordor Intelligence, 2020).

We focused this review on the peptides under clinical trials in the last 3 years, that are the direct application of the increased PPI knowledge and of the synthetic design and tactics evolution during the last 10 years. Only therapeutic peptides with a length up to 40 aa, according to the FDA definition, are discussed (FDA - U.S. Food and Drug Administration, 2018). We strictly considered therapeutic peptides targeting PPI, excluding diagnostic, radiotherapeutics, vaccines and conjugated peptides with different chemical modalities (Blanco and Gardinier, 2020).

The identification of peptides in clinical phase was not a simple task. The list of peptides under development discussed in this survey is the combination and critical evaluation of information coming from Cortellis-Clarivate, clinical trials databases (United States and Europe) and from companies' web sites, in order to really understand product status. In fact, during the drug discovery and development process few companies communicate NCEs elimination from the pipeline and most of the time the molecule simply disappears from official reports and websites. In addition, the same molecule can be identified with several codes and names due to product sales, co-development between companies, company mergers and acquisitions or definition of an international nonproprietary name. The list of discussed molecules includes 58 peptides in different clinical phases: 13 entered the Phase 1, 26 are in Phase 2, 15 are in Phase 3, while four are close to approval being the new drug application (NDA) already submitted to regulatory authorities (**Figure 1**). A striking difference in respect to the past is the increased number of amino acids, being the number of peptides with 20–40 residues prevailing on shorter peptides (26 *vs* 21) among the disclosed structures (47 of 58). However, this number should be even higher, considering that nine undisclosed structure are in diabetes and obesity segment, were peptides are typically longer than 20 AA.

With the only exception of two peptides, GT001 and Elsiglutide, that are produced through recombinant technology, all the other compounds with disclosed sequence are synthetically produced, commonly via solid phase approach (SPPS). In this context, many groups worldwide are targeting green innovative techniques (Lawrenson et al., 2017; Ferrazzano et al., 2019; Nuijens et al., 2019; Martin P. et al., 2020). As for the pathologies, diabetes, obesity, cancer and related pathologies are the major areas of interest.

Polypeptides have been classified according to Lau/Dunn definition (Lau and Dunn, 2018): **native** peptides have the same sequence of endogenous ligand, while **analogous** are products where the natural sequence has been modified in order to achieve a better pharmacological profile. **Heterologous** peptides have been discovered independently respect to the natural ligand and are based on a more classical medicinal chemistry approach (**Figure 2**). It is worth to notice that native peptides and their analogues represent more than 70% of the PPI targeting peptides in clinical trials, being in particular, the analogue ones accounting for 60% of the pipeline. The peptides have been discussed on the basis of the target pathology and, besides the clinical trial stage, the route of administration (RoA), as a symptom of peptide pharmacokinetic properties, has been considered (**Figure 3**).

CANCER AND RELATED PATHOLOGIES

The role of PPI in the development of tumors is strictly connected to protein-mediated signalling processes, able to activate several biological networks related to tumorigenesis, progression, invasion, and metastasis. For this reason, introducing perturbations in PPI represents an efficient strategy for interrupting cancer-related phenomena. Looking at different tumor phenotypes, specific proteins undergo modifications in their interaction pattern when they become part of carcinogenic phenomenology, with important effects on a patient' state of health. Depending on the tumor localization, it is possible to target different candidate proteins, generally transmembrane receptors or releasing hormone receptors, with theranostic performances useful in understanding cancer progression and improving treatment efficacy (Gulfidan et al., 2020).

Concerning the role of transmembrane receptors in cancer development, **Dolcanatide** was designed for the treatment of inflammatory bowel disease and functional gastrointestinal disorders to prevent colon cancer. In fact, cells belonging to intestinal epithelium are responsible for controlling toxic pathogens' efflux through the digestive apparatus and transport of nutrients, fluids, and bacterial flora (Rappaport

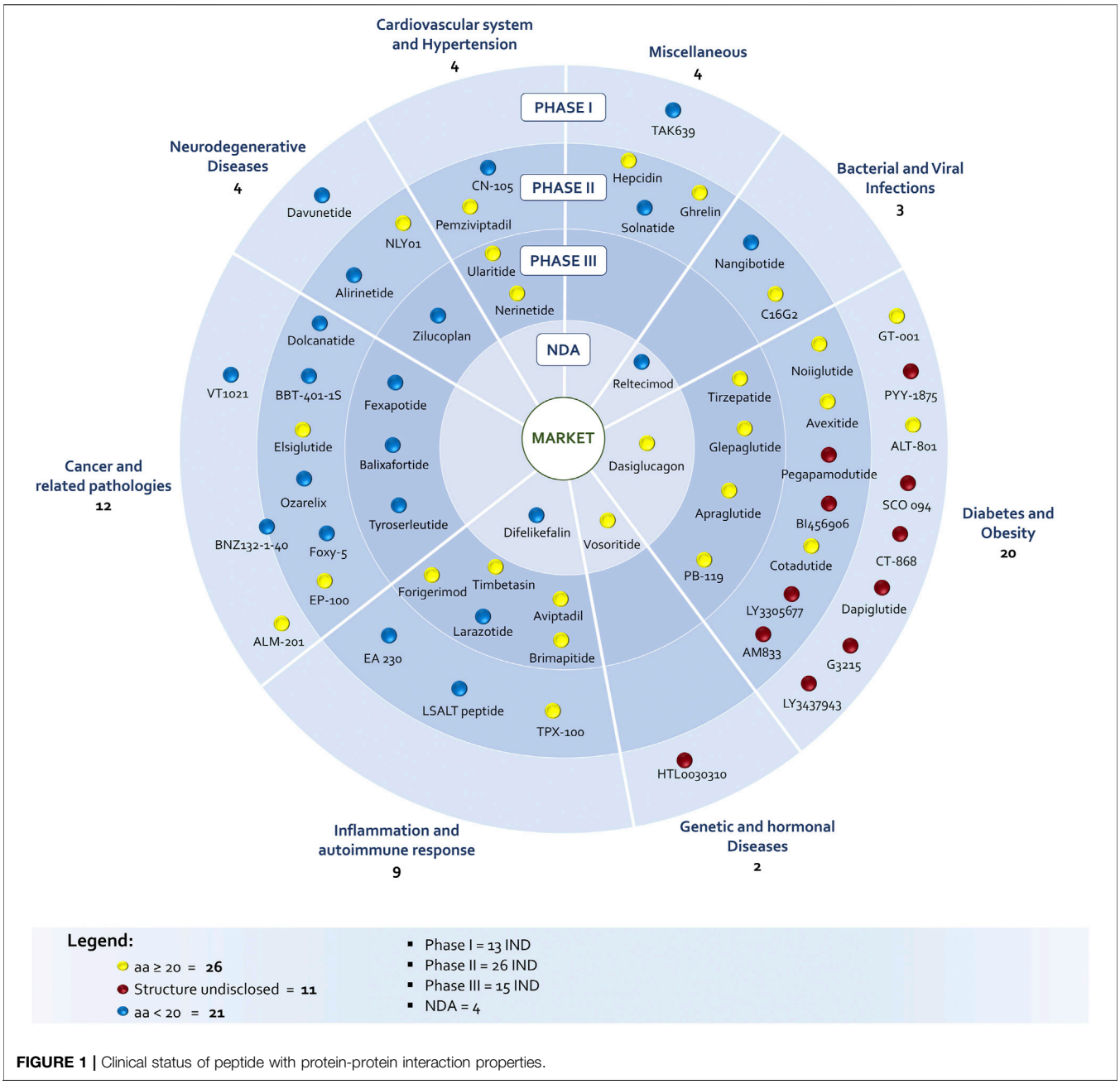

FIGURE 1 | Clinical status of peptide with protein-protein interaction properties.

and Waldman, 2018). To maintain homeostatic control of these processes the intestinal epithelial receptor, guanylate cyclase C (GUCY2C), and its cyclic nucleotide second messenger, cyclic guanosine monophosphate (cGMP), play a critical role. This heterodimeric transmembrane receptor can be activated by endogenous extracellular peptide ligands or other signalling agents, such as Ca^{2+} and nitric oxide (Boulete et al., 2018). Known ligands for GUCY2C receptor are the bacterial heat-stable enterotoxin, ST (cause of traveller's diarrhea), and the endogenous peptides, uroguanylin and guanylin. Dolcanatide was designed to be an analogue of uroguanylin with enhanced resistance to standard digestive breakdown by proteases in the intestine as consequence of the presence of a disulfide bridge. The peptide sequence differs from uroguanylin for the substitution of Asp with Glu at the 3-position at the N-terminus, for greater binding affinity, and for L-Asn1 and L-Leu16 replaced by D-Asn1 and D-Leu16 at the N- and C-termini, respectively, which are thought to provide enhanced biostability (Shailubhai et al., 2015). Dolcanatide is supposed to bind GUCY2C similarly to uroguanylin and the other known endogenous ligands, via the NH_2-terminal β-hairpin, by providing the third strand of a small triple-stranded antiparallel β-sheet (Lauber et al., 2003).

Similarly, **BBT-401** (structure undisclosed) is an orally available Pellino-1 protein-protein interaction inhibitor for the

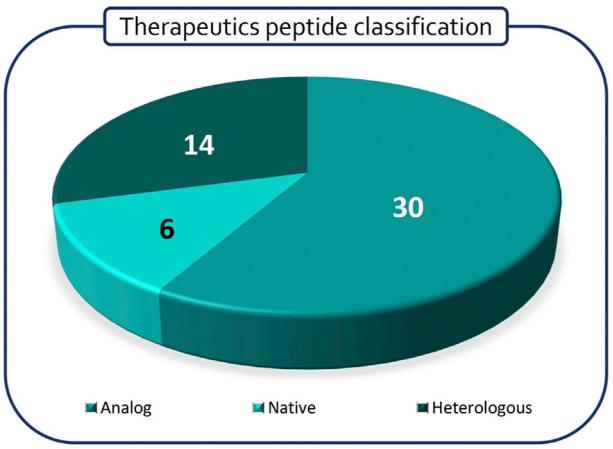

FIGURE 2 | Classification of discussed peptides according to Lau/Dunn classification.

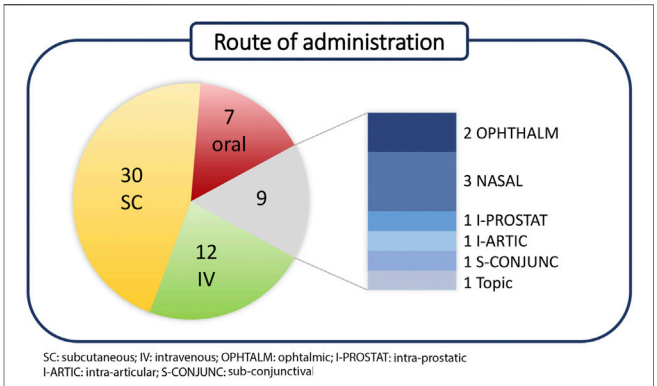

FIGURE 3 | Classification of discussed peptides on the basis of RoA.

treatment of patients affected by ulcerative colitis. This lipidated tetrapeptide binds Pellino-1 protein, interfering in its signalling cascade. BBT-401 efficiently inhibited the lipopolysaccharide-induced activation of the toll-like receptor proinflammatory signalling pathway, reducing proinflammatory cytokine expression as well. Studies on animal models showed that BBT-401 administration in colitis significantly improved symptoms and histopathological parameters associated to the disorder, and direct colon administration enhances considerably the therapeutic efficacy (Lee et al., 2019).

Interfering on surface receptors functions seems to be particularly relevant for solid and metastatic tumor progression. **Foxy-5** is a formylated WNT5A-derived six amino acid peptide, recently used in a Phase 1 trial in patients with metastatic breast, colon and prostate cancer and in a Phase 2 trial for early stage colon cancer. Its model protein, WNT5A, is a member of the Wnt protein family, which plays important roles in several physiological phenomena, like organ development, tissue orientation, cell polarity and migration. Its dysregulation has been associated with progression of various diseases as a consequence of its tumor-suppressive function in colon cancer, neuroblastoma, breast carcinomas, and leukemia (Säfholm et al., 2008; Canesin et al., 2017). In this contest, Foxy-5 has been characterized as a WNT5A-mimicking peptide, since it acts by triggering cytosolic free calcium signalling and by impairing migration and invasion of epithelial cancer cells. In silico prediction suggests that Foxy-5 could adopt in solution a short loop and alpha helical structure, a motif quite common in protein-protein interactions. In the structure of the full-length native protein, this segment is solvent exposed and could be involved in macromolecular interactions. Foxy-5 seems to be part of an exosite, expected to be critical for the interactions of WNT-5A with receptors and be part of a dimerization site (**Figure 4**, Villoutreix, 2017).

VT1021 is a cyclic pentapeptide developed by Vigeo Therapeutics whose structure is still undisclosed. It acts as a potent inducer of thrombospondin-1 (Tsp-1) expression in the tumor microenvironment (TME), which is then totally reprogrammed to reduce its immune-suppressive and tumor-promoting propensity, promoting instead the activation of the adaptive immune system and its tumor-inhibiting inclination (Harb et al., 2019). VT-1021 is at Phase 1 of clinical trials for the treatment of solid tumor since, in preclinical animal models, it showed robust anti-tumor activities on ovarian, pancreatic and breast cancer, with complete tumor regression and reprogramming of the immune TME.

Balixafortide is another good example of a potent and selective antagonist of the chemokine receptor CXCR4, which belongs to the transmembrane receptor family of G-coupled protein receptors (GPCR). This protein is largely expressed in several tumors type, including expression by cells of immune system in carcinogenic tissues. The role of CXCR4 in metastatic phenomena is particularly relevant, since this protein allows cancer cells to migrate to other sites where its natural ligand CXCL12 is expressed, like in the bone marrow of patients affected by breast cancer (Zimmermann et al., 2019). This evidence justifies the application of Balixafortide, in combination with eribulin, in Phase 3 trial for metastatic breast cancer and in a more recent Phase 1 trial for a dose-escalation study (Kaufmann et al., 2020).

In cancer progression and tumorigenesis, interleukin dysregulation has an important role, and its upregulation seems to be associated with many tumors. For this reason, controlling its functions is advantageous for blocking cancer development. **BNZ132-1-40** is a 19-mer pegylated peptide belonging to the anticytokine peptide family, active selectively on IL-15, IL-2 and IL-9, which drives T-cell mediated diseases including T-cell large granular lymphocyte leukemia (T-LGLL) and HTLV-1 driven adult T-cell leukemia (ATL) (Massoud et al., 2015; Wang et al., 2019). The peptide structure with helical conformation is responsible for the direct binding to γc receptor, present in all the above-mentioned cytokines which are fundamental for leukemia survival and lack of strong active therapies. Furthermore, the presence of a PEG-chain was required to increase the peptide half-life. The selectivity of BNZ132-1-40 for Tregs, $CD8^+$ T and NK cells was confirmed by the absence of adverse effects on other immune cells and the tolerance showed by healthy subjects reported in a recent Phase 1 clinical trial (Nata et al., 2015).

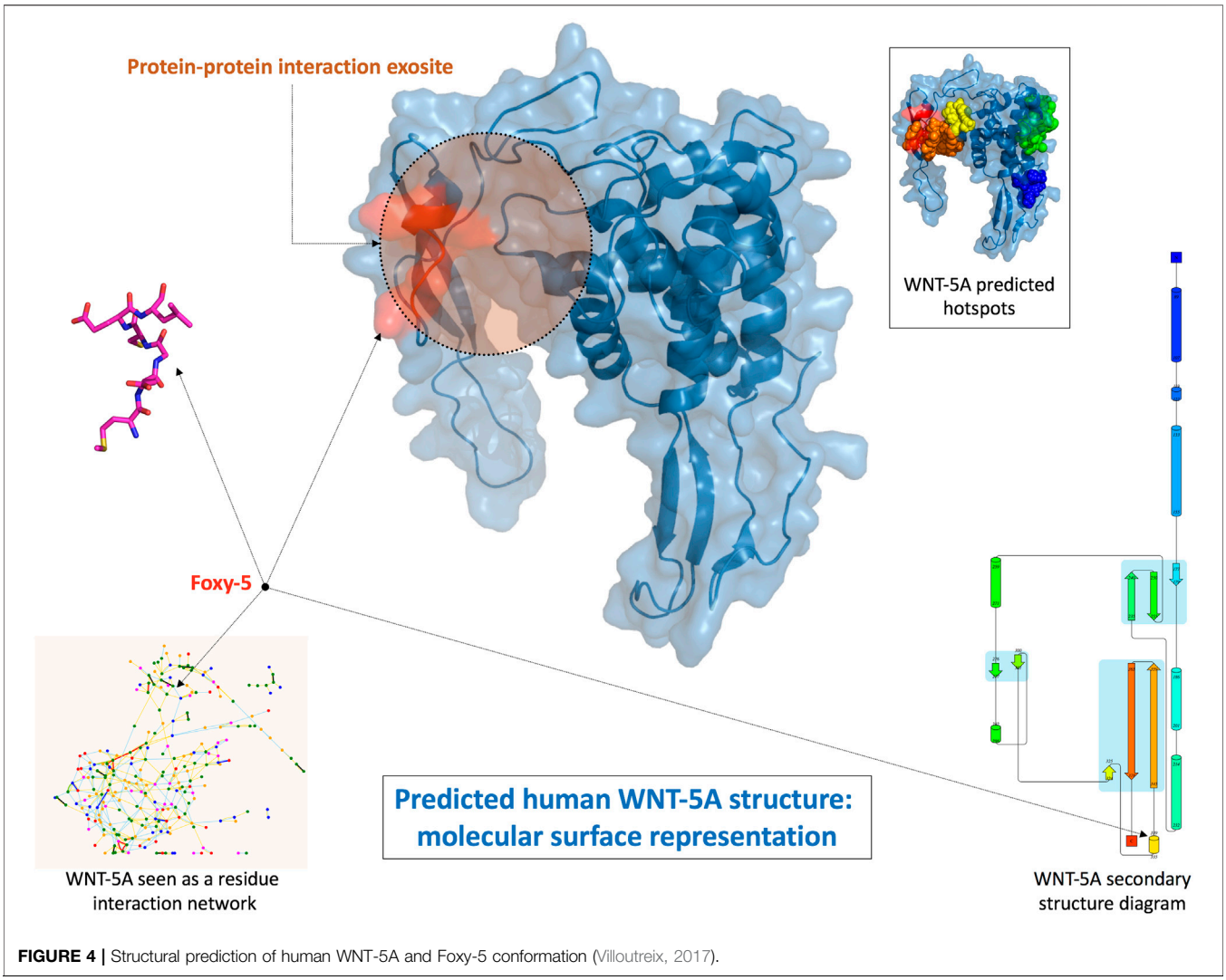

FIGURE 4 | Structural prediction of human WNT-5A and Foxy-5 conformation (Villoutreix, 2017).

ALM-201, that is a 23-mer peptide drug candidate, is a synthetic derivative of AD-01, a 24-mer peptide containing the sequence 34-58 of FK506-binding protein like (FKBPL). This protein, that showed prognostic potential in breast cancer, can be classified both as extracellular and intracellular protein: in the first case, it acts as a secreted anti-angiogenic protein targeting cell surface receptor CD44, upregulated in carcinogenic scenario, while intracellularly FKBPL shows a prognostic activity for breast cancer survival. As a consequence, FKBPL is involved in many cellular processes like cell cycle progression, signalling and differentiation (Annett et al., 2020). ALM201, like other FKBPL derivatives, inhibits breast cancer metastasis through Notch signalling, showing excellent safety profile in Phase 1 clinical trials, when applied for the treatment of ovarian cancer and solid tumor (McClements et al., 2019).

In some cases, the complexity of cancer physiopathology does not allow to clearly identify a single target protein to control cancer progression, even if efficient drug treatments can be applied. As an example, **Fexapotide triflutate** is a 17-mer peptide in clinical development for prostate cancer and hyperplasia. Even if its mechanism of action remains partially undisclosed, it is known that Fexapotide works stimulating several protein pathways, like caspase, tumor necrosis factor and BCL pathways in prostate glandular epithelial cells. It induces selective cell membrane permeability, mitochondrial metabolic arrest and reduces RNA, DNA lysis and aggregation, with subsequent cell fragmentation and loss, causing decompression of the urethral lumen (Shore et al., 2018). Studies on animal models revealed that Fexapotide direct injection in injured tissues, like bladder, urethra, rectum, periprostatic tissue, leaves unaffected adjacent tissues. For all these evidences, it reached Phase 3 in clinical trials for urinary-related pathologies.

Similarly, **Tyroserleutide** (YSL) is a tripeptide compound active on primary hepatocellular carcinoma, in Phase 3 of clinical trials. This short peptide, which showed very high activity and few side-effects, was originally purified from the hydrolysates of pig's spleen, but now obtained through chemical synthesis. To carry out its antitumor activity, YSL involves the second messenger Ca^{2+}, which is able to modulate cell function by

Ca^{2+}/calmodulin (CaM) pathway. In addition, CaM associates with phosphatidylinositol three kinase (PI3K), enhancing its activity and promoting upregulated cell proliferation (Zhao et al., 2008).

For the treatment of cancer types associated with the functioning of endocrine systems or for controlling side-effects related to other chemotherapeutic treatments, hormone receptors release appears a good targeting strategy to control and stop tumor escalation. **Elsiglutide**, a selective glucagon-like peptide of type 2 (GLP-2) derivative, was developed as adjuvant to chemotherapy to reduce induced diarrhoea. This new synthetic versions of GLP-2 and elsiglutide show longer half-life, reducing the frequency of administration. (Mayo et al., 2020). The peptide completed successfully a Phase 2 clinical trial.

Ozarelix is a fourth generation Luteinizing Hormone-Releasing Hormone (LHRH) antagonist acting on Gonadotropin-releasing hormone (GnRH) receptor, which controls the secretion of luteinizing and follicle-stimulating hormone from the anterior pituitary gland. As other LHRH analogues, it is a 10-mer peptide with several D-amino acids and bulky residues (in particular in position 6) to enhance stability against proteolysis. Gonadotropin-releasing hormone is a decapeptide (EHWSYGLRPG), displaying an *N*-terminal trimeric fragment responsible for agonist activity and a C-terminal trimer necessary for affinity to the receptor. Since the predominant bioactive conformer consists of a β-turn, where the two terminals are close together, analogues have been generally designed by replacing the central glycine in position 6 with residues able to stabilize the requested turn (Flanagan and Manilall, 2017). At first, Ozarelix was designed to stimulate secretion of gonadotropins, but continuous evidence demonstrates a decrease of pituitary hormone secretion, as a consequence of gonadotrophic cells desensitization and down-regulation of pituitary receptors (Festuccia et al., 2010). In fact, as GnRH antagonists, Ozarelix induces reduction in gonadotropin levels by inhibition of their secretion from the anterior pituitary gland. Ozarelix completed Phase 2 of clinical trials for the treatment of prostate cancer, showing higher solubility, definitive suppression of testosterone and any risk of clinical flare if compared to other antagonists (Schneider et al., 2010).

EP-100 is a synthetic LHRH natural ligand derivative made up 28 amino acid, 18 of which belong to the cationic α-helical lytic peptide (CLIP-71). Luteinizing-hormone-releasing hormone (LHRH) receptors overexpression has been found in several tumor types, like prostate, breast, ovarian, endometrial, pancreatic, bladder, colorectal, melanoma and non-Hodgkin lymphoma. For this reason, it has been selected as privileged target for treatment of solid and ovarian tumors, where EP-100 is in Phase 1 and 2 of clinical trials, respectively. LHRH sequence (HWSYGLRP) is responsible for the delivery of the lytic peptide to cancer cells via specific binding to the receptor LHRH on cell-surface receptors. The mode of action of EP-100 is not completely known. In fact, the negatively charged outer membrane of cancer cells determines the high selectivity of this peptide for carcinogenic tissues: after binding of LHRH targeting sequence, the positively charged portion of EP-100 interacts with the outer membrane of cancer cells in a disruptive manner, causing cell lysis and death (Curtis et al., 2014; Kim et al., 2020).

INFLAMMATION AND AUTOIMMUNE RESPONSE

Inflammation and autoimmune responses are essentials body's defence mechanisms. They are the processes by which the immune system recognizes and removes harmful and foreign stimuli and begins the healing processes (Pahwa et al., 2021). However, when an adaptive immune response develops against self-antigens or there is an upregulated recruitment of pro-inflammatory molecules, it is usually impossible for immune effector mechanisms to completely eliminate the antigen/pro-inflammatory molecules, and therefore a sustained response occurs (Janeway et al., 2001). In this perspective, peptide-based treatments able to interfere with the dysregulated body's defence were developed.

Forigerimod (ImmuPharma, 2019) is a synthetic 21-mer linear peptide, phosphorylated in correspondence of Ser11 position, produced by ImmuPharma and designed from the small nuclear ribonucleoprotein U1-70 (Zimmer et al., 2013). As suggested by its commercial name, Lupuzor™ is employed for the treatment of Systemic Lupus Erythematosus (SLE), a chronic, life-threatening autoimmune, inflammatory disease affecting multiple organs such as skin, joints, kidneys, blood cells, brain, heart and lungs. Due to the high relevance of this pathology, Lupuzor™ received fast-track designation from the FDA, which expedites the drug's approval process (ImmuPharma, 2021). Currently, the mechanism of action of Lupuzor™ has not been fully elucidated; however, several studies have shown that it displays tolerogenic and immunomodulatory effects leading to the inhibition of T cells' reactivity in presence of endogenous peptides.

On the other hand, for the treatment of Systemic Inflammatory Response Syndrome (SIRS) the intravenous infusion of **EA-230,** a synthetic 4-mer linear peptide produced by Exponential Biotherapies, is currently under investigation (Phase 2). The sequence was designed on the basis of the β-loop contained in the β subunit of the endogenous peptide human Chorionic Gonadotropin (hCG) (van den Berg et al., 2011). The SIRS pathology is caused by an upstream of pro-inflammatory agents (such as IL-6) and this dysregulated inflammatory response often results in tissue damage, failure of one or more organ systems, and high mortality. Even though the mechanism of action EA-230 is still unclear, biological evidence have demonstrated how changes of the hormonal milieu play a central role in the anti-inflammatory response (van Groenendael et al., 2019).

Another peptide employed to cure inflammation diseases is **Difelikefalin** acetate, a synthetic 5-mer linear D-peptide produced by Cara Therapeutics and designed starting from the sequence of the endogenous peptide Dinorphin A. As such, Difelikefalin acetate is an agonist of κ-opioid receptor (KOR) for the treatment of Chronic kidney disease-associated pruritus (CKD-aP), or uremic pruritus, and it has completed Phase 3

clinical trials in 2020 (Fishbane et al., 2020). CKD-aP is a severely distressing condition that occurs in more than 60% of patients undergoing dialysis and, even if the pathogenesis is still incompletely understood, opioid imbalance has been identified as a possible reason of the arise of this pathology (Lipman and Yosipovitch, 2020). Due to the ubiquitous nature of KOR (in peripheral and central nervous system), Difelikefalin acetate was designed as a selective agonist, avoiding the penetration into the CNS that aims to provide the benefits of minimizing itch through activation of the anti-pruritic KOR system without causing CNS side effects.

Moving to inflammation affecting the respiratory system, it is possible to mention the **LSALT peptide**, a synthetic 16-mer linear peptide developed by Arch Biopartners and still ongoing in Phase 2 clinical trials (Arch Biopartners, 2021) for the treatment of Acute Respiratory Distress Syndrome (ARDS). A hallmark feature of this inflammation is the recruitment of neutrophils from the bloodstream into inflamed tissue (Choudhury et al., 2019). In this context, dipeptidase-1 DPEP1, an anchored membrane protein, has been identified as the major adhesion receptor on the lung and liver endothelium for neutrophil sequestration, independently from its enzymatic activity. As a consequence, the inappropriate recruitment of neutrophils to various organs contributes to multi-organ dysfunction (such as pulmonary dysfunction). In order to prevent this healthy disfunctions, several experimental models have highlighted that LSALT peptide binds to DPEP-1 not inhibiting its enzymatic activity but preventing the neutrophils sequestration and the inflammation response.

Remaining within the ARDS treatment, **Avipdtadil** is a synthetic 28-mer linear peptide developed by NeuroRX and Relief Therapeutics Holding, designed starting from endogenous Vasoactive Intestinal Peptide (VIP) structure. This endogenous protein is involved in the development of pulmonary hypertension (PH), a progressive vascular disease caused by vasoconstriction and structural remodeling of arterioles, leading to dyspnea, fatigue, cough, chest pain, palpitations, peripheral edema, syncope, right heart failure, and death. Moreover, without treatment, PH can evolve in ARDS halving the survival rate within 5 years (Hu et al., 2015). As VIP analogue, Aviptadil through binding to G-protein coupled receptors (VPAC1, VPAC2 and PAC1) induces pulmonary vasodilation and shows anti-inflammatory properties. In fact, Aviptadil aerosol is still ongoing in Phase 2/3 for the treatment of ARDS leading to a small and temporary but significant selective pulmonary vasodilation, an to an improved stroke volume and mixed venous oxygen saturation (Leuchte et al., 2008).

Larazotide, a 9 m Biopharma's investigation drug (9 Meters Biopharma Inc., 2021), is the only therapeutic candidate for celiac disease adjuvant therapy, advanced to a Phase 3 clinical trial, that minimizes symptoms in tandem with gluten free diet. This octapeptide derives from the *Zonula Occludens* toxin secreted by *Vibrio cholerae* and it is an antagonist of zonulin, the only known physiological modulator of the intercellular tight junctions and a key player in regulation of the mucosal immune response in small intestine (Heickman et al., 2020).

Moving to more specific areas of the body, the treatment of the hearing and ocular inflammations is particularly interesting. **Brimapitide** is a synthetic dextrogyre 31-mer linear peptide developed by Auris Medical and designed from a combination of a 20-mer sequence of protein islet-brain 1 (IB-1) and 10-mer trans-activator of transcription sequence (TAT) of the HIVTAT protein, which allows its intracellular penetration. Its similarity with IB-1 makes this peptide a selective inhibitor of c-Jun N-terminal Kinase (JNK), a ubiquitous intracellular enzyme. (Chiquet et al., 2017). Its inhibition prevents formation of transcription complexes and further progress along the apoptotic pathway or activation of genes, which are encoding inflammatory molecules (such as cytokines). For this reason, Brimapitide is under investigation (Phase 3 clinical trials) for the treatment of acute sensorineural hearing loss (ASNHL) and ocular inflammation as biocompatible intratympanic hyaluronic acid gel and ophthalmic solution, respectively (Suckfuell et al., 2014).

Regarding the treatment of ocular inflammation, it is worth to mention **Timbetasin**, a synthetic 43-mer linear peptide produced by RegeneRX Biopharmaceuticals which behaves as analogue of the endogenous peptide Thymosin β4 from which it differs in the N-terminus acetylation. As such, Timbetasin is involved in the treatment of moderate to severe dry eye disease, thanks to its anti-inflammatory effect. Dry eye is a chronic ocular surface disease, causing visual morbidity that affects the quality of life, and it's associated with an increase in the levels of inflammatory cytokines in both the conjunctiva and tears (Sosne et al., 2015). Generally, endogenous Thymosin β4 promotes wound repair and regeneration in the skin, eye, heart, and nervous system in various animal models; moreover, it is known to modulate the expression of multiple signalling molecules, playing a role in the downregulation of transcription factors for inflammatory chemokines, cytokines, and metalloproteinases (Sosne and Ousler, 2015). For this reason, the topical supplementary administration as eye drop solution of Timbetasin is currently under investigation (Phase 3 clinical trials) for the promotion ocular surface healing, increase corneal epithelial cell migration, and decrease corneal pro-inflammatory cytokine levels.

Finally, for the treatment of inflammation of bone tissue, **TPX-100,** a synthetic 23-mer peptide which structure is currently undisclosed, is under investigation (OrthoTrophix, 2021). This peptide is produced by OrthoTrophix and designed starting from Matrix Extracellular Phosphoglycoprotein (MEPE), a protein belonging to the family of Small Integrin-Binding Ligand N-linked Glycoproteins (SIBLING) (McGuire et al., 2018). Evidence shows that these proteins play key roles in the mineralization of bones and dentin without a clear knowledge of the mechanism of action. It has been shown that the bone shape of the knee undergoes unidirectional and irreversible change over time, with a much greater rate of change in osteoarthritic knees than in normal ones (OrthoTrophix, 2021). Such accelerated bone shape mutation starts much earlier than cartilage degeneration and appears to be the most reliable structural marker, to date, for onset of osteoarthritis (OA). Even if the mechanism of action is still undisclosed, TPX-100 has completed Phase 2 clinical trial for the treatment of the knee osteoarthritis, inducing the

regeneration of normal tibiofemoral hyaline cartilage and highlighting a statistically significant correlation between stabilization of tibiofemoral cartilage and critical knee functions.

GENETIC AND HORMONAL DISEASES

Genetic disorders can be caused by a mutation in one gene (monogenic disorder), by mutations in multiple genes (multifactorial inheritance disorder), by a combination of gene mutations and environmental factors, or by damage to chromosomes (National Human Genome Research Institute NHGRI, 2021). On the other hand, hormonal disorders may result from a problem in the glands themself, or because the hypothalamic-pituitary axis (interplay of hormonal signals between the hypothalamus and the pituitary gland) provides too much or too little stimulations (Emanuele and Emanuele, 1997). In this context, peptide-based treatments can be employed both as complementary supply of the lacking endogenous molecules (genetic disorders) or/and as interfering agents on the mechanisms responsible for their dysregulated production (hormonal disorders).

HTL0030310 is a new synthetic peptide produced by Sosei Heptares which has recently completed Phase 1 of clinical trials for the evaluation of its safety and tolerability towards healthy subjects. Even though HTL0030310 structure is still undisclosed, Sosei Heptares designed this peptide as a selective SSTR5 (somatostatin 5) receptor agonist to treat endocrine disorders (Sosei Heptares, 2019) modulating the excess release of hormones from adenomas (benign tumors) of the pituitary gland. Highly elevated plasma levels of pituitary hormones result in a number of serious disorders including Cushing's Disease, a debilitating endocrine disorder caused by the overproduction of the hormone cortisol.

On the other hand, **Vosoritide** is a synthetic 39-mer cyclic peptide produced by BioMarin Pharmaceutical and currently in Phase 3 of clinical trials for the treatment of achondroplasia, the most common form of disproportionate short stature in humans (Savarirayan et al., 2020). This condition is caused by an autosomal dominant mutation in the fibroblast growth factor receptor 3 (FGFR3), a gene that constitutively activates the mitogen-activated protein kinase (MAPK), which inhibits endochondral ossification (Savarirayan et al., 2019). Since C-type natriuretic peptide (CNP) and its receptor, natriuretic peptide receptor 2 (NPR2), are potent stimulators of endochondral ossification, it was observed that a continuous intravenous infusion of exogenous C-type natriuretic peptide restores the impaired bone growth. Vosoritide was designed as a cyclic analogue of C-type natriuretic peptide in order to increase the half-life in comparison with its endogenous form.

DIABETES, OBESITY, SHORT BOWEL SYNDROME AND HYPERINSULINEMIA, THE PROGLUCAGON LEGACY

Over the last decades, a series of synthetic peptides derived from the gut endocrine system were identified as promising treatments for metabolic diseases such as Type 2 Diabetes Mellitus (T2DM) and obesity. These pathologies still remain global health problems in continuous increase, known to reduce quality of life and to lead to serious complications (Bastin and Andreeli, 2019). The therapy of T2DM involves agents targeting body weight and simultaneously maintaining blood glucose control.

The main synthetic therapeutic peptides have been designed by mimicking the sequences deriving from the pro-hormone proglucagon metabolic cleavage. This 158-mer small protein is submitted in pancreas, gut and central nervous system to specific posttranslational processing by prohormone convertase enzymes, leading to the generation of shorter fragments (**Figure 5**). Among them, glicentin-related pancreatic peptide (GRPP), glucagon, intervening peptide-1 (IP-1) and intervening peptide-2(IP-2), major proglucagon fragment (MPGF), oxyntomodulin (OXM), glucagon-like peptide-1 (GLP-1) and glucagon-like peptide-2 (GLP-2) have a prominent role in glucose control, energy balance and gut homeostasis and were hence proposed as models for drug design (Lafferty et al., 2021).

Glucagon Like Peptide-1 Receptor Targeting Peptides

One of the main biological targets for pharmaceutical action is the Glucagon like peptide-1 receptor (GLP-1R), a class BG-protein coupled receptor (GPCR), which is deeply involved in insulin secretion and homeostasis. Like other G-proteins, the GLP-1R is characterized by the seven transmembrane α-helices separated by three intracellular and three extracellular loops.

The GLP-1R activation is related to the secretion of glucagon like peptide 1 (GLP-1), an incretin glucoregulatory peptide released in the gut after food intakes. GLP-1 exists in two forms: GLP-1(7-37) and GLP-1(7-36) amide, with the latter being more abundant in circulation after eating. These peptides, interacting with GLP-1R, enhance the insulin secretion and normalize the glucose levels through the receptor signalling, *via* cyclic adenosine monophosphate (cAMP) production (Druker and Nauck, 2006). When the regulatory effect is complete, the GLP-1 is inactivated by proteolysis. Over this main effect, GLP-1 and its agonists can reduce the glucagon secretion, slow the gastric transit and decrease the energy consumption extending the effects on treatment of obesity. The key role of the GLP-1R/GLP-1 system is reflected by the efforts recently made in developing efficient GLP-1R peptide agonists for pharmacological treatment of T2DM (Sloop et al., 2018).

A great advance in the field was reached with the discovery of exendin-4 in the venom of the *Gila monster* lizard. Exendin-4 (or Exenatide, as it has been called its synthetic form) is a 39-mer peptide resistant to dipeptidyl peptidase 4 (DPP-4), which shows a better pharmacokinetic than GLP-1 thanks to a Gly^2 residue in its sequence. Exenatide was approved by FDA in 2005 and is dosed as a twice daily injection (Donnelly, 2012). Currently the best in class drugs for T2DM and obesity are liraglutide and more

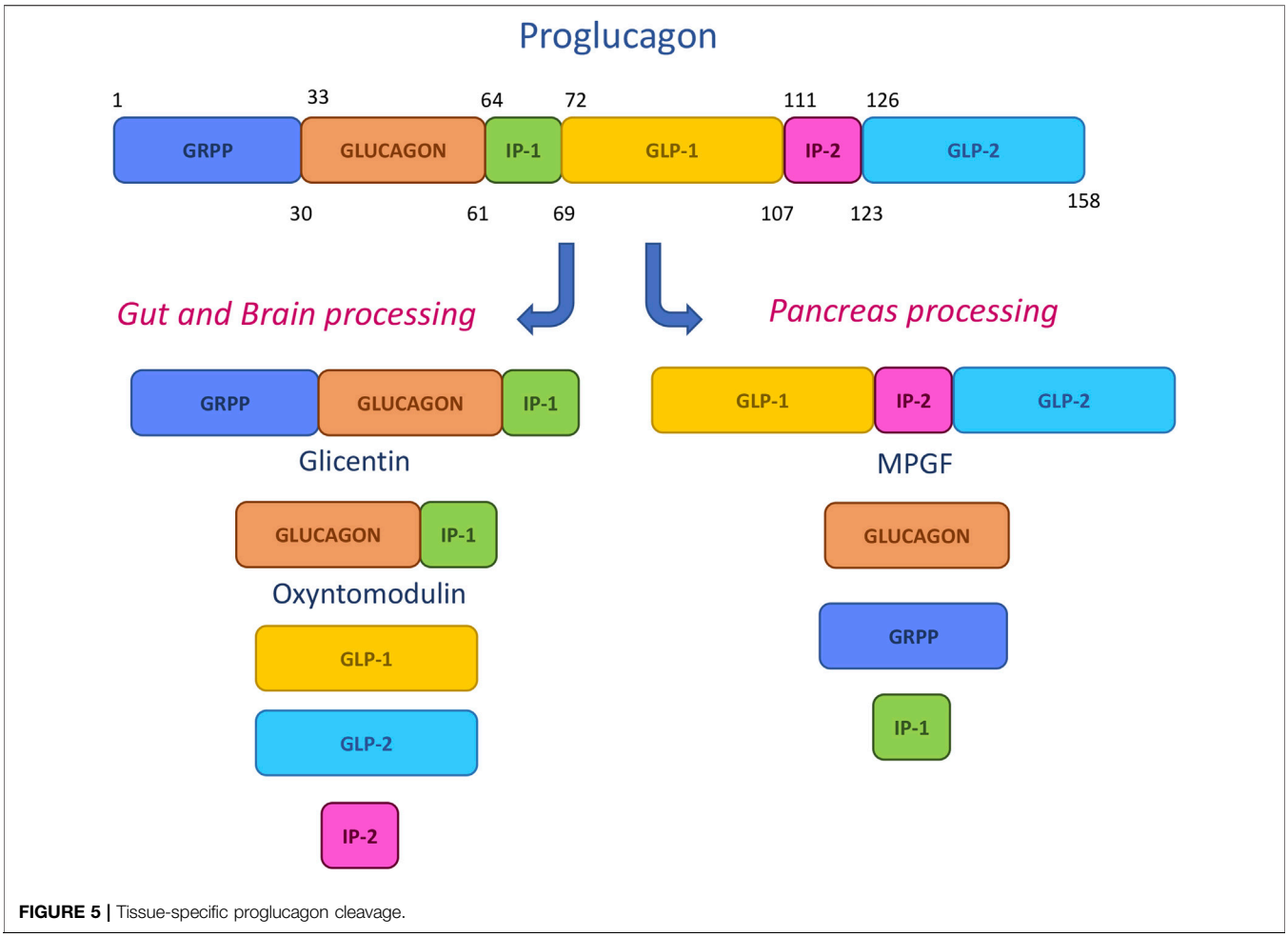

FIGURE 5 | Tissue-specific proglucagon cleavage.

recently the orally disposable semaglutide. These two molecules foster the research for better GLP-1 analogues with improved pharmacological profile.

Following these therapeutic needs, further modifications of the exenatide sequence led to slow-release compounds: an example is **PB-119**, a polyethylene glycosylated exenatide developed by PegBio and obtained by modification of a single amino acid in exenatide, replacing $Ser^{39}$with Cys (Min Xu et al., 2019). Even if the mechanism of action is identical to that of Exenatide, the PEGylation on the analogue PB-119 reduces the excretion rate in the kidneys, and its increased molecular weight causes steric hindrance toward DPP-4, prolonging the half-life and allowing one weekly subcutaneous injection dose regimen (Cui et al., 2020). The same concept of improved pharmacokinetic and resistance to DPP-4 was declined also by Jiangsu Hansoh Pharmaceutical through the development of the GLP-1R agonist **Noiiglutide**, a 40-mer exenatide analogue, currently in Phase 2 trials as subcutaneous injectable agent. Structurally, the presence of an unnatural Aib (α-amino isobutyric acid) residue in position two should guarantee a better resistance toward enzymatic hydrolysis while the condensation with palmitic acid on Lys^{1}-ξ-NH_2 enhances the hydrophilicity (Wang et al., 2012).

The GLP-1R agonist roster includes also **G3215** (structure undisclosed), developed by Imperial College, that completed its Phase 1 trials in 2019 (Serrano et al., 2017).

As above described, GLP-1R agonist peptides are receiving an increasing interest, with several agents advancing the clinical phases. In comparison, less efforts have been focused on studying GLP-1R antagonists. Nevertheless, Eiger BioPharmaceuticals is developing **Avexitide** for treating post-bariatric hypoglycemia (PBH), a form of hyperinsulinemic hypoglycemia (HH), as a new liquid formulation of Exendin 9–39 intended for subcutaneous injection administration. PBH is a rare disease without approved pharmacotherapy, caused by abnormal growth in insulin secretion, which is attributed to exaggerated postprandial secretion and to the large increase in meal induced GLP-1 release (Craig, 2020). Therefore, GLP-1R antagonism could represent a potential therapeutic strategy for managing this condition. Avexitide is a 31-mer peptide that selectively targets and blocks GLP-1R, normalizing insulin secretion and thus decreasing postprandial hypoglycemia. Data released from a

recent Phase 2 clinical trial showed that Avexitide produced consistent improvements in the incidence of hypoglycemia maintaining a good tolerability profile (Suzuki et al., 2020).

Glucagon Like Peptide-1 Receptor/GPCR Glucagon Receptor Targeting Peptides

The clinical success of GLP-1R agonist peptides has prompted the search for agents that could combine the benefits of GLP-1 with those of other key gut hormones, in order to target multiple signalling pathways with a single molecular entity. Moreover, this emerging dual pharmacological approach may lead to increased metabolic action compared to monotherapies, and a number of these candidates are being evaluated in clinical trials (Bastin et al., 2019).

Glucose homeostasis is regulated by the combinatorial action of insulin and glucagon. While insulin and its therapeutic applications were widely studied, the glucagon hormone, secreted by the pancreatic α-cells, has been receiving attention only in the last decades. Its main action consists in a counter-regulatory effect toward insulin, inducing hepatic glycogenolysis and gluconeogenesis by targeting the class B GPCR glucagon receptor (GCGR) (Herr, 2012). The use of native glucagon in the therapeutic approach to hypoglycaemia is not easily practicable (Patil et al., 2020) for its very low stability in physiological formulations and its consequent high tendency to aggregate in few hours, after reconstitution (Hövelmann et al., 2018). Thus, the development of new analogues/agonists of the native glucagon peptide is necessary in treatment of hypoglycaemia. Zealand Pharma developed, **Dasiglucagon** (NDA) which will be launched on the market in the first trimester of 2021 as Zegalogue®, a ready-to-use formulation administered by single-injection pen applicator. To avoid aggregation problems and fibril formations and to render it physically and chemically stable in aqueous solution, Dasiglucagon was designed introducing seven substitutions in the 29 amino acid sequence of the native glucagon, with the insertion of an Aib residue (Pieber et al., 2020).

On the other hand, glucagon enhances energy consumption and acts as food intake regulator, making its analogues also interesting for glucose regulation in T2DM and obesity (Suzuki et al., 2020). GLP-1 and glucagon have a high sequence homology: this aspect encouraged the development of multiple molecules with an integrate pharmacological profile targeting both GLP-1R and GCGR in a dual-agonism mechanism, where glycaemia and weight control are accompanied by adipose tissue lipolysis and appetite suppression (Capozzi et al., 2018). The native gut hormone peptide Oxyntomodulin (OXM), secreted after food ingestion, exhibits an antidiabetic effect and drives weight loss acting on appetite and satiety by activating both GLP-1R and GCGR, even if showing lower activity compared to GLP-1 and glucagon alone. Thus, oxyntomodulin has been chosen as a model for the development of GLP-1R/GCGR dual agonists.

Within this class, **Pegapamodutide** (OPK880033), by OPKO Health, completed phase 2 for once-weekly administration in treatment of T2DM. This drug candidate consists in a PEGylated analogue of OXM and displays a long action since the presence of two PEG moieties on $Cys^{38}$and Cys^{39} prevents enzymatic degradation (Sheetz et al., 2017) The resistance toward DPP-4 is also provided by the presence of two un-natural Aib residues along the sequence. In particular, Aib^2 enhances potency and selectivity at the GLP1-R. (Connop et al., 2020).

In addition, MedImmune, a subsidiary of AstraZeneca, is developing **Cotadutide** (MEDI0382), presently in Phase 2 as once-daily, subcutaneous therapy, to treat overweight or obese patients with T2DM. This novel dual GLP-1R/GCGR agonist was designed to improve glycaemic control and to facilitate weight loss through combined effects on appetite and energy expenditure (Ambery et al., 2018). Structurally, MEDI0382 is a 30-mer synthetic linear peptide, designed as OXM analogue, wherein the sequence of oxyntomodulin has been C-terminally depleted of seven residues, while seven of the remaining amino acids have been changed. Its extended half-life was achieved by enhancing stability to peptidase degradation: Gln^{20} and Gln^{24} were replaced with residues not susceptible to deamidation, whilst Arg^{17} was substituted with Glu to decrease proteolysis. Moreover, the insertion of a palmitic acid side chain at Lys^{10} through a γ-glutamate moiety promoted its reversible binding to albumin (Henderson et al., 2016). In such a way, this degradation resistant peptide is able to exert an optimally balanced dual agonism, inducing in clinical trials' patients an observed weight loss greater than that observed with GLP-1R alone.

Another long-acting GLP-1R/GCGR dual agonist, **BI456906**, is being developed by Zealand Pharma in collaboration with Boehringer Ingelheim. This peptide is an analogue of the natural OXM and is being investigated in Phase 2 for T2DM and obesity, (Zealand Pharma, 2020). Efficacy of BI456906 as a treatment for non-alcoholic steatohepatitis (NASH), the most severe form of non-alcoholic fatty liver disease (NAFLD), is also expected, due to the emerging successful approach for this pathology using dual GLP-1R/GCGR agonists.

In this field, **ALT-801** emerged as a novel peptide-based dual GLP-1R/GCGR agonist designed by AltImmune to treat the obesity and metabolic dysfunction caused by NASH. As observed in a preclinical model of the disease, ALT-801 induced significant weight loss compared to semaglutide, and accordingly the company recently announced the beginning of a Phase 1 clinical trial.

Its structure is based on a 29-mer sequence partially mimicking both GLP-1 for an improved weight loss and glucagon for restoring metabolic functions (Nestor et al., 2021). The insertion of an Aib residue was meant to prevent the proteolytic degradation, while a EuPort™ liposaccharide surfactant, formed by a D-glucoside linked to a methylene C18 chain, was introduced on Lys^{17} side chain to improve gastrointestinal tolerability. In addition, Glu^{16} and Lys^{20} side chains were conjugated to create a lactam ring, designed as a helix stabilizer to increase potency. These structural features afforded a high serum albumin binding, leading to a suitable once-weekly subcutaneous administration in patients (AltImmune, 2019). Finally, **LY3305677** (OXM3, IBI362) is an undisclosed peptide dual GLP-1R/GCGR agonist, reported by Ely Lilly as a third-generation analogue of Oxyntomodulin, that is currently under evaluation in Phase 2 clinical trials.

Glucagon Like Peptide-1 Receptor/GIPR Targeting Peptides

Another strategy to treat diabetes and obesity with dual active peptides is exploiting the agonism toward incretin receptors GLP-1R and GIPR. GIPR is the natural target of the native gut hormone glucose-dependent insulinotropic polypeptide (GIP), secreted by the *K*-cells after food intakes. This incretin peptide can stimulate insulin and glucagon secretion, like GLP-1, but with a weaker efficacy on the regulation of the insulinotropic effect. Studies on the receptor-ligand interaction pointed out the key role of the native peptide N-terminus in GIPR activation. This moiety interacts with a binding pocket in the transmembrane receptor, while the central residues bind to the extracellular domain of the receptor. Accordingly, a tuning of the N-terminal moiety could modulate the agonism or the antagonism of the peptide (Gasbjerg et al., 2018).

Therefore, the GIP agonism has been identified as a pharmaceutical strategy for the treatment of T2DM, even if it seems to be less relevant than GLP-1 agonism. Synthetic dual incretin receptor agonists, nicknamed "twincretins," have been investigated in the last years, with a few candidates actually in clinical development. The most advanced GLP-1R/GIPR agonist is **Tirzepatide** (LY3298176) from Eli Lilly, currently in Phase 3 trials. Tirzepatide is formulated as a synthetic 39-mer linear peptide, sharing 19 residues with native GIP. The peptide sequence incorporates the amidated C-terminus and two non-natural Aib residues at positions 2 and 13. Moreover, the structure is conjugated to a 20-carbon fatty diacid moiety *via* a hydrophilic linker connected to the Lys^{20} residue. This strategy was designed to promote albumin binding, prolonging Tirzepatide half-life to approximately 5 days and thus enabling once-weekly subcutaneous dosing regimen (Coskun et al., 2018). In phase 1 and 2 clinical trials, Tirzepatide produced significantly improved clinical efficacy, safety and tolerability in glucose control and weight loss compared with the GLP-1 agonist dulaglutide. GIPR binding affinity resulted comparable to that of native GIP, while a GLP-1R affinity five times lower than that of native GLP-1 was observed (Min and Bain, 2021).

It is worth mention that also the dual agonist peptide **SCO-094**, developed by Scohia Pharma in partnership with Takeda Pharmaceuticals (Clemmensen et al., 2019) belongs to this class of drug candidates. This molecule is being tested in both long-acting and oral formulations in Phase 1 with wide potential applications comprising diabetes, obesity and NASH.

Finally, the dual agonist **CT-868**, developed by Carmot Therapeutics, will enter in Phase 2 in the first half of 2021 as a promising treatment for diabetes, obesity and NASH (Kim and Kim, 2020). CT-868 dual agonist candidate was discovered using the Chemotype Evolution technology, as a peptide-small molecule hybrid compound, able to mimic the native GLP-1 hormone (Carmot Therapeutics Pipeline, 2021).

On the basis of the promising results of dual targeting peptides, some ternary agonists concurrently targeting GLP-1, GCGR and GIPR have been developed. The peptide **LY3437943** from Ely Lilly is the first member of this novel class of peptides, designed to be effective in T2DM and obesity treatment. The structure of this peptide is still undisclosed by the originator.

Y Receptor Type 2 Targeting Peptides

Other potential therapies for obesity and associate pathologies involve PYY and amylin agonists.

Peptide YY (PYY) is a gut hormone that is co-secreted from the entero-endocrine L cells, together with GLP-1 and oxyntomodulin, in response to feeding (Khoo and Tan, 2020). Although it exists in two major forms, the full length PYY1-36 and PYY3-36, the latest is the most commonly biologically active circulating form. PYY3-36 is a 34-mer peptide released postprandially by the gut. Its secretion activates appetite suppression and food intake decrease by acting, in the arcuate nucleus of the hypothalamus, on neuropeptide Y receptor type 2 (Y2R), a member of the neuropeptide Y receptor family that belongs to the GPCR family (Srivastava and Apovian, 2018).

Early clinical studies showed that PYY3–36 infusion in obese patients induced suppression of food intake with good tolerability, and limited side effects. Anyway, since native PYY short half-life (8 min) affects clinical stability, various approaches have been planned to increase its resistance to proteolytic inactivation (Will et al., 2017). In this context, alternative delivery of PYY is a challenge. Recently, Gila Therapeutics has developed **GT-001**, a PYY3–36 analogue that started Phase 1 trials with orally available sublingual formulation (Acosta et al., 2019). Novo Nordisk's pipeline also includes a novel analogue of the appetite-regulating hormone PYY, namely **PYY-1875**, whose structure is still undisclosed. This peptide is currently in Phase 1 and is intended as subcutaneous injection for once-weekly treatment (Novo Nordisk, 2020).

Amylin is a 37-mer peptide hormone mainly produced in the pancreatic beta cells and co-secreted with insulin during a meal. Amylin has a well-established role as a satiety signal; it acts by reducing food intake and postprandial glucagon secretion *via* binding to human amylin receptors (AMY) in specific areas of the brain (Zakariassen et al., 2020). AMY subtypes are GPCR consisting of a calcitonin receptor (CTR) and one of three receptor activity-modifying proteins (RAMP). Because of their mechanism of action, amylin mimetics are novel targets of study as anti-obesity drugs and several approaches (PEGylation, glycosylation or albumin binding) have been explored to extend their half-life and reduce their administration frequency. Novo Nordisk is currently testing **AM833** in phase 2 trial, a long-acting acylated analogue of the human amylin hormone, in once-weekly subcutaneous administration, AM833 has been evaluated in combination with the GLP-1 analogue semaglutide in a phase 1 clinical trial (Mathiesen et al., 2020).

Glucagon-Like Peptide-2 Receptor Targeting Peptides

Glucagon-like peptide-2 receptor (GLP-2R) is a GPCR superfamily member expressed in the gastrointestinal tract and, belonging to the family of seven trans-membrane receptors, it is closely related to GCGR and GLP-1R. Through binding to glucagon-like peptide-2 (GLP-2), GLP-2R directly

inhibits apoptosis and increases intestinal growth by stimulating cell proliferation in response to ligand activation. GLP-2 is a 33-mer hormone released by the enteroendocrine intestinal L-cells in response to nutrient ingestion (Brubaker, 2018).

Although the mechanisms by which GLP-2 mediates its effects still remain not completely understood, it is an important regulator for stimulating intestinal growth, increasing absorption, promoting healing and maintaining epithelial integrity, in both normal humans and patients with intestinal failure consequent to massive intestinal resection (short bowel syndrome, SBS). Indeed, patients with SBS might have impaired postprandial GLP-2 secretion, which is instead required for optimal intestinal adaptation. The use of GLP-2 as a therapeutic agent is limited because of its very short circulating half-life (approximately 7 min) due to cleavage by DPP-4 (Hargrove et al., 2020). Consequently, pharmacologically active GLP-2 analogues with a longer half-life and reduced clearance are under development against SBS, including phase 3 agents **Apraglutide** (VectivBio) and **Glepaglutide** (Zealand Pharma).

Glepaglutide is a highly potent GLP-2R selective 39-mer peptide, with a long-acting effect and an effective plasma half-life of approximately 50 h, allowing a less-than-once daily administration. Furthermore, it offers a more convenient dosing form *via* a ready-to-use autoinjector device, which removes the requirement for reconstitution from lyophilized powder and allows the formation of a subcutaneous depot at the site of the injection, from which it could be slowly released into the circulation (Naimi et al., 2019). Glepaglutide differs from native GLP-2 through the insertion of a C-terminal tail consisting of six lysine residues that modify the charge state aiding solubility and physicochemical properties. The N-terminal region was optimized by changing five amino acids for improving pharmacokinetic and potency properties, and by replacing other four residues with alanine in an internal region, ending in a globally nine amino acid substitution.

Apraglutide is another highly selective, potent GLP-2R agonist peptide, composed by a 33 amino acid sequence, with a molecular structure designed to preserve optimal pharmacological activity while increasing the half-life compared to native GLP-2 or other GLP-2 analogues (Martchenko et al., 2020). Specifically, native GLP-2 was modified at positions 2, 10, 11 and 16 with Gly, Nle, D-Phe and Leu respectively, and with a C-terminal amidation. The few amino acid substitutions translate into a superior pharmacokinetic profile that results in an exceptionally low clearance and in a high plasma protein binding, thus enabling a long *in vivo* elimination half-life after subcutaneous administration (30 h), without necessity of conjugation or other peptide modifications. Moreover, Apraglutide displays a good stability against DPP-4, allowing the possibility for only once-to-twice weekly treatment (Slim et al., 2019).

The effect of the native GLP peptides was investigated in SBS patients either as a selective agonist (GLP-1R or GLP-2R) or as a dual GLP agonist combination therapy, with the latter imparting superior efficacy and better patient outcomes compared to each single agent alone (Suzuki et al., 2020). This rationale supported the use of dual GLP receptor co-agonism for the treatment of metabolic and gastrointestinal diseases, even if clinical studies are still awaiting to confirm the therapeutic efficacy of its combination. Following this approach, Zealand Pharma is currently developing **Dapiglutide**, previously referred to as ZP7570. Even if its structure is still undisclosed, the company announced that this molecule completed Phase 1 trials in 2020 and showed a good safety and tolerability profile in healthy volunteers together with a plasma half-life allowing for once-weekly dosing (Zealand Pharma, 2020).

CARDIOVASCULAR SYSTEM AND HYPERTENSION

Cardiovascular diseases (CVD) are among the leading causes of death worldwide, taking an estimated 17.9 million lives each year. According to the World Health Organization (WHO), four out of five CVD deaths are due to heart attacks and strokes, and one third of these deaths occurs prematurely in people under 7 years of age (WHO, 2021). In the last years, proteins and peptides with unique biological activity and metabolism have successfully caught the attention of researchers as an alternative treatment for cardiovascular and hypertension diseases and several are still under clinical study waiting to be approved.

Ularitide, an atrial peptide agonist, was developed by Cardiorentis, a private biopharmaceutical company, specialized in the treatment of cardiovascular diseases, as an intravenous treatment for acute heart and kidney failure, and has completed the Phase 3 in 2018 (Emani et al., 2015). Ularitide is the chemically synthesized form of urodilatin, a human endogenous natriuretic peptide produced in the kidneys with the aim to regulate fluid balance and sodium homeostasis. This 32-mer-containing peptide has the same sequence of the 28 amino acid-containing atrial natriuretic peptide (ANP), except for the addition of four amino acids at the N-terminal extension. The crystal structure of ANP bound to the receptor showed that the complex contains two NPR-A molecules bound with one molecule of ANP and, since the ANP molecule has no internal symmetry, binding to the receptor is asymmetric and occurs through two different binding sites present in each NPR-A monomer (Ogawa et al., 2004). Ularitide binds primarily to the extracellular domain of natriuretic peptide receptor-A (NPR-A) which is expressed in the heart, kidney and other organs and activates the intracellular guanylate cyclase domain of the receptor (Anker et al., 2015). Guanylate cyclases catalyze the conversion of guanosine 5′ -triphosphate to cyclic guanosine-3′, 5′ -monophosphate (cGMP) causing vasodilation through vasorelaxation of smooth muscle cells and natriuresis and diuresis through inhibition of sodium reabsorption.In the treatment of stroke-associated pathologies, cationic arginine-rich peptides (CARPs) represent a new emerging class of neuroprotective agents with multimodal cytoprotective actions. Among them, **NA-1**, originally named TAT-NR2B9, is a lead compound being developed by NoNO for the treatment of stroke, traumatic brain injuries and subarachnoid hemorrhage and is currently in Phase 3 clinical trial. NA-1 is a 20-mer peptide consisting in a sequence (KLSSIESDV) derived from the intracellular terminal carboxylic

region of the N-methyl-D-aspartate (NMDA) receptor NR2B subunit protein, fused to the cationic arginine-rich cell penetrating peptide TAT (YGRKKRRQRRR), which facilitates the passage across the blood brain barrier (Ballarin and Tymianski 2018; Meloni et al., 2020). The NR2B9 9-mer peptide was selected to inhibit the postsynaptic density protein-95 (PSD95) adaptor protein, which binds to the NR2B subunit, and thereby blocks downstream cell signalling associated with overstimulation of the NMDA receptor.

CN-105, a small 5-mer apolipoprotein E (apoE) mimetic peptide, rich of arginine residues and deriving from the receptor binding region of apoE, is currently under development by AegisCN (formerly CereNova). This peptide is in Phase 2 for the treatment of hemorrhagic stroke and intracerebral hemorrhage. CN-105 has been developed based on the amino acids present in the parent neuroprotective peptide COG133, comprising the heparin binding and LDL receptor binding domains within the apoE (Meloni et al., 2020). ApoE is a multifunctional 299-mer protein that reduces neuroinflammation and mediates adaptive responses following ischemic and traumatic brain injury. However, the intact apoE holoprotein does not cross the blood-brain-barrier (BBB) limiting its therapeutic potential. CN-105 has the advantage of an increased CNS penetration and has demonstrated efficacy in experimental intracerebral hemorrhage, leading to an improvement of functional and histological outcomes after experimental ischemic stroke, and reducing microglial activation (Tu et al., 2017; Yeh et al., 2020).

The last peptide still in clinical trials for the treatment of cardiovascular disease through protein-protein interactions is **Pemziviptadil** (PB1046). PB1046 is a novel, subcutaneously injected vasoactive intestinal peptide (VIP) analogue, developed by PhaseBio Pharmaceutical that is currently tested in Phase 2 for the treatment of pulmonary arterial hypertension (PAH). VIP is a 28-mer peptide hormone that activates VPAC1 and VPAC2 receptors in the pulmonary vasculature and has been shown to relax pulmonary vascular smooth muscle, to neutralize pulmonary vasoconstrictors, and to inhibit cell proliferation (Chappe et al., 2014). The short half-life of VIP renders this peptide impractical as a pharmaceutical agent and modified versions of VIP are therefore needed to render the agent therapeutically useful (Sadeghi et al., 2015). PB1046 is 29-mer peptide linked to elastin-like polypeptide (ELP) biopolymer. The ELP component comprises structural peptide fragments that are related to the elastin protein. Such modified sequences are useful for improving important properties as absorption profile and circulating half-life (PhaseBio, 2020).

NEURODEGENERATIVE DISEASES

Neurodegenerative diseases are the result of a continuous process based on degenerative cell changes, which increasingly deteriorate over time. Aggregation of pathogenic proteins, mitochondrial dysfunction, oxidative stress, transcriptional dysfunction and apoptosis play an important role in the development of neurodegenerative disorders such as Parkinson's disease (PD), Alzheimer's disease (AD) and Amyotrophic lateral sclerosis (ALS) (Emerit et al., 2004). Up to now, no novel disease-modifying therapies have been shown to provide significant benefits for patients who suffer from these devastating disorders. Therefore, early diagnosis and the discovery of new drugs able to bind selectively specific targets are increasingly required on the market.

Davunetide (NAP, AL-108), is an intranasally administered, 8-mer peptide fragment deriving from the activity-dependent neuroprotective protein (ADNP), actually in Phase 1 for the treatment of progressive supranuclear palsy (PSP). Davunetide has preclinical evidence for neuroprotective, neurotrophic and cognitive protective properties by promoting microtubule stabilization. (Javitt et al., 2012). The protein tubulin, constituting the microtubule backbone, was shown to be the target of NAP, recently reported as an enhancer of the interaction between microtubules and microtubule associated proteins, and microtubule polymerization under conditions of zinc intoxication (Magen and Gozes, 2014). NAP has also been reported to reduce levels of neurotoxic and pro-inflammatory factors, such as nitric oxide (NO) and tumor necrosis factor (TNF) by blocking microglial activation. The microtubules end-binding (EB) proteins have been identified as the targets of NAP, through interaction of its SIP domain. The binding of davunetide to its receptor has been recently predicted using structural alignment of EB3 to EB1-EB3 complex with another peptide ligand (MACF) (Vaisburd et al., 2015)

NLY01 (Neuraly Inc.) is a pegylated long-acting analogue of exendin-4, (Yun et al., 2018). In the Phase 1 study, NLY01 was well-tolerated, and showed a half-life three times higher than shorter-acting GLP-1R agonists, which are often limited by side effects. In 2020 the approval of an investigational new drug application (IND) to initiate a Phase 2b clinical trial of NLY01 in patients with AD and a Phase 2 trial in patients with PD were announced.

In a previous study, it was shown that NLY01, through a favorable blood brain barrier penetration, binds upregulated GLP-1R, blocking pathological activation of microglia in animal models of neurodegenerative diseases, including Parkinson's (Sterling et al., 2020).

Myasthenia gravis (MG) is another serious degenerative disease, a chronic auto-immune condition in which auto-antibodies attack specific proteins in the neuro-muscular junction, resulting in muscle weakness and fatigue. **Zilucoplan** is a small synthetic 15-mer macrocyclic peptide by UCB Pharma, currently in Phase 3 clinical trial for MG, acting as a potent inhibitor of the terminal complement protein C5, with potential anti-inflammatory and cell protective activities (UCB Pharma, 2020). Upon subcutaneous administration, Zilucoplan binds to complement protein C5, blocking C5 cleavage into C5a and C5b and preventing the C5b-dependent assembly of the membrane-attack complex (MAC). Zilucoplan also inhibits the interaction between C5b and C6, thereby further blocking MAC assembly. (Gorman et al., 2021; Duda et al.,2020).

Last but not least, **GM604** (GM6, Alirinetide) is a cationic linear peptide drug that has been developed by Genervon Biopharmaceuticals and is in Phase 2 clinical trial for ALS

disease. The peptide consists of 6 amino acids, representing a subunit of the endogenous 33-mer peptide known as "motoneuronotrophic factor" (MNTF1) (Swindell et al., 2018). Preclinical tests suggest that MNTF regulates CNS biological functions, including neuronal differentiation, axonal regeneration, reinnervation, and inflammation and apoptosis, providing both neuroprotective and neuro-regenerative therapeutic effects. GM604 is expected to have a complex mechanism of action potentially involving stimulation of multiple receptors, signaling cascades and downstream gene expression responses (Ko et al., 2017). GM604 does not selectively interact with a single target, but rather interacts with multiple receptors linked to diverse pathways. These include insulin receptor, Notch receptors one to four and smoothened frizzled class receptor. Stimulation and activation of these and other receptors by GM6 is associated with the expression of thousands of genes leading to microtubule stability, synaptic transmission and axon guidance (Genervon, 2021).

BACTERIAL AND VIRAL INFECTIONS

Infectious diseases, caused by many pathogens, including bacteria, viruses, fungi, and parasites are extremely common worldwide, although a huge number of antibiotics and antiviral drugs are available on the market. Mutation of infectious microorganisms and development of resistant strains has to be continuously faced with new medicines and for this reason innovation if this area is a need. Up today, three peptides are in clinical phase with the purpose to treat these pathologies. Due to SARS-CoV-2 virus pandemic diffusion, in the last year all anti-infective peptides entered clinical trial to verify their possible use for this infection. Anyway, since these repositioning studies are not based on a medicinal chemistry approach targeting protein receptors, reliable results are still not available. For these reasons, we decided to exclude them from this overview.

Nangibotide (LR12) is a chemically synthesized 12-mer peptide derived from residues 94 to 105 of TREM-like transcript-1 (TLT-1). LR12, launched by Inotrem, is a specific TREM-1 inhibitor, interfering in the binding of TREM-1 and its ligand (Cuvier et al., 2018; Francois et al., 2020). TREM-1 is an amplifier of the innate immune response by synergizing with toll-like receptors and is a crucial mediator of septic shock. LR12 blocks TREM-1 by binding to its ligand and provides protective effects during sepsis such as inhibiting hyper-responsiveness, organ damage and death, without causing deleterious consequences (Inotrem, 2020). The protective effects of modulating TREM-1 signaling are also evident in other models of inflammation such as pancreatitis, hemorrhagic shock and inflammatory diseases. The drug is currently in a Phase 2b trial for treating septic shock and results are expected by the second half of 2021.

Reltecimod (AB103, p2TA; CD288–15) was discovered by Atox Bio as a drug candidate for the resolution of organ dysfunction or failure by attenuating the dysregulated immune response frequently seen in patients with necrotizing soft tissue infection (NSTI). It is an synthetic analogue peptide with homology to the fragment 8–15 of the T-lymphocyte receptor CD28. With its novel mechanism of action, it binds to the dimer interface of the costimulatory receptors and interferes with B7-2/CD28 engagement expressed on T-cells, thereby modulating the acute inflammation that leads to systemic organ failure (Kaempfer, 2018). Reltecimod completed the clinical trial process and its approval by regulatory organs is currently ongoing, suggesting the launch on the market in the next future. (Pipeline Overview AtoxBio, 2021).

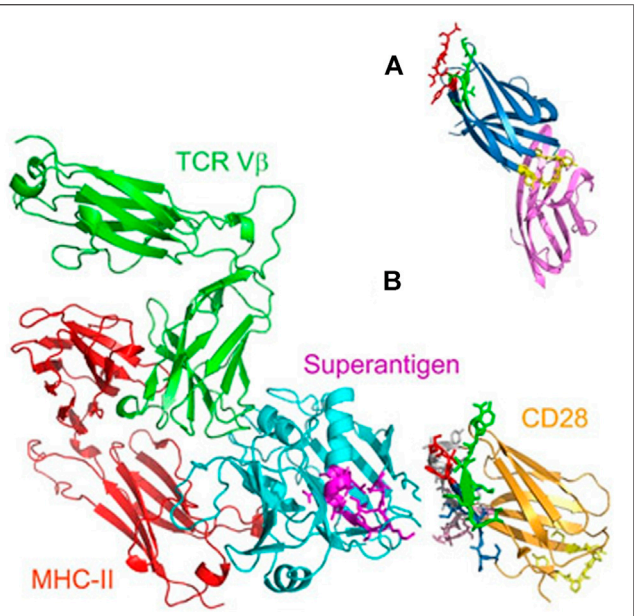

FIGURE 6 | (A) Predicted CD28 dimer interface domain **(B)** Model for superantigen action through binding to CD28 (adapted from Arad et al., 2011).

To understand the binding of bacterial superantigen toxins to the CD28 homodimer interface, reltecimod (SPMLVAYD) was explored, being a fragment of the CD28 dimer interface domain predicted from alignment with CTLA-4 (**Figure 6A**). In the available structure for CD28, reltecimod overlaps with the dimer interface, taking part to the complex functional superantigen binding site in CD28. The peptide competes with cell-surface CD28 for the β-strand/hinge/α-helix domain in the superantigen, in a site that is remote from other proteins (MHC-II, TCR Vβ) binding sites (**Figure 6B**).

Blocking the access of a superantigen to CD28 is sufficient to block acute inflammation lethal toxic shock (Arad et al., 2011)

C16G2 was developed by Armata Pharmaceuticals thanks to the design of a novel platform for the treatment of bacterial infections called "Specifically Targeted Antimicrobial Peptide (STAMP) platform". STAMPs are designed by mining bacterial genomes for targeting domains that confer pathogen-specific killing activity. Therefore, C16G2, targeting *S. mutans* in the dental caries, was created by matching a targeting domain for effective accumulation on the *S. mutans* cell surface, as the competence-stimulating peptide C16 pheromone, with a killing

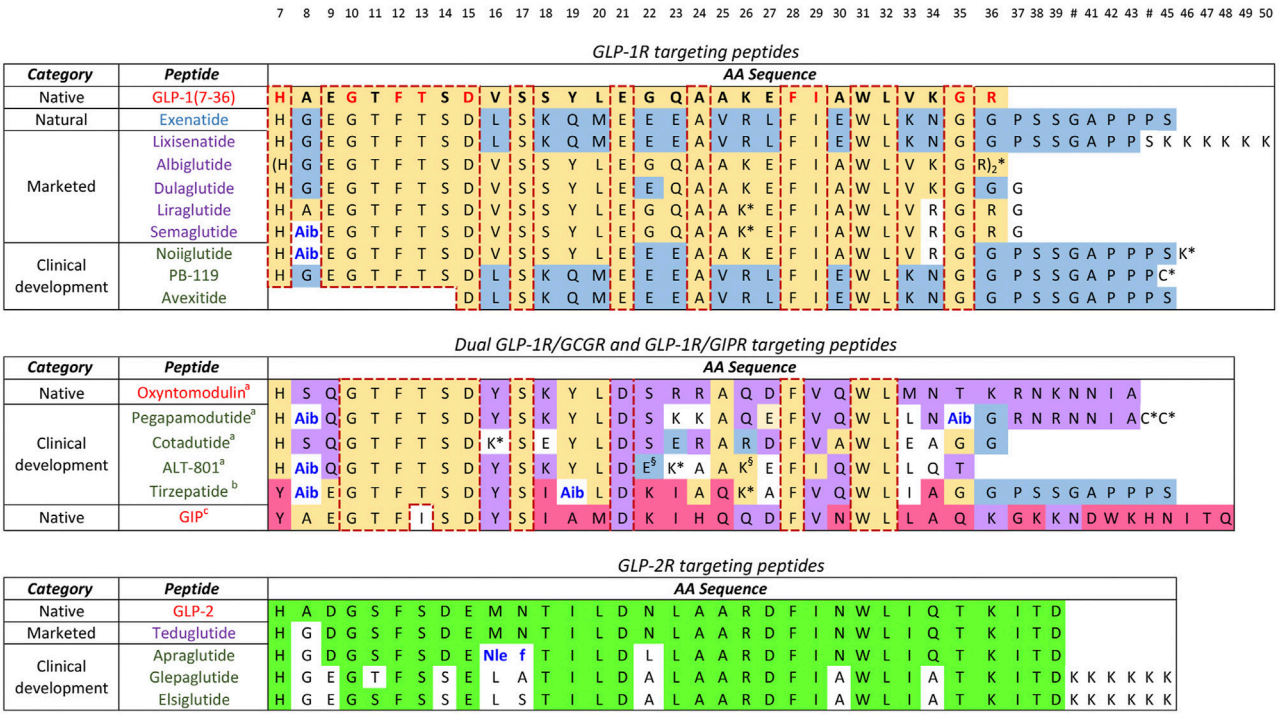

* indicates a lipophilic side chain on the marked residue; For clarity the nature of the side chian was omitted. § indicates a lactam linkage between the side chains of the marked residues; [a]Dual GLP-1R/GCGR targeting peptides; [b] dual GLP-1R/GIPR targeting peptides; [c] GIPR targeting peptide. AA sequence: residues colored in red = depicted from Ala scanning as important for biological activity; residues colored in blue = non natural aminoacids; highlighted in yellow: belonging to native GLP-1 sequence; highlighted in blue: belonging to Exenatide sequence; highlighted in purple: belonging to Oxyntomodulin sequence; highlighted in pink: belonging to GIP sequence; highlighted in green: belonging to GLP-2 sequence

FIGURE 7 | Alignment of analogue peptides with the corresponding native ones in T2DM/obesity and SBS treatment.

domain, that is the G2 sequence as a truncated version of the broad-spectrum killing peptide novispirin G. A flexible tri-glycine sequence links the two regions. C16G2 has finished the Phase 2 clinical trials demonstrating an acceptable safety and tolerability profile of the drug and a selective reduction of *S. mutans* in the oral cavity. However, the company elected not to proceed to Phase 3 to seek alternatives to lower STAMP cost of goods (Kaplan et al., 2011).

MISCELLANEOUS

In this section several peptides targeting different diseases have been collected, since they cannot be classified in one of the specific pathological areas described in this review.

LJPC-401 is a synthetic human hepcidin peptide, developed by La Jolla Pharmaceutical Company for the potential treatment of conditions characterized by iron overload. In healthy individuals, hepcidin prevents excessive iron accumulation in vital organs, such as the liver and heart, where it can cause significant damage and even result in death.

The feedback circuitry between hepcidin and iron levels in the body ensures systemic iron homeostasis. Hepcidin reduces the concentration of ferroportin-1 receptor (FPN-1) on the cell surface thereby inhibiting the entry of iron into plasma. Hepcidin binds FPN in a central cavity between the N and C domains, acting as a molecular cap to hinder the iron efflux pathway. The network of polar and hydrophobic interactions of the peptide with FPN has been assessed by evaluating decrease in binding affinity due to specific mutations (Billesbølle et al., 2020).

Binding of hepcidin to FPN-1 induces a modification in the receptor, leading to its internalization and degradation in lysosomes. In this way, the export of iron from reticuloendothelial macrophages, hepatocytes, and duodenal enterocytes is blocked (Casu et al., 2018). Hepcidin deficiency is a common feature of hereditary hemochromatosis (HH) and LJPC-401 has completed Phase 2 clinical trials for this therapeutic target, representing a "replacement therapy" to supplement inadequate hepcidin levels (Chawla et al., 2019).

OXE-103 (Oxeia Biopharmaceuticals) is a synthetic human ghrelin, an endogenous hormone, to treat concussions/mTBI. OXE-103 freely crosses the blood-brain-barrier and helps stabilizing metabolic and energy brain dysfunction following a concussion. OXE-103 uniquely targets the hippocampus region of the brain, an important area for cognition and memory. Treatment with OXE-103 has been shown to restore normal energy metabolism, and to reduce the toxic effects of reactive oxygen species that form in low energy states. In neurons, the uncoupling protein-2 (UCP2) stabilizes mitochondria by responding to sublethal stress. The exact neuroprotective role

of ghrelin is still unclear but UCP2-dependent mitochondrial stabilization effects in thalamic neurons have been suggested (Lopez et al., 2014). A Phase 2 study is running with the goal to reduce symptom burden with OXE103 treatment (Oxeia Biopharmaceutical, 2021).

Solnatide, is a synthetic cyclic 17-mer peptide whose molecular structure mimics the lectin-like domain (TIP) of human tumor necrosis factor (TNF) (Willam et al., 2017a, b), associated with high altitude pulmonary edema (HAPE) and adult respiratory distress syndrome (ARDS). Solnatide, also known as AP-301, has been developed by Apeptico Forschung und Entwicklung and is about to enter in Phase 2b in the treatment of various pulmonary diseases. Solnatide activates the lung epithelial sodium channel (ENaC), by directly binding to the crucial alpha-subunit of the channel and by stabilizing its open state, thus enhancing sodium ion uptake. The oligosaccharide-binding property of the TIP domain of TNF plays an important role in the mechanism by which TNF and solnatide interact with and activate ENaC, although the exact nature of this interaction is not yet understood.

TAK639 (Takeda) is a synthetic 9-mer linear peptide which has completed phase 1 clinical trials for the treatment of Primary Open-angle Glaucoma (POAG) and intraocular pressure (IOP) (Savinainen et al., 2019). It is estimated that in 2020 more than 75 million people worldwide have suffered from ocular glaucoma; in particular, POAG is a complex optic neuropathy characterized by atrophy of the optic nerve and retinal ganglion cells and their axons, leading to irreversible blindness. Clinical evidences indicate the key role of expression and function of the natriuretic peptide network in several ocular systems, including in human trabecular meshwork. C-type natriuretic peptide (CNP) is the most potent in the class at lowering IOP in rabbits and further studies have demonstrated the presence of functional natriuretic peptide receptor-B (NPR-B) in the eyes of these animals. However, this promising treatment is affected by administration issues owing to the difficulties of atrial natriuretic peptides in penetrating the cornea to lower IOP. To overcome this drawback, **TAK639** was designed as a cornea-permeable CNP derivative, exhibiting increased production and cellular concentrations of cyclic guanosine monophosphate (cGMP), able to lower IOP (Martin V. et al., 2020).

CURRENT CHALLENGES AND FUTURE PERSPECTIVES IN PEPTIDES DEVELOPMENT AS THERAPEUTIC AGENTS

The details of the industrial drug discovery and development process are normally performed under a very high degree of confidentiality. Most of the time, the structure is kept secret as long as possible and Markush structures are used in product patents, not only to enlarge the scope of the claim, but also to cover the real drug candidate formula. The structure of 11 of the 58 peptides that we have tracked down was not disclosed. In addition, for what concerns heterologous peptides most of the time also the binding mode, the hot spots of the protein-protein interaction, the modelling and the SARS are kept confidential to delay as much as possible potential competitors, since generation of "me-too" structures of peptides is quite simple.

Heterologous peptides for PPI are normally identified *via* a normal small molecule drug discovery approach, with the target to identify hot spots mainly via peptides library screening. Once the hit is identified, the structural changes have the target to shorten as much as possible the peptide length, to increase and stabilize the biological activity, to crystallize receptors/ligands or their fragments and to clearly identify the hot spots generating a docking model. The lead optimization to get the drug candidate will further optimize activity and selectivity, and will screen the amino acids that can be used to improve the pharmacological profile.

The approach to native/analogous peptides is completely different since, in this case, the active peptide sequence is normally well known as well as the protein-protein interaction. The critical issue is establishing the relationship of a specific PPI with a disease. Bioinformatics and a better understanding of human molecular physiology have a key role in decreasing time and cost in respect to experimental approaches for the identification of new targets (Muttenthaler et al., 2021). Starting from the native sequence, that has been already identified by nature, the challenge of the medicinal chemist is then similar to the one of heterologous peptides, with the target to file a product patent that identifies a series of new structure in a very competitive environment.

The most remarkable example of native/analogues peptides development is that of GLP-1R agonists for type-2 diabetes and obesity. The molecules in clinical trials have been already discussed in paragraph five, however, this segment, that is by far the most important PPI in terms of potential market and industrial competition, can be used for a critical evaluation. The first in class GLP-1R agonist for type-2-diabetes mellitus, exenatide, was approved by the FDA in 2012. This molecule is the synthetic version of exendin-4, a polypeptide found in the salivary excretion of the Gila Monster, that has a 53%

homology with GLP-1. While GLP-1 half-life is 1.5–5 min, exenatide is around 2.4 h. Since then, additional five molecules with a very high homology for GLP-1 or exenatide (>90%) have been approved and among them there are also the blockbusters liraglutide and semaglutide. From the alignments reported in **Figure 7**, it is easy to see that the amino acids that are critical for GLP-1R binding (Dods and Donnelly 2016), identified by site direct mutagenesis and Ala scanning (Knudsen and Lau 2019) have been conserved in all peptides (residues 7, 10, 12, 13, 15, 28, 29, 35, 36).

In fact, all modifications introduced in GLP-1 sequence and in the structures of dual inhibitors of GLP-1R/GIPR and GLP-1R/GCGR have the target to increase the pharmacological profile without perturbing the binding efficiency. With the only exception of liraglutide, in all the molecules already approved and in clinical trials, the Ala8 of GLP-1, that is sensitive to dipeptidyl peptidase-4 (DPP-4), has been replaced by Gly, Aib or Ser. In addition, side chains, known to prolong half-life and potentially increase oral bioavailability, were introduced in six of

the seven molecules in clinical trials and have been attached to amino acids that are not critical for GLP-1R binding (residues 16, 23, 26, 36, 44, 45, and 46). From the available data semaglutide has still the record in terms of half-life (7 days). The overall development of these drugs has been largely described and the new molecules in clinical trials have followed a similar development path. From a scientific point of view, it will be interesting to monitor the evolution of dual and triple inhibitors in clinical trials to understand if these approaches will deliver any real therapeutic advantage respect to the current blockbusters.

Still serendipity can play a major role, and a typical example is Drucker's discovery of the function of GLP-2 in the intestine that ultimately resulted in the commercialization of Teduglutide for the treatment of short bowel syndrome (Drucker 2019). The natural GLP-2 has a very short half-life, 7 min, while in Teduglutide the substitution of alanine with glycine at position two results in a peptide resistant to degradation by DPP-4 achieving a half-life of 2 h necessary for a daily treatment, in analogy with the GLP-1 analogues series (Marier et al., 2010). In other words, when the biological function of PPI is understood, the drug development is straightforward.

Therapeutic proteins (TP) have a consistently higher success rate than small molecules (Smietana et al., 2016). Peptides have performances similar to TP mainly because of the contribution of native/analogues and their high level of selectivity, that avoids out of target toxicity. On the other hand, heterologous peptides success rate is more similar to the one of small molecules and the target is, again, a very high level of selectivity, limiting the toxicological assessment to immunogenicity. When a market is saturated the impact of management and market considerations start to have a great impact on the attrition rate. Diabetes and obesity attracted the attention of several companies, since this is by far the most important market segment from a turnover point of view. We have described several native and analogue peptides that are targeting GLP-1R, GLP-1R/GCGR, GLP-1R/GIPR, Y2R actually in the clinic. However, there are already several peptides approved in this segment and, by the time the new ones will be approved, several potent and effective drugs will become generics. Therefore, the success rate of the molecules in the clinic will be not only related to efficacy but also by market positioning.

CONCLUSION

The PPI modulation is a fertile area for peptide development as shown by the overall peptide market and by the large pipeline discussed in this paper. The herein reported overview shows that targeting PPI represents a successful approach for a number of different pathologies, since the network of human interactome regulates all the physiological cascade events and the related disfunctions. The availability of powerful synthetic methodologies is able to sustain medicinal chemists in the exploration of the molecular space for the design of new structures with an improved pharmacological profile. From a technological standpoint, innovation is now needed in the greening of synthetic technologies to accomplish sustainability.

Although the number of peptides entering clinical trials pathways is always increasing, a huge number of PPI are still unexplored or undisclosed. In fact, it is important to underline that, with the exception of cancer related pathologies as well as diabetes/obesity, the number of molecules in Phase 1 is very limited. The drug discovery and development process and the regulatory and market dynamics of therapeutic peptides will evolve in the near future also because of the potentially enormous impact of PPI. In conclusion, behind the PPI understanding there is the Holy Grail of protein-protein cross talk alphabet that will open up a new era in the pharmaceutical development of safe and effective drugs where the peptide modality will play a major role.

AUTHOR CONTRIBUTIONS

All authors listed have made a substantial, direct and intellectual contribution to the work, and approved it for publication.

FUNDING

This work has been developed with fundings from Alma mater Studiorum University fo Bologna (RFO)

ACKNOWLEDGMENTS

We acknowledge Stefano Mureddu, Sylwia Malinowska and Antonio Ricci from Fresenius kabi for the extensive discussions on the subject and Fresenius kabi for the grants to GM, DC, and PC.

SUPPLEMENTARY MATERIAL

The Supplementary Material for this article can be found online at: https://www.frontiersin.org/articles/10.3389/fmolb.2021.697586/full#supplementary-material

REFERENCES

9 Meters Biopharma, Inc. (2021). Company Pipeline - Gastrointestinal Platform Company. Available at: https://9meters.com/pipeline/ (Accessed March 15, 2021)

Acosta, A., Vasicek, T., and Brown, B. A-S. (2019). *Peptide YY Pharmaceutical Formulations, Compositions and Methods*. Gila Therapeutics Inc.. U.S. Patent and Trademark Office, U.S. Patent Application No US2019/0231850

AltImmune (2021). *Corporate Presentation 2021*. Available at https://ir.altimmune.com/static-files/41e9a4ac-5982-4849-9cc4-0134553875da (Accessed June 4, 2021).

Ambery, P., Parker, V. E., Stumvoll, M., Posch, M. G., Heise, T., Plum-Moerschel, L., et al. (2018). MEDI0382, a GLP-1 and Glucagon Receptor Dual Agonist, in Obese or Overweight Patients with Type 2 Diabetes: A Randomised, Controlled, Double-Blind, Ascending Dose and Phase 2a Study. *The Lancet*. 391, 2607–2618. doi:10.1016/S0140-6736(18)30726-8

Anker, S. D., Ponikowski, P., Mitrovic, V., Peacock, W. F., and Filippatos, G. (2015). Ularitide for the Treatment of Acute Decompensated Heart Failure: from Preclinical to Clinical Studies. *Eur. Heart J.* 36, 715–723. doi:10.1093/eurheartj/ehu484

Annett, S., Moore, G., Short, A., Marshall, A., McCrudden, C., Yakkundi, A., et al. (2020). FKBPL-based Peptide, ALM201, Targets Angiogenesis and Cancer Stem Cells in Ovarian Cancer. *Br. J. Cancer*. 122, 361–371. doi:10.1038/s41416-019-0649-5

Arad, G., Levy, R., Nasie, I., Hillman, D., Rotfogel, Z., Barash, U., et al. (2011). Binding of Superantigen Toxins into the CD28 Homodimer Interface Is Essential for Induction of Cytokine Genes that Mediate Lethal Shock. *Plos Biol.* 9 (9), e1001149. doi:10.1371/journal.pbio.1001149

Arch Biopartners (2019). MetaBlock™. Available from: https://archbiopartners.com/index.php/our-science/our-key-platforms/metablok (Accessed March 15, 2021).

Ballarin, B., and Tymianski, M. (2018). Discovery and Development of NA-1 for the Treatment of Acute Ischemic Stroke. Acta Pharmacol. *Sin.* 39, 661–668. doi:10.1038/aps.2018.5

Bastin, M., and Andreelli, F. (2019). Dual GIP-GLP1-Receptor Agonists in the Treatment of Type 2 Diabetes: A Short Review on Emerging Data and Therapeutic Potential. *Diabetes Metab Syndr Obes.* Vol. 12, 1973–1985. doi:10.2147/DMSO.S191438

Billesbølle, C. B., Azumaya, C. M., Kretsch, R. C., Powers, A. S., Gonen, S., Schneider, S., et al. (2020). Structure of Hepcidin-Bound Ferroportin Reveals Iron Homeostatic Mechanisms. *Nature*. 586, 807–811. doi:10.1038/s41586-020-2668-z

Blanco, M. J., and Gardinier, K. M. (2020). New Chemical Modalities and Stratecgic Thinking in Early Drug Discovery. *ACS Med. Chem. Lett.* 11, 228–231. doi:10.121/acsmedchemlett.9b00582

Boulete, I.-M., Thadi, A., Beaufrand, C., Patwa, V., Joshi, A., Foss, J. A., et al. (2018). Oral Treatment with Plecanatide or Dolcanatide Attenuates Visceral Hypersensitivity via Activation of Guanylate Cyclase-C in Rat Models. *World J Gastroenterol.* 24 (17), 1888–1900. doi:10.3748/wjg.v24.i17.1888

Brubaker, P. L. (2018). Glucagon-like Peptide-2 and the Regulation of Intestinal Growth and Function. *Compr. Physiol.* 8, 1185–1210. doi:10.1002/cphy.c170055

Canesin, G., Evans-Axelsson, S., Hellsten, R., Krzyzanowska, A., Prasad, C. P., Bjartell, A., et al. (2017). Treatment with the WNT5A-Mimicking Peptide Foxy-5 Effectively Reduces the Metastatic Spread of WNT5A-Low Prostate Cancer Cells in an Orthotopic Mouse Model. *PLoS ONE*. 12 (9), e0184418. doi:10.1371/journal.pone.0184418

Capozzi, M. E., DiMarchi, R. D., Tschöp, M. H., Finan, B., and Campbell, J. E. (2018). Targeting the Incretin/Glucagon System with Triagonists to Treat Diabetes. *Endocr. Rev.* 39 (5), 719–738. doi:10.1210/er.2018-00117

Carmot Therapeutics Pipeline (2021). Available at: https://carmot-therapeutics.us/pipeline/ (Accessed March 10, 2021).

Casu, C., Nemeth, E., and Rivella, S. (2018). Hepcidin Agonists as Therapeutic Tools. *Blood*. 131, 1790. doi:10.1182/blood-2017-11-737411

Chappe, F., Arnold, S., Ballance, J., and Chappe, V. (2014). Vip-Elp Fusion Molecules Pb1120 and Pb1046 Correct F508del-Cftr Dysfunction. *Ped. Pulmon.* 49, 294–295.

Chawla, L. S., Beers-Mulroy, B., and Tidmarsh, G. F. (2019). Therapeutic Opportunities for Hepcidin in Acute Care Medicine. *Crit. Care Clin.* 35, 357–374. doi:10.1016/j.ccc.2018.11.014

Chiquet, C., Aptel, F., Creuzot-Garcher, C., Berrod, J.-P., Kodjikian, L., Massin, P., et al. (2017). Postoperative Ocular Inflammation: a Single Subconjunctival Injection of XG-102 Compared to Dexamethasone Drops in a Randomized Trial. *Am. J. Ophthalmol.* 174, 76–84. doi:10.1016/j.ajo.2016.10.012

Choudhury, S. R., Babes, L., Rahn, J. J., Ahn, B.-Y., Goring, K.-A. R., King, J. C., et al. (2019). Dipeptidase-1 Is an Adhesion Receptor for Neutrophil Recruitment in Lungs and Liver. *Cell.* 178 (5), 1205–1221. doi:10.1016/j.cell.2019.07.017

Clemmensen, C., Finan, B., Müller, T. D., DiMarchi, R. D., Tschöp, M. H., and Hofmann, S. M. (2019). Emerging Hormonal-Based Combination Pharmacotherapies for the Treatment of Metabolic Diseases. *Nat. Rev. Endocrinol.* 15, 90–104. doi:10.1038/s41574-018-0118-x

Connop, B. P., Spencer, D. M. L., Singh, J., Buczek, P. D., Halbleib, C. M., Kerkow, D. E., et al. (2020). *Oxyntomodulin Peptide Analog Formulations*. Washington, DC: OPKO Ireland Global Hldings Ltd. U.S. Patent and Trademark Office, U.S. Patent Application No, US2020/0262887

Coskun, T., Sloop, K. W., Loghin, C., Alsina-Fernandez, J., Urva, S., Bokvist, K. B., et al. (2018). LY3298176, a Novel Dual GIP and GLP-1 Receptor Agonist for the Treatment of Type 2 Diabetes Mellitus: from Discovery to Clinical Proof of Concept. *Mol. Metab.* 18, 3–14. doi:10.1016/j.molmet.2018.09.009

Craig, C. M. (2020). *Avexitide for the Treatment of Hyperinsulemic Hypoglycemia*. Geneva, Switzerland: Eiger Biopharmaceuticals, Inc.. World Intellectual Property Organization, PCT Patent Application No.WO2020/081534 A1

Cui, H., Zhao, C.-Y., Lv, Y., Wei, M.-J., Zhu, Y., Li, Y., et al. (2020). Safety, Tolerability and Pharmacokinetics of Single Dose Polyethylene Glycosylated Exenatide Injection (PB-119) in Healthy Volunteers. *Eur. J. Drug Metab. Pharmacokinet.* 45, 361–369. doi:10.1007/s13318-020-00605-9

Curtis, K. K., Sarantopoulos, J., Northfelt, D. W., Weiss, G. J., Barnhart, K. M., Whisnant, J. K., et al. (2014). Novel LHRH-Receptor-Targeted Cytolytic Peptide, EP-100: First-In-Human Phase I Study in Patients with Advanced LHRH-Receptor-Expressing Solid Tumors. *Cancer Chemother. Pharmacol.* 73, 931–941. doi:10.1007/s00280-014-2424-x

Cuvier, V., Lorch, U., Witte, S., Olivier, A., Gibot, S., Delor, I., et al. (2018). A First-In-Man Safety and Pharmacokinetics Study of Nangibotide, a New Modulator of Innate Immune Response through TREM-1 Receptor Inhibition. *Br. J. Clin. Pharmacol.* 84, 2270–2279. doi:10.1111/bcp.13668

Dods, R. L., and Donnelly, D. (2016). The Peptide Agonist-Binding Site of the Glucagon-like Peptide-1 (GLP-1) Receptor Based on Site-Directed Mutagenesis and Knowledge-Based Modelling. *Biosci. Rep.* 36, e00285. doi:10.1042/BSR20150253

Donnelly, D. (2012). The Structure and Function of the Glucagon-like Peptide-1 Receptor and its Ligands. *Br. J. Pharmacol.* 166, 27–41. doi:10.1111/j.1476-5381.2011.01687.x

Drucker, D. J., and Nauck, M. A. (2006). The Incretin System: Glucagon-like Peptide-1 Receptor Agonists and Dipeptidyl Peptidase-4 Inhibitors in Type 2 Diabetes. *The Lancet*. 368, 1696–1705. doi:10.1016/S0140-6736(06)69705-5

Drucker, D. J. (2019). The Discovery of GLP-2 and Development of Teduglutide for Short Bowel Syndrome. *ACS Pharmacol. Transl. Sci.* 2, 134–142. doi:10.1021/acsptsci.9b00016

Duda, P., Farzaneh-Far, R., Ma, Z., Zhu, N., Thackaberry, E., and Ricardo, A. (2020). *Neurological Disease Tratment with Zilucoplan. Patent No WO/2020/086506*. Cambridge: Ra Pharmaceuticals, Inc. doi:10.14311/tpfm.2020.008

Emani, S., Meyer, M., Palm, D., Holzmeister, J., and Haas, G. J. (2015). Ularitide: a Natriuretic Peptide Candidate for the Treatment of Acutely Decompensated Heart Failure. *Future Cardiol.* 11, 531–546. doi:10.2217/fca.15.53

Emanuele, N., and Emanuele, M. A. (1997). The Endocrine System: Alcohol Alters Critical Hormonal Balance. *Alcohol. Health Res. World*. 21 (1), 53

Emerit, J., Edeas, M., and Bricaire, F. (2004). Neurodegenerative Diseases and Oxidative Stress. *Biomed. Pharmacother.* 58, 39–46. doi:10.1016/j.biopha.2003.11.004

FDA - U.S. Food and Drug Administration (2018). Available online: https://www.fda.gov/about-fda/economic-impact-analyses-fda-regulations/definition-term-biological-product-proposed-rule-preliminary-regulatory-impact-analysis

Ferrazzano, L., Corbisiero, D., Martelli, G., Tolomelli, A., Viola, A., Ricci, A., et al. (2019). Green Solvent Mixtures for Solid-phase Peptide Synthesis: A Dimethylformamide-free Highly Efficient Synthesis of Pharmaceutical-Grade Peptides. *ACS Sustainable Chem. Eng.* 7, 12867–12877. doi:10.1021/acssuschemeng.9b01766

Festuccia, C., Dondi, D., Piccolella, M., Locatelli, A., Gravina, G. L., Tombolini, V., et al. (2010). Ozarelix, a Fourth Generation GnRH Antagonist, Induces Apoptosis in Hormone Refractory Androgen Receptor Negative Prostate Cancer Cells Modulating Expression and Activity of Death Receptors. *Prostate*. 70, a. doi:10.1002/pros.21169

Fishbane, S., Mathur, V., Germain, M. J., Shirazian, S., Bhaduri, S., Munera, C., et al. (2020). Randomized Controlled Trial of Difelikefalin for Chronic Pruritus in Hemodialysis Patients. *Kidney Int. Rep.* 5 (5), 600–610. doi:10.1016/j.ekir.2020.01.006

Flanagan, C. A., and Manilall, A. (2017). Gonadotropin-Releasing Hormone (GnRH) Receptor Structure and GnRH Binding. *Front. Endocrinol.* 8, 274. doi:10.3389/fendo.2017.00274

Fozgerau, K., and Hoffmann, T. (2015). Peptide Therapeutics: Current Status and Future Directions. *Drug Discov. Today* 20, 122–128. doi:10.1016/j.drudis.2014.10.003

François, B., Wittebole, X., Ferrer, R., Mira, J. P., Dugernier, T., Gibot, S., et al. (2020). Nangibotide in Patients with Septic Shock: a Phase 2a Randomized Controlled Clinical Trial. *Intensive Care Med.* 46, 1425–1437. doi:10.1007/s00134-020-06109-z

Gasbjerg, L. S., Gabe, M. B. N., Hartmann, B., Christensen, M. B., Knop, F. K., Holst, J. J., et al. (2018). Glucose-dependent Insulinotropic Polypeptide (GIP) Receptor Antagonists as Anti-diabetic Agents. *Peptides*. 100, 173–181. doi:10.1016/j.peptides.2017.11.021

Genervon (2021). Summary of Research Evaluating GM6 Mechanisms of Action and Efficacy in ALS. Available at: https://www.genervon.com/gm6-als-moa (Accessed March 15, 2021).

Gorman, D. M., Lee, J., Payne, C. D., Woodruff, T. M., and Clark, R. J. (2021). Chemical Synthesis and Characterisation of the Complement C5 Inhibitory Peptide Zilucoplan. *Amino Acids*. 53, 143–147. doi:10.1007/s00726-020-02921-5

Gulfidan, G., Turanli, B., Beklen, H., Sinha, R., and Arga, K. Y. (2020). Pan-cancer Mapping of Differential Protein-Protein Interactions. *Sci. Rep.* 10, 3272. doi:10.1038/s41598-020-60127-x

Hall, S., Isaacs, D., and Clements, J. N. (2018). Pharmacokinetics and Clinical Implications of Semaglutide: A New Glucagon-like Peptide (GLP)-1 Receptor Agonist. *Clin. Pharmacokinet.* 57, 1529–1538. doi:10.1007/s40262-018-0668-z

Harb, W., Patnaik, A., Mahalingam, D., Liu, J., Wen, P. Y., Shapiro, G. I., et al. (2019). A Phase I Open Label Dose Escalation Trial Evaluating VT1021 in Patients with Advanced Solid Tumours. *Ann. Oncol.* 30 (Suppl. l_5), v175–v193. doi:10.1093/annonc/mdz244.027

Hargrove, D. M., Alagarsamy, S., Croston, G., Laporte, R., Qi, S., Srinivasan, K., et al. (2020). Pharmacological Characterization of Apraglutide, a Novel Long-Acting Peptidic Glucagon-like Peptide-2 Agonist, for the Treatment of Short Bowel Syndrome. *J. Pharmacol. Exp. Ther.* 373, 193–203. doi:10.1124/jpet.119.262238

Heickman, L. K. W., DeBoer, M. D., and Fasano, A. (2020). Zonulin as a Potential Putative Biomarker of Risk for Shared Type 1 Diabetes and Celiac Disease Autoimmunity. *Diabetes/Metabolism Res. Rev.* 36, e3309. doi:10.1002/dmrr.3309

Henderson, S. J., Konkar, A., Hornigold, D. C., Trevaskis, J. L., Jackson, R., Fritsch Fredin, M., et al. (2016). Robust Anti-obesity and Metabolic Effects of a Dual GLP-1/glucagon Receptor Peptide Agonist in Rodents and Non-human Primates. *Diabetes Obes. Metab.* 18, 1176–1190. doi:10.1111/dom.12735

Herr, D. R. (2012). Potential Use of G Protein-Coupled Receptor-Blocking Monoclonal Antibodies as Therapeutic Agents for Cancers. *Int. Rev. Cel Mol. Biol.* 297, 45–81. doi:10.1016/B978-0-12-394308-8.00002-9

Hu, J., Xu, Q., McTiernan, C., Lai, Y.-C., Osei-Hwedieh, D., and Gladwin, M. (2015). Novel Targets of Drug Treatment for Pulmonary Hypertension. *Am. J. Cardiovasc. Drugs*. 15, 225–234. doi:10.1007/s40256-015-0125-4

Hövelmann, U., Væver Bysted, B., Mouritzen, U., Macchi, F., Lamers, D., Kronshage, B., et al. (2018). Pharmacokinetic and Pharmacodynamic Character of Dasiglucagon, a Novel Soluble and Stable Glucagon Analog. *Diabetes Care*. 41 (3), 531–537. doi:10.2337/dc17-1402

Janeway, C. A., Jr, Travers, P., Walport, M., and Shlomchik, M. J. (2001). *Immunobiology: The Immune System in Health and Disease*. 5th edition. New York: Garland Science. Autoimmune responses are directed against self-antigens. Available from: https://www.ncbi.nlm.nih.gov/books/NBK27155/ (Accessed March 15, 2021)

Javitt, D. C., Buchanan, R. W., Keefe, R. S. E., Kern, R., McMahon, R. P., Green, M. F., et al. (2012). Effect of the Neuroprotective Peptide Davunetide (AL-108) on Cognition and Functional Capacity in Schizophrenia. *Schizophrenia Res.* 136, 25–31. doi:10.1016/j.schres.2011.11.001

Jones, S., and Thornton, J. M. (1996). Principles of Protein-Protein Interactions. *Proc. Natl. Acad. Sci.* 93, 13–20. doi:10.1073/pnas.93.1.13

Inotrem (2020). *Inotrem Announces the Publication of its Phase IIa Clinical Study for Nangibotide in the Treatment of Septic Shock in Peer Review Journal "Intensive Care Medicine"*Available at: https://www.inotrem.com/2020/06/02/inotrem-announces-publication-phase-iia-clinical-study-nangibotide-treatment-septic-shock-peer-review-journal-intensive-care-medicine/ (Accessed March, 2021).

ImmuPharma (2019). *Lupuzor™*. Available from: https://www.immupharma.co.uk/folio/lupuzor-lupus/ (Accessed March 15, 2021).

Kaempfer, R. (2018). Bacterial Superantigen Toxins, CD28, and Drug Development. *Toxins*. 10, 459. doi:10.3390/toxins10110459

Kaplan, C. W., Sim, J. H., Shah, K. R., Kolesnikova-Kaplan, A., Shi, W., and Eckert, R. (2011). Selective Membrane Disruption: Mode of Action of C16G2, a Specifically Targeted Antimicrobial Peptide. *Antimicrob. Agents Chemother.* 55, 3446–3452. doi:10.1128/AAC.00342-11

Kaufmann, P., Cortes, J., Martin, M., Mayer, I., Vahdat, L., Pernas, S., et al. (2020). Abstract OT1-08-06: International, Phase 3 Trial: Balixafortide (A CXCR4 Antagonist) + Eribulin versus Eribulin Alone in Patients with HER2 Negative, Locally Recurrent or Metastatic Breast Cancer (FORTRESS) International, Phase 3 Trial: Balixafortide (A CXCR4 Antagonist) + Eribulin versus Eribulin Alone in Patients with HER2 Negative, Locally Recurrent or Metastatic Breast Cancer (FORTRESS). *Cancer Res.* 80 (4 Suppl. ment), OT1–08. doi:10.1158/1538-7445.SABCS19-OT1-08-06

Khoo, B., and Tan, T. M.-M. (2020). Combination Gut Hormones: Prospects and Questions for the Future of Obesity and Diabetes Therapy. *J. Endocrinol.* 246, R65–R74. doi:10.1530/JOE-20-0119

Kim, K., and Kim, K. H. (2020). Targeting of Secretory Proteins as a Therapeutic Strategy for Treatment of Nonalcoholic Steatohepatitis (NASH). *Int J Mol Sci.* 21 (7), 2296. doi:10.3390/ijms21072296

Kim, M. S., Ma, S., Chelariu-Raicu, A., Leuschner, C., Alila, H. W., Lee, S., et al. (2020). Enhanced Immunotherapy with LHRH-R Targeted Lytic Peptide in Ovarian Cancer. *Mol. Cancer Ther.* 19 (11), 2396–2406. doi:10.1158/1535-7163.MCT-20-0030

Knudsen, L. B., and Lau, J. (2019). The Discovery and Development of Liraglutide and Semaglutide. *Front. Endocrinol.* 10, 155. doi:10.3389/fendo.2019.00155

Ko, D., Kindy, M. S., Swindell, W. R., and Bojanowski, K. (2017). *Methods of Using GM604 in Modulating ALS Disease Biomarkers Leading to Prognosis and Therapeutic Treatment for ALS diseasePatent No US 2017/0157197*. Pasadena. Genevron Biopharmaceuticals, Inc

Lafferty, R. A., O'Harte, F. P. M., Irwin, N., Gault, V. A., and Flatt, P. R. (2021). Proglucagon-Derived Peptides as Therapeutics. *Front. Endocrinol.* 12, 689678. doi:10.3389/fendo.2021.689678

Lau, J. L., and Dunn, M. K. (2018). Therapeutic Peptides: Historical Perspectives, Current Development Trends, and Future Directions. *Bioorg. Med. Chem.* 26, 2700–2707. doi:10.1016/j.bmc.2017.06.052

Lauber, T., Neudecker, P., Rösch, P., and Marx, U. C. (2003). Solution Structure of Human Proguanylin. *J. Biol. Chem.* 278, 24118–24124. doi:10.1074/jbc.M300370200

Lawrenson, S. B., Arav, R., and North, M. (2017). The Greening of Peptide Synthesis. *Green. Chem.* 19, 1685–1691. doi:10.1039/c7gc00247e

Lee, G., Lee, Y., Chang, M., Kang, S. U. K., Ryou, J.-H., Lim, J.-J., et al. (2019). P120 BBT-401 Is a Selective Pellino-1 Protein-Protein Interaction Inhibitor in Clinical Development Targeting a First-In-Class Drug for UC Treatment. *Inflamm. Bowel Dis.* 25 (Suppl. ment_1), S58. doi:10.1093/ibd/izy393.131

Leuchte, H. H., Baezner, C., Baumgartner, R. A., Bevec, D., Bacher, G., Neurohr, C., et al. (2008). Inhalation of Vasoactive Intestinal Peptide in Pulmonary Hypertension. *Eur. Respir. J.* 32, 1289–1294. doi:10.1183/09031936.00050008

Lipman, Z. M., and Yosipovitch, G. (2020). An Evaluation of Difelikefalin as a Treatment Option for Moderate-To-Severe Pruritus in End Stage Renal Disease. *Expert Opin. Pharmacother.* 22, 549–555. doi:10.1080/14656566.2020.1849142

Lopez, N. E., Gaston, L., Lopez, K. R., Hageny, A. M., Putnam, J., Eliceiri, B., et al. (2014). Ghrelin Decreases Motor Deficits after Traumatic Brain Injury. *J. Surg. Res.* 187, 230–236. doi:10.1016/j.jss.2013.09.030

Mabonga, L., and Kappo, A. P. (2020). Peptidomimetics: A Synthetic Tool for Inhibiting Protein-Protein Interactions in Cancer. *Int. J. Pept. Res. Ther.* 26, 225–241. doi:10.1007/s10989-019-09831-5

Magen, I., and Gozes, I. (2014). Davunetide: Peptide Therapeutic in Neurological Disorders. *Curr Med Chem.* 21, 2591–2598. doi:10.2174/09298673216614021712 4945

Marier, J.-F., Mouksassi, M.-S., Gosselin, N. H., Beliveau, M., Cyran, J., and Wallens, J. (2010). Population Pharmacokinetics of Teduglutide Following Repeated Subcutanenous Administrations in Healthy Participants and in Patients with Short Bowel Syndrome and Crohn's Disease. *J.Clin. Pharmacol.* 50, 36–49. doi:10.1177/0091270009342252

Martchenko, S. E., Sweeney, M. E., Dimitriadou, V., Murray, J. A., and Brubaker, P. L. (2020). Site-Specific and Temporal Effects of Apraglutide, a Novel Long-Acting Glucagon-like Peptide-2 Receptor Agonist, on Intestinal Growth in Mice. *J. Pharmacol. Exp. Ther.* 373, 347–352. doi:10.1124/jpet.119.263947

Martin, P., Cohen, A., Uddin, S., Epelbaum, L., and Josiah, S. (2020). Randomized, Double-Masked, Placebo-Controlled Dose Escalation Study of TAK-639 Topical Ophthalmic Solution in Subjects with Ocular Hypertension or Primary Open-Angle Glaucoma. *Clin Ophthalmol.* Vol. 14, 885–896. doi:10.2147/opth.s242932

Martin, V., Egelund, P. H. G., Johansson, H., Thordal Le Quement, S., Wojcik, F., and Sejer Pedersen, D. (2020). Greening the Synthesis of Peptide Therapeutics: an Industrial Perspective. *RSC Adv.* 10, 42457–42492. doi:10.1039/d0ra07204d

Massoud, R., Enose-Akahata, Y., Tagaya, Y., Azimi, N., Basheer, A., and Jacobson, S. (2015). Common γ-chain Blocking Peptide Reduces *In Vitro* Immune Activation Markers in HTLV-1-Associated Myelopathy/tropical Spastic Paraparesis. *Proc. Natl. Acad. Sci. USA*. 112 (35), 11030–11035. doi:10.1073/pnas.1412626112

Mathiesen, D. S., Lund, A., Vilsbøll, T., Knop, F. K., and Bagger, J. I. (2020). Amylin and Calcitonin: Potential Therapeutic Strategies to Reduce Body Weight and Liver Fat. *Front. Endocrinol.* 11, 617400. doi:10.3389/fendo.2020.617400

Mayo, B. J., Secombe, K. R., Wignall, A. D., Bateman, E., Thorpe, D., Pietra, C., et al. (2020). The GLP-2 Analogue Elsiglutide Reduces Diarrhoea Caused by the Tyrosine Kinase Inhibitor Lapatinib in Rats. *Cancer Chemother. Pharmacol.* 85, 793–803. doi:10.1007/s00280-020-04040-0

McClements, L., Annett, S., Yakkundi, A., O'Rourke, M., Valentine, A., Moustafa, N., et al. (2019). FKBPL and its Peptide Derivatives Inhibit Endocrine Therapy Resistant Cancer Stem Cells and Breast Cancer Metastasis by Downregulating DLL4 and Notch4. *BMC Cancer*. 19, 351. doi:10.1186/s12885-019-5500-0

McGuire, D., Lane, N., Segal, N., Metyas, S., Barthel, H., Miller, M., et al. (2018). TPX-100 Leads to Marked, Sustained Improvements in Subjects with Knee Osteoarthritis: Pre-clinical Rationale and Results of a Controlled Clinical Trial. *Osteoarthritis and Cartilage*. 26, 243. doi:10.1016/j.joca.2018.02.502

Meloni, B. P., Blacker, D. J., Mastaglia, F. L., and Knuckey, N. W. (2020). Emerging Cytoprotective Peptide Therapies for Stroke. *Expert Rev. Neurotherapeutics*. 20, 887–890. doi:10.1080/14737175.2020.1788390

Min, T., and Bain, S. C. (2021). The Role of Tirzepatide, Dual GIP and GLP-1 Receptor Agonist, in the Management of Type 2 Diabetes: The SURPASS Clinical Trials. *Diabetes Ther.* 12, 143–157. doi:10.1007/s13300-020-00981-0

Min Xu, M., Lv, W., Zhang, Y., and Luo, X. (2019). *Composition Comprisining GLP-1 Receptor Agonist and Glucagon Receptor Agonist and Application of Thereof*. Washington, DC: PEGBIO Co., Ltd. U.S. Patent and Trademark Office, U.S. Patent Application No. US2019/0134161

Mordor Intelligelligence (2020). *Peptide Therapeutics Market 2020-2025 Mordor Intelligence*. Available at https://www.mordorintelligence.com/industry-reports/peptide-therapeutics-market (Accessed June 4, 2021).

Muttenthaler, M., King, G. F., Adams, D. J., and Alewood, P. F. (2021). Trends in Peptide Drug Discovery. *Nat. Rev. Drug Discov.* 20, 309–325. doi:10.1038/s41573-020-00135-8

Naimi, R. M., Hvistendahl, M., Enevoldsen, L. H., Madsen, J. L., Fuglsang, S., Poulsen, S. S., et al. (2019). Glepaglutide, a Novel Long-Acting Glucagon-like Peptide-2 Analogue, for Patients with Short Bowel Syndrome: a Randomised Phase 2 Trial. *Lancet Gastroenterol. Hepatol.* 4, 354–363. doi:10.1016/S2468-1253(19)30077-9

Nata, T., Zapata, J. C., Massoud, R., Jacobson, S., Azimi, N., and Tagaya, Y. (2015). A Multi-Cytokine Inhibitory Peptide (BNZ 132-1) that Is a Potential Therapeutic Agent for HAMTSP and Other Necrotizing Diseases. *Retrovirology*. 12 (Suppl. 1), O22. doi:10.1186/1742-4690-12-S1-O22

National Human Genome Research Institute NHGRI (2021). *"Genetic Disorders"*. Available from: https://www.genome.gov/For-Patients-and-Families/Genetic-Disorders (Accessed March 15, 2021).

Nestor, J. J., Zhang, X., Jaw-Tsai, S., Parkes, D. G., and Becker, C. K. (2021). Design and Characterization of a Surfactant-conjugated, Long-acting, Balanced GLP -1/glucagon Receptor Dual Agonist. *Pept. Sci.*, e24221. doi:10.1002/pep2.24221

Neumiller, J. J., and Campbell, R. K. (2009). Liraglutide: a Once-Daily Incretin Mimetic for the Treatment of Type 2 Diabetes Mellitus. *Ann. Pharmacother.* 43, 1433–1444. doi:10.1345/aph.1M134

Novo Nordisk (2020). *Annual Report 2020*. Available at https://www.novonordisk.com/annual-report.html (Accessed June 4, 2021).

Nuijens, T., Toplak, A., Schmidt, M., Ricci, A., and Cabri, W. (2019). Natural Occurring and Engineered Enzymes for Peptide Ligation and Cyclization. *Front. Chem.* 7, 829. doi:10.3389/fchem.2019.00829

Ogawa, H., Qiu, Y., Ogata, C. M., and Misono, K. S. (2004). Crystal Structure of Hormone-Bound Atrial Natriuretic Peptide Receptor Extracellular Domain. *J. Biol. Chem.* 279, 28625–28631. doi:10.1074/jbc.M313222200

OrthoTrophix (2021). *TPX-100*. Available from: http://www.orthotrophix.com/products-tpx-100.html (Accessed March 15, 2021)

Oxeia Biopharmaceuticals (2021). Available at: https://www.oxeiabiopharma.com/what-we-do/overview (Accessed March 12, 2021).

Pahwa, R., Goyal, A., Bansal, P., and Jialal, I. (2021). *Chronic Inflammation. [Updated 2020 Nov 20]. in: StatPearls [Internet]*. Treasure Island, United States: StatPearls Publishing. Available from: https://www.ncbi.nlm.nih.gov/books/NBK493173/ (Accessed March 15, 2021).

Patil, M., Deshmukh, N. J., Patel, M., and Sangle, G. V. (2020). Glucagon-based Therapy: Past, Present and Future. *Peptides*. 127, 170296. doi:10.1016/j.peptides.2020.170296

Pieber, T., Tehranchi, R., Hövelmann, U., Willard, J., Plum-Moerschel, L., and Aronoson, R. (2020). *Ready to Use Dasiglucagon Injection as a Fast and Effective Treatment for Severe Hypoglycaemia*. Madrid, Spain: Poster Presented at the ATTD 2020 Congress

Pipeline Overview AtoxBio (2021). Available at: https://www.atoxbio.com/pipeline/pipeline-overview/ (Accessed March 15, 2021).

Rappaport, J. A., and Waldman, S. A. (2018). The Guanylate Cyclase C-cGMP Signaling axis Opposes Intestinal Epithelial Injury and Neoplasia. *Front. Oncol.* 8, 299. doi:10.3389/fonc.2018.00299

Robertson, N., and Spring, D. (2018). Using Peptidomimetics and Constrained Peptides as Valuable Tools for Inhibiting Protein-Protein Interactions. *Molecules*. 23, 959. doi:10.3390/molecules23040959

Sadeghi, H., Dagher, S., and Turner, A. (2015). *Modified Vasoactive Intestinal Peptides. U.S. Patent No 9,029,505*. Washington, DC: Malvern, Phasebio Pharmaceuticals, Inc. U.S. Patent and Trademark Office, U.S. Patent No 9,029,505

Säfholm, A., Tuomela, J., Rosenkvist, J., Dejmek, J., Härkönen, P., and Andersson, T. (2008). The Wnt-5a-Derived Hexapeptide Foxy-5 Inhibits Breast Cancer Metastasis *In Vivo* by Targeting Cell Motility. *Clin. Cancer Res.* 14 (20), 6556–6563. doi:10.1158/1078-0432.CCR-08-0711

Savarirayan, R., Irving, M., Bacino, C. A., Bostwick, B., Charrow, J., Cormier-Daire, V., et al. (2019). C-type Natriuretic Peptide Analogue Therapy in Children with Achondroplasia. *N. Engl. J. Med.* 381, 25–35. doi:10.1056/NEJMoa1813446

Savarirayan, R., Tofts, L., Irving, M., Wilcox, W., Bacino, C. A., Hoover-Fong, J., et al. (2020). Once-daily, Subcutaneous Vosoritide Therapy in Children with Achondroplasia: a Randomised, Double-Blind, Phase 3, Placebo-Controlled, Multicentre Trial. *The Lancet*. 396 (10252), 684–692. doi:10.1016/S0140-6736(20)31541-5

Savinainen, A., Prusakiewicz, J. J., Oswald, J., Spencer, E., Lou, Z., Cohen, M. L., et al. (2019). Pharmacokinetics and Intraocular Pressure-Lowering Activity of TAK-639, a Novel C-type Natriuretic Peptide Analog, in Rabbit, Dog, and Monkey. *Exp. Eye Res.* 189, 107836. doi:10.1016/j.exer.2019.107836

Schneider, A., Lang, A., and Naumann, W. (2010). Fluorescence Spectroscopic Determination of the Critical Aggregation Concentration of the GnRH Antagonists Cetrorelix, Teverelix and Ozarelix. *J. Fluoresc.* 20, 1233–1240. doi:10.1007/s10895-010-0674-5

Serrano, J., Casanova-Martí, À., Blay, M. T., Terra, X., Pinent, M., and Ardévol, A. (2017). Strategy for Limiting Food Intake Using Food Components Aimed at Multiple Targets in the Gastrointestinal Tract. *Trends Food Sci. Technology*. 68, 113–129. doi:10.1016/j.tifs.2017.08.002

Shailubhai, K., Palejwala, V., Arjunan, K. P., Saykhedkar, S., Nefsky, B., Foss, J. A., et al. (2015). Plecanatide and Dolcanatide, Novel Guanylate Cyclase-C Agonists, Ameliorate Gastrointestinal Inflammation in Experimental Models of Murine Colitis. *World J Gastrointest Pharmacol Ther.* 6 (4), 213–222. doi:10.4292/wjgpt.v6.i4.213

Sheetz, M., Bray, R., Tham, R. B., Jones, C., Kinsella, J., and Violante-Ortiz, R. (2017). *Results of a Phase 2 Study of the Oxyntomodulin (OXM) Analogue LY2944876 in Patients with Type 2 Diabetes (T2DM)*. San Diego, CA: Poster presented at 77th Scientific Session American Diabetes Association; June 10

Shore, N., Tutrone, R., Efros, M., Bidair, M., Wachs, B., Kalota, S., et al. (2018). Fexapotide Triflutate: Results of Long-Term Safety and Efficacy Trials of a Novel Injectable Therapy for Symptomatic Prostate Enlargement. *World J. Urol.* 36, 801–809. doi:10.1007/s00345-018-2185-y

Slim, G. M., Lansing, M., Wizzard, P., Nation, P. N., Wheeler, S. E., Brubaker, P. L., et al. (2019). Novel Long-Acting GLP-2 Analogue, FE 203799 (Apraglutide), Enhances Adaptation and Linear Intestinal Growth in a Neonatal Piglet Model of Short Bowel Syndrome with Total Resection of the Ileum. *J. Parenter. Enteral Nutr.* 43 (7), 891–898. doi:10.1002/jpen.1500

Sloop, K. W., Briere, D. A., Emmerson, P. J., and Willard, F. S. (2018). Beyond Glucagon-like Peptide-1: Is G-Protein Coupled Receptor Polypharmacology the Path Forward to Treating Metabolic Diseases? *ACS Pharmacol. Transl. Sci.* 1, 3–11. doi:10.1021/acsptsci.8b00009

Smietana, k., Siatkowski, M., and Møller, M. (2016). Trends in Clinical success Rates. *Nat. Rev. Drug Discov.* 15, 379–380. doi:10.1038/nrd.2016.85

Sosei Heptares (2019). *Sosei Heptares Starts New Clinical Development Program - First Subject Dosed in Phase I Study of HTL0030310, a Selective SSTR5 (Somatostatin 5) Receptor Agonist in Development to Treat Endocrine Disorders"*. Available from: https://soseiheptares.com/news/496/129/Sosei-Heptares-starts-new-clinical-development-program-First-subject-dosed-in-Phase-I-study-of-HTL0030310-a-selective-SSTR5-somatostatin-5-receptor-agonist-in-development-to-treat-endocrine-disorders.html (Accessed June 4, 2021)

Sosne, G., and Ousler, G. W. (2015). Thymosin Beta 4 Ophthalmic Solution for Dry Eye: a Randomized, Placebo-Controlled, Phase II Clinical Trial Conducted Using the Controlled Adverse Environment (CAE™) Model. *Clin. Ophthalmol.* 9, 877–884. doi:10.2147/OPTH.S80954

Sosne, G., Dunn, S. P., and Kim, C. (2015). Thymosin β4 Significantly Improves Signs and Symptoms of Severe Dry Eye in a Phase 2 Randomized Trial. *Cornea.* 34 (5), 491–496. doi:10.1097/ICO.0000000000000379

Srivastava, G., and Apovian, C. (2018). Future Pharmacotherapy for Obesity: New Anti-obesity Drugs on the Horizon. *Curr. Obes. Rep.* 7, 147–161. doi:10.1007/s13679-018-0300-4

Sterling, J. K., Adetunji, M. O., Guttha, S., Bargoud, A. R., Uyhazi, K. E., Ross, A. G., et al. (2020). GLP-1 Receptor Agonist NLY01 Reduces Retinal Inflammation and Neuron Death Secondary to Ocular Hypertension. *Cel Rep.* 33, 108271. doi:10.1016/j.celrep.2020.108271

Stumpf, M. P. H., Thorne, T., de Silva, E., Stewart, R., An, H. J., Lappe, M., et al. (2008). Estimating the Size of the Human Interactome. *Proc. Natl. Acad. Sci.* 105 (19), 6959–6964. doi:10.1073/pnas.0708078105

Suckfuell, M., Lisowska, G., Domka, W., Kabacinska, A., Morawski, K., Bodlaj, R., et al. (2014). Efficacy and Safety of AM-111 in the Treatment of Acute Sensorineural Hearing Loss. *Otology & Neurotology.* 35 (8), 1317–1326. doi:10.1097/MAO.0000000000000466

Suzuki, R., Brown, G. A., Christopher, J. A., Scully, C. C. G., and Congreve, M. (2020). Recent Developments in Therapeutic Peptides for the Glucagon-like Peptide 1 and 2 Receptors. *J. Med. Chem.* 63, 905–927. doi:10.1021/acs.jmedchem.9b00835

Swindell, W. R., Bojanowski, K., Kindy, M. S., Chau, R. M. W., and Ko, D. (2018). GM604 Regulates Developmental Neurogenesis Pathways and the Expression of Genes Associated with Amyotrophic Lateral Sclerosis. *Transl. Neurodegener.* 7, 30. doi:10.1186/s40035-018-0135-7

Tu, T. M., Kolls, B. J., Soderblom, E. J., Cantillana, V., Ferrell, P. D., Moseley, M. A., et al. (2017). Apolipoprotein E Mimetic Peptide, CN-105, Improves Outcomes in Ischemic Stroke. *Ann. Clin. Transl. Neurol.* 4, 246–265. doi:10.1002/acn3.399

Vaisburd, S., Shemer, Z., Yeheskel, A., Giladi, E., and Gozes, I. (2015). Risperidone and NAP Protect Cognition and Normalize Gene Expression in a Schizophrenia Mouse Model. *Sci. Rep.* 5, 16300. doi:10.1038/srep16300

van den Berg, J. W., Dik, W. A., van der Zee, M., Bonthuis, F., van Holten-Neelen, C., Dingjan, G. M., et al. (2011). The β-human Chorionic Gonadotropin-Related Peptide LQGV Reduces Mortality and Inflammation in a Murine Polymicrobial Sepsis Model. *Crit. Care Med.* 39 (1), 126–134. doi:10.1097/CCM.0b013e3181fa3a93

van Groenendael, R., Beunders, R., Kox, M., van Eijk, L. T., and Pickkers, P. (2019). The Human Chorionic Gonadotropin Derivate EA-230 Modulates the Immune Response and Exerts Renal Protective Properties: Therapeutic Potential in Humans. *Semin. Nephrol.* 39 (5), 496–504. doi:10.1016/j.semnephrol.2019.06.009

Villoutreix, B. (2017). Structural Prediction of Human WNT-5A and Foxy-5. *Figgshare. Figure Repository*. doi:10.6084/m9.figshare.5354137.v1

Wang, T. T., Yang, J., Zhang, Y., Zhang, M., Dubois, S., Conlon, K. C., et al. (2019). IL-2 and IL-15 Blockade by BNZ-1, an Inhibitor of Selective γ-chain Cytokines, Decreases Leukemic T-Cell Viability. *Leukemia* 33, 1243–1255. doi:10.1038/s41375-018-0290-y

Wang, Y., Lü, A., Sun, C., and Yuan, H. (2012). *GLP-1 Analogues and Their Pharmaceutical Salts and Uses*. Washington, DC U.S. Patent and Trademark Office, U.S. Patent Application No US2012/0196798 A1

WHO (2021). *Cardiovascular Diseases*. Available at: https://www.who.int/westernpacific/health-topics/cardiovascular-diseases (Accessed March 15, 2021).

Will, S., Hornigold, D. C., Baker, D. J., Coghlan, M. P., Mesquita, M., Trevaskis, J. L., et al. (2017). Gut Check on Diabesity: Leveraging Gut Mechanisms for the Treatment of Type 2 Diabetes and Obesity. *Curr. Opin. Pharmacol.* 37, 10–15. doi:10.1016/j.coph.2017.07.010

Willam, A., Aufy, M., Tzotzos, S., El-Malazi, D., Poser, F., Wagner, A., et al. (2017a). TnF Lectin-like Domain Restores Epithelial Sodium Channel Function in Frameshift Mutants Associated with Pseudohypoaldosteronism Type 1B. *Front. Immunol.* 8, 601. doi:10.3389/fimmu.2017.00601

Willam, A., Lemmens-Gruber, R., Tzotzos, S., Fischer, B., Shabbir, W., Lucas, R., et al. (2017b). *Cyclic Polypeptide for the Treatment of PHA Type 1B. Patent No WO 2017/046124*. Wien: APEPTICO Forschung und Entwicklung

Yeh, C.-Y., Schulien, A. J., Molyneaux, B. J., and Aizenman, E. (2020). Lessons from Recent Advances in Ischemic Stroke Management and Targeting Kv2.1 for Neuroprotection. *Int J Mol Sci.* 21, 6107–6124. doi:10.3390/ijms21176107

Yun, S. P., Kam, T.-I., Panicker, N., Kim, S., Oh, Y., Park, J.-S., et al. (2018). Block of A1 Astrocyte Conversion by Microglia Is Neuroprotective in Models of Parkinson's Disease. *Nat. Med.* 24, 931–938. doi:10.1038/s41591-018-0051-5

Zakariassen, H. L., John, L. M., and Lutz, T. A. (2020). Central Control of Energy Balance by Amylin and Calcitonin Receptor Agonists and Their Potential for Treatment of Metabolic Diseases. *Basic Clin. Pharmacol. Toxicol.* 127, 163–177. doi:10.1111/bcpt.13427

Zealand Pharma (2020). *Growing as a Leader in Peptide Therapeutics. Annual Report 2020*. Available at https://static1.squarespace.com/static/58983777d1758e28995640b4/t/604a1939ec446c62bceeeb6f/1615468866056/Annual+report+for+2020.pdf (Accessed June 4, 2021).

Zhao, L., Zhao, Q., Lu, R., Fu, Z., Zhu, Z., Jia, J., et al. (2008). Effects of Tyroserleutide on Gene Expression of Calmodulin and PI3K in Hepatocellular Carcinoma. *J. Cel. Biochem.* 103, 471–478. doi:10.1002/jcb.21409

Zimmer, R., Scherbarth, H. R., Rillo, O. L., Gomez-Reino, J. J., and Muller, S. (2013). Lupuzor/P140 Peptide in Patients with Systemic Lupus Erythematosus: a Randomised, Double-Blind, Placebo-Controlled Phase IIb Clinical Trial. *Ann. Rheum. Dis.* 72, 1830–1835. doi:10.1136/annrheumdis-2012-202460

Zimmermann, J., Obrecht, D., and Remus, T. (2019). Abstract A003: Anti-angiogenic Activity of the CXCR4 Antagonist Balixafortide. *Mol. Cancer Ther.* 18 (12 Supplment), A003. doi:10.1158/1535-7163.TARG-19-A003

Conflict of Interest: The authors declare that the research was conducted in the absence of any commercial or financial relationships that could be construed as a potential conflict of interest.

frontiers in Molecular Biosciences

ORIGINAL RESEARCH
published: 01 July 2021
doi: 10.3389/fmolb.2021.690429

Peptide Based Inhibitors of Protein Binding to the Mitogen-Activated Protein Kinase Docking Groove

Anita Alexa[1], Orsolya Ember[1,2], Ildikó Szabó[3], Yousef Mo'ath[2], Ádám L. Póti[1], Attila Reményi[1] and Zoltán Bánóczi[2]**

[1]*Biomolecular Interactions Laboratory, Institute of Organic Chemistry, Research Centre for Natural Sciences, Budapest, Hungary,* [2]*Department of Organic Chemistry, Institute of Chemistry, Eötvös Loránd University, Budapest, Hungary,* [3]*MTA-ELTE Research Group of Peptide Chemistry, Eötvös Loránd Research Network (ELKH), Eötvös L. University, Budapest, Hungary*

OPEN ACCESS

Edited by:
M. Angeles Jimenez, Instituto de Química Física Rocasolano (IQFR), Spain

Reviewed by:
Thomas John Brett, Washington University in St. Louis, United States
Steven T. Whitten, Texas State University, United States
Anirban Chakraborty, University of Texas Medical Branch at Galveston, United States

***Correspondence:**
Anita Alexa
alexa.anita@ttk.hu
Zoltán Bánóczi
zoltan.banoczi@ttk.elte.hu

Specialty section:
This article was submitted to Molecular Recognition, a section of the journal Frontiers in Molecular Biosciences

Received: *02 April 2021*
Accepted: *18 June 2021*
Published: *01 July 2021*

Citation:
Alexa A, Ember O, Szabó I, Mo'ath Y, Póti ÁL, Reményi A and Bánóczi Z (2021) Peptide Based Inhibitors of Protein Binding to the Mitogen-Activated Protein Kinase Docking Groove. Front. Mol. Biosci. 8:690429. doi: 10.3389/fmolb.2021.690429

Mitogen-activated protein kinases (MAPK) are important regulatory units in cells and they take part in the regulation of many cellular functions such as cell division, differentiation or apoptosis. All MAPKs have a shallow docking groove that interacts with linear binding motifs of their substrate proteins and their regulatory proteins such as kinases, phosphatases, scaffolds. Inhibition of these protein–protein interactions may reduce or abolish the activity of the targeted kinase. Based on the wide range of their biological activity, this kind of inhibition can be useful in the treatment of many disorders like tumors, inflammation or undesired cell apoptosis. In this study a linear binding motif from the RHDF1 protein—a 15 amino acids long peptide—was selected for optimization to increase its cellular uptake but retaining its low micromolar binding affinity. First, we synthesized an octaarginine conjugate that showed efficient cellular uptake. Next, we set out to reduce the size of this construct. We were able to decrease the length of the original peptide, and to increase its cellular uptake with specific chemical modifications. These new constructs bound better to ERK2 and p38 kinases than the original peptide and they showed markedly increased cellular uptake. The new octaarginine conjugate and one of the minimized bicyclic derivatives could inhibit the phosphorylation of intracellular ERK or p38. However, the modulation of MAPK phosphorylation levels by these cell-penetrating peptides were complex, despite that in biochemical assays they all inhibited MAPK-substrate binding as well as phosphorylation. The optimized peptides depending on the applied concentration caused an expected decrease, but also some unexpected increase in MAPK phosphorylation patterns in the cell. This possibly reflects the complexity of MAPK docking groove mediated protein–protein interactions including bone fide MAPK clients such activator kinases, deactivating phosphatases or regulatory scaffolds. Thus, our findings with optimized cell-penetrating "inhibitory" peptides highlight the opportunities but also the pitfalls of docking peptide based MAPK activity regulation and call for a better quantitative understanding of MAPK mediated protein–protein interactions in cells.

Keywords: mitogen-activated protein kinase, protein–protein interaction, peptide inhibitor, cellular uptake, cell-penetrating peptide

INTRODUCTION

Mitogen-activated protein kinases (MAPK) are key regulators of cellular signaling since they play crucial roles in many cellular processes like cell division and survival, differentiation, gene expression, apoptosis and stress-response (Cargnello and Roux, 2011). They are found in eukaryotic cells and are activated by their upstream kinases (mitogen-activated protein kinase kinases, MAPK kinases or MAPKKs) which were previously activated by mitogen-activated protein kinase kinase kinases, MAPKKKs). These kinases form a multi-tiered kinase cascade in which the specific interactions between the activating kinase and their substrate kinase are very important. The activating MAPKKs bind to the docking groove of the cognate MAPK with a specific short linear motif. These linear docking motifs are composed of 8–20 amino acids and have a loose consensus sequence. They contain basic and hydrophobic amino acids which bind to the Common Docking (CD) and hydrophobic region of the docking groove, respectively with a consensus sequence of Ψ (1–3) × (3–7) Φ ×, where Ψ, Φ and × mark positively charged, hydrophobic or any intervening residues, respectively. The docking grooves of paralogous MAPKs are similar but also distinct in a few key amino acid positions, therefore the consensus sequence of the docking motifs has both common and different features.

There are three main subfamilies of mammalian MAPKs: extracellular signal-regulated kinases (ERKs), p38 mitogen-activated protein kinases (p38s), and c-Jun N-terminal kinases (JNKs) (Pearson et al., 2001). ERKs are activated by mitogen signals, while p38s and JNKs by cellular stress (osmotic stress, heat shock) and inflammatory cytokines. The same surface of the MAPK's docking groove serves as the binding site for not only the activator kinases but also for their inactivating phosphatases, downstream substrates, and any signaling partners having these motifs. By inhibition of the interaction between MAPKs and their signaling partners we may potentially influence MAPK signaling. These MAPKs play important roles in many pathological events as tumor genesis and progression, metastasis formation and inflammatory processes. Thus, these protein–protein interactions (PPIs) are ideal therapeutic targets, but their inhibition is very challenging. Designing small molecule PPI inhibitors may be more difficult, because of a) the interaction happens *via* a big surface, bigger than in the case of other interactions (e.g., enzyme-substrate, ligand-receptor) (Smith and Gestwicki, 2012) b) these surfaces are commonly flat and there are only few grooves or deep pockets (Hopkins and Groom, 2002), c) there are no small endogenous ligands that could be used as a template for drug design. Although there are several successful small molecule inhibitors (Nero et al., 2014; Lu et al., 2020), larger compounds may be better to inhibit PPI's. One extensively studied family of this kind of molecules is peptides (Nevola and Giralt, 2015; Tsomaia, 2015). They have several advantages (Craik et al., 2013), and their higher selectivity toward protein targets may result in less side effects. They can be easily modified with unnatural amino acids that increases their biological and chemical diversity. Their metabolism results in amino acids that are non-toxic products. Unfortunately, they have some disadvantages too; lower metabolic stability, cell-permeability and oral availability. Peptides that can bind to a protein have specificity because of their well-defined structure in their protein domains. Unfortunately, short peptides related to these parts of the binding domains lose these specific secondary structures. There are many chemical approaches to avoid this "side-effect" of size reduction of biologically active protein domains (Nevola and Giralt, 2015; Tsomaia, 2015), for example by producing cyclic peptides (Lennard et al., 2019; Sarkar et al., 2020; González-Muñiz et al., 2021), macrocyclic peptides (Dougherty et al., 2017; Krüger et al., 2017; González-Muñiz et al., 2021), stapled peptides (Walensky et al., 2004; Dietrich et al., 2017; Jeganathan et al., 2019), or bicyclic peptides (Trinh et al., 2016). Because the RAS-ERK signaling pathway plays an important role in the development of many tumors, it is a promising target to develop therapeutically active molecules (García-Gómez et al., 2018). Therefore, there has been considerable interest in developing small molecule inhibitors that bind to the MAPK docking groove (Burkhard et al., 2009; Sammons et al., 2019). The first peptide that inhibited the activation of ERK was derived from its activator protein kinase MEK1 (Kelemen et al., 2001). This 12 amino acids long peptide corresponding to the N-terminus of MEK1 inhibited the activation of ERK *in vitro* and its cell-permeable derivative was effective in cells. Further peptides were identified as inhibitors in later studies (Bardwell et al., 2003; Ho et al., 2003; Gaestel and Kracht, 2009). The linear docking motifs that are used by MAPKs to increase their signaling specificity (Tanoue and Nishida, 2002; Reményi et al., 2006) may all be good candidates to develop PPI inhibitors. The structural requirements and the mode of binding of these linear docking motifs was described earlier (Garai et al., 2012) and was used to identify further motifs (Zeke et al., 2015). One of these motifs (its sequence: SLQRKKPPWLKLDIPS) found in the Inactive rhomboid protease 1 (RHDF1) showed strong binding to ERK2 (Zeke et al., 2015). Although these peptides can bind very selectively and sometimes strongly to their target proteins, there are often limitations of their use in cells, due to their lack of cell-permeability in particular. The cellular uptake of these peptides can be increased using cell-penetrating peptides, and these positively charged peptides are known to be able to deliver a wide range of cargos into the cytosol (Hudecz et al., 2005). In former studies, we used these peptides successfully to deliver small molecules (Miklán et al., 2007; Bánóczi et al., 2008b; Szabó et al., 2016) or peptides (Bánóczi et al., 2007; Bánóczi et al., 2008a; Világi et al., 2008) into cells or tissue.

In this study we present the structural optimization of the linear binding motif from RHDF1 which, in turn, led to the development of cell-permeable modulator of MAPK phosphorylation. The synthesis and biological characterization of its cell-penetrating conjugate and modified derivatives are described and our results indicate that the sequence can be reduced and modified to enhance cellular uptake without compromising, or even slightly improving, MAPK binding. These new peptides may internalize efficiently and can inhibit the PPIs between ERK2 or p38 and their substrates, therefore, they may be suitable to modify the ERK or p38 signaling pathways in cells.

MATERIALS AND METHODS

All amino acid derivatives, and Rink-amide MBHA resins were purchased from IRIS Biotech GmbH (Marktredwitz, Germany), whereas N,N-diisopropylethylamine (DIEA), 1-hydroxybenzotriazole (HOBt), N,N′-diisopropylcarbodiimide (DIC), trifluoroacetic acid (TFA), 1.8-diazabicyclo[5.4.0]undec-7-ene (DBU), thioanisole, 5(6)-carboxyfluorescein (Cf), triisopropylsilane (TIS) and 1,2-ethanedithiol were FLUKA (Buchs, Switzerland) and Sigma Aldrich (Budapest, Hungary) products. Dabcyl acid [4-((4-(dimethylamino)phenyl)azo) benzoic acid] was ordered from (AAT Bioquest, Inc., Sunnyvale, CA). Solvents for syntheses and purification were obtained from Molar Chemicals Kft (Budapest, Hungary). The buffers were prepared with ion exchanged distilled water.

Synthesis of Peptides

All peptides were synthesized manually on Rink-amide MBHA resin (0.3 g, 0.69 mmol/g) by Fmoc/^{t}Bu strategy as was described earlier (Szabó et al., 2016). After the cleavage of the last Fmoc protecting group peptide for conjugation was chloroacetylated on the free *N*-terminal α-amino group using the pentachlorophenyl ester of chloroacetic acid in 5 eqv. on resin for overnight. The Cf and Dabcyl group were attached to the *N*-terminal of peptides too *via* the α-amino group using their acid and HOBt-DIC coupling reagents. When the peptid contained both Cf and Dabcyl a Lys was incorporated into the *C*-terminal and Cf was coupled to its ε-amino group in solution (DMF) using DIC-HOBt coupling reagents in 1.1 eqv. to the peptide. The chloroacetylated peptides were cleaved from the resin with 5 mL TFA containing 0.375 g phenol, 0.25 mL distilled water and 0.25 mL TIS as scavengers. Peptides without chloroacetyl group were cleaved using the same mixture but 0.25 mL thioanisole and 0.125 mL 1,2-ethanedithiol were applied instead of TIS. Crude products were precipitated by dry diethyl-ether, dissolved in 10% acetic acid and freeze-dried. The peptides were purified by RP-HPLC on a semipreparative Phenomenex Jupiter C18 column (250 × 10 mm I.D.) with 10 μm silica (300 Å pore size). Flow rate was 4 mL/min. Linear gradient elution was applied.

Conjugation was carried out in TRIS buffer (0.1 M, pH = 8.2). The cysteine containing peptides were added slowly to the solution of chloroacetylated peptide. The conjugate was isolated from the reaction mixture by RP-HPLC after lyophilisation.

The cyclic peptides were prepared by the formation of thioether bond between chloroacetyl (on the side chain of lysine) and thiol (in the side chain of cysteine) group. During the peptide synthesis the Lys residue was protected with Dde. After the coupling of Dabcyl group to the *N*-terminal amino group the Dde group was cleaved on the resin by 2% hydrazine hydrate (5 min + 5 min) and the resin was washed with DMF (8 × 0.5 min). After the cleavage chloroacetyl group was attached to the side chain of lysine using 5 eqv. of chloroacetic acid pentachlorophenyl ester on resin and the peptide was cleaved from the resin using TFA cleavage mixture. The cyclic peptide was produced by dissolving the purified peptide precursor (1 mg/mL) in 0.1 M TRIS buffer (pH 8.1) and stirring overnight at room temperature. The reaction solution was then lyophilized, and purified on HPLC.

For the synthesis of bicyclic peptides linear precursor peptides were prepared with three cysteine residues. Then the purified peptides were reacted with thiol reactive linker tris(bromomethyl)benzene (TBMB). The precursor peptides were dissolved in 0.1 M TRIS buffer (pH 8.1), while TBMB (1.5 eqv) was dissolved in acetonitrile. Then the two solutions were combined and stirred overnight, the final concentration of the peptide was 1 mM. The reaction solution was then evaporated to remove acetonitrile and lyophilized. The crude product was purified by RP-HPLC.

The purified compounds were characterized by analytical RP-HPLC and ESI-MS (**Table 1** and **Supplementary Material**).

In Vitro Cell Culturing

HL-60 (ATCC® CCL-240™) human promyelocytic leukemia cells were grown in RPMI-1640 supplemented with 10% FCS (L)-glutamine (2 mM) and gentamicin (160 μg/mL). Cells were maintained in plastic tissue culture dishes at 37°C with a humidified atmosphere containing 5% CO_2/95% air.

HEK-293T (ATCC, CRL-3216) were cultured in Dulbecco's modified Eagle's medium (DMEM, Gibco) supplemented with 10% fetal bovine serum (FBS) and gentamicin (50 μg/mL) at 37°C in an atmosphere of 5% CO_2.

Cellular Uptake Profile of Compounds by Flow Cytometry and Confocal Microscopy

To study the cellular uptake of fluorescent labeled peptides and conjugate by flow cytometry, 10^5 HL-60 cells per well were plated on 24-well plates and were incubated for 24 h at 37°C. Then cells were treated with the solution of compounds in serum-free media for 90 min. The cellular uptake was analysed at 1, 5 and 10 μM concentrations. Cells treated with serum-free media were the control. At the end of incubation, treatment solutions were removed, and the cells were treated with 100 μL trypsin for 2 min to remove the membrane proteins in order to eliminate non-specific binding of conjugates. The effect of trypsin was terminated by 900 μL HPMI containing 10% fetal calf serum, and the cell suspensions were transferred into FACS-tubes. After centrifugation at 216*g* at 4°C for 5 min the supernatant was removed. Then cells were resuspended in 500 μl HPMI, and the intracellular fluorescence intensity of HL-60 cells was monitored (on channel FITC LP505; emission at λ = 505 nm; LP 505, BP 530/30) by flow cytometry (BD LSR II, BD Bioscience, San Jose, CA, equipped with 488 nm; Coherent Sapphire, 22 mW laser.) which is proportional to the cellular uptake. Data were analysed with FACSDiVa 5.0 software. Statistical analysis was done using two-sided independent Student's *t*-test.

The cellular uptake of the fluorescent labeled peptide into HEK-293T cells were analyzed by fluorescence microscopy (Cytation 3, BioTek Instruments) and two peptides were further examined by confocal laser scanning microscopy (Zeiss LSM-710 system). Cells were incubated with peptides in serum-free medium (DMEM) for 3 h at 37 °C and then washed twice with 200 μl of serum-free medium before analyzing.

TABLE 1 | Characterisation of peptides.

Sequence	Code	R_t[a]	ESI-MS[b]		K_d (μM) ± sd[c]/EC_{50} (μM)[d]	
			$M_{cal.}$	$M_{meas.}$	ERK2	p38
H-SLQRKKPPWLKLDIPSC-NH_2	**1**		2007.1	2006.4	**1.8 ± 0.3**	**1.1 ± 0.3**
H-SLQRKKPPWLKLDIPSC-NH_2 CH_2-*CO*-RRRRRRRR-NH_2	**2**	10.7	3315.0	3315.4	**0.6 ± 0.3**	**n.d.**
Cf-SLQRKKPPWLKLDIPSC-NH_2 CH_2-*CO*-RRRRRRRR-NH_2	**3**	14.2	3673.4	3673.9	**n.d.**	**n.d.**
H-KKPPWLKLDI-NH_2	**4**	12.2	1236.5	1236.3	**15.0 ± 1.1**	**n.d.**
H-RRPPWLRLDI-NH_2	**5**	12.8	1319.8	1319.9	**19.5 ± 2.6**	**10.0 ± 1.1**
H-RRPPWLRLDIRR-NH_2	**6**	11.4	1633.0	1632.6	**5.2 ± 1.4/12.9[d]**	**n.d./3.7[d]**
Cf-RRPPWLRLDIRR-NH_2	**7**	12.2	1991.3	1991.2	**n.d.**	**n.d.**
H-RRRPPWLRLDIRR-NH_2	**8**	10.8	1788.1	1788.1	**1.3 ± 0.1/3.5[d]**	**1.4 ± 0.3/1.3[d]**
Cf- RRRPPWLRLDIRR-NH_2	**9**	13.3	2146.4	2146.1	**n.d.**	**n.d.**
Dabcyl-RRRPPWLRLDIRRK-NH_2	**10**	13.3	2167.5	2167.3	**4.6 ± 0.6/8.3[d]**	**1.0 ± 0.4/3.1[d]**
Dabcyl-RRRPPWLRLDIRRK(*Cf*)-NH_2	**11**	14.7	2525.8	2526.4	**n.d.**	**n.d.**
Dabcyl-RRRPPWK — LRLDRRC -NH_2 *CO*-CH_2	**12**	13.8	2197.2	2197.2	**4.1 ± 0.3**	**1.7 ± 0.4**
Dabcyl-RRRKPPWLRLDRRC -NH_2 *CO*-CH_2	**13**	13.8	2197.2	2198.0	**1.0 ± 0.2**	**1.0 ± 0.7**
Dabcyl-KRRRPPWLRLDRRC -NH_2 *CO*-CH_2	**14**	13.8	2197.2	2198.0	**5.1 ± 0.4**	**2.1 ± 0.6**
Dabcyl-RRRKPPWLRLDIRRC -NH_2 *CO*-CH_2	**15**	14.2	2310.3	2310.4	**1.5 ± 0.3**	**1.2 ± 0.6**
SCH_2PhCH_2S CH_2S Dabcyl-RRRCPPWCLRLDIRRC	**16**	14.7	2462.3	2462.5	**0.9 ± 0.2**	**1.4 ± 0.4**
SCH_2PhCH_2S CH_2S Dabcyl-RRRC PPWCLRLDRRC	**17**	14.8	2349.2	2349.2	**4.5 ± 0.6**	**3.2 ± 0.7**

[a]*Analytical RP-HPLC was done on Nucleosil 120-3 C18 column (4.6 mm × 150 mm, 5 μm, 100 Å). The applied linear gradient elution was 0 min 0% B, 2 min 0% B, 22 min 90% B at 1 mL/min flow rate. The detection was carried on at λ = 220 nm.*

[b]*ESI-MS.*

[c]K_d *was determined by fluorescence polarization assay.*

[d]EC_{50} *values were determined by an* in vitro *MAPK activity assay, n.d. not determined.*

All experiments were carried out at least in 3 independent measurements (Rt, retention time; Cf, carboxafluresceine).

In vitro MAPK Binding and Activity Assays

ERK2 and p38 proteins used for fluorescence polarization (FP) measurements were recombinantly expressed in *Escherichia coli* and purified according to Garai et al. The purified and concentrated proteins were subjected to fluorescence polarization based binding measurements (Garai et al., 2012) using 50 nM Cf-labeled Cf-RHDF (Cf-SLQRKKPPWLKLDIPSC) and the data was analyzed using OriginPro. For direct measurements the concentration of ERK2 and p38 protein was increased, and for competitive measurements the protein-labeled peptide complex at 60–80% complex formation was titrated with increasing concentration of unlabeled peptide and the amount of the protein-labeled peptide complex (fraction bound) was determined using Cytation 3 (BioTek Instruments) plate reader in 384-well black plates. The direct measurement gives the K_d between the labeled peptide and the MAPK, while the competitive titration experiment with the unlabeled peptide gives the Ki for the unlabeled peptide competing off the labeled peptide, which is a good proxy for the binding affinity of the unlabeled peptide to the protein. All of the FP measurements were performed in assay buffer: 20 mM Tris (pH 8.0), 100 mM NaCl, 0.05% Brij35, and 2 mM TCEP. Fraction bound of the labeled ligand was calculated based on direct binding and competitive binding equations described in (Roehrl et al., 2004; Simon et al., 2020). The Kd and Ki values were obtained by fitting the FP data, measured in triplicates, to a direct binding equation or to a competitive binding equation using the OriginPro software.

In order to determine the inhibitory effect of RHDF-peptides, we used a protein fragment complementation based assay. MAPK

activity was monitored based on the association of two protein constructs containing a phoshorylated substrate reporter sequence including a MAPK docking motif or a phospho-binding domain, where these had an the *N*-terminal or *C*-terminal fragment of the Nanobit Luciferase enzyme as a fusion tag (Promega Nanobit® PPI Starter Systems). Upon MAPK activity, these two proteins bind and form the active luciferase enzyme oxidizing its substrate (coelenterazine) and ultimately giving some luminescent signal. The initial rates of the reactions were calculated and were compared for the applied inhibitor's concentration, and then EC_{50} values were determined using dose response fitting (OriginPro) (see in **Supplementary Figure S26**). Reactions were carried out in a buffer of 50 mM HEPES, pH 7.5, 100 mM NaCl, 5 mM $MgCl_2$, 0.05% IGEPAL, 50 μM Coelenterazine h, 5% glycerol, 2 mM DTT, 1mM TCEP, 0.5 mg/ml BSA containing 1 nM active ERK2 (pp-ERK2) or p38 (pp-p38α) and were started by the addition of 2 mM ATP. Luminescence was measured using a luminescence plate reader (Cytation 3, BioTek) in white 96-well plates.

MAPK Phosphorylation Levels in Cells by Western-Blot Analysis

To study the effect of peptides on the ERK pathway EGF stimulation and Western-blot analysis were used. HEK-293T cells were plated on 48-well plate and were serum-starved for overnight. Then cells were treated with the Cf-peptide at 20μM for 5 h in 100 μL DMEM and then stimulated by addition of EGF (Sigma, E9644) in 100 ng/mL concentration. Stimulation was terminated at different time points by adding 35 μL 4× SDS loading buffer. Cells were lysed and 10 μL of each sample was subjected to SDS-PAGE. The proteins of the SDS-gel were transferred to PVDF-membrane by Trans-Blot Turbo Transfer System (Bio-Rad) and the membrane was incubated first by phospho-p44/42 MAPK (ERK1/2) (Thr202/Tyr204) rabbit primery antibody (Cell Signaling, #9101) in 1:2,000 dilution and then with goat anti-rabbit HRP conjugated secondary antibody (Cell Signaling, #7074) in 1:5,000, and after stripping the membrane by anti-p44/42 MAPK (ERK1/2) mouse primary antibody (Cell Signaling, #4696) in 1:2,000 and then with goat anti-mouse HRP conjugated secondary antibody (Merck Milipore, 401215) in 1:10,000. Immobilon® ECL Ultra Western HRP Substrate reagent (Millipor, WBK L S0500) and Fluorchem FC2 gel documentation system (Alpha Innotech) were used for developing the membrane. The intensities of the protein bands were determined by densitometry and monitored after the stimulation in time. Later the effect of the most effective peptide (bicyclic peptide **16**) on the ERK and p38 pathway was examined by Western-blot. In this case HEKT cells were treated with several concentrations of the peptide and then were stimulated by 50 or 200 ng/ml EGF for studying ERK pathway, and 0.4 M Sorbitol for the p38-pathway. Sorbitol induces osmotic stress to the cells which generates activated p38-level (pp-p38), since p38 protein is one of the stress-sensor of the cell. After 10 min cells were lysed and subjected to SDS-PAGE and then subjected to Western-blot as earlier described. Activated (i.e., phosphorylated) ERK and p38 were detected by phospho-p44/42 MAPK (ERK1/2) (see above) and phospho-p38 MAPK (Thr180/Tyr182) rabbit primary antibody (Cell Signaling, #9215) in 1:2000 dilution, respectively. The total ERK and p38 content of the samples were determined by anti-p44/42 MAPK (ERK1/2) mouse primary antibody and anti-p38α MAPK mouse mAb (Cell Signaling, #9228), respectively. Anti-alfa-tubulin mouse mAb antibody (Sigma, T6199) in 1:10,000 was used for loading control. As secondary antibody anti-rabbit antibody (IRDye® 800CW Goat anti-Rabbit IgG, #926-32211) in 1:5,000 and secondary anti-mouse antibody (IRDye® 680CW Goat anti-Mouse IgG, #926-68070 in 1: 10,000 were used. Protein bands were detected and quantified with LI-COR Odyssey® Clx infrared imaging system. Statistical analysis was done using two-sided independent Student's *t*-test.

RESULTS

Design of Inhibitor Peptides

MAPKs are important regulatory proteins with dozens of substrates and they bind their substrates with docking motifs. The S^{1}LQRKKPPWLKLDIPS^{16} peptide (**1**) located in the RHDF1 protein is one of these linear binding motifs and can bind to ERK2 and p38 in their docking groove. The bound peptide may inhibit protein–protein interaction and thus blocks the activity of these MAPKs. Our purpose was to develop cell-permeable inhibitors based on the RHDF1 motif. In the first trial a conjugate of the native sequence (**2**) with octaarginine as a cell-penetrating tag was synthesized. Then optimization of the original sequence was carried out to increase intracellular stability and cellular uptake. To reduce the size of the original peptide, several amino acids were eliminated from both termini (**4**). For MAPK binding the Lys^{6}, Lys^{7}, Leu^{10} and Leu^{12} were found to be important (Zeke et al., 2015). The presence of Ile^{14} as the third interacting site in the hydrophobic groove is not mandatory but may enhance the strength of binding. Thus, in our first truncated construct the flanking regions ("SLQR" on *N*- and "PS" on *C*-terminus) were removed but all necessary amino acids and Ile^{14} were retained in the sequence. As the docking groove prefers both Lys and Arg, all lysine residues were replaced by arginine in the next step (**5**). This modification may increase the cellular uptake of the peptide. For efficient internalization there is a necessary number of Arg residues (Mitchell et al., 2000; Futaki et al., 2001), thus additional arginines were added to both termini to enhance the internalization of the peptide (**6, 8**). Finally, a Dabcyl group as internalization enhancer was attached to the *N*-terminus (**10**). To improve the *in vivo* stability of linear peptides cyclization is often used. However, cyclization may increase the specificity, too. Therefore, cyclic and bicyclic derivatives (**12–17**) were prepared. In some cyclic and bicyclic constructs the Ile^{14} was left out to study its effect on binding. In order to study the cellular uptake fluorescently labeled peptides were synthesized. In these constructs 5(6)-carboxyfluorescein (Cf) was attached to the *N*-terminus or to the ε-amino group of Lys at the *C*-terminus (**3**, **7**, **9** and **11**). All peptides were produced by solid phase peptide synthesis using Fmoc/*t*Bu strategy. Peptides were purified by RP-HPLC and

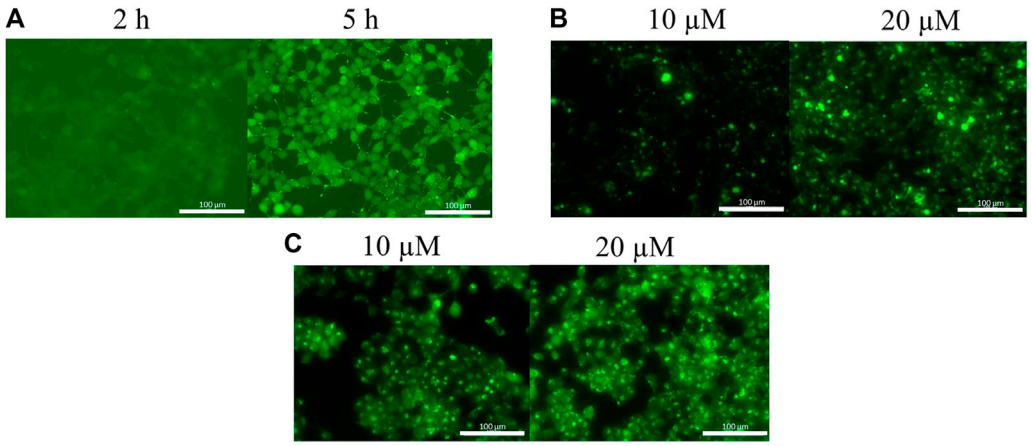

FIGURE 1 | Cellular uptake of peptides into HEK-293T cells. **(A)** *Cf*-RRRPPWLRLDIRR-NH_2 in 10 μM concentration, **(B)** *Cf*-RRRPPWLRLDIRR-NH_2 after 3 h, **(C)** *Dabcyl*-RRRPPWLRLDIRRK(*Cf*)-NH_2 after 3 h.

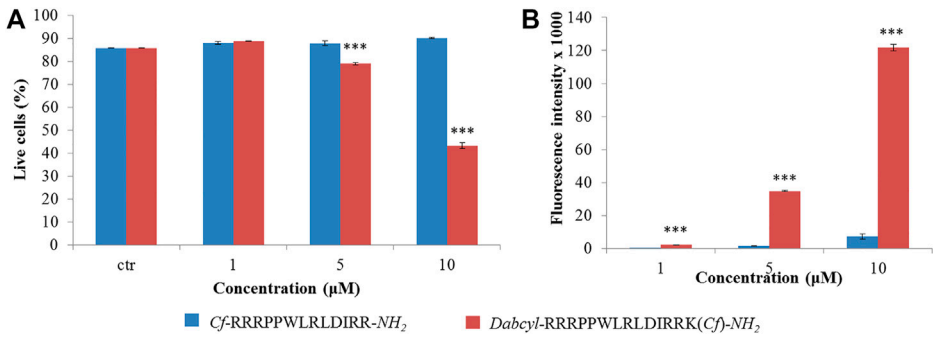

FIGURE 2 | Quantification of the internalization of *Cf*-RRRPPWLRLDIRR-NH_2 and *Dabcyl*-RRRPPWLRLDIRRK(*Cf*)-NH_2 into HL-60 cells by flow cytometry. The HL-60 cells were treated at different concentrations for 90 min and **(A)** the percent of live cells and **(B)** their average fluorescence intensity was determined by flow cytometry. Error bars show SD calculated based on three independent measurements. Statistical significance between the percent of live cells in the case of control and the peptide treated samples was determined with two-sided independent Student's *t*-test (***$p < 0.001$) **(A)**. Statistical significance between the internalization of two peptides was determined with two-sided independent Student's *t*-test (***$p < 0.001$) **(B)**.

characterized by analytical RP-HPLC and ESI-MS (**Table 1** and **Supplementary Material**).

Binding of Peptides to MAP Kinases

The binding of peptides was tested with two MAPKs, ERK2 and p38α. Fluorescently labeled RHDF-1 peptide was used as the binding partner of the MAPKs and fluorescence polarization was measured to calculate the binding constant. The binding affinity of peptides were determined in competitive binding assay (K_d or K_i) (**Table 1** and **Supplementary Figures S24,S25**). The conjugation of octaarginine, a cell-penetrating peptide (peptide **2**) slightly increased binding affinity. When the original peptide was shortened (**4**) its binding significantly decreased (8.3 times weaker). The substitution of Lys residues with arginines (**5**) resulted in no change in binding. Extension of the *C*-terminus by two Arg (**6**) enhanced the binding by 3.5 times; addition of one Arg to the *N*-terminus (**8**) further increased binding that became slightly better than that of the original sequence. The K_d value of cyclopeptides was dependent on the ring size. The best one was when the cycle contained all amino acids except of the positively charged *N*-terminus (three Arg residues) (**13**). The binding of this construct was one of the best and better than that of the original sequence. . It should be noted that the binding of cyclic peptides with (**15**) or without (**13**) Ile was the same. Based on these results bicyclic peptides with (**16**) or without (**17**) Ile were tested. In these cases the presence of Ile could increase the binding ability and this bicyclic peptide (**16**) showed the strongest binding to ERK2. The peptides bound to p38 similarly albeit with somewhat stronger K_d compared to ERK2 (with the exception of **16**).

As peptides could bind to both ERK2 and p38, their inhibitory effect on the activity of these enzymes was measured *in vitro* (**Table 1** and see **Supplementary Figure S26**). The EC_{50} was the lowest in case of the longest peptide that was extended by Arg residues at both termini (peptide **8**). Elimination of an Arg from the *N*-terminus (peptide **6**) reduced the inhibitory effect; its EC_{50} value was 3.7 times higher than that of the longer peptide (**8**).

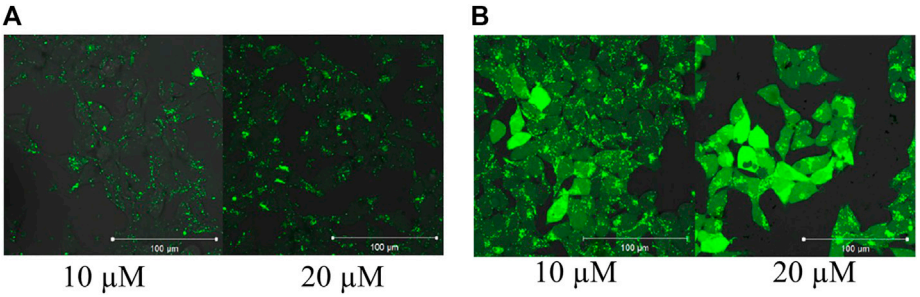

FIGURE 3 | Intracellular distribution of *Cf*-RRRPPWLRLDIRR-NH_2 and *Dabcyl*-RRRPPWLRLDIRRK(*Cf*)-NH_2 in HEK-293T cells. Cells were treated with 10 and 20 μM peptides for 3 h and the intracellular distribution of peptides was studied by fluorescence confocal microscopy.

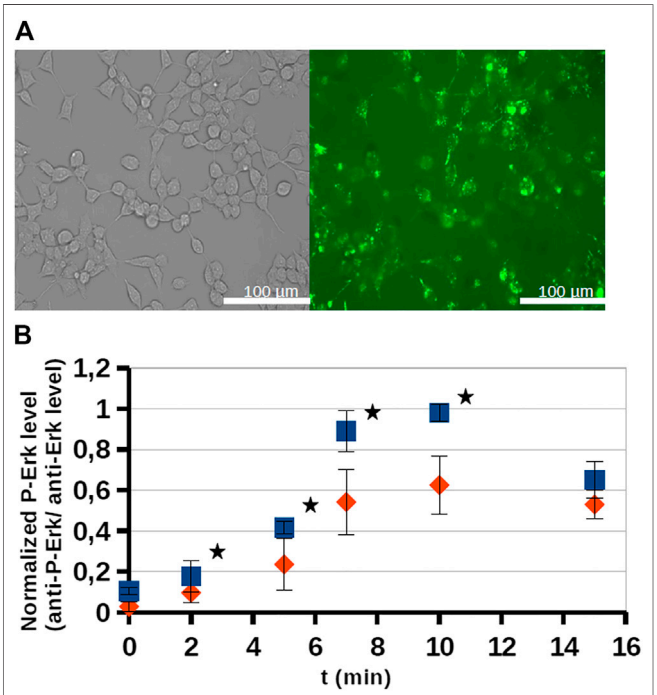

FIGURE 4 | Internalization and intracellular inhibitory activity of an octaarginine conjugate **(3).** The conjugate **(3)** treated cells (20 μM, 5 h) were analyzed by fluorescence microscopy **(A)**, or stimulated by EGF (100 ng/ml). The activity of ERK-pathway was followed by anti-P-ERK antibody using Western-blots **(B)**. The normalized phospho-ERK levels in untreated cells and peptide treated cells are labeled with blue and red, respectively. Error bars show SD calculated based on three independent measurements. * Indicates statistical significance between peptide-treated and control ($p < 0.05$ with two-sided independent Student's *t*-test).

Unfortunately, the attachment of Dabcyl group (peptide **10**) increased the EC_{50} value by 2.4 times. For ERK2, where the EC50 was measured parallel to the K_d for three peptides, we found that the best binding peptide had the lowest EC50 value, showing that binding affinity agrees with peptide mediated inhibition for this MAPK.

Cellular Uptake of Peptides and Conjugates

The uptake of the original peptide (**1**) and its shorter derivatives (**4** and **5**) was poor (data is not shown), but it could be enhanced by different modification, for example by additional arginine(s) (**7** and **9**) or a Dabcyl-group (**11**). When arginine residues were incorporated into the peptide at the *C*- (**Figure 1A**, peptide **7**) or at both termini (**Figure 1B**, peptide **9**) then time and concentration dependent internalization of peptides was noticeable. Addition of a Dabcyl-group to the *N*-terminus (**Figure 1C**, peptide **11**) increased the peptide internalization: cells had higher fluorescence intensity even at 10 μM concentration.

Because peptide **9** and **11** were the most effective based on fluorescence microscopy images, their internalization was further studied. Flow cytometry measurements were used to assess peptide internalization. HL-60 cells were treated by peptide **9** and **11** in 1, 5 and 10 μM concentrations for 90 min and the fluorescence intensity of cells was measured (**Figure 2**). The presence of live cells showed that the Dabcyl-containing peptide (**11**) affected cell viability at the two highest concentrations and the number of live cells decreased to 40% at 10 μM (**Figure 2A**). The fluorescence intensity of the Dabcyl-containing peptide at 1, 5 and 10 μM was 9.2, 23.5 and 16.9 times higher, respectively (**Figure 2B**).

When the internalization of the two peptides was confirmed by fluorescence microscopy, their intracellular distribution was examined. HEK-293T cells were treated with the solution of peptide **9** and **11** for 3 h and analyzed by fluorescence confocal microscopy (**Figure 3**). This analysis showed that the Dabcyl-group affected the peptide internalization pathway. Without the Dabcyl-group the peptide went through the cell membrane only *via* endocytosis since its intracellular distribution was punctuated (**Figure 3A**). The Dabcyl-group containing peptide showed a more diffuse distribution even at 10 μM which was further increased at 20 μM concentration (**Figure 3B**).

Inhibition of Intracellular ERK or p38 by an Octaarginine Conjugate and a Bicyclic Peptide

The effect of an octaarginine conjugate (**3**) on intracellular activity of ERK was studied on HEK-293T cells. First, the internalization of the conjugate was studied by fluorescence

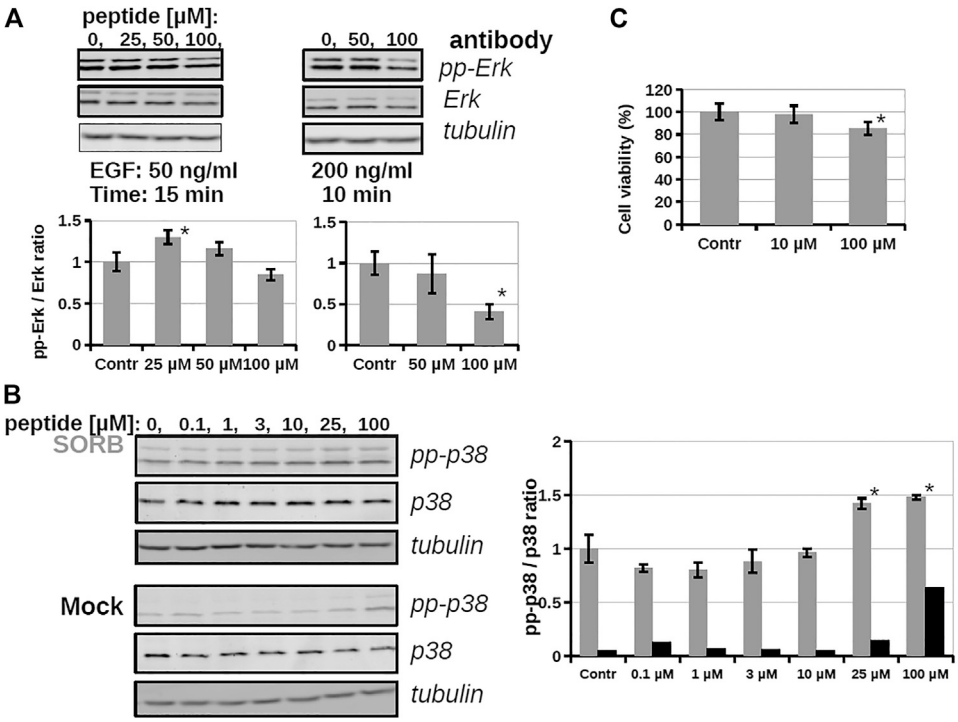

FIGURE 5 | The effect of a bicyclic peptide (16) on ERK and p38 pathways. **(A)** Serum-starved HEKT cells were pre-treated with 0, 25, 50, 100 μM peptide **16** for 2 h, and then stimulated by 50 ng/ml EGF for 15 min or 200 ng/ml EGF for 10 min. Samples were subjected to Western-blot analysis; activity of the ERK pathway was followed by anti-pp-ERK and anti-ERK antibody; anti-tubulin antibody was used as load control and demonstrates equal sample load in addition to the anti-ERK Western-blot signal. Bar charts show the ppERK2/ERK2 intensity ratio of each sample. **(B)** Serum-starved HEKT cells were pre-treated with the peptide **16** at 0.1, 1, 3, 10, 25, 100 μM for 1 h and then stimulated by 0.4 M Sorbitol for 10 min (upper panel) or treated only with the medium (lower panel; Mock). p38 activation was confirmed by using anti-pp-p38 antibody, and the total p38 amount of the samples by using the anti-p38 antibody. The graph shows the pp-p38/p38 intensity ratio of each band obtained from the densitometry of Western-blots in the case of Sorbitol (in grey) or medium (Mock; in black) treatment **(C)** Cell viability test with peptide **16**. HEKT cells were incubated with the peptide at 10 and 100 μM for 24 h, then the viability of cells was determined by PrestoBlue™ reagent according to the manufacturer's instructions (ThermoFisher Scientific, #A13261). Note that peptide incubation times before stimulation was only up to 2 h at maximun on Panel A and B. Error bars show SD of 3 independent measurements. *Indicates statistical significance between peptide-treated and control ($p < 0.05$ with two-sided independent Student's *t*-test).

microscopy (**Figure 4A**). It showed internalization after 5 h of treatment at 5 μM concentration.

As the conjugate could internalize into cells, its inhibitory effect on intracellular ERK activity was analyzed by using Western-blots (**Figure 4B**). The cells were stimulated by EGF and the time dependent phosphorylation of ERK1/2 was followed. After EGF stimulation phosphoERK levels normally increase (0–10 min), which at later time points (30–60 min) return to baseline (not shown). When the cells were pre-treated by conjugate **3** (20 μM, 5 h) some reduction was observed in the amount of phosphorylated ERK, meaning that the active form of ERK decreased and indicating that the conjugate attenuated ERK activation. In the case of the most active derivative (bicyclic peptide **16**) HEK-293T cells were pre-treated with the solution of inhibitor peptide (**16**) at 10, 25, 50, and 100 μM concentrations and cells were stimulated with EGF at 50 ng/ml for 15 min (**Figure 5A**), or with EGF at 200 ng/ml for 10 min. Unexpectedly, peptide **16** increased the phosphorylation of ERK at low concentration (with 30 and 16% at 25 and 50 μM, respectively) and inhibitory activity (15%) was detected only at the highest concentration (100 μM) at 50 ng/ml EGF and 60% at 200 ng/ml EGF. When the inhibition of intracellular p38 was studied the pre-treatment with peptide **16** (0.1, 1, 3, 10, 25, 100 μM) was for 1 h and we applied stimulation with sorbitol for 10 min. The effect of peptide **16** on p38 was somewhat different compared to on ERK1/2 (**Figure 5B**). At low concentration it inhibited the phosphorylation of p38 (with 18, 20, 12, 4% at 0.1, 1, 3, and 10 μM, respectively), but there was high increase in the phosphorylation of p38 at 25 μM, which was slightly enhanced further at 100 μM, with 42 and 48%, respectively. It is noteworthy, that pre-treatment with these peptides had only marginal effects on cell viability, which, however, was only apparent after long incubation (for 24 h, as shown on **Figure 5C**).

DISCUSSION

MAPKs are important components of intracellular signaling pathways and thus they are responsible for many biological process in cells (Cargnello and Roux, 2011). Their aberrant functions are crucial in many pathological symptoms. Development of inhibitors against them, and thus to attenuate

their effect in pathological alterations, has turned out to be challenging so far. The most applied strategy, inhibition of kinase activity *via* blocking ATP binding has several limitations. One of them is limited selectivity because of the high homology of ATP binding sites in different families of kinases (Knight and Shokat, 2005). Blocking the interaction of these kinases with their substrates can be a potent strategy to get selective inhibitors. The substrates of MAPKs contain docking motifs to bind to the kinase and this protein–protein interaction results in selectivity in downstream signaling. Many motifs were identified in various kinases and one of them was a sequence from the *N*-terminal part of RHDF1 protein. This peptide—SLQRKKPPWLKLDIPS—showed strong ERK2 and p38 binding (Zeke et al., 2015). This peptide was selected to develop new MAPK based inhibitor(s). In this systematic study our purpose was to develop efficient and cell permeable inhibitor peptide(s) based on the original sequence. As this sequence has good binding ability (K_d = 1.8 μM, **Table 1**) the first approach was to provide them with cell-penetrating tags to improve cellular uptake. These peptides were used successfully to develop cell-permeable MAPK inhibitor peptides (Kelemen et al., 2001; Fu et al., 2008; Gaestel and Kracht, 2009). Octaarginine was selected to deliver the peptide into cells, because it has been successfully used by us to deliver peptides into cells (Bánóczi et al., 2007; Bánóczi et al., 2008a; Világi et al., 2008). The conjugate retained MAPK binding ability and could penetrate into cells and had some inhibitory effect on the ERK pathway (**Figure 4**). Our hypothesis was that the low cellular stability may reduce the applicability of this construct. Thus, our interest turned toward the optimization of the binding peptide sequence, its cell-penetration and its in-cell stability. First the size of the peptide was reduced. The data suggested that despite that the flanking regions (SLQR and PS) may not act in binding directly based on available structural models of MAPK-docking motif complexes, they have some roles in it (**Table 1**). A short peptide (**4**) without these flanking regions showed weaker binding. To enhance cellular internalization of peptides, Lys-Arg substitutions were done (**5**) as it was proved that Arg residue(s) has high impact on cell penetration (Mitchell et al., 2000). This modification only slightly reduced binding *in vitro*. Based on these findings extension of both termini with Arg residues was done. While the number of Arg has a lower limit for efficient internalization (Mitchell et al., 2000; Futaki et al., 2001), there is high flexibility in their position (Futaki et al., 2002). The extension of the *C*-terminus with two Arg residues (**6**) induced stronger binding and the addition of an extra Arg to the *C*-terminus (**8**) resulted in the same binding as that of the original sequence. In addition to increased binding these peptides showed increased cellular uptake in HEK-293T cells. Because our latest findings showed that the Dabcyl-group may dramatically increase the internalization of oligoarginines this chromophore group was attached to the *N*-terminal amino group of peptide **8**. Coupling of this group (peptide **10**) slightly attenuated binding, but its fluorescent derivative (peptide **11**) had improved internalization ability into HL-60 and HEK-293T cells (**Figure 2D** and **Figures 3**, **4**). Its internalization was 10–24 times higher at different concentrations compared to the peptide without the Dabcyl-group. To improve the binding of peptide **10**, several cyclic and bicyclic peptide derivatives were synthesized. There are many examples where cyclic or bicyclic peptides were used as efficient PPI inhibitors (Cardote and Ciulli, 2016; Lennard et al., 2019; Colarusso et al., 2020). First, a medium sized cyclic peptide was made, where the hydrophobic binding region and the spacer sequence (**15**) was cyclized. This cyclic peptide had the same binding as the original peptide, suggesting that cyclization resulted in a structure that is compatible with binding. Next, the same cyclic derivative (**13**) without Ile^{14} was tested. This Ile may promote binding but it is not necessary for it. Our idea was that the cyclization may be enough for binding and the peptide can be shortened. Indeed, this shorter cyclic peptide (**13**) had a slightly better binding. The different size of the cycle may change the structure and the flexibility of the cyclic peptide. When only the region that is responsible for binding to the hydrophobic docking groove was cyclized (**12**) a smaller cyclic peptide was formed, likely having a more rigid structure. When all amino acids were in the cycle (**14**), the structural flexibility was presumably increased. Both cyclic peptides were designed without Ile^{14}. As both peptides had decreased binding ability, we could conclude that these cycles do not close the peptide into the proper structure. In the final attempt bicyclic peptides (**16** and **17**) were prepared. These peptides were designed on the basis of the best cyclic form (**13**), but instead of one cycle, the two parts of the peptide—the binding and spacer regions—were incorporated into two different loops. In these constructs the role of Ile^{14} was also examined. Interestingly, the bicyclic peptide with Ile^{14} (**16**) was more effective than the bicyclic peptide without Ile^{14} (**17**). This may suggest that in case of a more rigid structure the extra hydrophobic amino acid (Ile^{14}) could promote stronger interaction with the enzyme. It is noteworthy that only the best bicyclic peptide showed stronger binding to ERK2 than to p38. Cyclization can increase the stability of the peptides *in vivo*, suggesting that the bicyclic construct can be stable enough to have inhibitory activity on the intracellular activity of ERK2 or p38. Peptide **16** indeed affected ERK and p38 phosphorylation levels in cells, but our results also showed that it is not straightforward to predict the impact of cell-penetrating docking motif containing peptides on these signaling pathways. There are many interaction partners of these proteins in the cell which can all compete with each other and with the peptides for binding the MAPK docking. Further complexity comes from the fact that some of the MAPK partners are activators (MAPK kinases), others are deactivators (phosphatases) or regulatory proteins (scaffolds) and the relative concentration of all these—in comparison to the "inhibitory" MAPK docking groove targeting peptide's intracellular concentration—will collectively determine the final output. For example, **Figure 5** shows that peptide **16** at 100 μM has greater inhibitory effect at higher EGF concentration, because the relative concentrations of the interaction partners are different. In the case of p38 pathway activation by sorbitol, the inhibitory effect of peptide **16** was observed at low concentration only, but at higher concentrations the peptide enhanced p38 activation. In addition, the peptide in unstimulated cells (**Figure 5**, Mock) increased the p38 phosphorylation level, possibly because that peptide interferes with the binding of negative regulators such as

phosphatases in the resting state, too. A biological parable that demonstrates the complexity of MAPK docking is the case of the so-called "sevenmaker" mutation in the ERK2 MAPK docking groove (D319N). This mutation affects an important docking groove residue and causes elevated ERK2 pathway output in cells because the docking of phosphatases to this mutant is more affected than the binding of upstream activators or downstream substrates (Bott et al., 1994). This "biological" example shows that selective and engineered perturbation of this complex PPI system is conceptually possible but it also suggests that the impact of docking based "inhibitory" peptides on MAPK signaling pathways in cells could be more complex than simple blocking of MAPK phosphorylation. This provides challenges but also opportunities for MAPK activity modulation.

DATA AVAILABILITY STATEMENT

The original contributions presented in the study are included in the article/**Supplementary Material**, further inquiries can be directed to the corresponding authors.

AUTHOR CONTRIBUTIONS

AA carried out protein-peptide binding and biological assays, planned the experiments, and wrote the article. OE synthesized peptides, performed biological assays, and prepared figures. IS did the flow cytometry experiments and wrote the article. YM synthesized cyclic and bicyclic peptides. ÁP developed *in vitro* MAPK activity assays. AR analyzed and evaluated experimental data, and wrote the article. ZB synthesized peptides and conjugates, planned the experiment, and wrote the article.

FUNDING

The work was supported by the ELTE Thematic Excellence Programme 2020 supported by National Research, Development and Innovation Office—TKP2020-IKA-05 (to ZB), KKP 126963, VEKOP-2.3.3-15-2016-00011, FIEK16-1-2016-0005, the Tempus Public Foundation for the Stipendium Hungaricum Scholarship funding (to YM) and a Grant from the MedInProt project of the Hungarian Academy of Sciences (to AA and ZB). We thank Bálint Szeder for helping with confocal microscopy.

SUPPLEMENTARY MATERIAL

The Supplementary Material for this article can be found online at: https://www.frontiersin.org/articles/10.3389/fmolb.2021.690429/full#supplementary-material

REFERENCES

Bánóczi, Z., Alexa, A., Farkas, A., Friedrich, P., and Hudecz, F. (2008a). Novel Cell-Penetrating Calpain Substrate. *Bioconjug. Chem.* 19, 1375–1381. doi:10.1021/bc800021y

Bánóczi, Z., Peregi, B., Orbán, E., Szabó, R., and Hudecz, F. (2008b). Synthesis of Daunomycin-Oligoarginine Conjugates and Their Effect on Human Leukemia Cells (HL-60). Arkivoc *Part (iii)* 2008, 140–153. doi:10.3998/ark.5550190.0009.313

Bánóczi, Z., Tantos, Á., Farkas, A., Tompa, P., Friedrich, P., and Hudecz, F. (2007). Synthesis of Cell-Penetrating Conjugates of Calpain Activator Peptides. *Bioconjug. Chem.* 18, 130–137. doi:10.1021/bc0601976

Bardwell, A. J., Abdollahi, M., and Bardwell, L. (2003). Docking Sites on Mitogen-Activated Protein Kinase (MAPK) Kinases, MAPK Phosphatases and the Elk-1 Transcription Factor Compete for MAPK Binding and Are Crucial for Enzymic Activity. *Biochem. J.* 370, 1077–1085. doi:10.1042/BJ20021806

Bott, C. M., Thorneycroft, S. G., and Marshall, C. J. (1994). The Sevenmaker Gain-Of-Function Mutation in P42 MAP Kinase Leads to Enhanced Signalling and Reduced Sensitivity to Dual Specificity Phosphatase Action. *FEBS Lett.* 352, 201–205. doi:10.1016/0014-5793(94)00958-9

Burkhard, K., Smith, S., Deshmukh, R., MacKerell, A., Jr., and Shapiro, P. (2009). Development of Extracellular Signal-Regulated Kinase Inhibitors. *Ctmc* 9, 678–689. doi:10.2174/156802609789044416

Cardote, T. A. F., and Ciulli, A. (2016). Cyclic and Macrocyclic Peptides as Chemical Tools to Recognise Protein Surfaces and Probe Protein–Protein Interactions. *ChemMedChem.* 11, 787–794. doi:10.1002/cmdc.201500450

Cargnello, M., and Roux, P. P. (2011). Activation and Function of the MAPKs and Their Substrates, the MAPK-Activated Protein Kinases. *Microbiol. Mol. Biol. Rev.* 75, 50–83. doi:10.1128/mmbr.00031-10

Colarusso, S., De Simone, D., Frattarelli, T., Andreini, M., Cerretani, M., Missineo, A., et al. (2020). Optimization of Linear and Cyclic Peptide Inhibitors of KEAP1-NRF2 Protein-Protein Interaction. *Bioorg. Med. Chem.* 28, 115738. doi:10.1016/j.bmc.2020.115738

Craik, D. J., Fairlie, D. P., Liras, S., and Price, D. (2013). The Future of Peptide-Based Drugs. *Chem. Biol. Drug Des.* 81, 136–147. doi:10.1111/cbdd.12055

Dietrich, L., Rathmer, B., Ewan, K., Bange, T., Heinrichs, S., Dale, T. C., et al. (2017). Cell Permeable Stapled Peptide Inhibitor of Wnt Signaling that Targets β-Catenin Protein–Protein Interactions. *Cel Chem. Biol.* 24, 958–968.e5. doi:10.1016/j.chembiol.2017.06.013

Dougherty, P. G., Qian, Z., and Pei, D. (2017). Macrocycles as Protein-Protein Interaction Inhibitors. *Biochem. J.* 474, 1109–1125. doi:10.1042/BCJ20160619

Fu, J., Meng, X., He, J., and Gu, J. (2008). Inhibition of Inflammation by a P38 MAP Kinase Targeted Cell Permeable Peptide. *Mc* 4, 597–604. doi:10.2174/157340608786242106

Futaki, S., Nakase, I., Suzuki, T., Zhang, Z., and Sugiura, Y. (2002). Translocation of Branched-Chain Arginine Peptides through Cell Membranes: Flexibility in the Spatial Disposition of Positive Charges in Membrane-Permeable Peptides†. *Biochemistry* 41, 7925–7930. doi:10.1021/bi0256173

Futaki, S., Suzuki, T., Ohashi, W., Yagami, T., Tanaka, S., Ueda, K., et al. (2001). Arginine-rich Peptides. *J. Biol. Chem.* 276, 5836–5840. doi:10.1074/jbc.M007540200

Gaestel, M., and Kracht, M. (2009). Peptides as Signaling Inhibitors for Mammalian MAP Kinase Cascades. *Cpd* 15, 2471–2480. doi:10.2174/138161209788682299

Garai, A., Zeke, A., Gógl, G., Töro, I., Fördos, F., Blankenburg, H., et al. (2012). Specificity of Linear Motifs that Bind to a Common Mitogen-Activated Protein Kinase Docking Groove. *Sci. Signaling* 5, ra74. doi:10.1126/scisignal.2003004

García-Gómez, R., Bustelo, X. R., and Crespo, P. (2018). Protein–Protein Interactions: Emerging Oncotargets in the RAS-ERK Pathway. *Trends Cancer* 4, 616–633. doi:10.1016/j.trecan.2018.07.002

González-Muñiz, R., Bonache, M. Á., Pérez de Vega, M. J., Prokai-Tatrai, K., C Gomes, P. A., Galdiero, S., et al. (2021). Modulating Protein–Protein Interactions by Cyclic and Macrocyclic Peptides. Prominent Strategies and Examples. *Molecules* 26, 445. doi:10.3390/molecules26020445

Ho, D. T., Bardwell, A. J., Abdollahi, M., and Bardwell, L. (2003). A Docking Site in MKK4 Mediates High Affinity Binding to JNK MAPKs and Competes with

Similar Docking Sites in JNK Substrates. *J. Biol. Chem.* 278, 32662–32672. doi:10.1074/jbc.M304229200

Hopkins, A. L., and Groom, C. R. (2002). The Druggable Genome. *Nat. Rev. Drug Discov.* 1, 727–730. doi:10.1038/nrd892

Hudecz, F., Bánóczi, Z., and Csík, G. (2005). Medium-sized Peptides as Built in Carriers for Biologically Active Compounds. *Med. Res. Rev.* 25, 679–736. doi:10.1002/med.20034

Jeganathan, S., Wendt, M., Kiehstaller, S., Brancaccio, D., Kuepper, A., Pospiech, N., et al. (2019). Constrained Peptides with Fine-Tuned Flexibility Inhibit NF-Y Transcription Factor Assembly. *Angew. Chem. Int. Ed.* 58, 17351–17358. doi:10.1002/anie.201907901

Kelemen, B. R., Hsiao, K., and Goueli, S. A. (2002). Selective *In Vivo* Inhibition of Mitogen-Activated Protein Kinase Activation Using Cell-Permeable Peptides, *J. Biol. Chem.* 277, 8741, 8748. doi:10.1074/jbc.M108459200

Knight, Z. A., and Shokat, K. M. (2005). Features of Selective Kinase Inhibitors. *Chem. Biol.* 12, 621–637. doi:10.1016/j.chembiol.2005.04.011

Krüger, D. M., Glas, A., Bier, D., Pospiech, N., Wallraven, K., Dietrich, L., et al. (2017). Structure-Based Design of Non-natural Macrocyclic Peptides that Inhibit Protein–Protein Interactions. *J. Med. Chem.* 60, 8982–8988. doi:10.1021/acs.jmedchem.7b01221

Lennard, K. R., Gardner, R. M., Doigneaux, C., Castillo, F., and Tavassoli, A. (2019). Development of a Cyclic Peptide Inhibitor of the P6/UEV Protein–Protein Interaction. *ACS Chem. Biol.* 14, 1874–1878. doi:10.1021/acschembio.9b00627

Lu, H., Zhou, Q., He, J., Jiang, Z., Peng, C., Tong, R., et al. (2020). Recent Advances in the Development of Protein-Protein Interactions Modulators: Mechanisms and Clinical Trials. *Sig Transduct Target. Ther.* 5, 1–23. doi:10.1038/s41392-020-00315-3

Miklán, Z., Szabó, R., Zsoldos-Mády, V., Reményi, J., Bánóczi, Z., and Hudecz, F. (2007). New Ferrocene Containing Peptide Conjugates: Synthesis and Effect on Human Leukemia (HL-60) Cells. *Biopolymers* 88, 108–114. doi:10.1002/bip.20696

Mitchell, D. J., Steinman, L., Kim, D. T., Fathman, C. G., and Rothbard, J. B. (2000). Polyarginine Enters Cells More Efficiently Than Other Polycationic Homopolymers. *J. Pept. Res.* 56, 318–325. doi:10.1034/j.1399-3011.2000.00723.x

Nero, T. L., Morton, C. J., Holien, J. K., Wielens, J., and Parker, M. W. (2014). Oncogenic Protein Interfaces: Small Molecules, Big Challenges. *Nat. Rev. Cancer* 14, 248–262. doi:10.1038/nrc3690

Nevola, L., and Giralt, E. (2015). Modulating Protein-Protein Interactions: The Potential of Peptides. *Chem. Commun.* 51, 3302–3315. doi:10.1039/c4cc08565e

Pearson, G., Robinson, F., Beers Gibson, T., Xu, B.-e., Karandikar, M., Berman, K., et al. (2001). Mitogen-Activated Protein (MAP) Kinase Pathways: Regulation and Physiological Functions*. *Endocr. Rev.* 22, 153–183. doi:10.1210/edrv.22.2.0428

Reményi, A., Good, M. C., and Lim, W. A. (2006). Docking Interactions in Protein Kinase and Phosphatase Networks. *Curr. Opin. Struct. Biol.* 16, 676–685. doi:10.1016/j.sbi.2006.10.008

Roehrl, M. H. A., Wang, J. Y., and Wagner, G. (2004). A General Framework for Development and Data Analysis of Competitive High-Throughput Screens for Small-Molecule Inhibitors of Protein–Protein Interactions by Fluorescence Polarization†. *Biochemistry* 43, 16056–16066. doi:10.1021/bi048233g

Sammons, R. M., Perry, N. A., Li, Y., Cho, E. J., Piserchio, A., Zamora-Olivares, D. P., et al. (2019). A Novel Class of Common Docking Domain Inhibitors that Prevent ERK2 Activation and Substrate Phosphorylation. *ACS Chem. Biol.* 14, 1183–1194. doi:10.1021/acschembio.9b00093

Sarkar, P., Li, Z., Ren, W., Wang, S., Shao, S., Sun, J., et al. (2020). Inhibiting Matrix Metalloproteinase-2 Activation by Perturbing Protein–Protein Interactions Using a Cyclic Peptide. *J. Med. Chem.* 63, 6979–6990. doi:10.1021/acs.jmedchem.0c00180

Simon, M. A., Ecsédi, P., Kovács, G. M., Póti, Á. L., Reményi, A., Kardos, J., et al. (2020). High-throughput Competitive Fluorescence Polarization Assay Reveals Functional Redundancy in the S100 Protein Family. *FEBS J.* 287, 2834–2846. doi:10.1111/febs.15175

Smith, M. C., and Gestwicki, J. E. (2012). Features of Protein–Protein Interactions that Translate into Potent Inhibitors: Topology, Surface Area and Affinity. *Expert Rev. Mol. Med.* 14, e16. doi:10.1017/erm.2012.10

Szabó, I., Orbán, E., Schlosser, G., Hudecz, F., and Bánóczi, Z. (2016). Cell-penetrating Conjugates of Pentaglutamylated Methotrexate as Potential Anticancer Drugs against Resistant Tumor Cells. *Eur. J. Med. Chem.* 115, 361–368. doi:10.1016/j.ejmech.2016.03.034

Tanoue, T., and Nishida, E. (2002). Docking Interactions in the Mitogen-Activated Protein Kinase Cascades. *Pharmacol Ther.* 93, 193–202. doi:10.1016/S0163-7258(02)00188-2

Trinh, T. B., Upadhyaya, P., Qian, Z., and Pei, D. (2016). Discovery of a Direct Ras Inhibitor by Screening a Combinatorial Library of Cell-Permeable Bicyclic Peptides. *ACS Comb. Sci.* 18, 75–85. doi:10.1021/acscombsci.5b00164

Tsomaia, N. (2015). Peptide Therapeutics: Targeting the Undruggable Space. *Eur. J. Med. Chem.* 94, 459–470. doi:10.1016/j.ejmech.2015.01.014

Világi, I., Kiss, D. S., Farkas, A., Borbély, S., Tárnok, K., Halasy, K., et al. (2008). Synthetic Calpain Activator Boosts Neuronal Excitability without Extra Ca2+. *Mol. Cell Neurosci.* 38, 629–636. doi:10.1016/j.mcn.2008.05.012

Walensky, L. D., Kung, A. L., Escher, I., Malia, T. J., Barbuto, S., Wright, R. D., et al. (2004). Activation of Apoptosis *In Vivo* by a Hydrocarbon-Stapled BH3 helix. *Science* 305, 1466–1470. doi:10.1126/science.1099191

Zeke, A., Bastys, T., Alexa, A., Garai, Á., Mészáros, B., Kirsch, K., et al. (2015). Systematic Discovery of Linear Binding Motifs Targeting an Ancient Protein Interaction Surface on MAP Kinases. *Mol. Syst. Biol.* 11, 837. doi:10.15252/msb.20156269

Conflict of Interest: The authors declare that the research was conducted in the absence of any commercial or financial relationships that could be construed as a potential conflict of interest.

frontiers in Molecular Biosciences

MINI REVIEW
published: 21 July 2021
doi: 10.3389/fmolb.2021.703715

Peptide-Based Inhibitors of ADAM and ADAMTS Metalloproteinases

Stefano Pluda[1,2†], *Ylenia Mazzocato*[1†] *and Alessandro Angelini*[1,3*]

[1]Department of Molecular Sciences and Nanosystems, Ca' Foscari University of Venice, Venice, Italy, [2]Fidia Farmaceutici S.p.A., Abano Terme, Italy, [3]European Centre for Living Technology (ECLT), Venice, Italy

ADAM and ADAMTS are two large metalloproteinase families involved in numerous physiological processes, such as shedding of cell-surface protein ectodomains and extra-cellular matrix remodelling. Aberrant expression or dysregulation of ADAMs and ADAMTSs activity has been linked to several pathologies including cancer, inflammatory, neurodegenerative and cardiovascular diseases. Inhibition of ADAM and ADAMTS metalloproteinases have been attempted using various small molecules and protein-based therapeutics, each with their advantages and disadvantages. While most of these molecular formats have already been described in detail elsewhere, this mini review focuses solely on peptide-based inhibitors, an emerging class of therapeutic molecules recently applied against some ADAM and ADAMTS members. We describe both linear and cyclic peptide-based inhibitors which have been developed using different approaches ranging from traditional medicinal chemistry and rational design strategies to novel combinatorial peptide-display technologies.

Keywords: A-disintegrin and metalloproteinase (ADAM), A-disintegrin and metalloproteinase with thrombospondin motifs (ADAMTS), metalloproteinase, peptide inhibitors, linear peptides, cyclic peptides, macrocycles

OPEN ACCESS

Edited by:
Laura Belvisi,
University of Milan, Italy

Reviewed by:
Steven. T Whitten,
Texas State University, United States
Thomas John Brett,
Washington University in St. Louis, United States

****Correspondence:***
Alessandro Angelini
alessandro.angelini@unive.it

†These authors have contributed equally to this work and share first authorship

Specialty section:
This article was submitted to Molecular Recognition, a section of the journal Frontiers in Molecular Biosciences

Received: *30 April 2021*
Accepted: *30 June 2021*
Published: *21 July 2021*

Citation:
Pluda S, Mazzocato Y and Angelini A (2021) Peptide-Based Inhibitors of ADAM and ADAMTS Metalloproteinases. Front. Mol. Biosci. 8:703715. doi: 10.3389/fmolb.2021.703715

INTRODUCTION

The "A-disintegrin and metalloproteinase" (ADAM) and "A-disintegrin and metalloproteinase with thrombospondin motifs" (ADAMTS) are closely related matrix zinc-dependent metalloproteinases that belong to the adamlysin protein family (Takeda, 2016). Most ADAM metalloproteinases are membrane-anchored enzymes while the ADAMTS family comprises only secreted proteins. Both ADAM and ADAMTS proteins show a multi-domain structure and are mainly localised in the extracellular matrix (ECM) (Zhong and Khalil, 2019). Despite their structural similarities, each protein member possesses different variable domains which ensure both function and tissue specificity (**Supplementary Figure 1**). The domain organisation and function of each ADAM and ADAMTS protein has been extensively described elsewhere (Takeda, 2016). Briefly, ADAM proteins are responsible for shedding cell-surface protein ectodomains, such as the latent forms of growth factors, cytokines, receptors, and other molecules. Furthermore, ADAMs contribute to a wide array of biological processes, including cell adhesion, migration and signaling (Huovila et al., 2005; Seegar and Blacklow, 2019). From the twenty-one human ADAM members identified so far, only thirteen are proteolytically active (ADAM−8, −9, −10, −12, −15, −17, −19, −20, −21, −28, −30, −33, and −DEC1) whereas the other eight appear to be catalytically inactive (ADAM−2, −7, −11, −18, −22, −23, −29, and −32) (Edwards et al., 2009; Seegar and Blacklow, 2019). It has been shown that members of the latest group play important roles in development, and function as adhesion molecules rather than proteinases. However, the physiological function of the inactive ADAMs remains largely unknown.

Unlike ADAMs, all ADAMTS proteins are catalytically active and contain a varying number of C-terminal thrombospondin type-1 (TSP-1) motifs instead of the ADAM transmembrane and cytoplasmic domains (Apte, 2020). ADAMTSs participate in ECM maintenance, tissue morphogenesis and remodeling by cleaving a large number of matrix proteins (Kelwick et al., 2015; Apte, 2020). ADAMTS family consists of nineteen members that can be sub-classified according to their known substrates, namely aggrecanases or proteoglycanases (ADAMTS−1, −4, −5, −8, −9, −15 and −20), procollagen N-propeptidases (ADAMTS−2, −3 and −14), cartilage oligomeric matrix protein (also known as thrombospondin-5) cleaving proteinases (ADAMTS−7 and −12), von Willebrand factor (VWF) cleaving proteinase (ADAMTS-13) and a group of orphan enzymes (ADAMTS−6, −10, −16, −17, −18 and −19) (Kelwick et al., 2015; Apte, 2020).

Aberrant expression or dysregulation of ADAMs and ADAMTSs activity has been linked to the development of cancer (Sun et al., 2015; Jackson et al., 2017) and numerous inflammatory (Lambrecht et al., 2018; Mead and Apte, 2018), neurodegenerative (Duffy et al., 2009; Lemarchant et al., 2013) and cardiovascular (Zhong and Khalil, 2019; Santamaria and de Groot, 2020) diseases to name but a few. Hence, ADAM and ADAMTS proteins represent important drug targets for the prevention and treatment of several human diseases.

Inhibition of ADAM and ADAMTS metalloproteinases have been attempted using various small molecules. The majority of these molecules bear either the hydroxamate, carboxylate, thiolate, tartrate, phosphinate, thiadiazole, hydroxyquinoline or imida-zolidine-2,4-diones groups, which are capable of competitively binding the zinc ion present in the catalytic site of the metalloproteinase (Moss et al., 2001; Georgiadis and Yiotakis, 2008; Yiotakis and Dive, 2009). In addition, inhibitory molecules lacking a zinc-binding moiety have also been reported (Gilbert et al., 2011). Despite the different approaches attempted, these conventional small molecule-based inhibitors have mostly had limited success in the clinic (Georgiadis and Yiotakis, 2008; Moss and Minond, 2017). Failures have often been attributed to off-target effects due to structural similarities among the active sites of the different metalloproteinases and the consequent toxicities associated (**Supplementary Figure 2**) (Georgiadis and Yiotakis, 2008; Tortorella et al., 2009; Raeeszadeh-Sarmazdeh et al., 2020). As a result, there is a great interest in developing novel ADAM and ADAMTS inhibitors that can selectively target a single member of each family. Efforts to generate more effective therapies have led to the development of protein-based inhibitors such as monoclonal antibodies and tissue inhibitors of metalloproteinases (TIMPs) which are currently being tested in advanced clinical trials (Santamaria and de Groot, 2019; Raeeszadeh-Sarmazdeh et al., 2020). Unlike small molecule-based inhibitors, protein-based therapeutics offer a higher selectivity due to a larger surface of interaction and therefore, reduced toxicity. Indeed, most protein-based inhibitors do not bind the active site of the ADAM and ADAMTS enzymes but recognise surface-exposed loops that are poorly conserved between closely related family members. Inhibition appears to occur through a variety of mechanisms including i) binding at or near the active site to block substrate access (direct manner) or ii) binding to regions that are allosterically linked to the active site region (indirect manner) (Wu et al., 2007; Raeeszadeh-Sarmazdeh et al., 2020). A major drawback of protein-based therapeutics compared to small molecule inhibitors is that they are not orally available and therefore need to be injected either subcutaneously or intravenously.

While most of these small-molecules and protein-based inhibitors have been thoroughly described elsewhere (Moss et al., 2001; Georgiadis and Yiotakis, 2008; Yiotakis and Dive, 2009; Murumkar et al., 2010; Gilbert et al., 2011; El Bakali et al., 2014; Santamaria et al., 2017; Malemud, 2019) this mini review focuses exclusively on peptide-based inhibitors, an alternative and emerging type of ADAMs and ADAMTSs metalloproteinase inhibitors. Similar to the protein-based inhibitors, peptides inhibitors are capable of binding the target with a surface of interaction large enough to obtain high efficiency and selectivity (Pelay-Gimeno et al., 2015; Atangcho et al., 2019). Like small molecules, peptide-based inhibitors can be synthesised chemically, possess ease of modification, low toxicity, and reduced antigenicity. Their modular structure and the commercial availability of hundreds of amino acid building blocks simplifies the rapid development of peptides with tailored properties (Rastogi et al., 2018; Muttenthaler et al., 2021). Here, we will mention examples of both linear and cyclic peptide-based inhibitors and the different approaches undertaken for their development will be described.

PEPTIDE-BASED INHIBITORS OF ADAMs

To date, peptide-based inhibitors have been successfully developed against only two members of the ADAM family: ADAM-8 and ADAM-17 (**Figure 1** and **Supplementary Table 1**). The latter one, also known as tumor necrosis factor-α converting enzyme (TACE), is involved in shedding the proinflammatory cytokine tumor necrosis factor-a (TNF-α) at the cell surface (Zunke and Rose-John, 2017). Altered activity of ADAM-17 has been associated with the onset of numerous inflammatory diseases, such as cardiac hypertrophy, arthritis, Chron's disease and cancer (Feldmann and Maini, 2008; Moss and Minond, 2017; Lambrecht et al., 2018). The first peptide-based inhibitors targeting ADAM-17 were identified using synthetic combinatorial libraries of seven amino acids-long peptidomimetics (Hu et al., 2005a; Hu et al., 2005b). Libraries were designed to mimic the sequence of the cleavage sites in denatured collagen type II and include zinc-ion chelating side-groups. The screening revealed two low micromolar inhibitors, named regasepin 1 (**Figure 1A**) and regasepin 2, that inhibit related metalloproteinases MMP-8 and MMP-9 with similar potency (**Supplementary Table 1**; (Hu et al., 2005b; Dillen et al., 2006)). Further structure-based optimisation of regasepin 1 led to the generation of a small peptide repertoire bearing different D-form amino acids in place of Val and Lys in position P1′ at P2′, respectively. The best selected peptide, named

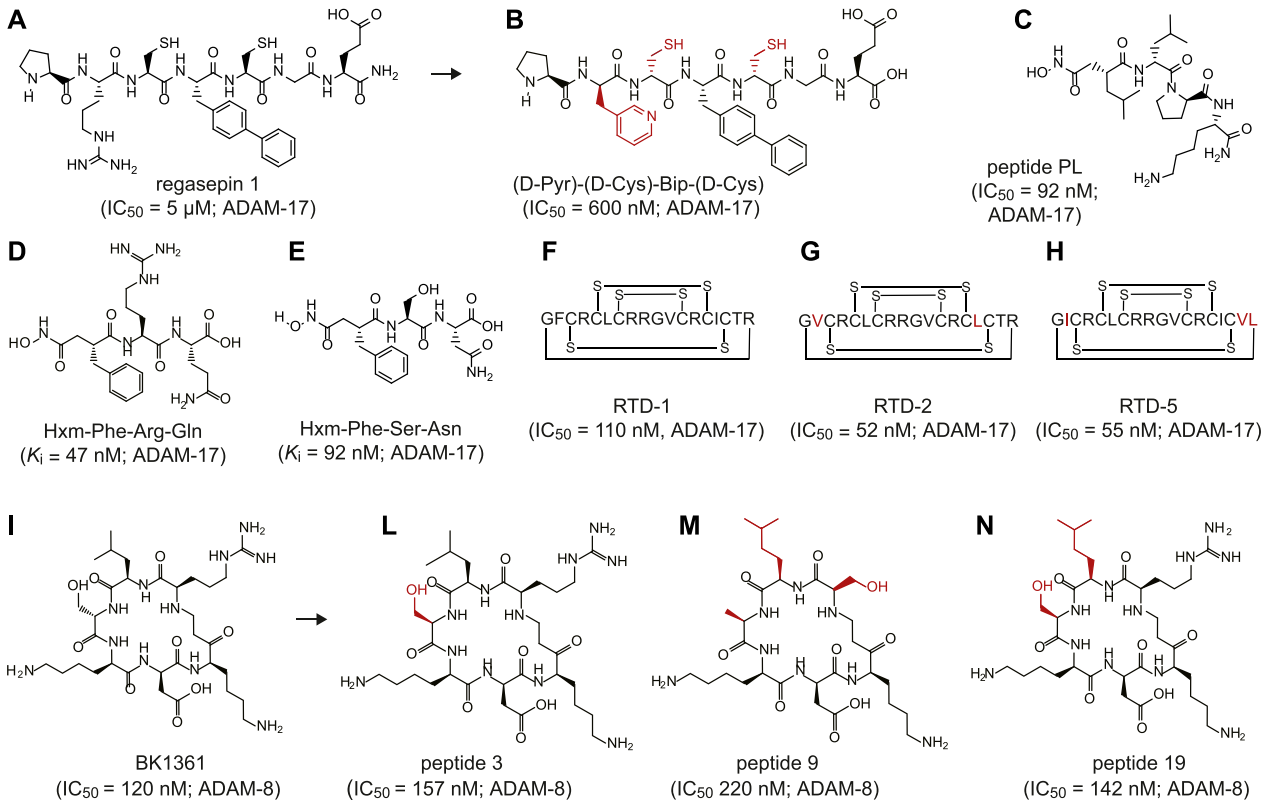

FIGURE 1 | Peptide inhibitors of ADAM proteins. **(A)** Chemical structure of regasepin 1 linear peptide (PRC(Bip)CGE); **(B)** Chemical structure of regasepin 1-derived linear peptide (D-Pyr)-(D-Cys)-Bip-(D-Cys); **(C)** Chemical structure of peptide PL (Hisb-LPK-NH2); **(D)** Chemical structure of linear peptide Hxm-FRQ; **(E)** Chemical structure of linear peptide Hxm-FSN; **(F)** Schematically depicted structure of polycyclic octadecapeptide rhesus θ-defensin-1 (RTD-1) peptide; **(G)** Schematically depicted structure of polycyclic octadecapeptide rhesus θ-defensin-2 (RTD-2) peptide; **(H)** Schematically depicted structure of polycyclic octadecapeptide rhesus θ-defensin-5 (RTD-5) peptide; **(I)** Chemical structure of cyclic peptide BK1361 (RLsKDK); **(L)** Chemical structure of cyclic peptide 3 (RLhS$_\beta$KDK); **(M)** Chemical structure of cyclic peptide 9 (RL*A$_\beta$KDK); **(N)** Chemical structure of cyclic peptide 19 (RL*hS$_\beta$KDK). Indicated half maximal inhibitory concentration (IC$_{50}$) and inhibition constant (*Ki*) values were reported as published. The targeted ADAM protein is reported near the IC$_{50}$ or K_i value. Legend: Bip = biphenylalanine, Pyr = pyridylalanine, Hisb = (R)-2-isobutylsuccin hydroxamate moiety, Hmx = hydroxamate moiety, s = D-serine; hS$_\beta$ = β-homoserine, A$_\beta$ = β-alanine, L* = homoleucine. The side chains that differentiate from the parental peptide are shown in red.

(D-Pyr)-(D-Cys)-Bip-(D-Cys) (**Figure 1B**), showed an 8-fold higher potency (IC$_{50}$ = 600 nM) than regasepin 1, 14-fold better selectivity against MMP-9 and 46-fold against MMP-3. However, no specificity for MMP-8 has been shown yet (**Supplementary Table 1**; (Qiu et al., 2012)). Similarly, Geurink and colleagues applied a synthetic combinatorial library of ninety-six enantiopure peptidomimetics bearing a zinc binding hydroxamate group at the N-terminal and identified eight peptide variants capable of inhibiting ADAM-17 with potencies in the sub-nanomolar to low micromolar range (Geurink et al., 2008). One peptide, named PL (**Figure 1C**), revealed an IC$_{50}$ of 92 nM against ADAM-17 and showed 40-fold better selectivity against MMP-9 but limited selectivity for MMP-12 (**Supplementary Table 1**). By using a virtual combinatorial library of peptides derived from the TNF protease inhibitor 2 (TAPI-2), a broad-spectrum peptide inhibitor of ADAM-17 bearing a hydroxamate group, Wang and colleagues identified two linear peptides, named Hxm-Phe-Arg-Gln (**Figure 1D**) and Hxm-Phe-Ser-Asn (**Figure 1E**) that exhibited high potency toward ADAM-17 (K_i = 47 and 92 nM, respectively) and moderate selectivity toward ADAM-10 (5-fold and 7-fold, respectively; **Supplementary Table 1**; (Wang et al., 2016)). Furthermore, Schaal and colleagues discovered novel peptide-based inhibitors of ADAMs by screening θ-defensins, a family of eighteen-amino acid macrocyclic peptides expressed exclusively in granulocytes and selected epithelia of Old World monkeys (Schaal et al., 2017)). The octadecapeptide rhesus θ-defensin-1 (RTD-1) includes six disulfide-linked cysteines (**Figure 1F**) and inhibited ADAM-17 and ADAM-10 with an IC$_{50}$ of 110 and 450 nM, respectively (**Supplementary Table 1**). Notably, RTD-1 showed at least 4-fold better selectivity toward a panel of related MMPs (IC$_{50}$ = 2–20 μM; **Supplementary Table 1**). When tested *in vivo* in a rodent model of rheumatoid arthritis, RTD-1 rapidly suppressed joint disease progression, restored limb mobility, and preserved normal joint architecture (Schaal et al., 2017). Further characterisation of five RTD isoforms (RTDs 1–5) revealed the presence of two macrocycles, RTD-2 (**Figure 1G**) and RTD-5 (**Figure 1H**), that inhibited ADAM-17 with IC$_{50}$ values of 52 and 55 nM, respectively (**Supplementary Table 1**; (Schaal et al., 2018)).

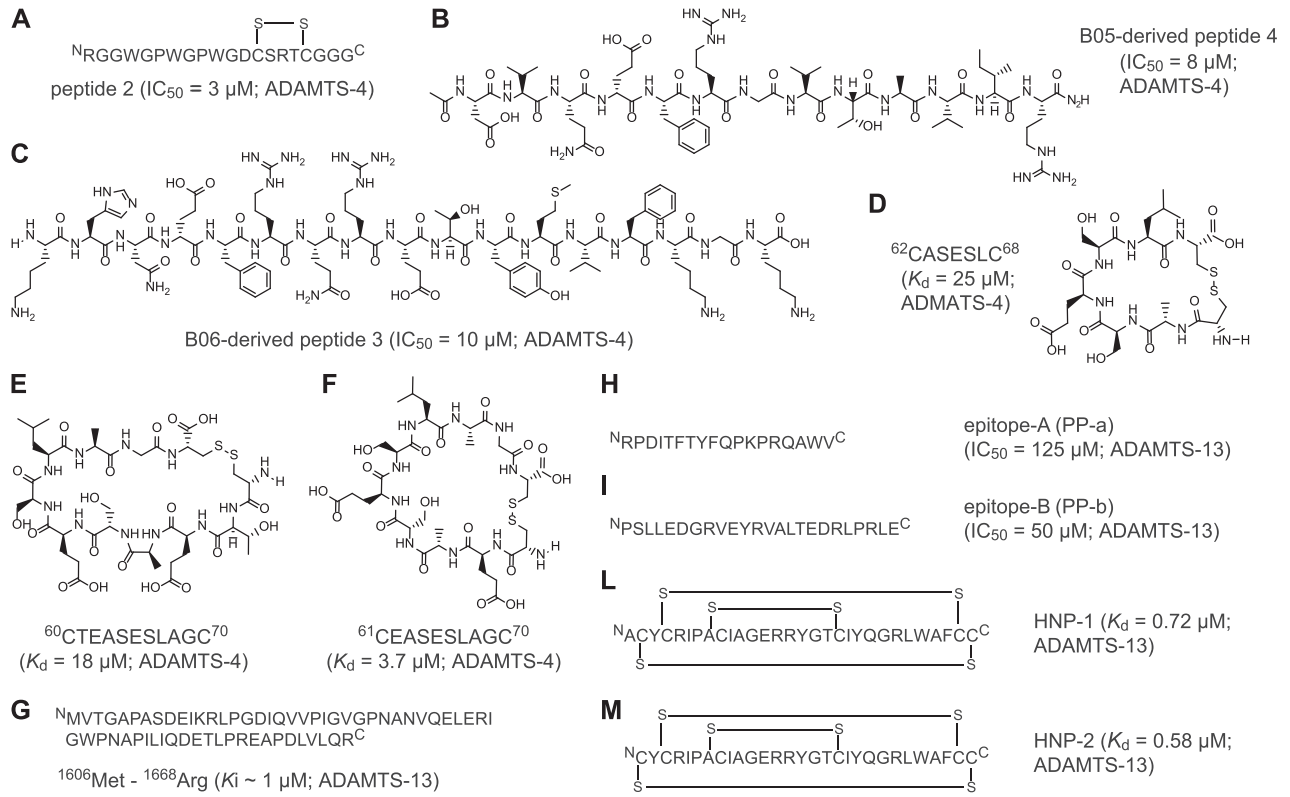

FIGURE 2 | Peptide inhibitors of ADAMTS proteins. **(A)** Aminoacidic sequence of linear peptide 2 derived from the C-terminus TSP-1 motif of aggrecanase-1; **(B)** Chemical structure of B05-derived linear peptide 4 (KHN(e)FRQRETYMVFKGK); **(C)** Chemical structure of B06-derived linear peptide 3 (DVQ(e)FRGVTAVIR); **(D)** Chemical structure of cyclic peptide ^{62}CASESLC^{68}; **(E)** Chemical structure of cyclic peptide ^{60}CTEASESLAGC^{70}; **(F)** Chemical structure of cyclic peptide ^{61}CEASESLAGC^{70}; **(G)** Aminoacidic sequence of linear peptide VWF-73 peptide (Met^{1606}-Arg^{166}) derived from C-terminal region of the multimeric von Willebrand factor (VWF); **(H)** Aminoacidic sequence of linear peptide epitope-A (PP-a); **(I)** Aminoacidic sequence of linear peptide epitope-B (PP-b); **(L)** Aminoacidic sequence of polycyclic human neutrophil peptide 1 (HNP-1); **(M)** Aminoacidic sequence of polycyclic human neutrophil peptide (HNP-2). Indicated half maximal inhibitory concentration (IC_{50}), inhibition constant (K_i) and dissociation constant (K_d) values were reported as published. The targeted ADAMTS protein is reported near the IC_{50}, K_i, or K_d value.

Another widely investigated sheddase is ADAM-8, a proteolytically active member of the ADAM protease family involved in numerous inflammatory processes (Schlomann et al., 2000) and neoplasia (Fritzsche et al., 2006; Romagnoli et al., 2014). By applying structural modeling and peptidomimetic approaches, Schlomann and colleagues generated a series of six amino acids cyclic peptides mimicking the RLSKDK motif of the mouse ADAM-8 (Schlomann et al., 2015). To enhance its potency and further increase its stability *in vivo*, the peptide sequence was constrained through cyclisation and modified with D-form amino acids in place of Arg, Leu, or Ser. The most potent cyclic peptide sequence contains a D-Ser ("s") (RLsKDK) (**Figure 1I**). The RLsKDK, also named BK-1361, inhibited ADAM-8 with IC_{50} of 182 nM. Importantly, BK-1361 showed more than 100-fold better selectivity toward other related metalloproteinases such as ADAM−9, −10, −12, −17 and MMP-2, −9, −14 (**Supplementary Table 1**). Notably, when tested in a mouse model of pancreatic ductal adenocarcinoma (PDAC), BK-1361 led to reduction of tumor load, infiltration and metastasis. Thus, further supporting the important role of ADAM-8 in PDAC development (Schlomann et al., 2015). Additional structure-activity relationship studies on BK-1361 enabled the generation of eighteen structural analogue peptidomimetics (Yim et al., 2016). Among all tested cyclic peptides, peptides 3 (**Figure 1L**), 9 (**Figure 1M**) and 19 (**Figure 1N**) showed comparable or slightly higher inhibitory potency than the parental BK-1361 (**Supplementary Table 1**) (Yim et al., 2016).

PEPTIDE-BASED INHIBITORS OF ADAMTSs

The physiological function of ADAMTSs and their role in numerous pathologies have been described only recently (Zhong and Khalil, 2019; Apte, 2020). The first member of this family, ADAMTS-1, was characterised for the first time in 1997 (Kuno et al., 1997). Since then, few examples of peptide-based inhibitors against ADAMTSs have been reported (Tortorella et al., 2000; Hills et al., 2007; Di Stasio et al., 2008; Moriki et al., 2010; Pillai et al., 2016; Zhang et al., 2018).

Recently, major efforts have been devoted to developing peptide-based inhibitors against two members of the ADAMTS family: ADAMTS-4 and ADAMTS-13 (**Figure 2** and **Supplementary Table 2**). ADAMTS-4 cleaves proteoglycans such as aggrecan and versican, which play a structural role in many tissues (Fosang and Little, 2008). In fact, degradation of aggrecan is a clinical hallmark of degenerative joint disorders such as osteoarthritis Zhang et al. (2013), Yang et al. (2017) and rheumatoid arthritis (Mead and Apte, 2018). The first peptide-based inhibitors targeting ADAMTS-4 were identified using linear peptides derived from the TSP-1 motif located at the C-terminus of the aggrecanase-1, an enzyme involved in cartilage degradation. The best selected peptide, peptide 2 (**Figure 2A**), showed an IC_{50} of 3 μM against ADAMTS-4 (**Supplementary Table 2**; (Tortorella et al., 2000)). With the aim of identifying the cleavage motif of ADAMTS-4, Hills and co-workers applied phage display of random thirteen-amino acid linear peptide libraries to isolate seven-amino acid cleaved peptides with a wide range of potencies (Hills et al., 2007). Two linear peptides, B05 and B06, inhibited ADAMTS-4 with potencies in the micromolar range (IC_{50} = 35 μM) and exhibited good selectivity toward the homologue ADAMTS-5 (**Supplementary Table 2**; Hills et al., 2007). Further studies revealed the importance of Glu in position P1 for substrate recognition and led to the development of novel synthetic peptides with modified stereochemistry of P1 and P1'. These two selected peptides inhibited ADAMTS-4 with IC_{50} values of 8 μM (peptide 4, **Figure 2B**) and 10 μM (peptide 3, **Figure 2C**) (Hills et al., 2007). Recently, Zhang and colleagues used computational modeling to develop peptide-based inhibitors from a loop of the N-terminal domain of TIMP3, a protein inhibitor of ADAMTS-4 (Zhang et al., 2018). Further peptide cyclisation diminished flexibility and enabled the generation of constrained molecules with reduced entropic penalty and improved binding affinities. Cyclised peptides ^{62}CASESLC^{68} (**Figure 2D**), ^{61}CEASESLAGC^{70} (**Figure 2F**) and ^{60}CTEASESLAGC^{70} (**Figure 2E**) showed bindings constants in the micromolar range (K_d = 25 μM, K_d = 3.7 μM and K_d = 18 μM, respectively) and three- to 9-fold increased affinity over the linear peptides (**Supplementary Table 2**).

In addition to ADAMTS-4, peptide-based inhibitors against ADAMTS-13 have been also developed. ADAMTS-13 is a metalloproteinase which cleaves the von Willebrand factor (VWF), a blood glycoprotein involved in haemostasis (Zheng, 2013). The levels of ADAMTS-13 correlate with ischaemic stroke risk, thrombotic thrombocytopenic purpura and microvascular thrombosis (South and Lane, 2018; Santamaria and de Groot, 2020). The first peptide-based inhibitor of ADAMTS-13 was identified by analysing the C-terminal region of the multimeric VWF factor, the VWF-73 peptide (Glu^{1660}—Arg^{1668}; **Figure 2G**) (Di Stasio et al., 2008). By elucidating the interaction of linear VWF-73 peptide with ADAMTS-13, Di Stasio and colleagues determined that inhibition occurs with a K_i value of 1 μM (**Supplementary Table 2**). Furthermore, Moriki and colleagues applied phage display technology to identify two novel ADAMTS-13-derived peptide epitopes capable of binding VWF factor. Selected synthetic linear peptides PP-a and PP-b (**Figures 2H,I**) exhibited K_d values of 4.1 and 0.3 μM, respectively, and inhibited ADAMTS-13 with IC_{50} values of 125 μM (PP-a) and 50 μM (PP-b) (**Supplementary Table 2**) (Moriki et al., 2010). Finally, Pillai and co-workers showed that polycyclic human neutrophil peptides (HNP) inhibit the proteolytic cleavage of peptide VWF-73 and multimeric von Willebrand factor in a concentration-dependent manner. HNP-1 and -2 (**Figures 2L,M**) showed inhibitory concentrations in the low micromolar range and binding constants in the sub-micromolar range (**Supplementary Table 2**) (Pillai et al., 2016).

CONCLUSIONS AND PERSPECTIVES

ADAM and ADAMTS metalloproteinases play a significant yet complex role in several types of cancer, as well as in diverse inflammatory, neurodegenerative and cardiovascular diseases. Thus, a plethora of small chemical molecules and a few large proteins, such as monoclonal antibodies, have been developed to inhibit ADAM and ADAMTS metalloproteinases. While small chemical molecules often lack specificity and turn to be toxic, therapeutic proteins require high manufacturing costs and subcutaneous or intravenous administration. In this sense, peptide-based drugs offer a good alternative strategy with a surface of interaction large enough to obtain both high potency and selectivity, and yet small enough to diffuse into tissues. Other distinctive properties of peptides include chemical synthesis, ease of modification, low toxicity and reduced antigenicity. However, despite these favourable traits, peptides often have a relatively short circulating half-life and exhibit poor membrane permeability, which limit their broad applicability. While their systemic half-life can be prolonged by chemical conjugation to synthetic and natural polymers, or through non-covalent binding to endogenous proteins, such as serum albumin (Zorzi et al., 2019), reaching intracellular targets, on the other hand, is still a daunting task for peptide-based drugs. Although recent developments in chemical cyclization, methylation and the use of non-proteinogenic amino acids have led to promising results to overcome this problem, more accessible targets would also help to bypass the delivery strategies challenges (Cunningham et al., 2017; Lenci and Trabocchi, 2020). In this regard, ADAM and ADAMTS proteins have a peripheral extracellular localisation, which makes them ideal targets of peptide-based drugs. Moreover, the existence of multiple ADAM and ADAMTS homologues leverage the better selectivity of peptides (driven by their larger surface area and chiral complexity) over small-molecule drugs. The majority of linear and cyclic peptide inhibitors described in this mini review were developed using traditional medicinal chemistry approaches and structure–activity relationship studies on natural substrates and/or endogenous inhibitors. However, the specificity of some of the peptide inhibitors described here have not been fully investigated and none of them have reached a pre-clinical stage yet. Nevertheless, their development demonstrates that peptides represent valid molecular modalities for blocking the activity of ADAM and ADAMTS proteins. Indeed, the advent of novel DNA-encoded chemical libraries (Neri and Lerner, 2018) and superior peptide display technologies (Linciano et al., 2019; Sohrabi et al., 2020; Peacock and Suga, 2021) will enable the high-throughput screening of large combinatorial libraries, facilitating the discovery of novel potent and selective compounds with improved properties on short timescales (Sohrabi et al., 2020). Integration of these powerful

combinatorial approaches with better automation, innovative chemical modification strategies and emerging computational methods will contribute to the development of better peptide-based inhibitors against ADAM and ADAMTS proteins, which have the potential to be used in the clinic in the near future.

AUTHOR CONTRIBUTIONS

SP, YM, and AA conceived the work. SP and YM analyzed data, prepared figures and wrote the first draft of the manuscript. AA supervised the work and edited the manuscript. All authors contributed to manuscript revision, read, and approved the submitted version.

FUNDING

The authors declare that this study received funding from Fidia Farmaceutici S.p.A. The funder was not involved in the study design, collection, analysis, interpretation of data, the writing of this article or the decision to submit it for publication.

SUPPLEMENTARY MATERIAL

The Supplementary Material for this article can be found online at: https://www.frontiersin.org/articles/10.3389/fmolb.2021.703715/full#supplementary-material

REFERENCES

Apte, S. S. (2020). ADAMTS Proteins: Concepts, Challenges, and Prospects. *Methods Mol. Biol.* 2043, 1–12. doi:10.1007/978-1-4939-9698-8_1

Atangcho, L., Navaratna, T., and Thurber, G. M. (2019). Hitting Undruggable Targets: Viewing Stabilized Peptide Development through the Lens of Quantitative Systems Pharmacology. *Trends Biochem. Sci.* 44, 241–257. doi:10.1016/j.tibs.2018.11.008

Bakali, J. E., Gras-Masse, H., Maingot, L., Deprez, B., Dumont, J., Leroux, F., et al. (2014). Inhibition of Aggrecanases as a Therapeutic Strategy in Osteoarthritis. *Future Med. Chem.* 6, 1399–1412. doi:10.4155/FMC.14.84

Bessette, P. H., Rice, J. J., and Daugherty, P. S. (2004). Rapid Isolation of High-Affinity Protein Binding Peptides Using Bacterial Display. *Protein Eng. Des. Sel.* 17, 731–739. doi:10.1093/protein/gzh084

Cunningham, A. D., Qvit, N., and Mochly-Rosen, D. (2017). Peptides and Peptidomimetics as Regulators of Protein-Protein Interactions. *Curr. Opin. Struct. Biol.* 44, 59–66. doi:10.1016/j.sbi.2016.12.009

Daugherty, P. S. (2007). Protein Engineering with Bacterial Display. *Curr. Opin. Struct. Biol.* 17, 474–480. doi:10.1016/j.sbi.2007.07.004

Di Stasio, E., Lancellotti, S., Peyvandi, F., Palla, R., Mannucci, P. M., and De Cristofaro, R. (2008). Mechanistic Studies on ADAMTS13 Catalysis. *Biophysical J.* 95, 2450–2461. doi:10.1529/biophysj.108.131532

Dillen, C., Fiten, P., Chaltin, P., Hu, J., Dubois, V., Van den Steen, P., et al. (2006). Inhibition of Lethal Endotoxin Shock with an L-Pyridylalanine Containing Metalloproteinase Inhibitor Selected by High-Throughput Screening of a New Peptide Library. *Cchts* 9, 599–611. doi:10.2174/138620706778249758

Duffy, M. J., McKiernan, E., O'Donovan, N., and McGowan, P. M. (2009). Role of ADAMs in Cancer Formation and Progression. *Clin. Cancer Res.* 15, 1140–1144. doi:10.1158/1078-0432.CCR-08-1585

Edwards, D., Handsley, M., and Pennington, C. (2008). The ADAM Metalloproteinases. *Mol. Aspects Med.* 29, 258–289. doi:10.1016/j.mam.2008.08.001

Feldmann, M., and Maini, S. R. N. (2008). Role of Cytokines in Rheumatoid Arthritis: an Education in Pathophysiology and Therapeutics. *Immunol. Rev.* 223, 7–19. doi:10.1111/j.1600-065X.2008.00626.x

Fosang, A. J., and Little, C. B. (2008). Drug Insight: Aggrecanases as Therapeutic Targets for Osteoarthritis. *Nat. Rev. Rheumatol.* 4, 420–427. doi:10.1038/ncprheum0841

Fritzsche, F. R., Jung, M., Xu, C., Rabien, A., Schicktanz, H., Stephan, C., et al. (2006). ADAM8 Expression in Prostate Cancer Is Associated with Parameters of Unfavorable Prognosis. *Virchows Arch.* 449, 628–636. doi:10.1007/s00428-006-0315-1

Georgiadis, D., and Yiotakis, A. (2008). Specific Targeting of Metzincin Family Members with Small-Molecule Inhibitors: Progress toward a Multifarious challenge. *Bioorg. Med. Chem.* 16, 8781–8794. doi:10.1016/j.bmc.2008.08.058

Geurink, P., Klein, T., Leeuwenburgh, M., Van Der Marel, G., Kauffman, H., Bischoff, R., et al. (2008). A Peptide Hydroxamate Library for Enrichment of Metalloproteinases: Towards an Affinity-Based Metalloproteinase Profiling Protocol. *Org. Biomol. Chem.* 6, 1244–1250. doi:10.1039/b718352f

Gilbert, A. M., Bikker, J. A., and O'Neil, S. V. (2011). Advances in the Development of Novel Aggrecanase Inhibitors. *Expert Opin. Ther. Patents* 21, 1–12. doi:10.1517/13543776.2011.539204

Heinis, C., and Winter, G. (2015). Encoded Libraries of Chemically Modified Peptides. *Curr. Opin. Chem. Biol.* 26, 89–98. doi:10.1016/j.cbpa.2015.02.008

Hills, R., Mazzarella, R., Fok, K., Liu, M., Nemirovskiy, O., Leone, J., et al. (2007). Identification of an ADAMTS-4 Cleavage Motif Using Phage Display Leads to the Development of Fluorogenic Peptide Substrates and Reveals Matrilin-3 as a Novel Substrate. *J. Biol. Chem.* 282, 11101–11109. doi:10.1074/jbc.M611588200

Hu, J., Fiten, P., Van Den Steen, P. E., Chaltin, P., and Opdenakker, G. (2005a). Simulation of Evolution-Selected Propeptide by High-Throughput Selection of a Peptidomimetic Inhibitor on a Capillary DNA Sequencer Platform. *Anal. Chem.* 77, 2116–2124. doi:10.1021/ac048631p

Hu, J., Van Den Steen, P. E., Dillen, C., and Opdenakker, G. (2005b). Targeting Neutrophil Collagenase/matrix Metalloproteinase-8 and Gelatinase B/matrix Metalloproteinase-9 with a Peptidomimetic Inhibitor Protects against Endotoxin Shock. *Biochem. Pharmacol.* 70, 535–544. doi:10.1016/j.bcp.2005.04.047

Huang, Y., Wiedmann, M. M., and Suga, H. (2019). RNA Display Methods for the Discovery of Bioactive Macrocycles. *Chem. Rev.* 119, 10360–10391. doi:10.1021/acs.chemrev.8b00430

Huovila, A.-P. J., Turner, A. J., Pelto-Huikko, M., Kärkkäinen, I., and Ortiz, R. M. (2005). Shedding Light on ADAM Metalloproteinases. *Trends Biochem. Sci.* 30, 413–422. doi:10.1016/j.tibs.2005.05.006

Jackson, H. W., Defamie, V., Waterhouse, P., and Khokha, R. (2017). TIMPs: Versatile Extracellular Regulators in Cancer. *Nat. Rev. Cancer* 17, 38–53. doi:10.1038/nrc.2016.115

Kelwick, R., Desanlis, I., Wheeler, G. N., and Edwards, D. R. (2015). The ADAMTS (A Disintegrin and Metalloproteinase with Thrombospondin Motifs) Family. *Genome Biol.* 16, 113. doi:10.1186/s13059-015-0676-3

Kuno, K., Kanada, N., Nakashima, E., Fujiki, F., Ichimura, F., and Matsushima, K. (1997). Molecular Cloning of a Gene Encoding a New Type of Metalloproteinase-Disintegrin Family Protein with Thrombospondin Motifs as an Inflammation Associated Gene. *J. Biol. Chem.* 272, 556–562. doi:10.1074/jbc.272.1.556

Lambrecht, B. N., Vanderkerken, M., and Hammad, H. (2018). The Emerging Role of ADAM Metalloproteinases in Immunity. *Nat. Rev. Immunol.* 18, 745–758. doi:10.1038/s41577-018-0068-5

Lemarchant, S., Pruvost, M., Montaner, J., Emery, E., Vivien, D., Kanninen, K., et al. (2013). ADAMTS Proteoglycanases in the Physiological and Pathological central Nervous System. *J. Neuroinflammation* 10, 133. doi:10.1186/1742-2094-10-133

Lenci, E., and Trabocchi, A. (2020). Peptidomimetic Toolbox for Drug Discovery. *Chem. Soc. Rev.* 49, 3262–3277. doi:10.1039/d0cs00102c

Linciano, S., Pluda, S., Bacchin, A., and Angelini, A. (2019). Molecular Evolution of Peptides by Yeast Surface Display Technology. *Med. Chem. Commun.* 10, 1569–1580. doi:10.1039/c9md00252a

Malemud, C. J. (2019). Inhibition of MMPs and ADAM/ADAMTS. *Biochem. Pharmacol.* 165, 33–40. doi:10.1016/j.bcp.2019.02.033

Mead, T. J., and Apte, S. S. (2018). ADAMTS Proteins in Human Disorders. *Matrix Biol.* 71-72, 225–239. doi:10.1016/j.matbio.2018.06.002

Moriki, T., Maruyama, I. N., Igari, A., Ikeda, Y., and Murata, M. (2010). Identification of ADAMTS13 peptide sequences binding to von Willebrand factor. *Biochem. Biophysical Res. Commun.* 391, 783–788. doi:10.1016/j.bbrc.2009.11.138

Moss, M. L., and Minond, D. (2017). Recent Advances in ADAM17 Research: A Promising Target for Cancer and Inflammation. *Mediators Inflamm.* 2017, 1–21. doi:10.1155/2017/96735372017

Moss, M. L., White, J. M., Lambert, M. H., and Andrews, R. C. (2001). TACE and Other ADAM Proteases as Targets for Drug Discovery. *Drug Discov. TodayToday* 6, 417–426. doi:10.1016/S1359-6446(01)01738-X

Murumkar, P. R., DasGupta, S., Chandani, S. R., Giridhar, R., and Yadav, M. R. (2010). Novel TACE Inhibitors in Drug Discovery: A Review of Patented Compounds. *Expert Opin. Ther. Patents* 20, 31–57. doi:10.1517/13543770903465157

Muttenthaler, M., King, G. F., Adams, D. J., and Alewood, P. F. (2021). Trends in Peptide Drug Discovery. *Nat. Rev. Drug Discov.* 20, 309–325. doi:10.1038/s41573-020-00135-8

Neri, D., and Lerner, R. A. (2018). DNA-encoded Chemical Libraries: A Selection System Based on Endowing Organic Compounds with Amplifiable Information. *Annu. Rev. Biochem.* 87, 479–502. doi:10.1146/annurev-biochem-062917-012550

Peacock, H., and Suga, H. (2021). Discovery of De Novo Macrocyclic Peptides by Messenger RNA Display. *Trends Pharmacol. Sci.* 42, 385–397. doi:10.1016/j.tips.2021.02.004

Pelay-Gimeno, M., Glas, A., Koch, O., and Grossmann, T. N. (2015). Structure-Based Design of Inhibitors of Protein-Protein Interactions: Mimicking Peptide Binding Epitopes. *Angew. Chem. Int. Ed.* 54, 8896–8927. doi:10.1002/anie.201412070

Pillai, V. G., Bao, J., Zander, C. B., McDaniel, J. K., Chetty, P. S., Seeholzer, S. H., et al. (2016). Human neutrophil peptides inhibit cleavage of von Willebrand factor by ADAMTS13: A potential link of inflammation to TTP. *Blood* 128, 110–119. doi:10.1182/blood-2015-12-688747

Plückthun, A. (2012). Ribosome Display: A Perspective. *Methods Mol. Biol.* 805, 3–28. doi:10.1007/978-1-61779-379-0_1

Qiu, Z., Yan, M., Li, Q., Liu, D., Van den Steen, P. E., Wang, M., et al. (2012). Definition of Peptide Inhibitors from a Synthetic Peptide Library by Targeting Gelatinase B/matrix Metalloproteinase-9 (MMP-9) and TNF-α Converting Enzyme (TACE/ADAM-17). *J. Enzyme Inhib. Med. Chem.* 27, 533–540. doi:10.3109/14756366.2011.599323

Raeeszadeh-Sarmazdeh, M., Do, L., and Hritz, B. (2020). Metalloproteinases and Their Inhibitors: Potential for the Development of New Therapeutics. *Cells* 9, 1313. doi:10.3390/cells9051313

Rastogi, S., Shukla, S., Kalaivani, M., and Singh, G. N. (2019). Peptide-based Therapeutics: Quality Specifications, Regulatory Considerations, and Prospects. *Drug Discov. Today* 24, 148–162. doi:10.1016/j.drudis.2018.10.002

Romagnoli, M., Mineva, N. D., Polmear, M., Conrad, C., Srinivasan, S., Loussouarn, D., et al. (2014). ADAM 8 Expression in Invasive Breast Cancer Promotes Tumor Dissemination and Metastasis. *EMBO Mol. Med.* 6, 278–294. doi:10.1002/emmm.201303373

Santamaria, S., and de Groot, R. (2020). ADAMTS Proteases in Cardiovascular Physiology and Disease. *Open Biol.* 10, 200333. doi:10.1098/rsob.200333

Santamaria, S., and de Groot, R. (2019). Monoclonal Antibodies against Metzincin Targets. *Br. J. Pharmacol.* 176, 52–66. doi:10.1111/bph.14186

Santamaria, S., Fedorov, O., McCafferty, J., Murphy, G., Dudhia, J., Nagase, H., et al. (2017). Development of a Monoclonal Anti-ADAMTS-5 Antibody that Specifically Blocks the Interaction with LRP1. *MAbs* 9, 595–602. doi:10.1080/19420862.2017.1304341

Schaal, J. B., Maretzky, T., Tran, D. Q., Tran, P. A., Tongaonkar, P., Blobel, C. P., et al. (2018). Macrocyclic θ-defensins Suppress Tumor Necrosis Factor-α (TNF-α) Shedding by Inhibition of TNF-α-Converting Enzyme. *J. Biol. Chem.* 293, 2725–2734. doi:10.1074/jbc.RA117.000793

Schaal, J. B., Tran, D. Q., Subramanian, A., Patel, R., Laragione, T., Roberts, K. D., et al. (2017). Suppression and Resolution of Autoimmune Arthritis by Rhesus θ-defensin-1, an Immunomodulatory Macrocyclic Peptide. *PLoS One* 12, e0187868. doi:10.1371/journal.pone.0187868

Schlomann, U., Koller, G., Conrad, C., Ferdous, T., Golfi, P., Garcia, A. M., et al. (2015). ADAM8 as a Drug Target in Pancreatic Cancer. *Nat. Commun.* 6, 1–16. doi:10.1038/ncomms7175

Schlomann, U., Rathke-Hartlieb, S., Yamamoto, S., Jockusch, H., and Bartsch, J. W. (2000). Tumor Necrosis Factor α Induces a Metalloprotease-Disintegrin, ADAM8 (CD 156): Implications for Neuron-Glia Interactions during Neurodegeneration. *J. Neurosci.* 20, 7964–7971. doi:10.1523/jneurosci.20-21-07964.2000

Seegar, T. C., and Blacklow, S. C. (2019). Domain Integration of ADAM Family Proteins: Emerging Themes from Structural Studies. *Exp. Biol. Med. (Maywood)* 244, 1510–1519. doi:10.1177/1535370219865901

Simonetti, L., and Ivarsson, Y. (2020). Genetically Encoded Cyclic Peptide Phage Display Libraries. *ACS Cent. Sci.* 6, 336–338. doi:10.1021/acscentsci.0c00087

Sohrabi, C., Foster, A., and Tavassoli, A. (2020). Methods for Generating and Screening Libraries of Genetically Encoded Cyclic Peptides in Drug Discovery. *Nat. Rev. Chem.* 4, 90–101. doi:10.1038/s41570-019-0159-2

South, K., and Lane, D. A. (2018). ADAMTS-13 and von Willebrand factor: a dynamic duo. *J. Thromb. Haemost.* 16, 6–18. doi:10.1111/jth.13898

Sun, Y., Huang, J., and Yang, Z. (2015). The Roles of ADAMTS in Angiogenesis and Cancer. *Tumor Biol.* 36, 4039–4051. doi:10.1007/s13277-015-3461-8

Takeda, S. (2016). ADAM and ADAMTS Family Proteins and Snake Venom Metalloproteinases: A Structural Overview. *Toxins* 8, 155. doi:10.3390/toxins8050155

Tortorella, M. D., Tomasselli, A. G., Mathis, K. J., Schnute, M. E., Woodard, S. S., Munie, G., et al. (2009). Structural and Inhibition Analysis Reveals the Mechanism of Selectivity of a Series of Aggrecanase Inhibitors. *J. Biol. Chem.* 284, 24185–24191. doi:10.1074/jbc.M109.029116

Tortorella, M., Pratta, M., Liu, R.-Q., Abbaszade, I., Ross, H., Burn, T., et al. (2000). The Thrombospondin Motif of Aggrecanase-1 (ADAMTS-4) Is Critical for Aggrecan Substrate Recognition and Cleavage. *J. Biol. Chem.* 275, 25791–25797. doi:10.1074/jbc.M001065200

Wang, Z., Wang, L., Fan, R., Zhou, J., and Zhong, J. (2016). Molecular Design and Structural Optimization of Potent Peptide Hydroxamate Inhibitors to Selectively Target Human ADAM Metallopeptidase Domain 17. *Comput. Biol. Chem.* 61, 15–22. doi:10.1016/j.compbiolchem.2015.12.003

Wu, Y., Eigenbrot, C., Liang, W.-C., Stawicki, S., Shia, S., Fan, B., et al. (2007). Structural Insight into Distinct Mechanisms of Protease Inhibition by Antibodies. *Proc. Natl. Acad. Sci.* 104, 19784–19789. doi:10.1073/pnas.0708251104

Yang, C.-Y., Chanalaris, A., and Troeberg, L. (2017). ADAMTS and ADAM Metalloproteinases in Osteoarthritis - Looking beyond the 'usual Suspects'. *Osteoarthritis and Cartilage* 25, 1000–1009. doi:10.1016/j.joca.2017.02.791

Yim, V., Noisier, A. F. M., Hung, K.-y., Bartsch, J. W., Schlomann, U., and Brimble, M. A. (2016). Synthesis and Biological Evaluation of Analogues of the Potent ADAM8 Inhibitor cyclo(RLsKDK) for the Treatment of Inflammatory Diseases and Cancer Metastasis. *Bioorg. Med. Chem.* 24, 4032–4037. doi:10.1016/j.bmc.2016.06.042

Yiotakis, A., and Dive, V. (2008). Synthetic Active Site-Directed Inhibitors of Metzincins: Achievement and Perspectives. *Mol. Aspects Med.* 29, 329–338. doi:10.1016/j.mam.2008.06.001

Zhang, E., Yan, X., Zhang, M., Chang, X., Bai, Z., He, Y., et al. (2013). Aggrecanases in the Human Synovial Fluid at Different Stages of Osteoarthritis. *Clin. Rheumatol.* 32, 797–803. doi:10.1007/s10067-013-2171-0

Zhang, W., Zhong, B., Zhang, C., Wang, Y., Guo, S., Luo, C., et al. (2018). Structural Modeling of Osteoarthritis ADAMTS4 Complex with its Cognate Inhibitory Protein TIMP3 and Rational Derivation of Cyclic Peptide Inhibitors from the Complex Interface to Target ADAMTS4. *Bioorg. Chem.* 76, 13–22. doi:10.1016/j.bioorg.2017.10.017

Zheng, X. L. (2013). Structure-function and Regulation of ADAMTS-13 Protease. *J. Thromb. Haemost.* 11, 11–23. doi:10.1111/jth.12221

Zhong, S., and Khalil, R. A. (2019). A Disintegrin and Metalloproteinase (ADAM) and ADAM with Thrombospondin Motifs (ADAMTS) Family in Vascular Biology and Disease. *Biochem. Pharmacol.* 164, 188–204. doi:10.1016/j.bcp.2019.03.033

Zorzi, A., Linciano, S., and Angelini, A. (2019). Non-covalent Albumin-Binding Ligands for Extending the Circulating Half-Life of Small Biotherapeutics. *Med. Chem. Commun.* 10, 1068–1081. doi:10.1039/c9md00018f

Zunke, F., and Rose-John, S. (2017). The Shedding Protease ADAM17: Physiology and Pathophysiology. *Biochim. Biophys. Acta (Bba) - Mol. Cel Res.* 1864, 2059–2070. doi:10.1016/j.bbamcr.2017.07.001

Conflict of Interest: SP is an employee of Fidia Farmaceutici S.p.A.

The remaining authors declare that the research was conducted in the absence of any commercial or financial relationships that could be construed as a potential conflict of interest.

frontiers in Molecular Biosciences

ORIGINAL RESEARCH
published: 31 August 2021
doi: 10.3389/fmolb.2021.707661

Shedding Light on the Molecular Recognition of Sub-Kilodalton Macrocyclic Peptides on Thrombin by Supervised Molecular Dynamics

*Mahdi Hassankalhori, Giovanni Bolcato, Maicol Bissaro, Mattia Sturlese and Stefano Moro **

Molecular Modeling Section (MMS), Department of Pharmaceutical and Pharmacological Sciences, University of Padova, Padova, Italy

Macrocycles are attractive structures for drug development due to their favorable structural features, potential in binding to targets with flat featureless surfaces, and their ability to disrupt protein–protein interactions. Moreover, large novel highly diverse libraries of low-molecular-weight macrocycles with therapeutically favorable characteristics have been recently established. Considering the mentioned facts, having a validated, fast, and accurate computational protocol for studying the molecular recognition and binding mode of this interesting new class of macrocyclic peptides deemed to be helpful as well as insightful in the quest of accelerating drug discovery. To that end, the ability of the in-house supervised molecular dynamics protocol called SuMD in the reproduction of the X-ray crystallography final binding state of a macrocyclic non-canonical tetrapeptide—from a novel library of 8,988 sub-kilodalton macrocyclic peptides—in the thrombin active site was successfully validated. A comparable binding mode with the minimum root-mean-square deviation (RMSD) of 1.4 Å at simulation time point 71.6 ns was achieved. This method validation study extended the application domain of the SuMD sampling method for computationally cheap, fast but accurate, and insightful macrocycle–protein molecular recognition studies.

Keywords: molecular recognition, macrocyclic, supervised molecular dynamics, thrombin, tetrapeptide

OPEN ACCESS

Edited by:
Luca Domenico D'Andrea, National Research Council (CNR), Italy

Reviewed by:
Jinan Wang, University of Kansas, United States
Klaus R. Liedl, University of Innsbruck, Austria

***Correspondence:**
Stefano Moro
stefano.moro@unipd.it

Specialty section:
This article was submitted to Molecular Recognition, a section of the journal Frontiers in Molecular Biosciences

Received: *10 May 2021*
Accepted: *15 July 2021*
Published: *31 August 2021*

Citation:
Hassankalhori M, Bolcato G, Bissaro M, Sturlese M and Moro S (2021) Shedding Light on the Molecular Recognition of Sub-Kilodalton Macrocyclic Peptides on Thrombin by Supervised Molecular Dynamics. Front. Mol. Biosci. 8:707661. doi: 10.3389/fmolb.2021.707661

INTRODUCTION

The ever-increasing expeditious development of computer hardware, software, and algorithms has positively contributed to many domains of research such as drug design. The developed computational methods, namely, molecular docking and molecular dynamics (MD) simulations, to name but two, greatly reduce the time and cost of drug development, in a way that *in silico* modeling tools are highly utilized in the research ambit of drug discovery (Muegge et al., 2017; Salmaso et al., 2017; Lin & Li, 2020). Particularly, the investigation of the binding mode, following the steps of varied ligand–target recognition pathways, and exploring their interactions have been claimed to be the area of impressive application of MD computational protocols (Salmaso et al., 2017).

Molecular dynamics simulations are considered an endorsed computational method in which by integrating the numerical solution of the Newton equation of motion, the time-dependent evolution of a molecular system can be revealed and described. However, obtaining a complete molecular recognition trajectory leading to binding, from the unbound to the bound state, is a rare event, and to

capture moments of importance, therapeutically speaking, *via* a free classical molecular dynamics approach requires a long microsecond timescale and therefore massive computing resources even with the novel GPU-based protocols (Buch et al., 2011; Dror et al., 2011; Shan et al., 2011).

Our in-house alternative MD approach, compared to the classical method, named supervised molecular dynamics (SuMD), improves the efficiency of sampling a binding event and decreases the simulation time from a microsecond (μs) to a nanosecond (ns) timescale (Sabbadin and Moro, 2014). To do that, it applies a tabu-like algorithm to monitor the distance between the ligand center of mass and the target binding site center of mass during a short classical MD simulation; only productive simulations in terms of reducing this distance are considered productive. Despite the exploration of the recognition event, SuMD has been previously proved to be able to reproduce the experimental bound state of various kinds of complexes with great geometric accuracy. Its already validated application domain covers the molecular recognition simulation of small molecules, natural linear peptides, most classic peptidomimetics, and nucleic acids (Bissaro et al., 2020).

Among different classes of compounds, macrocycles are attractive structures for drug development, due to their potential in binding to "undruggable and canonical small molecules or proteins" (Kale et al., 2019). Macrocyclic peptides represent an efflorescing class of molecules potentially targeting numerous disease-related protein targets otherwise intractable *via* established pharmacological approaches (Passioura, 2020). Several remarkable characteristics can be considered for this class of molecules. First, compared to linear peptides, they are relatively stable and less prone to protease degradation. The cyclization also confers advantages such as having a compromised state between a flexible and a preorganized structure required for dynamic interactions with protein targets with a conformational bias; a reduced binding entropy cost can be imagined compared to their linear counterparts (Giordanetto and Kihlberg, 2014). However, it is worth to mention that due to the reduced accessible conformational states, shifting the structure—upon macrocyclization—toward states that can anticipate bioactivity for a specific target binding site is consequential because otherwise the non-bioactive conformation stabilization can slow down the binding. Therefore, identification of highly populated conformations of macrocycles is of significance when it comes to drug design (Kamenik et al., 2018). Moreover, it has been shown that macrocyclic peptides are capable of selectively binding to relatively shallow, flat, and featureless protein surfaces often involved in clinically important protein–protein interactions (PPIs), in a fashion similar to antibody-based therapeutics and conversely to small molecules which generally need a pocket to bind (Deyle et al., 2017; Vinogradov et al., 2019). Furthermore, thanks to their amino acid composition, a low innate toxicity is anticipated which is of advantage as therapeutic modalities. Being synthetically accessible makes possible lead optimization attempts and altering biophysical properties in terms of binding affinity and specificity, proteolytic stability, and/or solubility improvement for a particular purpose. A variety of macrocyclization reactions have been devised over the years, and now different topologies can be easily synthetically available (Vinogradov et al., 2019). However, this interesting class of molecules has been underrepresented in numbers and diversity in the available libraries (Kale et al., 2019). In recent years, innovative approaches evolved for further development of cyclic peptides, such as generating and screening large combinatorial cyclic peptide libraries using *in vitro* display. These attempts have increased the availability and potential screening of ten to hundreds of thousands up to 1 trillion compounds or more highly diverse macrocycles with extraordinary target affinity, selectivity, and bioactivity (Deyle et al., 2017; Taylor et al., 2017; Kale et al., 2019; Passioura, 2020). In a recent research project of Kale et al., *via* novel thiol-to-amine cyclization reactions, they introduced a strategy that enables the generation of a high-yield purification-free large library of diverse macrocycles to screen for various targets in an efficient, relatively small-effort manner. Generating a library containing 8,988 macrocycles of sub-kilodalton molecular weight (ideal for addressing the lingering challenge of macrocycles) and screening of this library against thrombin and other homologous targets identified a potent selective thrombin inhibitor called P2 (Ki = 42 ± 5 nM) (Kale et al., 2019).

Given the emerged perspective stemming from all referred above, having a reasonably fast and accurate computational method like SuMD for studying the molecular recognition pathway and reproduction of an experimentally comparable binding mode of this promising macrocyclic class of peptides is deemed significant. With that intent, through this study, the ability of the SuMD protocol in the reproduction of the X-ray crystallography final bound state of the candidate macrocyclic peptide P2 as a potent thrombin inhibitor was evaluated.

P2 is a tetrapeptide composed of "glycine"–"L-beta-homoproline"–" arginine"–"cysteine" cyclized with a linker of di-bromomethyl benzyl and an N-(2-(hydroxymethyl)benzyl) substituent coming from an additional reaction of the linker (**Figure 1**). P2 is proved to be a highly selective inhibitor for thrombin with a snug fit of the specific backbone to the target, while it did not show any considerable inhibition for other homologous structurally and functionally similar proteases such as activated protein C (APC) and tissue plasminogen activator (tPA), to name but two (Kale et al., 2019). A representation of thrombin in complex with the P2 structure is shown in **Figure 1**. During library screening, another macrocycle called P1 with a similar structure to P2 and merely lacking the hydroxymethyl-benzyl moiety showed three orders of magnitude lower inhibition constant than P2 (Kale et al., 2019). Given that and the fact of any experimentally reported binding state not being available for P1, the idea to try simulating a probable binding mode of P1 in addition and possibly hypothesizing the inhibition potency difference through our *in silico* studies was emerged.

The protein target in this study, thrombin, is a typical trypsin-like serine protease and the final generated protease during the blood coagulation cascade. It is worth raising the point that distinct structural features are present in this single protease for the recognition ability of different substrates in a specific

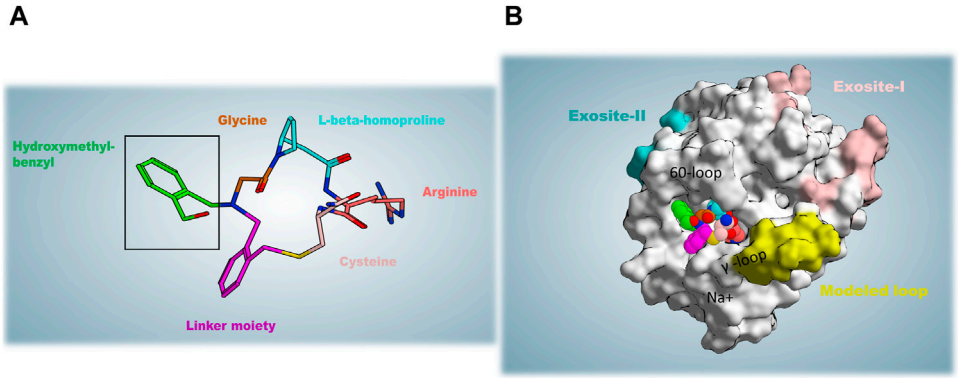

FIGURE 1 | (A) The structure of P2 is shown; the hydroxymethyl-benzyl moiety (in green) that is lacking in the P1 macrocycle is highlighted by a black frame. **(B)** Thrombin in complex with P2; thrombin structural determinants for its function and client recognition are also reported.

manner (Huntington, 2005; Huntington, 2008). As reported in **Figure 1**, the walls of a deep active site cleft—often referred to as canyon—are formed by the two insertion loops known as the 60-loop and γ-loop. The upper 60-loop, is a rigid, hydrophobic cap over the active site, while the more hydrophilic and flexible γ-loop is situated at the downside of the cleft. A constricted access to the catalytic site of thrombin is provided only to proteins with long, flexible substrate loops (Huntington, 2005). The substrate recognition within the active site of thrombin occurs thanks to favorable interactions between the P1 residue [according to the Schechter and Berger nomenclature of amino acid residues around the substrate scissile bond (Schechter and Berger, 1967)] and the deep acidic S1 pocket (Asp189, Ser190, Gly219), as well as the presence of hydrophobic/aromatic residues N-terminal to P1 occupying the S2 pocket (Tyr60A and Trp60D as the main residues) and S3 (the aryl-binding pocket composed of Trp215, Leu99, Ile174) (Huntington, 2005; He et al., 2015; Fong, 2017). Apart from the active site, three other regions are involved in the diverse specific recognition of different substrates. There are two electropositive exosites, termed anion-binding exosites (ABEs) and a sodium-binding site. The all-natural thrombin substrate directly or *via* cofactor mediation establishes contacts with at least one exosite and usually both; this represents the prerequisite event to form initial stable complex conformation needed for the peptide bond cleavage (Chahal et al., 2015; Huntington, 2005, 2008). The sodium-binding site, 15 Å away from the catalytic triad (His57, Asp102, Ser195), with Na^+ coordinated to the main chain oxygen atoms of Arg221a and Lys224 and four conserved water molecules, is considered another allosteric activity modulator site of this protease, helping the maintenance of the hemostatic balance. Upon binding to sodium, thrombin shifts toward a conformation known as "fast conformation" able to cleave all procoagulant substrates such as fibrinogen- and protease-activated receptors more readily. On the contrary, in the Na-unbound "slow" state, the protein C anticoagulant pathway is preferentially activated. Under physiologic conditions, the 140 mmol/L Na^+ concentration in the blood would not saturate the site, and a present 2:3 ratio of slow: fast states accounts for optimal allosteric regulation of anticoagulant: procoagulant activities and hemostasis (Di Cera, 2003; Huntington, 2008; Kahler et al., 2020).

MATERIALS AND METHODS

Computational Study Infrastructure

This project was carried out on a hybrid GPU–CPU Linux cluster of 280 CPU cores and 30 NVIDIA graphic cards.

Structure Preparation

To begin with the simulation, the three-dimensional coordinates of the crystal structure of thrombin bound to the P2 macrocycle (PDB ID: 6GWE) were retrieved from the RCSB Protein Data Bank (PDB) with a resolution of 2.3 Å (Kale et al., 2019). Then, using MOE suite (*Molecular Operating Environment (MOE)* & Chemical Computing Group ULC) version 2019.01, the structure was checked and modeled (*via* the loop modeler plugin) for the missing loop, 3D protonated, and energy minimized regarding the energy of the added hydrogens and their positions. For this study, one of each unique chain which is chain A with 257 residues and chain B with 30 residues in their sequence, in addition to the sodium ion bound to the chain A sodium binding loop, was kept. The modeled eight-residue missing loop between Glu146 and Gly150 amino acid sequences comprised of TWTANVGK.

Solvated System Setup and Equilibration

All MD simulations were carried out using AMBERTools14 (Case et al., 2014). To parameterize the ligand, the *Antechamber* tool (Wang et al., 2006) in conjunction with a general Amber force field (GAFF) (Wang et al., 2004) was utilized to classify atom and bond types, assign charges, and estimate force field parameters. The charge method AM1-BCC of the GAFF which is semi-empirical was used in this study. The solvation box with charge neutrality and physiological ionic strength (0.154 M in Na^+ and Cl^- ions), as well as complex system parameters and topology files, was prepared using tLEaP (Case et al., 2005).

Protein and water were represented by Amber *ff14SB* (Maier et al., 2015) and TIP3P (Jorgensen et al., 1983) models, respectively, in the prepared system. In all SuMD replicas, simulation starts with the ligand located 40 Å far from the orthosteric active site at time zero, which is a distance bigger than the electrostatic cut-off term used in the simulation (9 Å with the Amber force field), to avoid premature interaction during the initial phases of SuMD simulations.

All simulation systems were energy minimized through two equilibration steps. Considering 2 fs as a time step equal to the vibrational frequency of bonds, 500,000 steps (1 ns) of NVT in addition to 500,000 steps (1 ns) of NPT simulations were carried out. Gradual reduction of harmonic positional constraints by a force constant of 5 kcal mol^{-1} $Å^{-2}$ was applied in both steps. In the first equilibration, ions (except bounded Na^+ in the sodium-binding loop) and water were kept free, while protein and ligand atoms were constrained. However, in the second equilibration, the constraints were kept only on the alpha carbons of the protein, as well as ligand atoms and the loop sodium. In both steps, the temperature was maintained at 310 K by a Langevin thermostat with low damping of 0.1 ps^{-1}, and in the second NPT step, the pressure was maintained at 1 atm by a Berendsen barostat as well (Berendsen et al., 1984). To calculate electrostatic interactions with a cubic spline interpolation and a 9.0 Å cut-off for Lennard–Jones interactions, the particle-mesh Ewald (PME) method was utilized (Essmann et al., 1995).

Supervised Molecular Dynamics Production

The SuMD simulations were done in NVT conditions with the temperature equal to 310 K, while the pressure of the system was free to change. To perform a supervised MD simulation, the topology and coordinates of the last frame of the second equilibration phase were used as the starting point. In the configuration file of SuMD, three selected amino acid residues Glu97A, Gly219, Cys191 whose center of mass (CM) approximately defines the binding site CM were inputted. SuMD applies a dynamic selection on the indicated residue position to calculate the center of mass of the binding site. MOE suite was used to determine the center of mass of the co-crystallized ligand regarded as the center of mass of the thrombin active site to be then visually selecting a combination of residues that their center of mass could represent the approximate position of the binding site guiding the supervision. Each SuMD replica was produced on a graphics machine using ACEMD3 (Harvey et al., 2009) as the MD engine. The length of the SuMD steps for SuMD replicas was set to either a 600 ps or a 1 ns time window.

Free (Unsupervised) Classical Molecular Dynamics Production

For each cMD, after system preparation and equilibration steps, the ACEMD3 (Harvey et al., 2009) engine was used with the same settings, except for the simulation length, of the cMD simulation in each SuMD step.

Visualization of the Molecular Dynamics Trajectories

Visual Molecular Dynamics (VMD) (Humphrey et al., 1996) and MOE suite (*Molecular Operating Environment (MOE)* & Chemical Computing Group ULC) were utilized during this project for molecular visualization and analysis of the trajectories.

Trajectory Versus Trajectory Root-Mean-Square Deviation Calculation

Using MDAnalysis (Michaud-Agrawal et al., 2011; Gowers et al., 2016), a matrix of frames related to the cMD of reference against frames of each SuMD replica was set for comparative root-mean-square deviation (RMSD) calculation. Then *via* the Seaborn Python library (Waskom et al., 2020), a heat map of the resulting RMSD calculation was illustrated (**Figure 2**).

MM-GBSA Energetic Profile Analysis and Clustering

All total free energy calculations in this work were computed using the MMPBSA.py tool (Miller et al., 2012) using the GB-OBC(II) Born solvation model and no entropy calculation. To identify other energetically favorable binding sites and elucidate a P2 ligand–protein recognition scenario, the trajectories of 99 SuMD replicas of P2 were first solvent-dried, aligned, merged, and ten times strided as input for positional clusterization. To do so, ligand sets of coordinates (each set of coordinates corresponds to the ligand conformation in a frame) after discarding noise sets considering a cosine similarity value of 0.01 were clusterized using the OPTICS algorithm of Scikit-learn (Pedregosa et al., 2011). Thereafter, given the MM-GBSA value of the included ligand coordinates in each cluster, the representative ligand conformation with the most favorable energetic value was selected for the corresponding cluster.

RESULTS

Study Principal Outcomes

This study was conducted aiming to extend the application domain of our molecular dynamics supervision method for studies related to models of the sub-kilodalton macrocyclic peptide–protein binding event. As a case study, the SuMD ability to reproduce the X-ray crystallography bound state of the P2 macrocyclic peptide to thrombin was evaluated. To that end, 99 SuMD simulations were performed starting from an unbound state obtained by separating P2 from its binding site by around 40 Å. Among 99 SuMD replicas, 84 trajectories finished with the ligand arriving in the proximity of the binding site and its sub-pockets with different binding orientations and conformations, while 15 trajectories ended with the ligand stopping over a varied site categorized as "failed" based on SuMD termination criteria (far from the binding site). Overall, five trajectories concluded with the ligand reaching the narrow S1

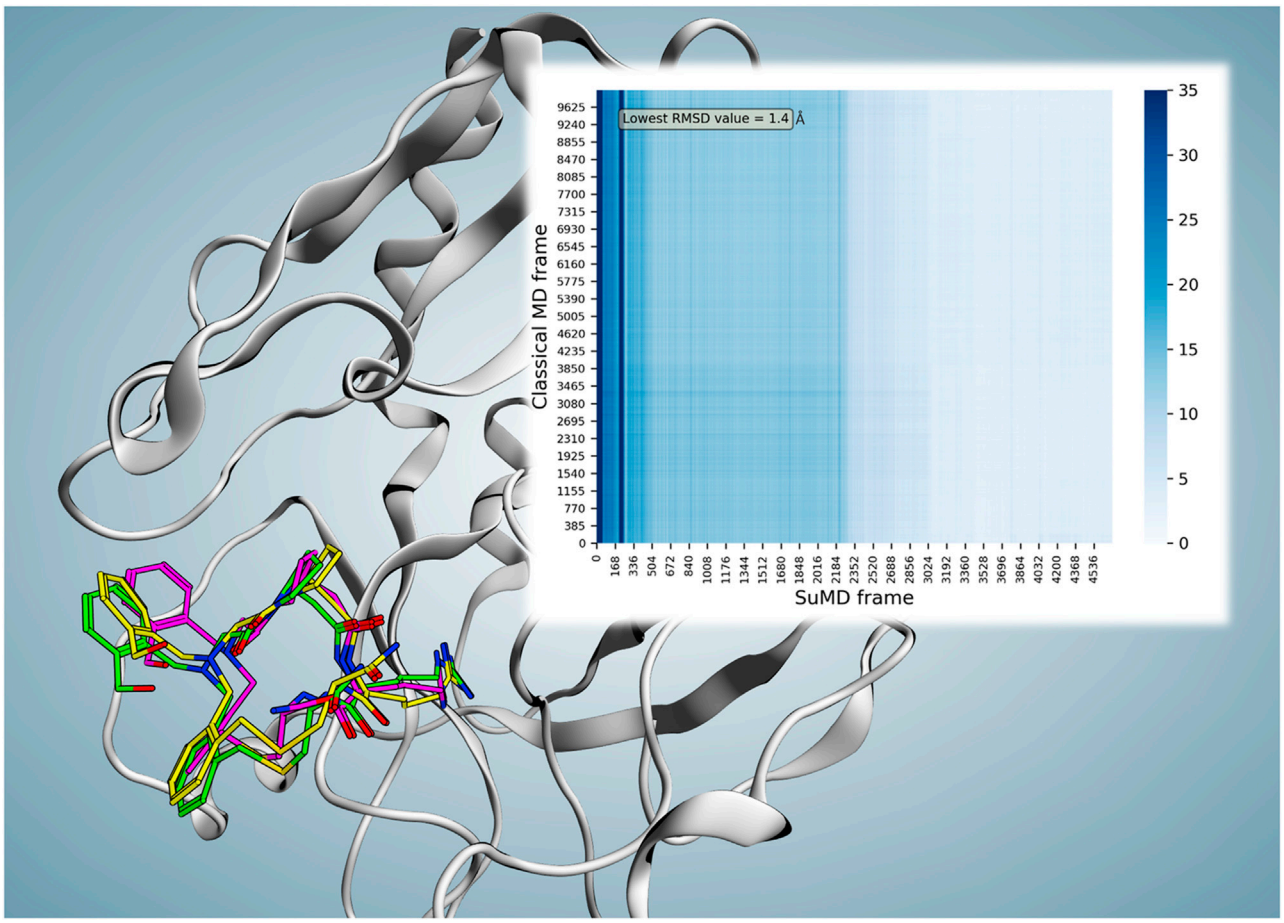

FIGURE 2 | Superposition of the P2-reported X-ray crystallography conformation (magenta), frame number 102 (2.04 ns) of reference cMD (green), and frame number 3,579 (71.56 ns) of replica 74 (yellow; the frame with the lowest RMSD value compared to both reported binding conformation and the parallel trajectory analysis reference resulted in the frame). The minimum obtained RMSD compared to the reported binding conformation showed a value of 2.27 Å at time point 71.56 ns. However, considering the observed instability of the reported conformation, parallel frame RMSD calculation of the replica 74 trajectory versus reference cMD trajectory was performed which resulted in the minimum RMSD value of 1.4 Å at 71.56 ns for frame number 3,579 (the same frame with the lowest RMSD value compared to the reported binding conformation). The heat map of the parallel trajectory RMSD analysis of replica 74 versus reference cMD is shown on the top right.

pocket (guanidinium moiety entering S1), all below 100 ns of SuMD-productive simulation time.

To better compare the SuMD results with the experimental structure, the X-ray crystallography complex (reference) was subjected to 200 ns of cMD, allowing to have both systems in similar conditions: equilibrated and relaxed in a fully explicit solvent environment. In fact, during the initial 4 ns of the cMD, a fluctuation within the range of experimental resolution (2.3 Å) was observed, while after 4 ns, a more significant shift of the macrocycle occurred as confirmed by a drop of its RMSD values to above 3 Å and below 5.66 Å until the end (200 ns) was detected (**Supplementary Video S1**). The mean calculated RMSD during this trajectory was 3.57 ± 0.47 Å (**Supplementary Figure S1**). Those RMSD values highlight a discrepancy between the experimental bound conformation and the one assumed once the system is equilibrated in a fully explicit solvent suggesting that the cMD could represent a more adequate comparison for SuMD. Indeed, we performed a frame-to-frame analysis of the SuMD trajectory versus cMD trajectory monitoring the ligand RMSD. Among all replicas, replica 74 is deemed the best-produced binding event trajectory for P2. This SuMD simulation (replica 74) with 94 ns duration reproduced a possible binding event trajectory with the most comparability to the X-ray crystallography binding mode. The minimum obtained RMSD compared to the X-ray conformation showed a value of 2.27 Å at time point 71.56 ns. However, considering the cMD trajectory as a reference, the minimum RMSD value is 1.4 Å at the same time point (71.56 ns, frame number 3,579) versus frame number 102 (2.04 ns) of reference cMD (**Figure 2**).

The simulation started with P2 located 40 Å far from the orthosteric active site (AS) at time zero (**Supplementary Video S2**), and then upon approaching the AS, the first stable binding occurred from time point 5.5 ns until 43 ns with a mean MM-GBSA free energy (ΔG) of −27.1 kcal/mol. As this stopover had enough residence time to break the progressive and continual approach of the ligand, it can be defined as a meta-stable binding

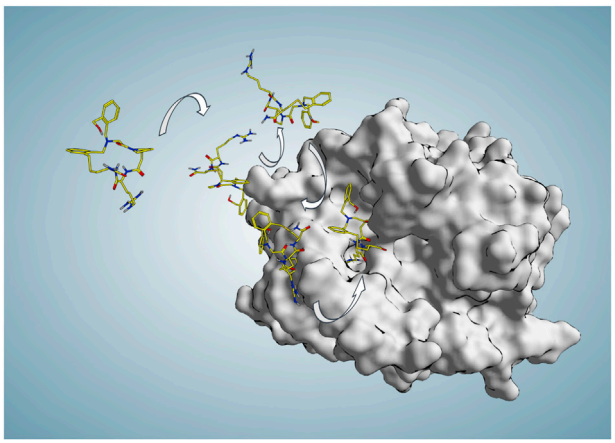

FIGURE 3 | Some representative P2 poses along the binding trajectory (94 ns) produced in SuMD replica 74 during which P2 starts approaching the active site from 30 Å far from any protein atom at time zero and reaches the binding site and S1 pocket in an experimentally comparable binding mode ($RMSD_{min}$ = 1.4 Å at 71.56 ns).

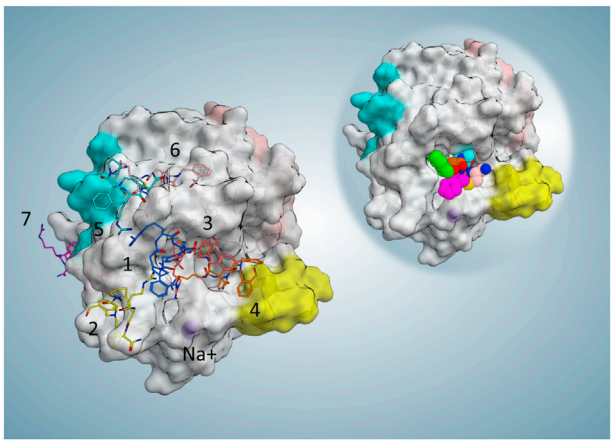

FIGURE 4 | Representative frame (minimum MM-GBSA free binding energy in each cluster) and position of each cluster. For the collective illustration of all representing poses on one protein surface, the molecular surface of the reference PDB is selected to be shown here. On the top right reference, the complex is shown to indicate the active site position.

site. Afterward, for around 4 ns from time point 48 ns, another stable contact near the active site (ΔG = −18.9 kcal/mol) was seen as the ligand was transitioning to the active site area. Then, from 54 ns, a favorable orientation of P2 facilitated the entrance of the fundamental guanidinium moiety to the S1 pocket. From that point, an initial evolution of the final binding state phase was followed by fluctuating but stable similar conformations until the end. The mean total ΔG of the last 22.44 ns (from the $RMSD_{min}$ frame until the end) resulted in a value of −27.3 kcal/mol compared to the calculated mean total ΔG value of −32.2 kcal/mol in the same duration (22.44 ns) of reference cMD, showing a similar with no meaningful MM-GBSA difference (ΔΔG < 5 kcal/mol) energetic profile. Some of the most relevant ligand P2 conformations during this binding trajectory are presented in **Figure 3**. To evaluate the P2 flexibility, we calculated its RMSD during the best five trajectories; the ligand fluctuates until 5.7 Å, suggesting that a certain flexibility is explored during the recognition (**Supplementary Figure S2**). To identify significant states during the P2 recognition and their corresponding metastable binding sites, all the conformations sampled during all the SuMD trajectories were geometrically clustered resulting in seven clusters (**Figure 4**). All the clusters showed a favorable average of MM-GBSA binding free energy values compared to the calculated value for the reference binding conformation in the canonical binding site (active site) (**Table 1**). This outcome suggests multiple energetically favorable binding patches on the thrombin surface for P2. Among all the clusters, the seventh cluster comprised of 2–3 times higher number of frames with the minimum average free energy value of −33 kcal/mol. The position of this cluster population was identified near exosite II. Given high population of the seventh cluster, a highly favorable binding free energy value—closely comparable to the canonical binding site—of this positional cluster is near exosite II which is considered an important contact point for natural thrombin substrates to form an initial stable complex conformation required for the peptide bond cleavage; it can be hypothesized that thrombin inhibition by P2 might be resulted from dual-site inhibition, i.e., allosterically preventing the selective stable recognition of substrates in addition to occupying the orthosteric proteolysis site and thus being a potent thrombin inhibitor.

Elucidation of the Role of Hydroxymethyl-Benzyl Moiety

Asp1 shares the same structure of P2 except for the presence of a hydroxymethyl-benzyl structure on the latter; a similar binding mode and orientation of the ligand with the guanidinium moiety entering the S1 pocket and the macrocycle occupying the rest of the active site could be hypothesized. For further witnessing of SuMD helpful implication in depicting the molecular basis of the recognition of this class of compounds, we investigate the hydroxymethyl-benzyl role that leads to an increased inhibition activity (three orders of magnitude); SuMD simulations for P1 were additionally performed until reaching a representative replica (**Supplementary Video S3**) in which P1 fully enters the active site S1 pocket to establish a salt bridge with Asp189. After 18 replicas (in 16 replicas, P1 reached the binding site in different final binding modes, among which six replicas had the supposed orientation and one had expected orientation while entering the S1 pocket), we obtained a possible binding trajectory in which during 34.84 ns of simulation, P1 reached the active site with guanidinium partly inside the S1 pocket as supposed. For further evolution and reaching the most stable conformation, the simulation continued with 50 ns of cMD. After that, a stable conformation was achieved, having a salt bridge with Asp189 and contacting four of the same reference P2 interacting residues (Asp189, Cys220, Gly216, Glu217) (**Figure 5**).

To compare P1 and P2 from an energetic point of view, the mean total MM-GBSA binding free energy during 50 ns of cMD

TABLE 1 | Size and energetic analysis of all the clusters obtained during P2 SuMD simulations.

Cluster No.	Number of included frames	Average MM-GBSA total ΔG (kcal/mol) (rounded)
1	459	−22
2	309	−28
3	460	−27
4	356	−32
5	438	−26
6	275	−28
7	890	−33

Several conformations showed a favorable MM-GBSA binding free energy value suggesting multiple energetically favorable binding states on the thrombin surface for P2.

trajectories was taken into consideration. The calculated total $\Delta G_{P1} = -20.2$ kcal/mol and total $\Delta G_{P2} = -29.3$ kcal/mol show a more favorable energy profile in P2 as expected. To be confident about the compared value correctly associated with the final evolved stable P1 binding conformation, similar total $\Delta G_{P1} = -20.37$ kcal/mol was obtained for the last 6 ns of the P1 continued cMD ($RMSD_{last\ 6\ ns} = 1.4 \pm 0.4$ Å). The energy landscape of P1 and P2 trajectories (**Figure 6**) indicates a similar profile characterized by a large number of energetically stable frames when the distance between the centers of mass ($dcm_{L\text{-}R}$) is in the range of 3–7.5 Å. This observation suggests that many ligand states, even if they present different binding modes, contribute to a stable protein–ligand association. The presence of metastable binding sites far from the active site ($dcm_{L\text{-}R} > 10$ Å) is slightly more pronounced in the representative trajectory of P2 where three transient spikes are evident at $dcm_{L\text{-}R}$ 9, 15, and 20 Å.

Additionally, to compare P1 and P2 structural characteristics and their possible effects on each ligand dynamics and binding during the SuMD condition, the representative replica of P2 and the P1 residue were selected for further analysis. Given the experimental final binding state of P2, an internal hydrogen bond (2.15 Å/H-O) between the hydrogen atom of the hydroxyl group of the hydroxymethyl-benzyl moiety and the nearby carbonyl group of the macrocycle ring can be seen. This hydrogen bond during the produced binding event trajectory (replica 74) sustains an average value of 2.72 Å (H-O). Considering that, it could be hypothesized that this present internal bond thanks to the hydroxymethyl-benzyl moiety which is absent in P1 contributes to a less flexible structure and a biased maintained conformation necessary for the observed favorable snug-fit binding. To corroborate this idea, the average RMSD of the mutual macrocycle ring of P2 and P1 during the time, in addition to the RMSD of the whole structure of each ligand along their representative SuMD trajectory, was calculated. For this RMSD calculation, all frames of each representative replica were aligned on the comprising atoms of the mutual ring of the corresponding replica's first frame separately. The calculations obtained in this way indicate the flexibility of the

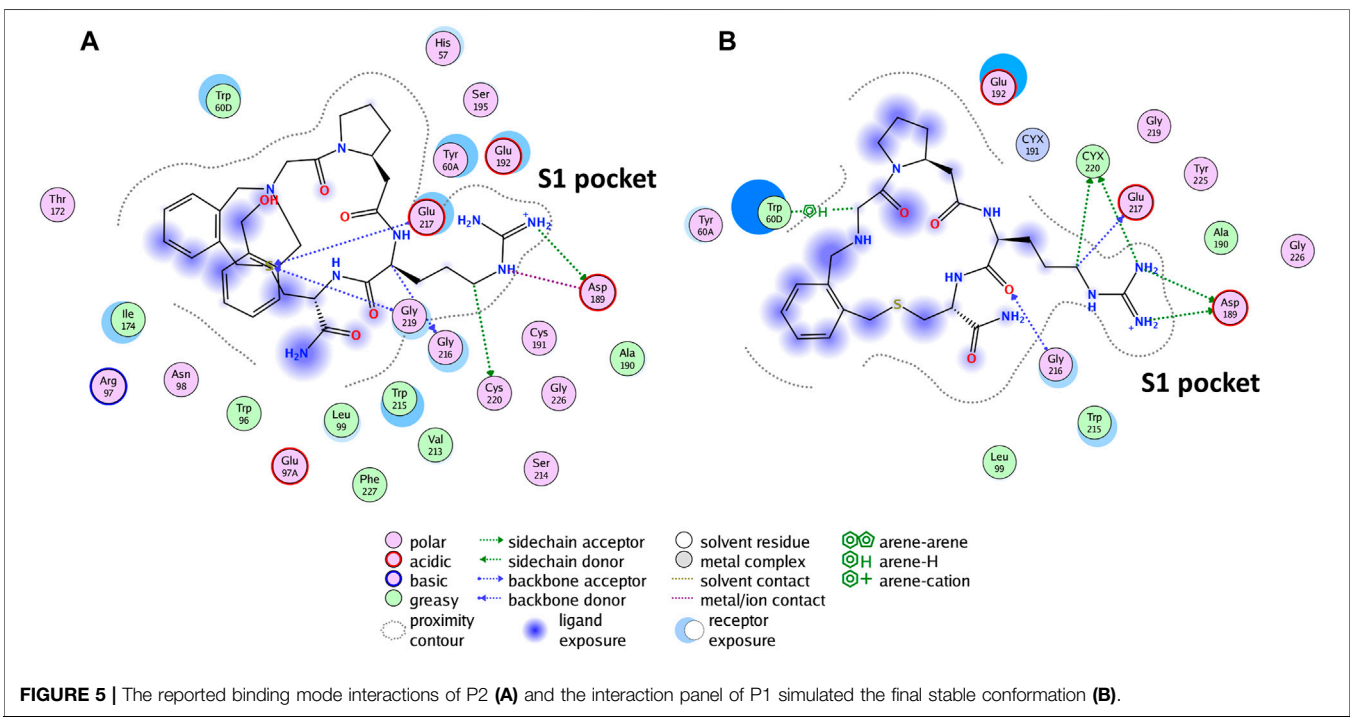

FIGURE 5 | The reported binding mode interactions of P2 **(A)** and the interaction panel of P1 simulated the final stable conformation **(B)**.

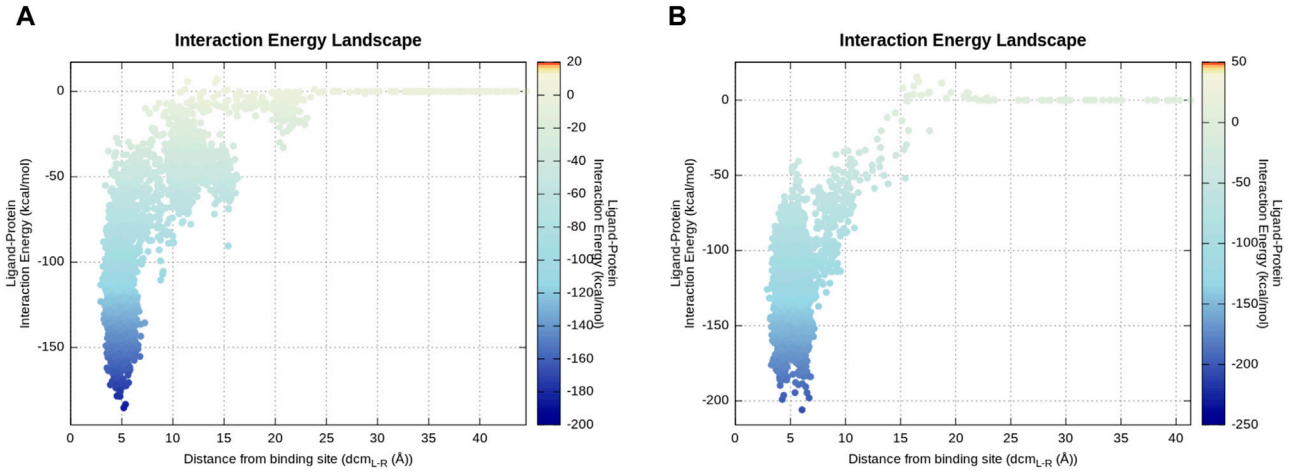

FIGURE 6 | Energy landscape of P2 **(A)** and P1 **(B)** representative produced trajectories. The interaction energy calculation is based on the *mdenergy* function of VMD (Humphrey et al., 1996) and plotted *via* an in-house pepSuMD analyzer (Salmaso et al., 2017). **(A)** Along this trajectory, 2–3 local minima can be seen which correspond to meta-stable binding sites for P2. **(B)** P1 directly goes to the canonical active site during this representative trajectory.

mutual ring and each ligand and not the ligand transition during their molecular dynamics trajectory. The achieved values of the mutual ring and the whole ligand in the P2 trajectory were, respectively, four times and 2.7 times less than calculated values for P1 (average $RMSD_{ring/P2} = 0.41 \pm 0.15$ Å, average $RMSD_{ligand/P2} = 1.62 \pm 0.4$ Å; average $RMSD_{ring/P1} = 1.68 \pm 0.22$ Å, average $RMSD_{ligand/P1} = 4.43 \pm 0.56$ Å). Thus, as expected, this result can quantitatively show a more biased stable conformation for P2 during time compared to P1.

DISCUSSION

In this study, the ability of the SuMD protocol in the reproduction of the X-ray crystallography final binding state of the candidate macrocyclic tetrapeptide P2—from a novel library of 8,988 sub-kilodalton macrocyclic peptides—bound to thrombin to inhibit its activity was successfully investigated (minimum RMSD of 1.4 Å at 71.56 ns). The outcomes reported that more than 80 percent of trajectories reached the canonical binding surface in varied conformations below or around a hundred nanoseconds, and near five percent mimic the experimentally solved final bound state for this class of macrocyclic peptides to a challenging target, characterized by a narrow active site cleft and deep significant-for-activity sub-pocket (S1). These results reiterated and extended SuMD high value as a computational protocol to explore the recognition pathway. Additionally, based on the observations, SuMD can be regarded as an insightful tool in terms of meta-stable binding site identification, as well as the binding mode and molecular recognition pattern elucidation of sub-kilodalton macrocyclic peptides (with different scaffolds than natural peptides or small molecules) to a protein target with relatively low computational expense. Therefore, this study further validated and expanded the applicability of SuMD as a valuable protocol in studying varied molecular complex recognition.

The main advantages of the method used in this work are being able to correctly parameterize the ligand P2 of this class of macrocyclic peptides with a general Amber force field (GAFF) similar to small molecules and thus having no need for tailored parameterization due to the presence of unnatural amino acids and linkers, as well as the possibility to simulate the trajectory of a binding event in the nanosecond timescale thanks to SuMD. Consider that the association event starting from an unbound state is a rare event to be observed by cMD without the implementation of an enhanced sampling strategy. For instance, in **Supplementary Video S4**, a comparative cMD starting from the same state of SuMD is reported; during the 900 ns of simulation, P2 never approached thrombin, confirming the different sampling rate of the two methods. The opportunity of performing an efficient high-throughput molecular dynamics study of the remaining macrocyclic peptides of the same class, after further optimization and validation, can be envisioned. Therefore, the prospective use of this study's findings would be toward using SuMD to perform high-throughput molecular dynamics studies of other available macrocyclic peptides of the same class, enjoying a highly diverse scaffold, to find probable hit candidates for various protein targets of interest and predict their binding mode as an adjunct predictive and screening tool, similarly to what was recently reported for fragments (Ferrari et al., 2021), narrowing down the requirement of going through experimental structural studies for each molecular complex of interest. On the contrary, a particular attention should be paid to the starting conformation of the macrocycle that could affect the recognition sampling since its flexibility could be rather pronounced. Specific methods (e.g., low-mode MD) are used to preprocess a novel ligand for selecting at least one of the few adequate starting conformations in solution. It should also be considered that a particularly flexible sub-kDa macrocycle could

present more issue in sampling the bound conformation during the recognition. Anyway, all of these prospective enhancements would lead to the main goal of achieving computationally cheap molecular dynamics study methods with ever-increasing power in predicting experimentally equivalent final binding states and recognition of key elements and patterns of complexes.

DATA AVAILABILITY STATEMENT

The original contributions presented in the study are included in the article/**Supplementary Material**, and further inquiries can be directed to the corresponding author.

AUTHOR CONTRIBUTIONS

SM and MS conceived the research idea and approach. MH, GB, MB and MS carried out all computational simulations. MH, MS, and SM wrote the manuscript. All authors discussed the results and reviewed the manuscript.

FUNDING

This scientific work was financially supported by MIUR (PRIN 2017, no. 2017MT3993) and by the University of Padova under the STARS Grants program (SUMD4FBDD).

ACKNOWLEDGMENTS

MMS Lab is very grateful to Chemical Computing Group, OpenEye, and Acellera for the scientific and technical partnership. MMS Lab gratefully acknowledges the support of NVIDIA Corporation for the donation of the Titan V GPU, used in this research.

SUPPLEMENTARY MATERIAL

The Supplementary Material for this article can be found online at: https://www.frontiersin.org/articles/10.3389/fmolb.2021.707661/full#supplementary-material

REFERENCES

Berendsen, H. J. C., Postma, J. P. M., Van Gunsteren, W. F., Dinola, A., and Haak, J. R. (1984). Molecular Dynamics with Coupling to an External bath. *J. Chem. Phys.* 81 (8), 3684–3690. doi:10.1063/1.448118

Bissaro, M., Sturlese, M., and Moro, S. (2020). Exploring the RNA-Recognition Mechanism Using Supervised Molecular Dynamics (SuMD) Simulations: Toward a Rational Design for Ribonucleic-Targeting Molecules? *Front. Chem.* 8, 107. doi:10.3389/fchem.2020.00107

Buch, I., Giorgino, T., and De Fabritiis, G. (2011). Complete Reconstruction of an Enzyme-Inhibitor Binding Process by Molecular Dynamics Simulations. *Proc. Natl. Acad. Sci.* 108 (25), 10184–10189. doi:10.1073/pnas.1103547108

Case, D. A., Cheatham, T. E., Darden, T., Gohlke, H., Luo, R., Merz, K. M., et al. (2005). The Amber Biomolecular Simulation Programs. *J. Comput. Chem.* 26 (16), 1668–1688. doi:10.1002/jcc.20290

Case, D., Babin, V., Berryman, J., Betz, R., Cai, Q., Cerutti, D., et al. (2014). *Amber 2014*. San Francisco: University of California.

Chahal, G., Thorpe, M., and Hellman, L. (2015). The Importance of Exosite Interactions for Substrate Cleavage by Human Thrombin. *PLoS One* 10 (6), e0129511. doi:10.1371/journal.pone.0129511

Deyle, K., Kong, X.-D., and Heinis, C. (2017). Phage Selection of Cyclic Peptides for Application in Research and Drug Development. *Acc. Chem. Res.* 50 (8), 1866–1874. doi:10.1021/acs.accounts.7b00184

Di Cera, E. (2003). Thrombin Interactions. *Chest*, 124(3), 11S–17S. doi:10.1378/chest.124.3_suppl.11S

Dror, R. O., Pan, A. C., Arlow, D. H., Borhani, D. W., Maragakis, P., Shan, Y., et al. (2011). Pathway and Mechanism of Drug Binding to G-Protein-Coupled Receptors. *Proc. Natl. Acad. Sci. USA* 108 (32), 13118–13123. doi:10.1073/pnas.1104614108

Essmann, U., Perera, L., Berkowitz, M. L., Darden, T., Lee, H., and Pedersen, L. G. (1995). A Smooth Particle Mesh Ewald Method. *J. Chem. Phys.* 103 (19), 8577–8593. doi:10.1063/1.470117

Ferrari, F., Bissaro, M., Fabbian, S., De Almeida Roger, J., Mammi, S., Moro, S., et al. (2021). HT-SuMD: Making Molecular Dynamics Simulations Suitable for Fragment-Based Screening. A Comparative Study with NMR. *J. Enzyme Inhib. Med. Chem.* 36 (1), 1–14. doi:10.1080/14756366.2020.1838499

Fong, C. (2017). "The Binding of Ligands to Thrombin, Trypsin and Avidin: Validation of a Structure Activity Model,". [Research Report] Eigenenergy (Adelaide, Australia: ffhal-01659878v2). doi:10.5176/2251-1679_cgat17.13

Giordanetto, F., and Kihlberg, J. (2014). Macrocyclic Drugs and Clinical Candidates: What Can Medicinal Chemists Learn from Their Properties? *J. Med. Chem.* 57 (2), 278–295. doi:10.1021/jm400887j

Gowers, R. J., Linke, M., Barnoud, J., Reddy, T. J. E., Melo, M. N., Seyler, S. L., et al. (2016). *MDAnalysis: A Python package for the rapid analysis of molecular dynamics simulations. In S. Benthall and S. Rostrup, editors, Proceedings of the 15th Python in Science Conference United States*. Austin, TX, 278–295. doi:10.25080/majora-629e541a-00e

Harvey, M. J., Giupponi, G., and Fabritiis, G. D. (2009). ACEMD: Accelerating Biomolecular Dynamics in the Microsecond Time Scale. *J. Chem. Theor. Comput.* 5 (6), 1632–1639. doi:10.1021/ct9000685

He, L.-W., Dai, W.-C., and Li, N.-G. (2015). Development of Orally Active Thrombin Inhibitors for the Treatment of Thrombotic Disorder Diseases. *Molecules* 20 (6), 11046–11062. doi:10.3390/molecules200611046

Humphrey, W., Dalke, A., and Schulten, K. (1996). VMD: Visual Molecular Dynamics. *J. Mol. Graphics*, 14(1), 33–38. doi:10.1016/0263-7855(96)00018-5

Huntington, J. A. (2008). How Na+ Activates Thrombin - a Review of the Functional and Structural Data. *Biol. Chem.* 389 (8), 1025–1035. doi:10.1515/bc.2008.113

Huntington, J. A. (2005). Molecular Recognition Mechanisms of Thrombin. *J. Thromb. Haemost.* 3 (8), 1861–1872. doi:10.1111/j.1538-7836.2005.01363.x

Jorgensen, W. L., Chandrasekhar, J., Madura, J. D., Impey, R. W., and Klein, M. L. (1983). Comparison of Simple Potential Functions for Simulating Liquid Water. *J. Chem. Phys.* 79 (2), 926–935. doi:10.1063/1.445869

Kahler, U., Kamenik, A. S., Kraml, J., and Liedl, K. R. (2020). Sodium-induced Population Shift Drives Activation of Thrombin. *Sci. Rep.* 10 (1), 1086. doi:10.1038/s41598-020-57822-0

Kale, S. S., Bergeron-Brlek, M., Wu, Y., Kumar, M. G., Pham, M. V., Bortoli, J., et al. (2019). Thiol-to-amine Cyclization Reaction Enables Screening of Large Libraries of Macrocyclic Compounds and the Generation of Sub-kilodalton Ligands. *Sci. Adv.* 5 (8), eaaw2851. doi:10.1126/sciadv.aaw2851

Kamenik, A. S., Lessel, U., Fuchs, J. E., Fox, T., and Liedl, K. R. (2018). Peptidic Macrocycles - Conformational Sampling and Thermodynamic Characterization. *J. Chem. Inf. Model.* 58 (5), 982–992. doi:10.1021/acs.jcim.8b00097

Lin, X., Li, X., and Lin, X. (2020). A Review on Applications of Computational Methods in Drug Screening and Design. *Molecules* 25 (6), 1375. doi:10.3390/molecules25061375

Maier, J. A., Martinez, C., Kasavajhala, K., Wickstrom, L., Hauser, K. E., and Simmerling, C. (2015). ff14SB: Improving the Accuracy of Protein Side Chain

and Backbone Parameters from ff99SB. *J. Chem. Theor. Comput.* 11 (8), 3696–3713. doi:10.1021/acs.jctc.5b00255

Michaud-Agrawal, N., Denning, E. J., Woolf, T. B., and Beckstein, O. (2011). MDAnalysis: a Toolkit for the Analysis of Molecular Dynamics Simulations. *J. Comput. Chem.* 32 (10), 2319–2327. doi:10.1002/jcc.21787

Miller, B. R., McGee, T. D., Swails, J. M., Homeyer, N., Gohlke, H., and Roitberg, A. E. (2012). MMPBSA.py: An Efficient Program for End-State Free Energy Calculations. *J. Chem. Theor. Comput.* 8 (9), 3314–3321. doi:10.1021/ct300418h

Molecular Operating Environment (MOE), & Chemical Computing Group ULC (2020). *1010 Sherbooke St. West, Suite #91*. Montreal, QC: Canada, H3A 2R7.

Muegge, I., Bergner, A., and Kriegl, J. M. (2017). Computer-aided Drug Design at Boehringer Ingelheim. *J. Comput. Aided Mol. Des.* 31 (3), 275–285. doi:10.1007/s10822-016-9975-3

Passioura, T. (2020). The Road Ahead for the Development of Macrocyclic Peptide Ligands. *Biochemistry* 59 (2), 139–145. doi:10.1021/acs.biochem.9b00802

Pedregosa, F., Varoquaux, G., Gramfort, A., Michel, V., Thirion, B., Grisel, O., et al. (2011). Scikit-learn: Machine Learning in Python. *J. machine Learn. Res.* 12, 2825–2830.

Sabbadin, D., and Moro, S. (2014). Supervised Molecular Dynamics (SuMD) as a Helpful Tool to Depict GPCR-Ligand Recognition Pathway in a Nanosecond Time Scale. *J. Chem. Inf. Model.* 54 (2), 372–376. doi:10.1021/ci400766b

Salmaso, V., Sturlese, M., Cuzzolin, A., and Moro, S. (2017). Exploring Protein-Peptide Recognition Pathways Using a Supervised Molecular Dynamics Approach. *Structure*, 25(4), 655–662.e652. doi:10.1016/j.str.2017.02.009

Schechter, I., and Berger, A. (1967). On the Size of the Active Site in Proteases. I. Papain. *Biochem. Biophysical Res. Commun.* 27 (2), 157–162. doi:10.1016/s0006-291x(67)80055-x

Shan, Y., Kim, E. T., Eastwood, M. P., Dror, R. O., Seeliger, M. A., and Shaw, D. E. (2011). How Does a Drug Molecule Find its Target Binding Site? *J. Am. Chem. Soc.* 133 (24), 9181–9183. doi:10.1021/ja202726y

Taylor, R. D., Rey-Carrizo, M., Passioura, T., and Suga, H. (2017). Identification of Nonstandard Macrocyclic Peptide Ligands through Display Screening. *Drug Discov. Today Tech.* 26, 17–23. doi:10.1016/j.ddtec.2017.10.005

Vinogradov, A. A., Yin, Y., and Suga, H. (2019). Macrocyclic Peptides as Drug Candidates: Recent Progress and Remaining Challenges. *J. Am. Chem. Soc.* 141 (10), 4167–4181. doi:10.1021/jacs.8b13178

Wang, J., Wang, W., Kollman, P. A., and Case, D. A. (2006). Automatic Atom Type and Bond Type Perception in Molecular Mechanical Calculations. *J. Mol. Graphics Model.* 25 (2), 247–260. doi:10.1016/j.jmgm.2005.12.005

Wang, J., Wolf, R. M., Caldwell, J. W., Kollman, P. A., and Case, D. A. (2004). Development and Testing of a General Amber Force Field. *J. Comput. Chem.*, 25 (9), 1157–1174. doi:10.1002/jcc.20035

Waskom, M., Botvinnik, O., Gelbart, M., Ostblom, J., Hobson, P., Lukauskas, S., et al. (2020). Seaborn: statistical data visualization. *J. Open Source Softw.*, 6 (60), 3021–1174. doi:10.21105/joss.03021

Conflict of Interest: The authors declare that the research was conducted in the absence of any commercial or financial relationships that could be construed as a potential conflict of interest.

Publisher's Note: All claims expressed in this article are solely those of the authors and do not necessarily represent those of their affiliated organizations, or those of the publisher, the editors and the reviewers. Any product that may be evaluated in this article, or claim that may be made by its manufacturer, is not guaranteed or endorsed by the publisher.

frontiers in Molecular Biosciences

BRIEF RESEARCH REPORT
published: 01 September 2021
doi: 10.3389/fmolb.2021.718941

Peptides Targeting the Interaction Between Erb1 and Ytm1 Ribosome Assembly Factors

*Lidia Orea-Ordóñez, Susana Masiá and Jerónimo Bravo**

Department Genomics and Proteomics, Instituto de Biomedicina de Valencia, Spanish National Research Council (CSIC), Valencia, Spain

Ribosome biogenesis is an emerging therapeutic target. It has been proposed that cancer cells are addicted to ribosome production which is therefore considered a druggable pathway in cancer therapy. Cancer cells have been shown to be more sensitive to inhibition of the ribosome production than healthy cells. Initial attempts of inhibiting ribosome biogenesis have been focused on the inhibition of transcription by targeting RNA Pol I. Despite being a promising field of research, several limitations have been identified during the development of RNA Pol I inhibitors, like the lack of specificity or acquired resistance. Ribosome biogenesis is a multistep process and additional points of intervention, downstream the very initial stage, could be investigated. Eukaryotic ribosome maturation involves the participation of more than 200 essential assembly factors that will not be part of the final mature ribosome and frequently require protein–protein interactions to exert their biological action. Using mutagenesis, we have previously shown that alteration of the complex interface between assembly factors impairs proper ribosome maturation in yeast. As a first step toward the developing of ribosome biogenesis inhibitory tools, we have used our previously solved crystal structure of the *Chaetomium thermophilum* complex between the assembly factors Erb1 and Ytm1 to perform a structure-guided selection of interference peptides. The peptides have been assayed *in vitro* for their ability to bind their cellular partner using biophysical techniques.

Keywords: structural-guided peptide selection, interference peptides, targeting ribosome biogenesis, protein–protein interactions, Erb1/Ytm1 complex

OPEN ACCESS

Edited by:
Luca Domenico D'Andrea, National Research Council (CNR), Italy

Reviewed by:
Helmut Bergler, University of Graz, Austria
Xiyuan Yao, The Scripps Research Institute, United States

****Correspondence:***
Jerónimo Bravo
jbravo@ibv.csic.es

Specialty section:
This article was submitted to Molecular Recognition, a section of the journal Frontiers in Molecular Biosciences

Received: *01 June 2021*
Accepted: *20 July 2021*
Published: *01 September 2021*

Citation:
Orea-Ordóñez L, Masiá S and Bravo J (2021) Peptides Targeting the Interaction Between Erb1 and Ytm1 Ribosome Assembly Factors. Front. Mol. Biosci. 8:718941. doi: 10.3389/fmolb.2021.718941

INTRODUCTION

The synthesis of ribosomes in eukaryotes is a sophisticated and energy-demanding process requiring the participation of more than 200 assembly factors that will not be part of the final mature ribosome although are required for a correct ribosome biogenesis. The initial steps of ribosome assembly take place in the nucleolus where rRNA is transcribed by RNA polymerase I (RNA pol I) [reviewed in (Baßler and Hurt, 2019)] under the regulation of both tumor suppressor genes (including p53, Rb, and Arf) and oncogenes (including MYC, MAPK/ERK, PI3K, and AKT) (Montanaro et al., 2008; Morcelle et al., 2019). Increased ribosome biogenesis is important for cell transformation or tumorigenesis and it is assumed as a general trend in cancer cells that need to make extra ribosomes in order to produce more proteins to sustain uncontrolled cell division (Orsolic et al., 2016) (Truitt and Ruggero, 2016). Interestingly, it has been shown that cell proliferation can be

blocked by inhibiting the production of new ribosomes since impaired ribosome biogenesis induces a checkpoint control that prevents cell cycle progression (Volarević et al., 2000). It is therefore not surprising that biogenesis of the ribosomes has been accumulating growing attention as a potential new therapeutic target.

Initial attempts to specifically target ribosome biogenesis have been focused on the downregulation of RNA pol I. Several recently described small molecules like CX-5461, CX-3543, BMH-21, or CID-765471 are now providing evidence that inhibition of ribosome biogenesis by targeting transcription of ribosomal DNA has a promising therapeutic potential (Bywater et al., 2012; Colis et al., 2014). However, lack of specificity and acquired resistance suggest that a new generation of Pol I inhibitors should be developed. Moreover, the only inhibitor that reached clinical trials has shown additional activities contributing to its toxicity profile and resistance, and therefore, additional points of intervention during the ribosome maturation process should be explored apart from the inhibition of transcription (Catez et al., 2019; Ferreira et al., 2020). Despite the fact that the complexity of the process yields a large repertoire of potential targets, only very few chemical inhibitors of ribosome biogenesis are known so far (Awad et al., 2019). Apart from the lack of molecular details in the process, the main reason for this limited number of inhibitors is that the complex ribosome biogenesis pathway is orchestrated by a wide range of macromolecular interactions sequentially coordinated to promote the correct ribosome maturation. Ribosome assembly factors frequently require protein–protein interactions in order to exert their biological actions (Li et al., 2017) and these have been traditionally hard to target by small molecule drugs given the absence of grooves or binding pockets in the interaction surface.

Nop7, Erb1, and Ytm1 are assembly factors that form a discrete heterotrimer that can be detected in isolation from the pre-ribosomal particles (Tang et al., 2008). The so-called Nop7 complex (PeBoW in mammals) is essential for a correct maturation of the ribosomal 60S subunit. The three components guarantee the correct maturation of 5' end of 5.8S rRNA, thus facilitating its association with 25S rRNA in the mature ribosome (Granneman et al., 2011). We have previously reported the structural resolution of the *Chaetomium thermophilum* Erb1/Ytm1 complex (Marcin et al., 2015; Wegrecki et al., 2015). The crystal structure shows Ytm1 bound to the carboxy-terminal portion of Erb1. Integrity of the heterotrimer assembly is essential for exerting its biological action. In fact, we previously showed that compromising the stability of the Erb1/Ytm1 interaction has an effect on proliferation in yeast (Wegrecki et al., 2015).

Using our previous Erb1/Ytm1 structure, we have performed a structure-guided selection of a set of peptides derived from their sequences and test their ability to bind to their respective cellular partners, Erb1 or Ytm1. Our results open the possibility to obtain peptides with the ability to interfere in the ribosome biogenesis pathway. To our knowledge, this is the first report of peptides designed to target ribosome biogenesis.

MATERIALS AND METHODS

Cloning, Expression, and Purification of Ytm1 and Erb1

Protein expression and purification was carried out following the protocol described in a study by Wegrecki et al. (2015). The *YTM1* gene from *Chaetomium thermophilum* was obtained by total cDNA amplification and cloning in pOPIN-F using an In-Fusion cloning system commercial kit (Clontech). Sf9 insect cells were grown in the Sf900 II SFM medium (Gibco) and were transfected with Ytm1-pOPINF and linearized Ian Jones bacmid (Zhao et al., 2003). Baculovirus generated were amplified and used to induce protein expression for 72 h at 27°C. Erb1 was cloned in a pET28-NKI/LIC 6His/3C vector (from NKI Protein Facility, Amsterdam) by the ligase independent cloning (LIC) method and expressed in *Escherichia coli* (DE3) BL21 CodonPlus (RIPL) using an auto-induction system (Studier, 2005). The 6xHis tagged Ytm1 and Erb1 proteins were purified using a Histrap-HP Ni charged column (GE Healthcare) eluting with a 20–500 mM imidazole gradient. An additional step of a HiTrap Heparin HD column (GE Healthcare) eluting with 0.2–1.5 M NaCl gradient was included for Erb1. A final polish step of size exclusion chromatography (HiLoad 16/60 Superdex 200 column, GE Healthcare) was performed for both proteins that were flash cooled under liquid nitrogen and stored at −80°C until use.

Biolayer Interferometry Assays

Peptides were commercially obtained from Synpeptide Co., Ltd., Shanghai, China. All experiments have been made in triplicates and include control curves for bait and analyte only.

Peptide Interference Experiments

Potential interference peptide samples were evaluated by their ability to interfere the kinetics and affinity of the complex between Erb1 and Ytm1 as measured by Biolayer Interferometry (BLItz, Pall FortéBio Corp.) using Ni-NTA biosensors (FortéBio) and 50 mM HEPES, pH 7.5; 150 mM NaCl; 5% (v/v) glycerol; and 2 mM β-mercaptoethanol (BME) buffer. To set the reference K_D, an 80 μg/ml solution of Erb1 was immobilized to the biosensor in order to obtain binding curves for increasing concentrations of Ytm1. According to this, an evaluation of Erb1-derived peptides (P1–P3) was performed using 5 μM Ytm1 previously incubated during 30 min at equimolar concentrations of each peptide. New K_D values were determined. Similarly, an 80 μg/ml solution of Ytm1 was immobilized to the biosensor in order to obtain binding curves for increasing concentrations of Erb1. 20 μM Erb1concentration was selected for the analyte. Each Ytm1-derived peptide (P4–P6) was evaluated by preincubation of equimolar concentrations with 20 μM Erb1 assayed against immobilized Ytm1 of 80 μg/ml.

Peptide Affinity Experiments

BLI was used to determine the affinity between Ytm1 and biotinylated peptides using streptavidin biosensors (FortéBio). The biosensors were hydrated 10 min in the same buffer used on the interference assay, with 0.05% (w/v) bovine serum albumin

(BSA). 50 μg/ml of biotinylated peptide was immobilized at the streptavidin biosensor. Increasing concentrations of Ytm1 were used to calculate the K_D values using the Blitz Pro 1.2 software using the implemented equations for association and dissociation:

Association phase:

$$y = R_{max} \frac{1}{1 + \frac{k_d}{k_a * [Analyte]}} \left(1 - e^{-\left(k_a * [\text{Analyte}] + k_d\right) x}\right).$$

Dissociation phase:

$$y = y_0 \, e^{-k_d (x - x_0)}.$$

$$y0 = R_{max} \frac{1}{1 + \frac{k_d}{k_a * [Analyte]}} \left(1 - e^{-\left(k_a * [\text{Analyte}] + k_d\right) x_0}\right).$$

Differential Scanning Fluorimetry

Thermofluor assays (Pantoliano et al., 2001) were performed on a 7,500 Fast Real-Time PCR System (Applied Biosystems) measuring the gradual fluorescence generated by a 1:1,000 dilution of SYPRO Orange Protein Stain Gel (Supelco, Merck-Sigma) along with 1°C/min temperature increase from 20°C until 85°C.

The samples were mixed containing the protein Ytm1 at 5 μM in 50 mM HEPES pH 7.5, 150 mM NaCl and peptides P1-P3 at 1 mM concentration. Previously, lyophilized P2 and P3 were resuspended in the same Ytm1 buffer and P1 was solubilized in 10 mM Tris (hydroxymethyl)-methylamine (Tris-HCl), pH 8.8 for P1. Data of triplicated experiments were analyzed using GraphPad Prism 5.01 software.

MicroScale Thermophoresis

Microscale thermophoresis (MST) was used to determine the binding affinity between Ytm1 and P1. Ytm1 was labeled with a Red-NHS second-generation dye kit (100 μl at 10 μM of protein +300 μM dye solution) for 30 min at room temperature in the dark. 5 nM of labeled Ytm1 in 50 mM HEPES pH 7.5, NaCl 150 mM supplemented with 0.1% (v/v) Pluronic F-127 was used for the assay. P1 stock is diluted in 10 mM Tris (hydroxymethyl)-methylamine (Tris-HCl), pH 8.8. Ytm1 and P1 were mixed at 1:1 molar ratio in sixteen serial dilutions (1,230 μM–0.0751 μM) using the same buffer. Measurements were taken on a Monolith NT.115 instrument (NanoTemper Technologies). Similarly biding between Ytm1 and P3 using MST was tested using the same Ytm1 buffer also for P3. Curve fitting and K_D calculations every 10 min were analyzed from three independent experiments with MO. Maximum binding was observed at 50 min. Curves were analyzed using Affinity Analysis Software (NanoTemper Technologies).

Bioinformatics

Buried surface calculations were performed using the protein interfaces, surfaces, and assemblies service PISA at the European Bioinformatics Institute (http://www.ebi.ac.uk/pdbe/prot_int/pistart.html) (Krissinel and Henrick 2007) using PDB ID 5cxb and in silico alanine scanning of the interaction surface was performed using the DrugScorePPI Web Interface (https://cpclab.uni-duesseldorf.de/dsppi/) (Krüger and Gohlke, 2010) only considering polypeptide atoms. ΔG computed for alanine mutants for each 5cxb polypeptide chain is compared to ΔG computed from the wild type complex. Resulting ΔΔG predicts the contribution of a given side chain to the wild type complex stability (ΔΔG = ΔGALAcomplex−ΔGWTcomplex). Interacting atoms between Erb1 and Ytm1 were also analyzed using the 5cxb coordinates program contact in the CCP4 suite (Winn et al., 2011). Molecular graphics in **Figure 1** were performed with UCSF Chimera (Pettersen et al., 2004).

RESULTS

Interaction Surface Analysis and Peptide Selection

Our Erb1/Ytm1 heterodimer crystal structure (PDB ID 5CXB) (Wegrecki et al., 2015) shows that the central part of the β-propeller of Ytm1 provides a large docking surface for the bottom face of blades 1, 2, and 7 from Erb1 that is additionally held in place by two lateral extensions from Ytm1. The Ytm1 β-propeller top face, away from the N-terminal Ubiquitin-like domain, establishes extensive contacts with the side face of Erb1 C-terminal β-propeller (**Figure 1A**) with a predominant role of blade 7. The Erb1/Ytm1 heterodimer is mainly maintained by electrostatic forces with some hydrophobic regions also involved in the interaction (**Figure 1B**). No clear grooves have been detected in the heterodimer interaction surface.

Manual inspection of the interaction surface between Erb1 and Ytm1 combined with buried surface area upon binding calculations using PISA (Krissinel and Henrick, 2007), together with an analysis of the interactions and an alanine scanning of the interacting residues to locate hotspots using DrugScore^{PPI} (Krüger and Gohlke, 2010), revealed several areas of interaction (**Figure 1C**, **Supplementary Table S1, S2**). The last β-strand ("1d") of blade 7 in Erb1 contacts loop "6d-6a" and a long extension that appears between strands "7d" and "7a" of Ytm1 (the knob formed by residues 444–460). A second interaction area involves the entrance of the central tunnel of Ytm1 as a docking site for a loop between strands "1c–2d" from the first blade of Erb1 (481–486) (**Figure 1C**). The loop contains three well conserved residues: E481, T484, and R486 that establish a network of electrostatic interactions with also conserved amino acids from blades 1, 2, 3, and 7 of Ytm1. We have previously reported the relevance of the second area of interaction since the R486E point mutation decreased the affinity of the interaction by two orders of magnitude without affecting structural integrity. The equivalent mutation in yeast impaired growth in yeast and affected 60S subunit biogenesis (Wegrecki et al., 2015). As indicated by the in silico alanine scanning analysis, this interacting region also suggests a hot spot between Erb1 and Ytm1 (**Figure 1C**, **Supplementary Table S1**). Erb1 a-b

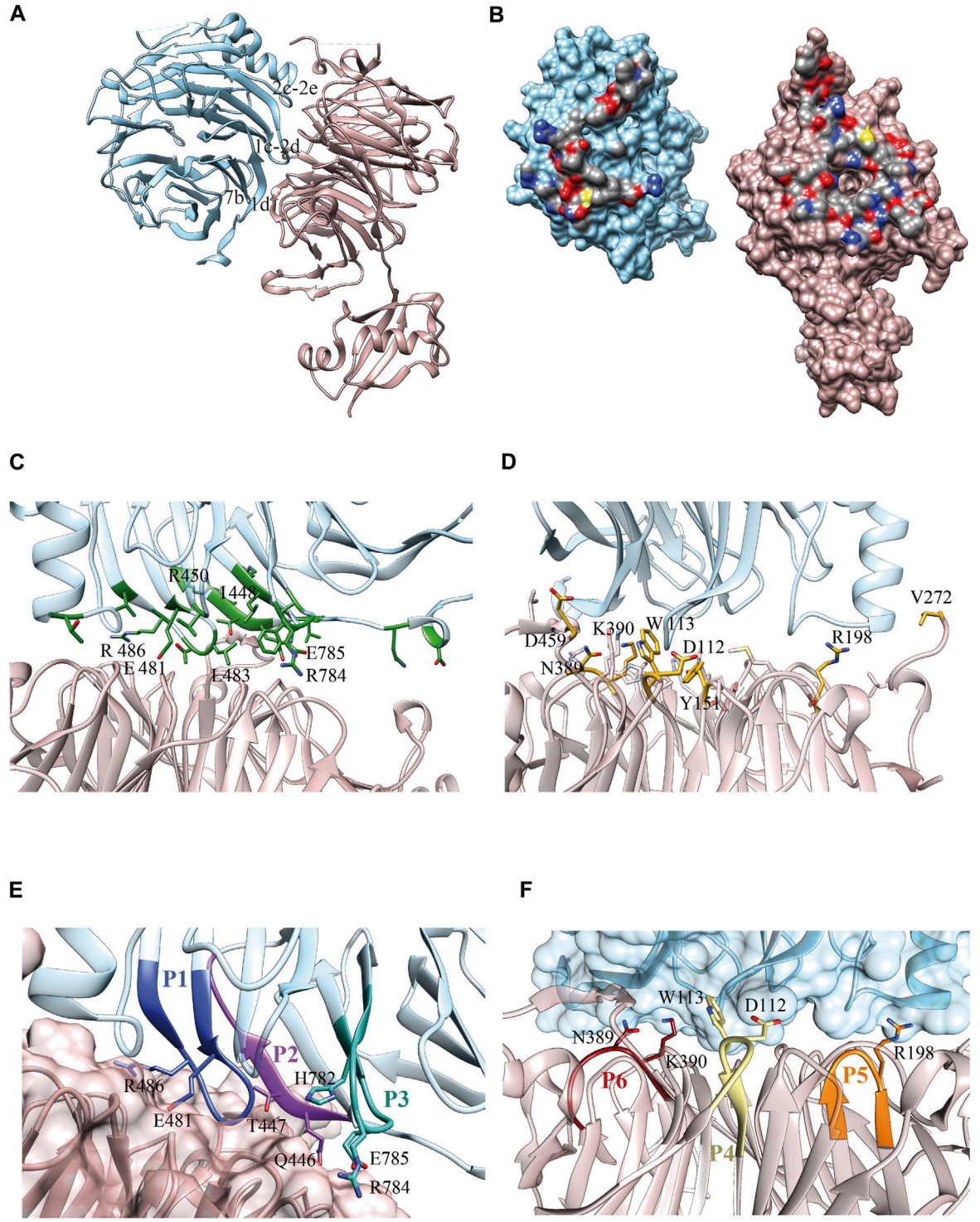

FIGURE 1 | Erb1/Ytm1 interaction. **(A)** Ribbon representation of the heterodimer. Top face of Ytm1 β-propeller in pale pink interacts with Erb1 β-propeller's side in blue. The main secondary structure-interacting motifs are shown in Erb1 **(B)** Surface representation of the individual components with the interaction areas facing toward the observer. Atoms from residues involved in the interaction are colored by atom, carbon in grey, oxygen in red, and nitrogen in blue. The rest of the surface is colored in blue for Erb1 and pale pink for Ytm1. **(C)** Calculated Erb1 ΔΔG values from in silico alanine scan. Residues from Erb1 with calculated ΔΔG>0.5 kcal/mol are depicted in green. **(D)** Calculated Ytm1 ΔΔG values from in silico alanine scan. Ytm1 residues with calculated ΔΔG>1.0 kcal/mol are represented in yellow. **(E)** Selected peptides derived from Erb1. Each peptide is colored with a different shade of blue and is labeled according to **Table 1**. Side chains of interacting residues establishing electrostatic interactions are shown. **(F)** Selected peptides derived from Ytm1. The three selected peptides are depicted in brown, yellow, and orange for P6, P4, and P5, respectively (**Table 1**). Side chains of interacting residues establishing electrostatic interactions are shown.

TABLE 1 | Peptides used in this study. Residue numbering is referred to the *Chaetomium thermophilum* sequences.

Peptide	Sequence	Protein	Residues
P1	VWELLTGRQVW	Erb1	479–489
P2	QQTIFRGH	Erb1	445–452
P3	DWHPREPWCV	Erb1	780–789
P4	HDDWVSA	Ytm1	110–116
P5	AGMDRTV	Ytm1	194–200
P6	RGHANKV	Ytm1	385–391
Biot-P1	Biotin-VWELLTGRQVW	Erb1	479–489
Biot-P3	Biotin-DWHPREPWCV	Erb1	780–789
Biot-P6	Biotin-RGHANKV	Ytm1	385–391

loop from blade 7 participates in another interaction area with Ytm1 loops from blade 3. Finally an insertion in blade 2 of the β-propeller of Erb1 between 2c and 2e (**Supplementary Figure S1**) interacts with loops from blades 2 and 3 and an extension between strands 3c and 4d from Ytm1 (**Supplementary Figure S2**). This Erb1 insertion area shows poor sequence conservation (**Supplementary Figure S1**) and will not be taken it into further consideration. Ytm1 residues interacting with Erb1 appear to cluster mostly on one side of the interaction surface (**Figure 1D**) although they do not show sequence continuity of interacting residues (**Figure 1D**, **Supplementary Figure S2** and **Supplementary Table S2**).

According to the previous observations, a set of six peptides, summarized in **Table 1**, were selected derived from Erb1 sequence and Ytm1 (**Figures 1E,F** and **Supplementary Figures S1, S2**).

Peptide Competition Assay

Biolayer interferometry interference assays were used to evaluate the ability of each peptide to interfere in the *in vitro* formation of the Erb1/Ytm1 complex. Erb1 was immobilized to a Ni-NTA biosensor and Ytm1 was used as analyte for testing direct interaction. The binding affinity is 3.2e-8M (**Supplementary Table S3**), similar to the previously reported values using microcalorimetry (Wegrecki et al., 2015). Peptides were evaluated for their ability to decrease in the Erb1/Ytm1 complex formation by preincubating the analyte with each peptide derived from the immobilized partner. **Figures 2A,B** show typical curves from the interference assay using biolayer interferometry. The black line depicts the reference curve obtained in the absence of peptide preincubation. Erb1-derived peptides were evaluated by their ability to decrease Erb1/Ytm1 complex affinity. Each P1-3 peptide was preincubated for half an hour at 4°C with an equimolar concentration of Ytm1 used as an analyte for binding with Erb1, previously immobilized to the Ni-NTA biosensor (**Figure 2A**). Peptides P1 and P3 showed a decrease of more than one order of magnitude (1.9 and 1.7e-7M respectively) with respect the Erb1/Ytm1 binding curve, in the absence of peptide. Similarly, an assay immobilizing Ytm1 to the Ni-NTA biosensor was used with Erb1 as analyte preincubated at equimolar concentrations with P4-6 Ytm1-derived peptides. Only peptide P6 showed a significant decrease (2.4e-6M) with respect to the reference Ytm1/Erb1 binding curve (**Figure 2B**).

Direct Peptide Binding Assays

According to P1, P3, and P6 results, a new N-terminal biotynilated peptide synthesis was ordered using the same sequences (Biot-P1, Biot-P3, and Biot-P6, **Table 1**). Biotynilated peptides Biot-P1 and Biot-P3 were immobilized to the streptavidin biosensor and Ytm1 binding was measured. Similarly, Biot-P6 was immobilized to the streptavidin biosensor followed by Erb1 binding. As indicated in **Figure 2C**, we could not detect binding for Biot-P6/Erb1. Peptides Biot-P1 and Biot-P3 showed an affinity for Ytm1 in the mM range (**Figures 2D,E**). To further confirm the interaction a differential scanning fluorimetry assay was performed. A thermofluor assay of Ytm1 on its own and in the presence of 1 mM P3 did not show any significant thermal shift (**Figure 2F**) Similarly, no significant thermal shift in Ytm1 was observed in the presence of 1 mM P2 (**Supplementary Figure S3**). A shift of several degrees in the Tm was observed in the presence of 1 mM P1 indicating binding with Ytm1 (**Figure 2G**). Inconsistent results were obtained in DSF using Erb1 and a proper Tm could not be obtained so thermal shift could not be evaluated for P6. To further demonstrate the ability of P1 to interact with Ytm1, the binding was also monitored in free solution by the change in the thermophoresis of Ytm1 upon interaction with P1. Binding affinity determined using microscale thermophoresis showed a Kd in the mM range (8.2e-6M, **Supplementary Table S3**) consistent with affinities observed using interferometry and further confirming a direct interaction between P1 and Ytm1 (**Figure 2H**). Experimental limitations with maximum ligand concentration did not allow the calculation of binding stoichiometry. A tendency toward binding was also detected using MST with the P3 peptide at a maximum concentration of 1,580 μM but data quality would not allow a proper fitting for obtaining the K_D values (**Supplementary Figure S4**).

DISCUSSION

Erb1 surface appears to be more suitable for the selection of peptides targeting the complex, as compared to Ytm1 that, despite showing some degree of clustering (**Figure 1D**) reveals scattered interacting residues and fragmented regions (**Supplementary Figure S2**). In fact, we did not obtain clear experimental binding results for Ytm1-derived peptides. Apart from the peptides derived from Ytm1 selected in this study, additional regions that might have been considered are 224–229 that shows a rather continuous interaction with Erb1. It has, however, been initially discarded given the small differences in calculated ΔΔG upon *in vitro* alanine substitution with respect WT Ytm1 in the complex (**Supplementary Table S2**). An additional region includes V272 that shows reasonable ΔΔG values and continuity (S265-V272) of neighboring residues in *Chaetomium*. However, it is located in an evolutionary poorly conserved region (**Supplementary Figure S2**). Sequence elongation of the selected Ytm1-derived peptides might also provide better interaction results.

The combination of in silico hot spot analysis with contact analysis in the interface and residue conservation suggested an

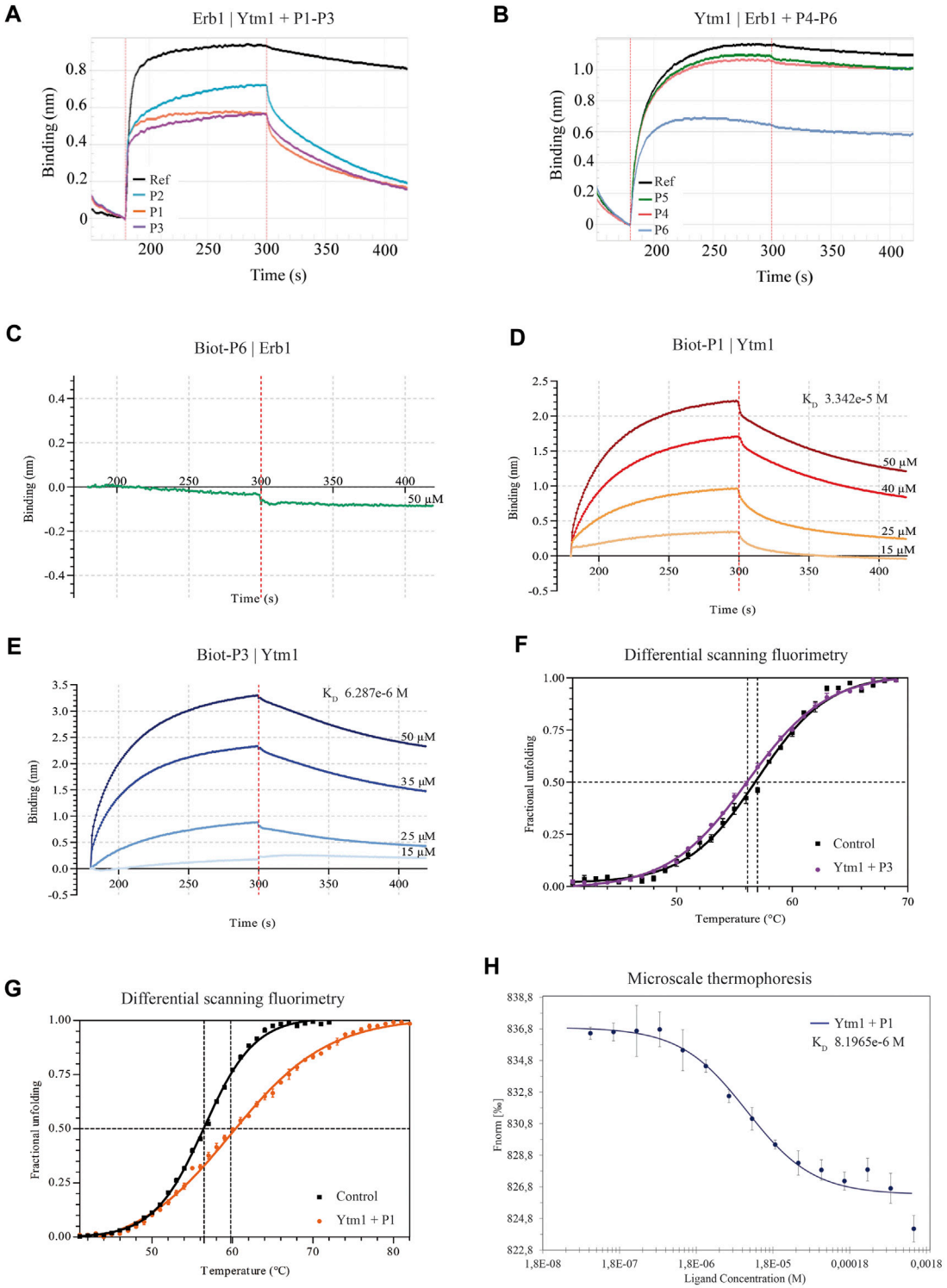

FIGURE 2 | Binding properties of Erb1- and Ytm1-derived peptides to Ytm1 and Erb1, respectively. **(A)** Biolayer interferometry curves of preincubated peptides P1–3 with equimolar amounts of Ytm1 (5 µM). The ability to interfere with Erb1/Ytm1 complex formation (black line) is evaluated using immobilized Erb1 and Ytm1 as an analyte. The reference K_D for the Erb1/Ytm1 complex is 3.228e-8M. K_D decrease for preincubated Ytm1-P2 is less than one order of magnitude (**Supplementary Table S3**) whereas it is more than one order of magnitude for preincubated Ytm1-P1 and Ytm1-P3. **(B)** The equivalent competition BLI experiment preincubating equimolar concentrations of peptides P4–6 with 20 µM Erb1 and using immobilized Ytm1 as bait. K_D values of Erb1-P5 and Erb1-P4 are similar to the reference K_D (2.292e-7M) using only Erb1 as an analyte. K_D values of Erb1-P6 are almost one order of magnitude lower than the reference (**Supplementary Table S3**). **(C–E)** Biolayer

(*Continued*)

FIGURE 2 | interferometry curves using inmobilized biotynilated peptides. **(C)** Immobilized biot-P6 did not show binding when using Erb1 as analyte. **(D)** BLI Ytm1 binding curves obtained using immobilized biot-P1. **(E)** BLI Ytm1 binding curves using biot-P3 as bait. **(F)** Thermal shift curves obtained by differential scanning fluorimetry (DSF) of Ytm1 isolated (black line) and in the presence of 1 mM P3 peptide. **(G)** Similarly, DSF thermal shift curves of Ytm1 isolated (black line) and in the presence of 1 mM P1 peptide (orange). **(H)** Microscale thermoforesis binding curve for Ytm1 with peptide P1. Ytm1 was labeled using the Red-NHS second-generation dye for the binding affinity with the peptide P1 (NanoTemper Technologies). Fnorm indicates normalized fluorescence.

initial set of six peptides in the Erb1/Ytm1 interface. Three of them showed some degree of interference in the complex formation on a competition assay. Best candidates (P1, P3, and P6) were further tested immobilizing the peptide to the biosensor. We have observed some differences for peptide P6 in the competition assays with respect biotinylated peptide assay using biolayer interferometry. Biotin itself could be affecting the binding to Erb1; however, this is unlikely to be the case since the N-terminus of P6 is not involved in the interaction according to the structure of the Erb1/Ytm1 complex (**Figure 1**). An obvious difference is the immobilization of the peptide that might be impairing a proper conformation of P6 for the interaction with Erb1 to take place. Immobilized peptide in the biotynilated P1 experiment can also explain the slight difference observed in the Kds obtained by BLI and MST. Tm values for Erb1 using DSF could not be obtained. Moreover, several of the selected peptides did not show any effect on the interference biolayer interferometry assay. Alternative methodological approaches should be considered for the detection of low affinity interactions in BLI or proteins with potential hydrophobic exposed areas in DSF. We have been able to detect direct *in vitro* interactions of P1 and Biot-P1 with Ytm1 at a low mM affinity range indicating that at least for these conditions biolayer interferometry is a suitable methodological approach. MST also represented a good alternative for evaluating the interaction with initial binding detected for Ytm1-P3 and proper affinity determination for Ytm1-P1. Erb1 and Ytm1 form a part of the Nop7 complex which is a heterotrimeric complex. Assembly of the three subunits is required for the correct maturation of 60S ribosomal subunit. Once the Nop7 complex has exerted its molecular function it is sequentially removed from the pre60S subunit (Tang et al., 2008; Baßler and Hurt, 2019). Individual Nop7, Erb1, and Ytm1 will then reassemble to repeat the process with a new preribosome. It is at this stage when a peptide targeting the Erb1/Ytm1 interaction could play its interference role since the P1 peptide affinity shown for Ytm1 is lower than the one observed for the Erb1/Ytm1 complex.

Ribosome biogenesis has recently been accumulating growing attention as a potential new therapeutic target, since the observation that cell proliferation can be blocked by inhibition of new ribosomes production. Several RNA pol I inhibitors have been reported to date (Ferreira et al., 2020) and molecules like CX-3543, CX-5461, and BMH-21 are currently under investigation for treating cancer, as rapidly dividing cancer cells are particularly dependent on high levels of RNA pol I transcription. CX-5461 is phase I clinical trial in patients with advanced haematological cancers and breast cancer (Hilton et al., 2018; Khot et al., 2019). CX-3543 reached phase II clinical trial but was withdrawn due to bioavailability issues (Balasubramanian et al., 2011). While extremely promising, these compounds targeting RNA pol I are associated with additional activities, like DNA damage, which possibly contributes to its efficacy, toxicity profile, and resistance mechanisms. These observations suggest that it may be necessary to look for other points of intervention during this multistep process of ribosome maturation. One relevant question in this new field of targeting ribosome biogenesis is whether downstream specific targets would behave the same or differ to those RNA pol I transcription inhibitors currently developed. We had previously shown that altering the interaction surface between the ribosome assembly factors Erb1 and Ytm1 hinders cell proliferation in yeast. We have now developed a peptide derived from the Erb1 sequence capable of interacting with Ytm1 at a low mM range and interfere in the Erb1/Ytm1 complex formation negatively affecting this extensive and highly conserved protein–protein interaction. This result opens the possibility to investigate the *in vivo* action of RNA pol I downstream targets in the ribosome biogenesis process. Delivery methods like cell penetrating peptides or nanoparticles should be considered for internalization of the peptide into the cell in order to test future inhibitory strategies *in vivo*.

DATA AVAILABILITY STATEMENT

The raw data supporting the conclusions of this article will be made available by the authors, without undue reservation.

AUTHOR CONTRIBUTIONS

LO-O performed the interaction assays, interaction surface analysis, elaborated tables, and figures, contributed to scientific discussion, and manuscript writing. SM contributed in the peptide selection, interaction surface analysis, provided technical assistance for binding experiments and critical discussion. JB contributed to the peptide selection, methodological approach, graphical imaging, and manuscript writing.

FUNDING

Funding was obtained from the Spanish Ministry of Economy, Industry and Competitiveness SAF2017-89901-R and Generalitat Valenciana PROMETEO/2018/055. Open access publication fees have been partially funded by URICI from Consejo Superior de Investigaciones Científicas (CSIC). Molecular graphics and analyses were performed with UCSF Chimera, developed by the Resource for Biocomputing, Visualization, and Informatics at the University of California, San Francisco, with support from NIH P41-GM103311.

ACKNOWLEDGMENTS

We would like to thank Ma del Valle Morales Cuenca, Clara Arenas, and Guilherme Dim for technical support. Molecular

graphics and analyses were performed with UCSF Chimera, developed by the Resource for Biocomputing, Visualization, and Informatics at the University of California, San Francisco, with support from NIH P41-GM103311 (https://www.cgl.ucsf.edu/chimera/docs/credits.html).

SUPPLEMENTARY MATERIAL

The Supplementary Material for this article can be found online at: https://www.frontiersin.org/articles/10.3389/fmolb.2021.718941/full#supplementary-material

REFERENCES

Awad, D., Prattes, M., Kofler, L., Rössler, I., Loibl, M., Pertl, M., et al. (2019). Inhibiting Eukaryotic Ribosome Biogenesis. *BMC Biol.* 17 (1), 1–16. doi:10.1186/s12915-019-0664-2

Balasubramanian, S., Hurley, L. H., and Neidle, S. (2011). Targeting G-Quadruplexes in Gene Promoters: A Novel Anticancer Strategy? *Nat. Rev. Drug Discov.* 10 (4), 261–275. doi:10.1038/nrd3428

Baßler, J., and Hurt, E. (2019). Eukaryotic Ribosome Assembly. *Annu. Rev. Biochem.* 88 (1), 281–306. doi:10.1146/annurev-biochem-013118-110817

Bywater, M. J., Poortinga, G., Sanij, E., Hein, N., Peck, A., Cullinane, C., et al. (2012). Inhibition of RNA Polymerase I as a Therapeutic Strategy to Promote Cancer-specific Activation of P53. *Cancer Cell* 22 (1), 51–65. doi:10.1016/j.ccr.2012.05.019

Catez, F., Dalla Venezia, N., Marcel, V., Zorbas, C., Lafontaine, D. L. J., Diaz, J.-J., et al. (2019). Ribosome Biogenesis: An Emerging Druggable Pathway for Cancer Therapeutics. *Biochem. Pharmacol.*, 159, 74–81. doi:10.1016/j.bcp.2018.11.014

Colis, L., Peltonen, K., Sirajuddin, P., Liu, H., Sanders, S., Ernst, G., et al. (2014). DNA Intercalator BMH-21 Inhibits RNA Polymerase I Independent of DNA Damage Response. *Oncotarget* 5 (12), 4361–4369. doi:10.18632/oncotarget.2020

Ferreira, R., Schneekloth, J. S., Panov, K. I., Hannan, K. M., and Hannan, R. D. (2020). Targeting the RNA Polymerase I Transcription for Cancer Therapy Comes of Age. *Cells* 9, 266. doi:10.3390/cells9020266

Granneman, S., Petfalski, E., and Tollervey, D. (2011). A Cluster of Ribosome Synthesis Factors Regulate Pre-RRNA Folding and 5.8S RRNA Maturation by the Rat1 Exonuclease. *EMBO J.* 30 (19), 4006–4019. doi:10.1038/emboj.2011.256

Hilton, J., Cescon, D. W., Bedard, P., Ritter, H., Tu, D., Soong, J., et al. (2018). CCTG IND.231: A Phase 1 Trial Evaluating CX-5461 in Patients with Advanced Solid Tumors. *Ann. Oncol.* 29, iii8. doi:10.1093/annonc/mdy048.003

Khot, A., Brajanovski, N., Cameron, D. P., Hein, N., Maclachlan, K. H., Sanij, E., et al. (2019). First-in-Human RNA Polymerase I Transcription Inhibitor CX-5461 in Patients with Advanced Hematologic Cancers: Results of a Phase I Dose-Escalation Study. *Cancer Discov.* 9 (8), 1036–1049. doi:10.1158/2159-8290.CD-18-1455

Krissinel, E., and Henrick, K. (2007). Inference of Macromolecular Assemblies from Crystalline State. *J. Mol. Biol.* 372 (3), 774–797. doi:10.1016/j.jmb.2007.05.022

Krüger, D. M., and Gohlke, H. (2010). DrugScorePPI Webserver: Fast and Accurate In Silico Alanine Scanning for Scoring Protein-Protein Interactions. *Nucleic Acids Res.* 38 (Suppl. 2), W480–W486. doi:10.1093/nar/gkq471

Li, Z., Ivanov, A. A., Su, R., Gonzalez-Pecchi, V., Qi, Q., Liu, S., et al. (2017). The OncoPPi Network of Cancer-Focused Protein-Protein Interactions to Inform Biological Insights and Therapeutic Strategies. *Nat. Commun.* 8, 14356. doi:10.1038/ncomms14356

Marcin, W., Neira, J. L., and Bravo, J. (2015). The Carboxy-Terminal Domain of Erb1 Is a Seven-Bladed SS-Propeller that Binds RNA. *PLoS ONE* 10 (4), e0123463. doi:10.1371/journal.pone.0123463

Montanaro, L., Treré, D., and Derenzini, M. (2008). Nucleolus, Ribosomes, and Cancer. *Am. J. Pathol.* 173, 301–310. doi:10.2353/ajpath.2008.070752

Morcelle, C., Menoyo, S., Morón-Duran, F. D., Tauler, A., Kozma, S. C., Thomas, G., et al. (2019). Oncogenic MYC Induces the Impaired Ribosome Biogenesis Checkpoint and Stabilizes P53 Independent of Increased Ribosome Content. *Cancer Res.* 79 (17), 4348–4359. doi:10.1158/0008-5472.CAN-18-2718

Orsolic, I., Jurada, D., Pullen, N., Oren, M., Eliopoulos, A. G., and Volarevic, S. (2016). The Relationship between the Nucleolus and Cancer: Current Evidence and Emerging Paradigms. *Semin. Cancer Biol.*, 37-38, 36–50. doi:10.1016/j.semcancer.2015.12.004

Pantoliano, M. W., Petrella, E. C., Kwasnoski, J. D., Lobanov, V. S., Myslik, J., Graf, E., et al. (2001). High-Density Miniaturized Thermal Shift Assays as a General Strategy for Drug Discovery. *J. Biomol. Scree.* 6 (6), 429–440. doi:10.1177/108705710100600609

Pettersen, E. F., Goddard, T. D., Huang, C. C., Couch, G. S., Greenblatt, D. M., Elaine, C. M., et al. (2004). UCSF Chimera?A Visualization System for Exploratory Research and Analysis. *J. Comput. Chem.* 25 (13), 1605–1612. doi:10.1002/jcc.20084

Studier, F. W. (2005). Protein Production by Auto-Induction in High-Density Shaking Cultures. *Protein Expr. Purif.* 41 (1), 207–234. doi:10.1016/j.pep.2005.01.016

Tang, L., Sahasranaman, A., Jakovljevic, J., Schleifman, E., and Woolford, J. L. (2008). Interactions Among Ytm1, Erb1, and Nop7 Required for Assembly of the Nop7-Subcomplex in Yeast Preribosomes. *Mol. Biol. Cel* 19 (7), 2844–2856. doi:10.1091/mbc.E07-12-1281

Truitt, M. L., and Ruggero, D. (2016). New Frontiers in Translational Control of the Cancer Genome. *Nat. Rev. Cancer* 16, 288–304. doi:10.1038/nrc.2016.27

Volarevic, S., Stewart, M. J., Ledermann, B., Zilberman, F., Terracciano, L., Montini, E., et al. (2000). Proliferation, but Not Growth, Blocked by Conditional Deletion of 40S Ribosomal Protein S6. *Science* 288 (5473), 2045–2047. doi:10.1126/science.288.5473.2045

Wegrecki, M., Rodríguez-Galán, O., de la Cruz, J., and Bravo, J. (2015). The Structure of Erb1-Ytm1 Complex Reveals the Functional Importance of a High-Affinity Binding between Two β-Propellers During the Assembly of Large Ribosomal Subunits in Eukaryotes. *Nucleic Acids Res.* 43 (22), 11017–11030. doi:10.1093/nar/gkv1043

Winn, M. D., Ballard, C. C., Cowtan, K. D., Eleanor, J. D., Paul, E., Dodson, E. J., et al. (2011). Overview of theCCP4 Suite and Current Developments. *Acta Crystallogr. D Biol. Cryst.* 67, 235–242. doi:10.1107/S0907444910045749

Zhao, Y., Chapman, D. A. G., and Jones, I. M. (2003). Improving Baculovirus Recombination. *Nucleic Acids Res.* 31 (2), E6. doi:10.1093/nar/gng006

Conflict of Interest: The authors declare that the research was conducted in the absence of any commercial or financial relationships that could be construed as a potential conflict of interest.

Publisher's Note: All claims expressed in this article are solely those of the authors and do not necessarily represent those of their affiliated organizations, or those of the publisher, the editors and the reviewers. Any product that may be evaluated in this article, or claim that may be made by its manufacturer, is not guaranteed or endorsed by the publisher.

frontiers in Molecular Biosciences

ORIGINAL RESEARCH
published: 07 September 2021
doi: 10.3389/fmolb.2021.742903

Differential Modulation of the Voltage-Gated Na^+ Channel 1.6 by Peptides Derived From Fibroblast Growth Factor 14

Aditya K. Singh[1], Nolan M. Dvorak[1,2,3], Cynthia M. Tapia[1,3], Angela Mosebarger[1,2,3], Syed R. Ali[1], Zaniqua Bullock[1], Haiying Chen[1], Jia Zhou[1] and Fernanda Laezza[1]**

[1]Department of Pharmacology and Toxicology, Galveston, TX, United States, [2]Pharmacology and Toxicology Graduate Program, Galveston, TX, United States, [3]Presidential Scholarship Program, University of Texas Medical Branch, Galveston, TX, United States

The voltage-gated Na^+ (Nav) channel is a primary molecular determinant of the initiation and propagation of the action potential. Despite the central role of the pore-forming α subunit in conferring this functionality, protein:protein interactions (PPI) between the α subunit and auxiliary proteins are necessary for the full physiological activity of Nav channels. In the central nervous system (CNS), one such PPI occurs between the C-terminal domain of the Nav1.6 channel and fibroblast growth factor 14 (FGF14). Given the primacy of this PPI in regulating the excitability of neurons in clinically relevant brain regions, peptides targeting the FGF14:Nav1.6 PPI interface could be of pre-clinical value. In this work, we pharmacologically evaluated peptides derived from FGF14 that correspond to residues that are at FGF14's PPI interface with the CTD of Nav1.6. These peptides, Pro-Leu-Glu-Val (PLEV) and Glu-Tyr-Tyr-Val (EYYV), which correspond to residues of the β12 sheet and β8-β9 loop of FGF14, respectively, were shown to inhibit FGF14:Nav1.6 complex assembly. In functional studies using whole-cell patch-clamp electrophysiology, PLEV and EYYV were shown to confer differential modulation of Nav1.6-mediated currents through mechanisms dependent upon the presence of FGF14. Crucially, these FGF14-dependent effects of PLEV and EYYV on Nav1.6-mediated currents were further shown to be dependent on the N-terminal domain of FGF14. Overall, these data suggest that the PLEV and EYYV peptides represent scaffolds to interrogate the Nav1.6 channel macromolecular complex in an effort to develop targeted pharmacological modulators.

Keywords: voltage-gated sodium channels, protein-protein interactions, intracellular fibroblast growth factors, split-luciferase complementation assays, patch-clamp electrophysiology

OPEN ACCESS

Edited by:
Luca Domenico D'Andrea, National Research Council (CNR), Italy

Reviewed by:
Angelika Lampert, University Hospital RWTH Aachen, Germany
Steve Peigneur, KU Leuven, Belgium

****Correspondence:***
Aditya K. Singh
adsingh@utmb.edu
Fernanda Laezza
felaezza@utmb.edu

Specialty section:
This article was submitted to Molecular Recognition, a section of the journal Frontiers in Molecular Biosciences

Received: *16 July 2021*
Accepted: *23 August 2021*
Published: *07 September 2021*

Citation:
Singh AK, Dvorak NM, Tapia CM, Mosebarger A, Ali SR, Bullock Z, Chen H, Zhou J and Laezza F (2021) Differential Modulation of the Voltage-Gated Na^+ Channel 1.6 by Peptides Derived From Fibroblast Growth Factor 14. Front. Mol. Biosci. 8:742903. doi: 10.3389/fmolb.2021.742903

INTRODUCTION

Voltage-gated Na^+ (Nav) channels are responsible for the initiation and propagation of action potentials in excitable cells (Catterall, 2012). This functionality is largely conferred via the pore-forming α subunit of Nav channels, of which nine different isoforms (Nav1.1-Nav1.9) have been described. In addition to molecular differences among these nine isoforms of the Nav channel α subunit, they also diverge with respect to their tissue distribution. Specifically, Nav1.1-Nav1.3 and

Nav1.6 are expressed in the central nervous system (CNS); Nav1.4 is expressed in skeletal muscle; Nav1.5 is expressed in cardiac muscle; and Nav1.7-Nav1.9 are expressed in the peripheral nervous system (PNS) (Goldin et al., 2000; Yu and Catterall, 2003; Catterall et al., 2005; Chahine et al., 2008; Savio-Galimberti et al., 2012; Dib-Hajj et al., 2015). Given this ubiquitous expression throughout the body, it is unsurprising that mutations to specific Nav channel isoforms give rise to an array of disease-states including autism spectrum disorder (Sanders et al., 2012; Tavassoli et al., 2014), ataxia (Savio-Galimberti et al., 2012), Dravet syndrome, cognitive impairment, epilepsy (Claes et al., 2001; Mantegazza et al., 2005, 2010; Catterall et al., 2010; Volkers et al., 2011; Schaefer et al., 2013; Oyrer et al., 2018), Brugada syndrome (Probst et al., 2009), pain-related syndromes (Woods et al., 2015; Wright et al., 2016), primary erythromelalgia (Tang et al., 2015), paroxysmal extreme pain disorder (Dib-Hajj et al., 2009; Lampert et al., 2010); and cardiac arrhythmias (Wang et al., 1995; Musa et al., 2015).

Given their essential role in regulating physiology throughout the body, Nav channels have historically been a traditional target for drug development. Unfortunately, current therapeutics targeting Nav channels bind to structural motifs of the α subunit that display high amino acid sequence homology among the nine Nav channels isoforms, which results in these therapeutics lacking isoform selectivity and giving rise to deleterious off-target side effects due to modulation of off-target Nav channel isoforms (Catterall and Swanson, 2015). To address this challenge, the identification of novel Nav channel drug-binding sites is a necessary pre-requisite to identify therapeutics with improved selectivity (Dvorak et al., 2021).

Among structural components of the Nav channel that could be pharmacologically targeted to achieve improved selectivity, C-terminal domains (CTD) of Nav channels stand out as promising surfaces to target, as they display amino acid sequence divergence among isoforms that enables structurally and functionally specific protein:protein interactions (PPI) with auxiliary proteins (Lou et al., 2005; Laezza et al., 2007, 2009; Tseng et al., 2007; Wang et al., 2011; Pitt and Lee, 2016; Effraim et al., 2019; Lu et al., 2020). In the central nervous system (CNS), one salient example of such a PPI occurs between the CTD of Nav1.6 and its auxiliary protein fibroblast growth factor 14 (FGF14) (Liu et al., 2003; Lou et al., 2005; Goetz et al., 2009; Laezza et al., 2009; Ali et al., 2016, 2018; Hsu et al., 2016; Singh et al., 2020; Wadsworth et al., 2020). Specifically, this PPI regulates the transient and resurgent Na+ currents of neurons through a mechanism thought to depend upon the N-terminus of FGF14 (Yan et al., 2014; White et al., 2019), as well as the action potential (AP) firing of neurons in clinically relevant brain regions, including the nucleus accumbens (NAc) (Ali et al., 2018) and hippocampus (Hsu et al., 2016). Translationally, perturbation of this PPI is increasingly being associated with a myriad of neurologic and neuropsychiatric disorders (Di Re et al., 2017; Paucar et al., 2020), highlighting its potential clinical relevance as a pharmacological target.

To guide drug discovery efforts targeting the PPI interface between FGF14 and the CTD of Nav1.6, we previously developed and interrogated a homology model of the PPI interface to identify putative clusters of amino acids central to assembly of the complex (Ali et al., 2014, 2016). These investigations identified the Phe-Leu-Pro-Lys (FLPK) and Pro-Leu-Glu-Val (PLEV) motifs on the β12 sheet of FGF14, and the Glu-Tyr-Tyr-Val (EYYV) motif on the β8-β9 loop of FGF14, as being putatively essential for FGF14:Nav1.6 complex assembly (Ali et al., 2014, 2016). To investigate if short peptides derived from these clusters of amino acids could exert functionally relevant modulation of the Nav1.6 channel macromolecular complex, we previously reported our pharmacological evaluation of the FLPK tetrapeptide (Singh et al., 2020). In that work, we showed that FLPK inhibited FGF14:Nav1.6 complex assembly, reversed FGF14-mediated regulatory effects on Nav1.6 channel activity and affected neuronal excitability of MSNs of the NAc (Singh et al., 2020). Based upon this premise, we sought in the current work to investigate the modulatory effects of PLEV and EYYV on the Nav1.6 channel macromolecular complex. By employing the split-luciferase complementation assay (LCA) and whole-cell patch clamp electrophysiology, we show that these two short peptides derived from FGF14 confer inhibitory effects on FGF14:Nav1.6 complex assembly. Correspondingly, both peptides confer functionally relevant modulation of Nav1.6 channel activity in a manner dependent on the N-terminal domain of FGF14. Overall, this study demonstrates that short peptides derived from "hot spot" (London et al., 2010, 2013) of PPI interfaces could serve as innovative probes to guide drug discovery efforts.

MATERIAL AND METHODS

Materials

D-luciferin (Gold Biotechnology, St. Louis, MO) was prepared as a 30 mg/ml stock solution in phosphate-buffered saline (PBS), and stored at −20 C. PLEV and EYYV peptides were synthesized with 98% purity from Zhejiang Ontores Biotechnologies Co. (Yuhang District, Hangzhou, Zhejiang, China). Peptides were reconstituted in 100% dimethyl sulfoxide (DMSO) as 50 mM stock solutions and stored −20°C.

Plasmid Constructs

Plasmid constructs used in this study were derived from the following clones: human FGF14-1b isoform (accession number: NM_175929.2); human Nav1.6 (accession number: NM_014191.3). The CLuc-FGF14, CD4-Nav1.6-NLuc constructs and the pcDNA3.1 vector (Invitrogen, Carlsbad, CA) were engineered and characterized as previously described (Goetz et al., 2009; Shavkunov et al., 2012; Shavkunov et al., 2013; Shavkunov et al., 2015; Ali et al., 2016, 2018; Wadsworth et al., 2019, 2020; Singh et al., 2020). The plasmid pGL3 expressing full-length Firefly (*Photinus pyralis*) luciferase was a gift from P. Sarkar (Department of Neurology, UTMB). To perform electrophysiological studies, FGF14-GFP and FGF14-ΔNT-GFP (64–252 amino acid residues) were sub-cloned into the GFP plasmid pQBI-fC2 (Quantum Biotechnology Inc., Montreal, Canada) as previously described (Singh et al., 2020).

Homology Model-Based Docking of PLEV and EYYV to FGF14

The homology model-based docking was run with Schrödinger Small-Molecule Drug Discovery Suite using the FGF14 chain of a previously described FGF14:Nav1.6 homology model (Ali et al., 2016; Singh et al., 2020). The structure for protein was prepared by using Protein Prepared Wizard and peptide fragments (PLEV or EYYV containing N-terminal acetylation and C-terminal amidation) were prepared with LigPrep and further initial lowest energy conformation was obtained. The grid box coordinates, grid generation, docking employment, docking poses were analyzed as previously described (Singh et al., 2020).

Cell Culture

HEK293 cells were cultured in a 1:1 mixture of Dulbecco's Modified Eagle Medium (DMEM) with 1 g/L glucose and F-12 (Invitrogen, Carlsbad, CA, United States) that was additionally supplemented with 10% fetal bovine serum, 100 units/ml of penicillin, and 100 µg/ml streptomycin (Invitrogen). HEK293 cells stably expressing CLuc-FGF14 and CD4-Nav1.6-NLuc constructs were maintained similarly except for the addition of 500 µg/ml G418 and 100 ug/ml puromycin (Invitrogen) to maintain stable expression. This cell line was developed and characterized in previous studies and is hereafter coded as "Clone V" cells (Wadsworth et al., 2019). Cells were grown at 37°C. The HEK293 cells stably expressing human $Na_v1.6$ channels have previously been described (Ali et al., 2016, 2018; Singh et al., 2020; Wadsworth et al., 2020). For transient transfections, the Lipofectamine 2000 protocol was followed (Invitrogen, Waltham, MA, United States), and the amount of cDNA used was 1 µg for each. For whole-cell, patch-clamp recordings HEK293-Nav1.6 cells were washed and replated at very low density prior to incubating the cells with peptides for recordings (Ali et al., 2016, 2018; Wadsworth et al., 2019, 2020; Singh et al., 2020).

In Cell Split Luciferase Assay

HEK293 cells stable expressing CLuc-FGF14 and CD4-Nav1.6-NLuc (Clone-V) were grown for 24–48 h. Clone-V cells were detached using TrypLE (Gibco, Waltman, MA, United States), triturated in medium, and seeded in white, clear-bottom CELLSTAR µClear® 96-well tissue culture plates (Greiner Bio-One) at ~0.8 × 105 cells per well in 200 µl of medium. The cells were treated for 12 h in a growth medium supplemented with 100 µl of serum-free, phenol red–free DMEM/F12 medium (Invitrogen) containing PLEV or EYYV (1–250 µM). The final concentration of DMSO was maintained at 0.5% for all wells. Following 12 h incubation at 37°C, the luminescence reaction was initiated by injection of 100 µl substrate solution containing 1.5 mg/ml of D-luciferin dissolved in PBS (final concentration = 0.75 mg/ml) by the Synergy™ H4 Multi-Mode Microplate Reader (BioTek). LCA readings were performed at 2 min intervals for 20–30 min, integration time 0.5 s, while cells were maintained at 37°C throughout the measurements. Detailed LCA method can be found in previous studies (Shavkunov et al., 2012; Ali et al., 2014, 2016, 2018; Hsu et al., 2015; Wadsworth et al., 2019, 2020; Singh et al., 2020).

Electrophysiology in Heterologous Cells

Whole-cell voltage-clamp recordings in heterologous cell systems were performed as previously described (Ali et al., 2016, 2018; Singh et al., 2020; Wadsworth et al., 2020). The HEK293 cells cultured as described above were dissociated using TrypLE and re-plated at very low density onto glass coverslips. HEK293 cells were then allowed at least 3–4 h for attachment before coverslips were transferred to the recording chamber. The recording chamber was filled with a freshly prepared extracellular recording solution comprised of: 140 mM NaCl; 3 mM KCl; 1 mM $MgCl_2$; 1 mM $CaCl_2$; 10 mM HEPES; and 10 mM glucose (pH = 7.3; all salts purchased from Sigma-Aldrich, St. Louis, MO, United States). For control recordings, DMSO was added to the extracellular solution to obtain a final concentration of 0.1%. For the peptide conditions a PLEV and EYYV peptides were added to the extracellular solution to obtain their final concentrations. Cells were pre-incubated for at least 30 min in either DMSO or peptides containing extracellular solutions prior to the recordings. The pipettes were filled with an intracellular solution: 130 mM CH_3O_3SCs; 1 mM EGTA; 10 mM NaCl; and 10 mM HEPES (pH = 7.3; all salts purchased from Sigma-Aldrich). The glass pipettes (Harvard Apparatus, Holliston, MA, United States) with a resistance of 3–5 MΩ were fabricated using a PC-100 vertical Micropipette Puller (Narishige International Inc., East Meadow, NY, United States). Recordings were obtained using an Axopatch 700B or 200B amplifier (Molecular Devices, Sunnyvale, CA, United States). Membrane capacitance and series resistance were estimated using the dial settings on the amplifier, and capacitive transients and series resistances were compensated by 70–80%. Data acquisition and filtering occurred at 20 and 5 kHz, respectively, before digitization and storage. Clampex 9.2 software (Molecular Devices) was used to set experimental parameters, and electrophysiological equipment interfaced to this software using a Digidata 1,200 analog-digital interface (Molecular Devices). Analysis of electrophysiological data was performed using Clampfit 9 software (Molecular Devices) and GraphPad Prism 7 software (La Jolla, CA, United States). After GΩ seal formation and entry into the whole-cell configuration, the voltage-clamp protocols were employed such as the current-voltage (IV) protocol which entailed voltage-steps from −100 mV to +60 mV from a holding potential of −70 mV. The voltage-dependence of steady-state inactivation was calculated using a paired-pulse protocol during which, from the holding potential, cells were stepped to varying test potentials between −20 mV and +20 mV prior to a test pulse to −20 mV.

Current densities were obtained by dividing Na^+ current (I_{Na}) amplitude by membrane capacitance. Current-voltage relationships were then assessed by plotting current density as a function of applied voltage. Tau (τ) of fast inactivation was calculated by fitting the decay phase of currents at the -10 mV voltage step with a one-term exponential function. To assess voltage-dependence of activation, conductance (G_{Na}) was first calculated using the following equation:

$$G_{Na} = \frac{I_{Na}}{(V_m - E_{rev})}$$

where I_{Na} is the current amplitude at voltage V_m, and E_{rev} is the Na^+ reversal potential. Activation curves were then generated by plotting normalized G_{Na} as a function of the test potential. Data was then fitted with the Boltzmann equation to determine $V_{1/2}$ of activation using the following equation:

$$\frac{G_{Na}}{G_{Na,\,max}} = 1 + e^{V_a - E_m/k}$$

where $G_{Na,max}$ is the maximum conductance, V_a is the membrane potential of half-maximal activation, E_m is the membrane voltage, and k is the slope factor. For steady-state inactivation, normalized current amplitude ($I_{Na}/I_{Na,max}$) at the test potential was plotted as a function of pre-pulse potential (V_m) and fitted using the Boltzmann equation:

$$\frac{I_{Na}}{I_{Na,max}} = \frac{1}{1 + e^{V_h - E_m/k}}$$

where V_h is the potential of half-maximal inactivation, E_m is the membrane voltage, and k is the slope factor.

To study long-term inactivation (LTI), a four-sweep protocol consisting of four 20 ms duration, 0 mV depolarizing pulses separated by 40 ms duration −90 mV interpulse recovery phases from a -90 mV holding potential was employed (Dover et al., 2010; Barbosa et al., 2017; Liu et al., 2019; Tapia et al., 2020).

Cumulative inactivation was examined by applying a 2 ms test pulse to −10 mV 20 times at frequency10 Hz from a holding potential of −80 mV. Current responses were normalized to the first recorded pulse and the currents at the 20th pulses were compared (Laezza et al., 2009; Effraim et al., 2019).

Data Analysis

Results are expressed as mean ± standard error of the mean (SEM). Except where otherwise noted, statistical significance was determined using a Student's *t*-test or one way ANOVA Tukey's multiple comparisons test, comparing cells treated with vehicle (DMSO) or PLEV and EYYV, with $p < 0.05$ being considered statistically significant. The analysis was performed by using GraphPad Prism^R (La Jolla, CA) software.

RESULTS

Homology Model-Based Docking of PLEV and EYYV to the Protein-Protein Interaction Interface Between FGF14 and the CTD of Nav1.6

The peptides used in this study were developed based upon segments of FGF14 that are known to be at the interface of the FGF14:Nav1.6 macromolecular complex. PLEV corresponds to an amino acid sequence on the β12 sheet of FGF14, and EYYV corresponds to a sequence on the *β*8-*β*9 loop of FGF14 (Ali et al., 2014). These peptides were docked to a homology model of the PPI interface between FGF14 and the CTD of Nav1.6. (Ali et al., 2016, 2018; Dvorak et al., 2020). In our previous study (Singh et al., 2020) we predicted that PLEV and EYYV were interacting toward the periphery of FGF14 at the β5 strand and N-terminus. We further showed the interactions of PLEV and EYYV with key residues at the FGF14:Nav1.6 PPI interface (modified **Figure 1**, Singh et al., 2020). The molecular docking of PLEV and EYYV revealed predicted interactions with residues at the FGF14:Nav1.6 PPI interface suggestive of the ability to disrupt FGF14:Nav1.6 complex assembly. For example, PLEV and EYYV displayed conserved interactions with R117 on the *β*5 strand of FGF14, a residue that is a crucial constituent of the core domain of FGF14 and is essential for enabling FGF14-mediated regulatory effects on transient I_{Na} and resurgent I_{Na} (Yan et al., 2014). Additionally, PLEV and EYYV displayed conserved interactions with K74 of the N-terminus of FGF14, which could be predictive of these peptides displaying functional activity due to the central role of the N-terminus of FGF14 in conferring modulatory effects on Nav channel inactivation and resurgent I_{Na} (Laezza et al., 2007; Yan et al., 2014; White et al., 2019). Despite these conserved interactions, PLEV and EYYV also displayed divergent interactions with residues at the FGF14:Nav1.6 PPI interface, such as with P203, which could be suggestive of differential effects on Nav1.6 channel activity. Based upon these predicted interactions with residues at the FGF14:Nav1.6 PPI interface *in silico*, both PLEV and EYYV were further investigated in biological systems to interrogate potential modulatory effects on the Nav1.6 channel macromolecular complex.

In-Cell Testing of PLEV and EYYV Using the Split Luciferase Complementation Assay

To evaluate the hypothesis that PLEV and/or EYYV could modulate FGF14:Nav1.6 complex assembly, an in-cell assay was used with a HEK293 cell line (hereafter coded as "Clone V" cells) stably expressing both CLuc-FGF14 and CD4-Nav1.6-NLuc (Shavkunov et al., 2012; Shavkunov et al., 2013; Shavkunov et al., 2015; Ali et al., 2016, 2018; Wadsworth et al., 2019, 2020; Dvorak et al., 2020, 2021; Singh et al., 2020; Wang et al., 2020). In this assay, upon binding of FGF14 to the Nav1.6 C-terminal tail, there is reconstitution of the NLuc and CLuc halves of the luciferase enzyme, which produces luminescence in the presence of substrate D-luciferin (**Figures 2A,D**). Employing this assay in the current study, Clone V cells were seeded into 96 well plates and then treated with various concentrations (1–250 μM) of PLEV, EYYV, or 0.5% DMSO. After incubation, luciferin was dispensed, and the luminescence observed in each well was recorded. The max luminescence observed in each well was then normalized to the average max luminescence observed in per plate control wells. These investigations revealed that PLEV and EYYV displayed dose-dependent inhibitory effects on FGF14:Nav1.6 complex assembly. Specifically, sigmoidal fitting of the dose response curve for PLEV and EYYV revealed IC_{50} values of 41.1 ± 4.4 μM and 35.7 ± 4.7 μM, respectively. (**Figures 2B,C,E,F**). Having demonstrated their inhibitory effects on FGF14:Nav1.6 complex assembly, the functional effects of these peptides on Nav1.6 channel activity were subsequently assessed using whole-cell patch-clamp electrophysiology in heterologous cells.

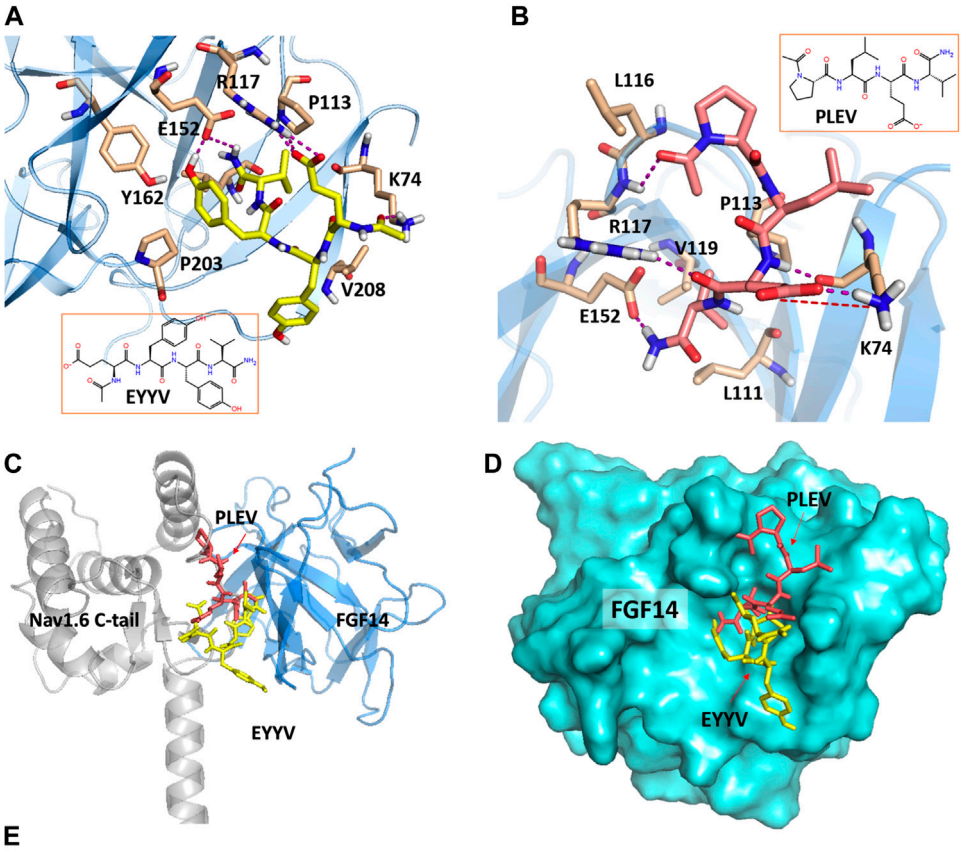

E

Homology model-based docking and interaction of peptides at Nav1.6:FGF14 complex

FGF14 Location	Residues at Nav1.6:FGF14 complex	PLEV	EYYV
β9	N157, Y158, Y159, V160	E152 (H-bond), No interaction with N157,Y158, Y159 and V160	E152 (H-bond), No interaction with N157,Y158, Y159 and V160
β12	L202, P203, P205, V208	P203 (No interaction)	P203, V208 (hydrophobic)
β5	L116, L117	R117 (H-bond) L116, P113 (hydrophobic)	R117(H-Bond, salt bridge), P113 (hydrophobic)
N-terminus	K74, I76	K74 (H-Bond, Salt Bridge) I76 (No interaction)	K74 (H-bond), I76 (hydrophobic)

FIGURE 1 | PLEV and EYYV docking to the FGF14:Nav1.6 complex (modified Singh et al., 2020. Physiol Rep. PMID: 32671946). **(A,B)** Representation of PLEV (pink-orange) and EYYV (yellow) peptide fragments docked into the FGF14 chain of the FGF14:Nav1.6 C-terminal tail homology model. FGF14 has depicted as sky blue ribbons. Key interaction residues are highlighted as stick representations. H-bonds are shown as purple dotted lines, salt bridges are shown as red dotted lines. Residues shown in the map are within 4 Å cut-off. **(C)** Overlay of PLEV (pink-orange) and EYYV (yellow) docked poses and FGF14. Nav1.6 C-terminal tail complex homology model. The FGF14 chain is depicted as sky blue ribbons and the Nav1.6 C-terminal tail is highlighted as gray ribbons. The overlay analysis demonstrated the peptides bound with FGF14 to the different locations at the FGF14:Nav1.6 C-tail protein-protein interaction (PPI) interface. **(D)** Surface representation of PLEV (pink-orange) and EYYV (yellow) peptide fragments docked pose overlay with FGF14 (cyan). **(E)** table representing the Key interacting residues of FGF14:Nav1.6 C-terminal tail PPI with PLEV and EYYV.

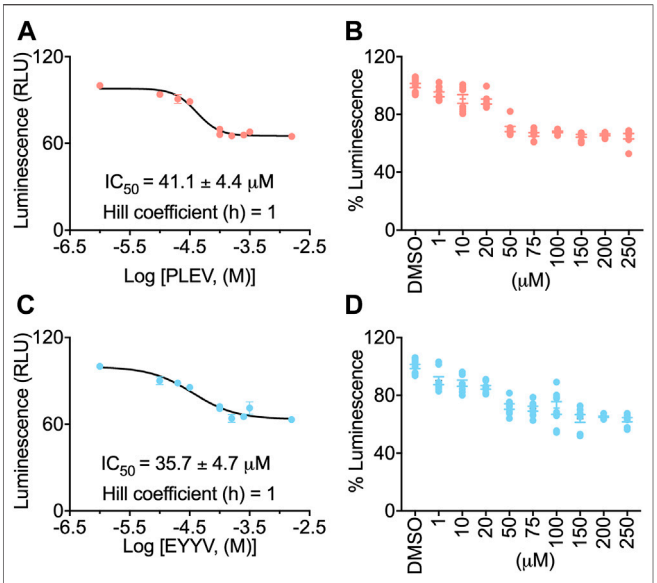

FIGURE 2 | In-cell evaluation of dose-dependent effects of the PLEV and EYYV tetrapeptides on FGF14:Nav1.6 complex assembly using the LCA. **(A)** Percent luminescence plotted as a function of log concentration of PLEV to characterize the dose-dependent effects of the tetrapeptide on FGF14: Nav1.6 complex assembly. **(B)** Bar graph showing dose-response as depicted in panel A. **(C)** Percent luminescence plotted as a function of log concentration of EYYV to characterize the dose-dependent effects of the tetrapeptide on FGF14:Nav1.6 complex assembly. **(D)** Bar graph showing dose-response as depicted in panel B. PLEV or EYYV concentrations were used (1, 10, 25, 50, 75, 100, 150, and 250 μM; n = 8 per concentration) for dose response. Data were normalized to per plate wells treated with 0.5% DMSO, and non-linear regression curve was performed using GraphPad Prism to calculate IC Data represented as mean ± SEM.

PLEV and EYYV Differentially Modulate Peak Transient INa in the Presence of FGF14

Having determined the in-cell potency with which PLEV and EYYV inhibit FGF14:Nav1.6 complex assembly, we next used electrophysiology to evaluate whether PLEV or EYYV displayed modulatory effects on Nav1.6-mediated currents. These recordings were performed in HEK293 cells stably expressing Nav1.6 and transiently transfected with GFP (Nav1.6-GFP) or FGF14-GFP (Nav1.6-FGF14-GFP). The cells were incubated for at least 30 min with 0.1% DMSO or either one of the two tetrapeptides at 50 μM final concentration in a static bath before recording. After incubation, the modulatory effects of PLEV and EYYV on Nav1.6-mediated currents were assessed using whole-cell patch-clamp recordings (**Figures 3**, **4** and **Table 1**). In agreement with previous studies (Ali et al., 2016, 2018; Singh et al., 2020; Wadsworth et al., 2020), expression of FGF14-GFP suppressed the Nav1.6-mediated peak transient Na^+ current (I_{Na}) density (−20.58 ± 3.03 pA/pF, n = 12 vs −59.63 ± 5.33 pA/pF, n = 15; p < 0.001; one-way ANOVA Tukey's multiple comparison test; **Figures 3A,B** and **Table 1**). In the presence of PLEV, the FGF14-mediated suppression of Nav1.6 current was partially reversed compared to control (FGF14-GFP + PLEV: −39.51 ± 5.54 pA/pF, n = 8; FGF14-GFP + DMSO: −20.58 ± 3.03 pA/pF, n = 12; p = 0.0428; one-way ANOVA Tukey's multiple comparison test). Conversely, EYYV failed to modulate the FGF14-mediated regulatory effects on Nav1.6 peak transient I_{Na} density as compared to control (FGF14-GFP + EYYV: −18.1 ± 3.92 pA/pF, n = 10; FGF14-GFP + DMSO: −20.58 ± 3.03 pA/pF, n = 12; p = 0.9890; **Figures 3A,B** and **Table 1**). However, both PLEV and EYYV had no effect when tested in the channel alone experimental group (HEK-Nav1.6-GFP), as the Nav1.6-mediated transient peak I_{Na} density was not significantly changed (PLEV: −64.66 ± 9.1 pA/pF, n = 11; EYYV: −57.09 ± 4.66, n = 14) compared to DMSO (−59.63 ± 5.33 pA/pF, n = 15; **Figures 3A,B** and **Table 1**). Consistent with previous studies (Ali et al., 2016, 2018), co-expression of FGF14 with Nav1.6 increased the decay time constant (τ) of fast inactivation (1.72 ± 0.24 ms, n = 14 versus 1.06 ± 0.06 ms, n = 12 for FGF14-GFP + DMSO versus GFP + DMSO, respectively; p < 0.05). Despite this FGF14-mediated regulatory effect on the entry of Nav1.6 channels into fast inactivation, neither PLEV nor EYYV displayed effects on τ in the presence or absence of FGF14 (**Figure 3D**; **Table 1**).

PLEV and EYYV Display Convergent Modulatory Effects on Steady-State Inactivation, But Divergent Modulatory Effects on Long-Term and Cumulative Inactivation

Consistent with previous investigations (Ali et al., 2016, 2018; Singh et al., 2020), co-expression of FGF14 with Nav1.6 resulted in depolarizing shifts in the voltage-dependence of Nav1.6 channel activation (−24.21 ± 1.02 mV, n = 12 versus 27.98 ± 1.48 mV, n = 14 for FGF14-GFP + DMSO and GFP + DMSO, respectively; p < 0.05; **Figures 4A,B** and **Table 1**) and Nav1.6 channel steady-state inactivation (−56.67 ± 0.69 mV, n = 14 versus −60.93 ± 1.3 mV, n = 13 for FGF14-GFP + DMSO and GFP + DMSO, respectively; p < 0.05; **Figures 4C,D** and **Table 1**). Whereas neither peptide displayed modulatory effects on the voltage-dependence of activation (**Figures 4A,B** and **Table 1**), both peptides reversed the FGF14-mediated depolarizing shift in Nav1.6 channel steady-state inactivation (**Figures 4C,D**). Similar to the results shown in **Figure 3**, both peptides displayed no effects in the absence of FGF14 on either Nav1.6 channel activation or steady-state inactivation.

In contrast to their conserved effects on Nav1.6 channel steady-state inactivation, PLEV and EYYV displayed divergent effects on long-term inactivation (LTI) and cumulative inactivation induced by applying a 2 ms test pulse to −10 mV 20 times at frequency of 10 Hz from a holding potential of −80 mV. Similar to results shown in **Figure 3** and **Figures 4A–D**, both PLEV and EYYV displayed no effect on LTI or cumulative inactivation in the absence of FGF14 (**Figures 4E–H** and **Table 1**). Additionally, EYYV displayed no effects on LTI or cumulative inactivation in the presence of FGF14 (**Figures 4E–H** and **Table 1**). Notably, however, in the presence of FGF14, PLEV

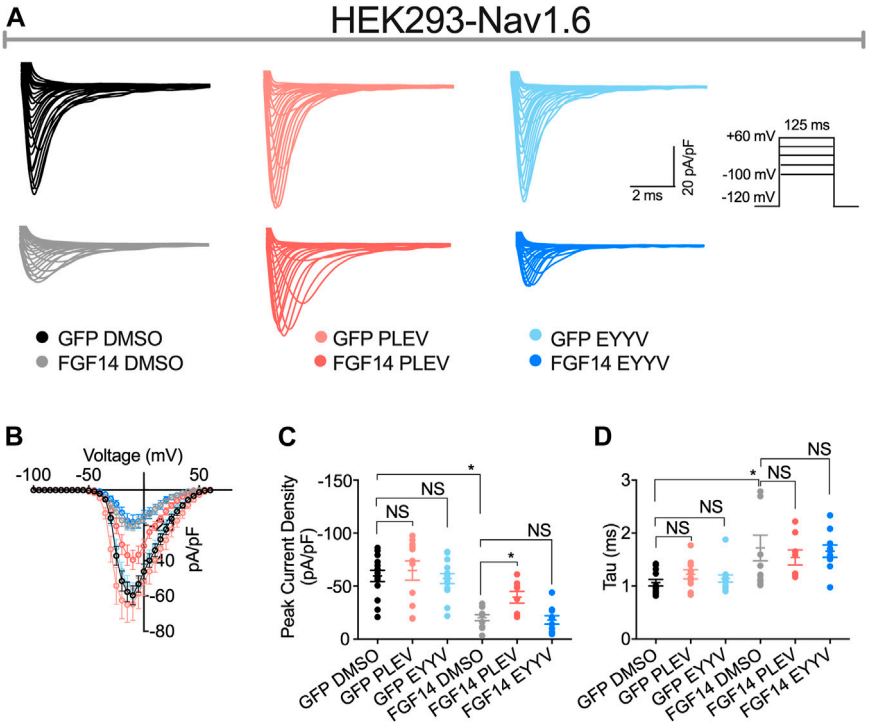

FIGURE 3 | PLEV and EYYV differentially modulate peak transient INa density in the presence of FGF14. **(A)** Representative traces of transient Na+ currents elicited by HEK293-Nav1.6 cells co-expressing either GFP of FGF14-GFP that had been treated with 0.1% DMSO, 50 μM PLEV, or 50 μM EYYV in response to voltage-steps from −100 mV to +60 mV from a holding potential of − 70 mV (inset). **(B)** Current-voltage relationships for experimental groups described in (A). (C,D) Comparison of peak transient INa density **(C)** and tau (τ) of fast inactivation **(D)** for the indicated experimental groups. Data are mean ± SEM. Significance was assessed using a one-way ANOVA Tukey's multiple comparisons test. NS = non-significant; *, p at least < 0.05 (detailed p values and summary of results are reported in **Table 1**).

markedly altered the function of FGF14 as it pertains to its regulatory effects on LTI and cumulative inactivation. Specifically, treatment of HEK-Nav1.6 cells co-expressing FGF14 with PLEV resulted in an increased fraction of channels entering into LTI compared to HEK-Nav1.6 cells co-expressing FGF14 treated with vehicle (**Figures 4E,F** and **Table 1**). Paradoxically, treatment of HEK293-Nav1.6 cells co-expressing FGF14 with PLEV resulted in an increased number of available channels after repetitive stimulation, whereas treatment of HEK293-Nav1.6 cells co-expressing FGF14 with DMSO (control) resulted in roughly the same number of available channels before and after repetitive stimulation (**Figures 4G,H** and **Table 1**). Consistent with the results of the molecular modeling study shown in **Figure 1**, the results of these functional studies highlight conserved and divergent modulatory effects of PLEV and EYYV on the Nav1.6 channel macromolecular complex.

Functional Effects of PLEV and EYYV on Nav1.6 Channel Activity Are Dependent Upon the Presence of the N-terminal Domain of FGF14

The role of the N-terminal domain of FGF14 in conferring its functional regulation of Nav channel activity is widely recognized (Lou et al., 2005; Laezza et al., 2007; Yan et al., 2014; White et al., 2019). According to current models of iFGF-mediated regulation of Nav channel activity, it is proposed that the core domain of FGF14 interacts with the CTD of Nav1.6, which resultantly orients the N-terminal domain of FGF14 such that it can occlude the internal mouth of the pore (Yan et al., 2014; White et al., 2019). Resultantly, both mutating residues of the core domain of FGF14 that enable its PPI with the CTD of Nav1.6 and truncation of the N-terminal domain of FGF14 have been shown to reverse FGF14-mediated regulation of Nav1.6 channel activity (Yan et al., 2014). Based upon this model of FGF14-mediated regulation of Nav1.6 channel activity, we next sought to investigate if PLEV and EYYV, which are derived from the core domain of FGF14, exert their modulatory effects on Nav1.6 channel activity through a mechanism dependent upon the N-terminal domain of FGF14. To do so, HEK293-Nav1.6 cells were transiently transfected with a cDNA construct corresponding to a FGF14 protein product with a truncated N-terminal domain (FGF14-ΔNT-GFP, 64–252 amino acid residues). Transiently transfected cells were then treated with 0.1% DMSO, 50 μM PLEV, or 50 μM EYYV, after which whole-cell patch-clamp electrophysiology was performed as described for **Figure 3** and **Figure 4**.

In these studies, we observed the previously identified (Laezza et al., 2007; Singh et al., 2020) phenotype in which co-expression

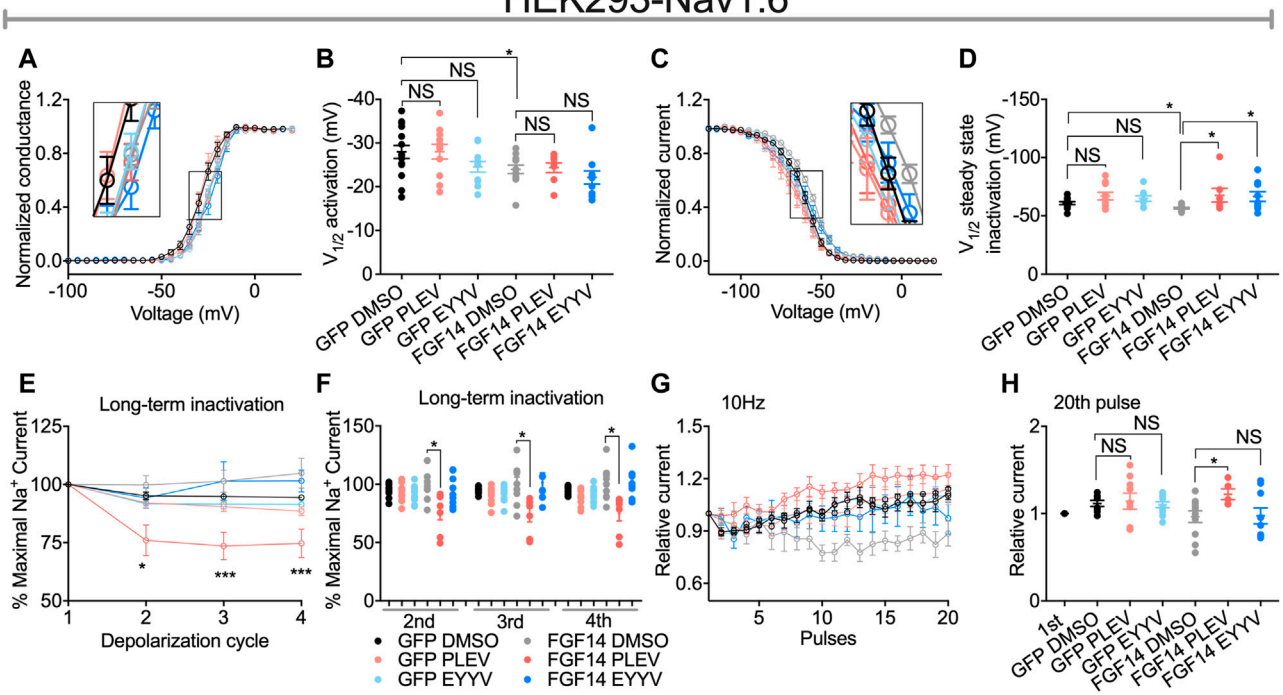

FIGURE 4 | Functional regulation of Nav1.6-mediated currents by PLEV and EYYV. **(A)** Conductance-voltage relationships for Nav1.6 cells co-expressing GFP or FGF14-GFP treated with 0.1% DMSO, 50 μM PLEV and 50 μM EYYV. **(B)** Comparison of V1/2 of activation between the indicated experimental groups. **(C)** Normalized current as a function of membrane potential to characterize the effects of 0.1% DMSO, 50 μM PLEV, and 50 μM EYYV on steady-state inactivation. **(D)** Comparison of V1/2 of steady-state inactivation between the indicated experimental groups. **(E)** Ratio maximal INa plotted as a function of depolarization cycle to characterize the effects of 0.1% DMSO, 50 μM PLEV, or 50 μM EYYV on entry of Nav1.6 channels into long-term inactivation (LTI) in the presence and absence of FGF14. Cells were subjected to four 0 mV 16 ms depolarizations separated by −90 mV 40 ms recovery intervals. **(F)** Bar graph represented 2nd, 3rd, and 4th pulse of LTI. (G,H) Characterization of cumulative inactivation of Nav1.6 channels in the presence or absence of FGF14 exposed to 0.1% DMSO, 50 μM PLEV, or 50 μM EYYV. It was examined by applying a 2 ms test pulse to −10 mV, 20 times at frequency10 Hz from a holding potential of −80 mV. Data are mean ± SEM. Significance was assessed using a one-way ANOVA Tukey's multiple comparisons test. NS = non-significant; *, *p* value at least < 0.05 (detailed *p* values and summary of results are reported in **Tables 1**, **3**).

TABLE 1 | Nav1.6 currents in the presence of FGF14 and tetrapeptides PLEV, EYYV.

Condition	Peak density	Activation	K_{act}	Steady-state inactivation	K_{inact}	Tau (τ)
	pA/pF	mV	mV	mV	mV	Ms
GFP DMSO	−59.63 ± 5.33 (14)	−27.98 ± 1.48 (15)	5.23 ± 0.55 (12)	−60.93 ± 1.3 (13)	5.88 ± 0.59 (13)	1.06 ± 0.06 (12)
GFP PLEV	−64.66 ± 9.1 (11)	−28.01 ± 1.67 (11)	3.97 ± 0.57 (11)	−66.9 ± 3.25 (10)	5.90 ± 0.87 (10)	1.48 ± 0.25 (11)
GFP EYYV	−57.09 ± 4.66 (14)	−24.56 ± 1.20 (11)	4.37 ± 0.40 (11)	−64.93 ± 2.31 (9)	6.57 ± 0.37 (9)	1.14 ± 0.06 (13)
FGF14-GFP DMSO	−20.58 ± 3.03 (11)[a]	−24.21 ± 1.02 (12)[b]	6.66 ± 0.84 (12)	−56.67 ± 0.69 (14)[c]	6.52 ± 0.74 (14)	1.72 ± 0.24 (14)[d]
FGF14-GFP PLEV	−39.51 ± 5.54 (8)[e]	−24.35 ± 1.10 (8)	4.55 ± 0.39 (8)	−67.66 ± 5.85 (7)[f]	7.89 ± 0.90 (7)	1.54 ± 0.14 (8)
FGF14-GFP EYYV	−18.1 ± 3.92 (10)	−22.11 ± 1.49 (10)	5.97 ± 0.69 (10)	−66.59 ± 4.16 (9)[g]	6.91 ± 0.65 (9)	1.66 ± 0.12 (10)

Data are mean ± SEM. ns, non-significant.

[a]p < *0.0001, one-way ANOVA post hoc Tukey's multiple comparisons test compared to GFP DMSO.*

[b]p = *0.0428, Student's* t*-test compared to GFP DMSO.*

[c]p = *0.007, Student's* t*-test compared to GFP DMSO.*

[d]p = *0.0337, one-way ANOVA post hoc Tukey's multiple comparisons test compared to GFP DMSO.*

[e]p = *0.0258, one-way ANOVA post hoc Tukey's multiple comparisons test compared to GFP DMSO.*

[f]p = *0.0497, one-way ANOVA post hoc Tukey's multiple comparisons test compared to FGF14-GFP DMSO.*

[g]p = *0.0084, Student's* t*-test compared to FGF14-GFP DMSO.*

of FGF14-ΔNT with Nav1.6 resulted in a potentiation of Nav1.6 mediated peak transient I_{Na} density compared to co-expression of GFP (FGF14-ΔNT DMSO: −85.26 ± 8.59 pA/pF, n = 13 compared to GFP DMSO: −59.63 ± 5.33 pA/pF, n = 14; p = 0.0162, Student's *t*-test; **Figures 5A,B** and **Tables 1**, **2**). Unlike the effects of PLEV on peak transient I_{Na} density observed in the presence of FGF14 (see **Figure 3**), the peptide displayed no effects on this electrophysiological parameter when the

TABLE 2 | Nav1.6 currents in the presence of FGF14-ΔNT and tetrapeptides PLEV, EYYV.

Condition	Peak density	Activation	K_{act}	Steady-state Inactivation	K_{inact}	Tau (τ)
	pA/pF	MV	mV	mV	mV	ms
FGF14-ΔNT-GFP DMSO	−85.26 ± 8.59 (13)	−23.13 ± 1.79 (13)	5.23 ± 0.55 (13)	−71.71 ± 3.54 (11)	5.88 ± 0.59 (11)	1.07 ± 0.08 (13)
FGF14-ΔNT-GFP PLEV	−74.19 ± 10.22 (12)	−25.65 ± 1.81 (11)	3.97 ± 0.57 (11)	−69.29 ± 3.58 (9)	5.90 ± 0.87 (9)	1.21 ± 0.15 (9)
FGF14-ΔNT-GFP EYYV	−72.25 ± 13.46 (11)	−22.96 ± 0.87 (11)	4.37 ± 0.40 (11)	−69.24 ± 2.22 (13)	6.57 ± 0.37 (13)	1.11 ± 0.14 (13)

Data are mean ± SEM; ns = nonsignificant.

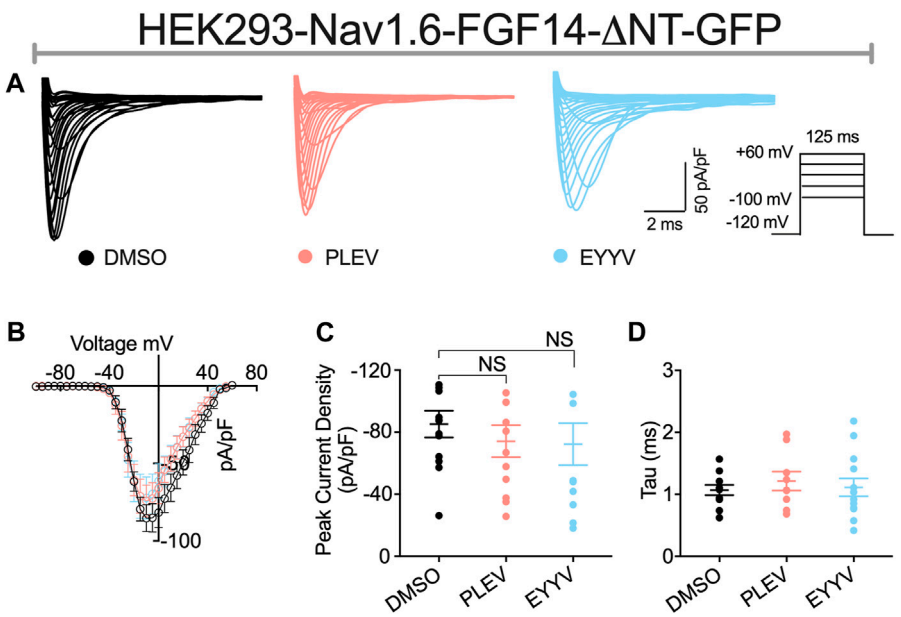

FIGURE 5 | The N-terminal domain of FGF14 is required for functional activity of peptides on peak transient INa density. **(A)** Representative traces of transient Na+ currents elicited by HEK293-Nav1.6 cells co-expressing FGF14-ΔNT-GFP treated with 0.1% DMSO, 50 μM PLEV and 50 μM EYYV in response to voltage steps from −100 mV to +60 mV, holding potential of −70 mV (inset). **(B)** Current-voltage relationships for experimental groups described in **(A)**. **(C,D)** Comparison of peak transient INa density (C) and tau (τ) of fast inactivation (D) for the indicated experimental groups. Data are mean ± SEM. Significance was assessed using Student's *t*-test comparing cells treated with 0.1% DMSO, 50 μM PLEV and 50 μM EYYV. NS = non-significant. Table summary of results is shown in **Table 2**.

TABLE 3 | Nav1.6 channel LTI in the presence of FGF14 and tetrapeptides PLEV, EYYV.

Condition	LTI (% Maximal Na^+ current)		
	2nd Pulse	3rd Pulse	4th Pulse
GFP DMSO	95.12 ± 1.66 (11)	94.82 ± 0.83 (11)	94.41 ± 1.05 (11)
GFP PLEV	92.1 ± 2.22 (11)	90.48 ± 2.03 (11)	88.55 ± 1.87 (11)
GFP EYYV	91.69 ± 2.11 (11)	91.53 ± 2.01 (11)	91.48 ± 1.93 (11)
FGF14-GFP DMSO	99.77 ± 4.01 (11)	101.4 ± 4.74 (11)	104.9 ± 6.39 (11)
FGF14-GFP PLEV	76.06 ± 8.44 (7)[a]	73.56 ± 5.92 (7)[b]	74.69 ± 8.05 (7)[c]
FGF14-GFP EYYV	94.24 ± 4.33 (9)	101.4 ± 8.29 (9)	101.5 ± 6.16 (9)

Data are mean ± SEM. ns, non-significant.
[a]p = *0.0125, one-way ANOVA post hoc Tukey's multiple comparisons test compared to FGF14-GFP DMSO.*
[b]p = *0.0009, one-way ANOVA post hoc Tukey's multiple comparisons test compared to FGF14-GFP DMSO.*
[c]p = *0.0002, one-way ANOVA post hoc Tukey's multiple comparisons test compared to FGF14-GFP DMSO.*

N-terminal domain of FGF14 was truncated (**Figures 5A–C**). EYYV similarly displayed no effects on peak transient I_{Na} density in the presence of FGF14-ΔNT (**Figures 5A–C**). The lack of effects of both peptides on peak transient I_{Na} density in the presence of FGF14-ΔNT were accompanied by lack of effects on τ of fast inactivation (**Figure 5D**).

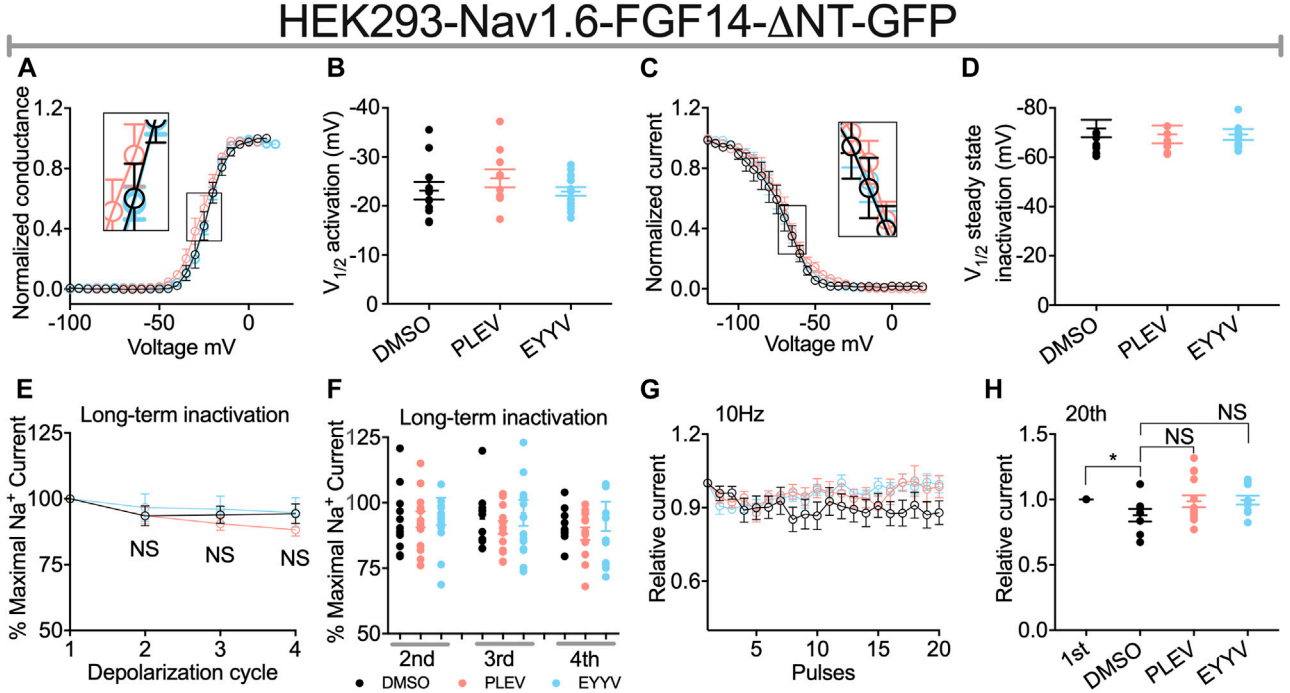

FIGURE 6 | The N-terminal domain of FGF14 is required for peptides to exert modulatory effects on Nav1.6 channel inactivation. **(A)** Conductance-voltage relationships for HEK293-Nav1.6 cells co-expressing FGF14-ΔNT-GFP treated with 0.1% DMSO, 50 μM PLEV and 50 μM EYYV. **(B)** Comparison of V1/2 of activation between the indicated experimental groups. **(C)** Normalized current as a function of membrane potential to characterize the effects of 0.1% DMSO, 50 μM PLEV and 50 μM EYYV on steady-state inactivation. **(D)** Comparison of V1/2 of steady-state inactivation between the indicated experimental groups. **(E)** Ratio maximal INa plotted as a function of depolarization cycle to characterize entry of Nav1.6 channels exposed to 0.1% DMSO, 50 μM PLEV, or 50 μM EYYV in the presence of FGF14-ΔNT. Cells were subjected to four 0 mV 16 ms depolarizations separated by −90 mV 40 ms recovery intervals. **(F)** Bar graph represented 2nd, 3rd, and 4th pulse of LTI. **(G,H)** Assessment of cumulative inactivation of Nav1.6 channels exposed to 0.1% DMSO, 50 μM PLEV, or 50 μM EYYV in the presence of FGF14-ΔNT. It was examined by applying a 2 ms test pulse to −10 mV 20 times at frequency10 Hz from a holding potential of −80 mV. Data are mean ± SEM. Significance was assessed using an Student's *t*-test comparing cells treated with 0.1% DMSO, 50 μM PLEV and 50 μM EYYV. NS = non-significant; *, *p* at least < 0.05 (detailed *p* values and summary of results are reported in **Tables 2**, **4**).

TABLE 4 | Nav1.6 channel LTI in the presence of FGF14-ΔNT and tetrapeptides PLEV, EYYV.

Condition	LTI (% Maximal Na^+ current)		
	2^{nd} Pulse	3^{rd} Pulse	4^{th} Pulse
FGF14-ΔNT-GFP DMSO	92.82 ± 4.57 (9)	93.21 ± 3.97 (9)	94.17 ± 4.52 (9)
FGF14-ΔNT-GFP PLEV	91.27 ± 3.10 (12)	88.4 ± 2.33 (12)	86.91 ± 2.58 (12)
FGF14-ΔNT-GFP EYYV	98.12 ± 7.34 (10)	97.66 ± 6.87 (10)	93.37 ± 8.12 (10)

Data are mean ± SEM; ns = nonsignificant.

Similar to their lack of effects on Nav1.6 channel activation in the presence of FGF14, PLEV and EYYV displayed no effects on this electrophysiological parameter in the presence of FGF14-ΔNT (**Figures 6A,B**). Notably, however, whereas both PLEV and EYYV reversed FGF14-mediated regulatory effects on Nav1.6 channel steady-state inactivation (**Figures 4C,D**), neither peptide displayed effects on this parameter in the presence of FGF14-ΔNT (**Figures 6C,D**). Furthermore, the additional modulatory effects of PLEV on LTI and cumulative inactivation observed in the presence of FGF14 were also not observed in the presence of FGF14-ΔNT (**Figures 6E–H**). Overall, these studies provide strong evidence that these two peptides, despite being derived from the core domain of FGF14, exert their effects on Nav1.6 channel activity through a mechanism dependent upon the presence of the N-terminal domain of FGF14.

DISCUSSION

PLEV and EYYV represent previously identified tetrapeptides that correspond to clusters of amino acids on the β12 sheet and β8-β9 loop of FGF14, respectively, that are at the FGF14's PPI interface with the CTD of Nav1.6 (Ali et al., 2014, 2016; Singh

et al., 2020). Given the primacy of these structural motifs of FGF14 in enabling FGF14:Nav1.6 complex assembly, we investigated if short peptides corresponding to these motifs of FGF14 could confer functionally relevant modulation of the Nav1.6 channel macromolecular complex. Given that perturbation of the PPI between FGF14 and the CTD of Nav1.6 gives rise to neural circuitry aberrations that are linked to neurologic and neuropsychiatric disorders (Di Re et al., 2017; Paucar et al., 2020), such peptides could represent promising "small-molecular inhibitor starting points (SMISP)" to develop PPI-targeting neuromodulators (Koes and Camacho, 2012a; 2012b). To pharmacologically evaluate the PLEV and EYYV tetrapeptides as potential SMISPs, we employed an amalgam of complementary and orthogonal approaches including *in silico* molecular modeling, the LCA, and whole-cell patch-clamp electrophysiology. These results demonstrated that PLEV and EYYV both displayed functional modulation of the Nav1.6 channel macromolecular. Despite displaying mostly convergent modulatory effects on Nav1.6 channel activity, PLEV and EYYV displayed some divergent effects, consistent with their derivation from different structural motifs of FGF14. Overall, these studies provide strong evidence that PLEV and EYYV could serve as promising scaffolds for the development of chemical probes targeting the PPI interface between FGF14 and the CTD of Nav1.6. Additionally, this study further support the notion that short peptides derived from "hot spot" (London et al., 2010, 2013) of PPI interfaces could serve as innovative probes to guide drug discovery efforts.

PLEV and EYYV Disrupt FGF14:Nav1.6 Complex Assembly Through Predicted Interactions With Resides at the PPI Interface

In our previous study (Singh et al., 2020), we pharmacologically evaluated all three tetrapeptides at a single concentration of 50 μM using the LCA. In the FGF14:Nav1.6 wild type condition, all three tetrapeptides displayed comparable single concentration activity. In conditions in which putative "hot spot" residues at the FGF14:Nav1.6 PPI interface were mutated, such as Y158 and V160 (Ali et al., 2016, 2018), the three peptides displayed some divergent effects. For example, in the $FGF14^{V160A}$ condition, all three peptides lost activity, whereas in the $FGF14^{Y158A}$ condition, FLPK retained its inhibitory effects on FGF14:Nav1.6 complex assembly, whereas PLEV and EYYV were shown to increase FGF14:Nav1.6 complex assembly.

Based upon these divergent effects of PLEV and EYYV compared to FLPK, we elected to further pharmacologically evaluate these two tetrapeptides in the present investigation. In dose-response analyses studies, PLEV and EYYV were shown to inhibit FGF14:Nav1.6 complex assembly with IC_{50} values of 41.1 ± 4.4 μM and 35.7 ± 4.7 μM, respectively. These in-cell studies, considered collectively with the *in silico* molecular modeling studies, highlight potential residues of FGF14 that, when occupied by a ligand, inhibit FGF14:Nav1.6 complex assembly. For example, PLEV and EYYV have predicted interactions with residues of the core domain of FGF14 including R117 and E152, as well as predicted interactions with residues of the N-terminal domain of FGF14 including K74. Given these predicted modes of binding coupled with the inhibitory effects of PLEV and EYYV on FGF14:Nav1.6 complex assembly, these residues could represent potential "hot spots" for the development of small molecular modulators targeting the FGF14:Nav1.6 PPI interface.

PLEV and EYYV Modulates Nav1.6 Channel Activity

To test whether PLEV and EYYV affected Nav1.6-mediated currents, we employed whole-cell patch-clamp electrophysiology in heterologous cell systems. We used HEK cells stably expressing human Nav1.6 (HEK-Nav1.6), and transiently transfected with GFP (HEK293-Nav1.6-GFP) or FGF14-GFP (HEK293-Nav1.6-FGF14-GFP) and treated with 50 μM PLEV and EYYV or 0.1% DMSO (**Figures 3**, **4**). Both peptides did not show measurable effect in the absence of FGF14 (Nav1.6-GFP); however, PLEV partially reversed the FGF14-mediated regulatory effects on peak transient I_{Na} density (**Figures 3A–C**; **Table 1**). This effect was not observed due to treatment with EYYV, highlighting the divergent mechanisms of action of the two tetrapeptides. Unlike their differential modulation of FGF14-mediated regulatory effects on peak transient I_{Na} density, PLEV and EYYV displayed conserved effects in terms of reversing FGF14-mediated regulatory effects on Nav1.6 channel steady-state inactivation (**Figures 4C,D**; **Table 1**). Whereas PLEV and EYYV displayed conserved modulatory effects on Nav1.6 channel steady-state inactivation, PLEV also displayed distinct effects on LTI and cumulative inactivation that were not observed due to treatment with EYYV. Specially, PLEV increased the fraction of Nav1.6 channels that entered into LTI in a FGF14-dependent fashion, indicating a complex mechanism of action where treatment with PLEV results in altered function of FGF14. PLEV similarly altered the function of FGF14 as it related to cumulative inactivation, as HEK293-Nav1.6-FGF14-GFP cells treated with PLEV displayed an increased number of available channels after repetitive stimulation, whereas the same cells treated with DMSO displayed no change in the number of available channels before and after repetitive stimulation. All together, these effects demonstrate that PLEV and EYYV display both convergent and divergent effects on Nav1.6 channel activity, which could be attributable to their derivation from different structural motifs of FGF14 and differential interactions with residues at the FGF14:Nav1.6 PPI interface.

FGF14-1b N-Terminus Domain Required to Modulate Nav1.6 Channel Activity

The N-terminal domain of FGF14-1b, the splice variant of FGF14 studied in the present investigation, is essential for conferring FGF14-mediated regulation of Nav1.6 channel

activity, as deletion of the N-terminus of FGF14-1b abolishes the regulatory effects of FGF14 on a myriad of electrophysiological properties of Nav1.6 channels (Laezza et al., 2007; Yan et al., 2014). In line with previous studies, FGF14-ΔNT potentiates Nav1.6 current densities (**Figures 3A–C**, **5A–C**; **Tables 1**, **2**), causes a depolarizing shift in the voltage-dependence of Nav1.6 channel activation, a hyperpolarizing shift in the voltage-dependence of Nav1.6 channel steady-state inactivation, while having no effects on LTI or cumulative inactivation of Nav1.6 channels (**Figures 3**, **5E–H**; **Tables 1**, **2**) (Laezza et al., 2007, 2009; Ali et al., 2018; Singh et al., 2020). In contrast to the modulatory effects of PLEV and EYYV on Nav1.6 channel activity in the presence of FGF14, the peptides display no effects in the presence of FGF14-ΔNT. As such, while the peptides are derived from clusters of amino acids constituent to the core domain of FGF14, their mechanisms of action are nevertheless dependent upon the N-terminal domain of FGF14. Given the central role of the N-terminus of FGF14-1b in the generation of resurgent I_{Na} and the repetitive firing of action potentials (Yan et al., 2014), these results have important implications for anticipating the functional effects of both tetrapeptides in the native system. As FGF14-1b is highly enriched in clinically relevant brain regions, including the nucleus accumbens (Ali et al., 2018) and hippocampus (Hsu et al., 2016), along with Nav1.6, these peptides that disrupt their complex assembly could represent promising scaffolds for their development of PPI-targeting neuromodulators (Dvorak et al., 2021).

CONCLUSION

We have studied the modulatory effects of the tetrapeptides PLEV and EYYV, which correspond to residues of FGF14 that are at its PPI interface with the CTD of the Nav1.6 channel, on FGF14: Nav1.6 complex assembly and the functional activity of the Nav1.6 channel macromolecular complex. We have shown that both peptides functionally modulate Nav1.6 channel activity in a manner dependent upon the N-terminal domain of FGF14. Whereas both tetrapeptides inhibited FGF14:Nav1.6 complex assembly and reversed the FGF14-mediated depolarizing shift in the voltage-dependence of Nav1.6 channel steady-state inactivation, PLEV exerted additional modulatory effects not observed due to treatment with EYYV. Specially, PLEV increased the fraction of Nav1.6 channels that entered into LTI and modulated the fraction of channels that re-open during repetitive stimulation in a FGF14-depedent manner, indicating a complex mechanism of action where treatment with PLEV results in altered function of FGF14. Consistent with the molecular modeling studies shown in **Figure 1**, these nonoverlapping modulatory effects on Nav1.6 channel activity could be attributable to the tetrapeptides being derived from different structural motifs of FGF14 and resultantly displaying divergent interactions with residues at the FGF14:Nav1.6 PPI interface.

DATA AVAILABILITY STATEMENT

The original contributions presented in the study are included in the article/supplementary files, further inquiries can be directed to the corresponding authors.

AUTHOR CONTRIBUTIONS

Conceptualization, AS and FL; formal analysis, AS; investigation, AS, and FL; data curation, AS, ND., CT, AM; technical, SA and ZB; writing—original draft preparation, AS; writing-review and editing, AS, ND and FL; visualization, AS, and FL; supervision, AS, and FL; docking, HC; resources, JZ and FL; project administration, JZ and FL; funding acquisition, JZ, and FL. All authors have read and agreed to the published version of the manuscript.

FUNDING

This work was supported by the Houston Area Molecular Biophysics Program Grant No. T32 GM008280 (ND), National Institute of Environmental Health Sciences T32-ES007254 (Tapia), R25 GM069285 training grant (ZB), National Institutes of Health (NIH) Grants 1R01MH12435101 (FL), R01MH111107 (JZ and FL), P30 DA028821 (JZ), John D. Stobo, M.D. Distinguished Chair Endowment Fund at UTMB (JZ), John Sealy Memorial Endowment Fund (FL) and the UTMB Technology Commercialization Program (JZ and FL).

ACKNOWLEDGMENTS

We thank Jully Singh for technical support. We acknowledge the Sealy Center for Structural Biology and Molecular Biology at the University of Texas Medical Branch at Galveston for providing research resources.

REFERENCES

Ali, S. R., Liu, Z., Nenov, M. N., Folorunso, O., Singh, A., Scala, F., et al. (2018). Functional Modulation of Voltage-Gated Sodium Channels by a FGF14-Based Peptidomimetic. *ACS Chem. Neurosci.* 9, 976–987. doi:10.1021/acschemneuro.7b00399

Ali, S. R., Singh, A. K., and Laezza, F. (2016). Identification of Amino Acid Residues in Fibroblast Growth Factor 14 (FGF14) Required for Structure-Function Interactions with Voltage-Gated Sodium Channel Nav1.6. *J. Biol. Chem.* 291, 11268–11284. doi:10.1074/jbc.M115.703868

Ali, S., Shavkunov, A., Panova, N., Stoilova-McPhie, S., and Laezza, F. (2014). Modulation of the FGF14:FGF14 Homodimer Interaction through Short Peptide Fragments. *Cnsnddt* 13, 1559–1570. doi:10.2174/1871527313666141126103309

Barbosa, C., Xiao, Y., Johnson, A. J., Xie, W., Strong, J. A., Zhang, J.-M., et al. (2017). FHF2 Isoforms Differentially Regulate Nav1.6-mediated Resurgent Sodium Currents in Dorsal Root Ganglion Neurons. *Pflugers*

Arch. - Eur. J. Physiol. 469, 195–212. doi:10.1007/s00424-016-1911-9.FHF2

Catterall, W. A., Goldin, A. L., and Waxman, S. G. (2005). International Union of Pharmacology. XLVII. Nomenclature and Structure-Function Relationships of Voltage-Gated Sodium Channels. *Pharmacol. Rev.* 57, 397–409. doi:10.1124/pr.57.4.4.and

Catterall, W. A., Kalume, F., and Oakley, J. C. (2010). NaV1.1 Channels and Epilepsy. *J. Physiol.* 588, 1849–1859. doi:10.1113/jphysiol.2010.187484

Catterall, W. A., and Swanson, T. M. (2015). Structural Basis for Pharmacology of Voltage-Gated Sodium and Calcium Channels. *Mol. Pharmacol.* 88, 141–150. doi:10.1124/mol.114.097659

Catterall, W. A. (2012). Voltage-gated Sodium Channels at 60: Structure, Function and Pathophysiology. *J. Physiol.* 590, 2577–2589. doi:10.1113/jphysiol.2011.224204

Chahine, M., Chatelier, A., Babich, O., and Krupp, J. (2008). Voltage-gated Sodium Channels in Neurological Disorders. *Cnsnddt* 7, 144–158. doi:10.2174/187152708784083830

Claes, L., Del-Favero, J., Ceulemans, B., Lagae, L., Van Broeckhoven, C., and De Jonghe, P. (2001). De Novo mutations in the Sodium-Channel Gene SCN1A Cause Severe Myoclonic Epilepsy of Infancy. *Am. J. Hum. Genet.* 68, 1327–1332. doi:10.1086/320609

Di Re, J., Wadsworth, P. A., and Laezza, F. (2017). Intracellular Fibroblast Growth Factor 14: Emerging Risk Factor for Brain Disorders. *Front. Cel. Neurosci.* 11, 1–7. doi:10.3389/fncel.2017.00103

Dib-Hajj, S. D., Black, J. A., and Waxman, S. G. (2015). NaV1.9: a Sodium Channel Linked to Human Pain. *Nat. Rev. Neurosci.* 16, 511–519. doi:10.1038/nrn3977

Dib-Hajj, S. D., Black, J. A., and Waxman, S. G. (2009). Voltage-gated Sodium Channels: Therapeutic Targets for Pain. *Pain Med.* 10, 1260–1269. doi:10.1111/j.1526-4637.2009.00719.x

Dover, K., Solinas, S., D'Angelo, E., and Goldfarb, M. (2010). Long-term Inactivation Particle for Voltage-Gated Sodium Channels. *J. Physiol.* 588, 3695–3711. doi:10.1113/jphysiol.2010.192559

Dvorak, N. M., Wadsworth, P. A., Wang, P., Chen, H., Zhou, J., and Laezza, F. (2020). Bidirectional Modulation of the Voltage-Gated Sodium (Nav1.6) Channel by Rationally Designed Peptidomimetics. *Molecules* 25, 3365. doi:10.3390/molecules25153365

Dvorak, N. M., Wadsworth, P. A., Wang, P., Zhou, J., and Laezza, F. (2021). Development of Allosteric Modulators of Voltage-Gated Na+ Channels: A Novel Approach for an Old Target. *Ctmc* 21, 841–848. doi:10.2174/1568026621666210525105359

Effraim, P. R., Huang, J., Lampert, A., Stamboulian, S., Zhao, P., Black, J. A., et al. (2019). Fibroblast Growth Factor Homologous Factor 2 (FGF-13) Associates with Nav1.7 in DRG Neurons and Alters its Current Properties in an Isoform-dependent Manner. *Neurobiol. Pain* 6, 100029. doi:10.1016/j.ynpai.2019.100029

Goetz, R., Dover, K., Laezza, F., Shtraizent, N., Huang, X., Tchetchik, D., et al. (2009). Crystal Structure of a Fibroblast Growth Factor Homologous Factor (FHF) Defines a Conserved Surface on FHFs for Binding and Modulation of Voltage-Gated Sodium Channels. *J. Biol. Chem.* 284, 17883–17896. doi:10.1074/jbc.M109.001842

Goldin, A. L., Barchi, R. L., Caldwell, J. H., Hofmann, F., Howe, J. R., Hunter, J. C., et al. (2000). Nomenclature of Voltage-Gated Sodium Channels. *Neuron* 28, 365–368. doi:10.1016/s0896-6273(00)00116-1

Hsu, W.-C., Nenov, M. N., Shavkunov, A., Panova, N., Zhan, M., and Laezza, F. (2015). Identifying a Kinase Network Regulating FGF14:Nav1.6 Complex Assembly Using Split-Luciferase Complementation. *PLoS One* 10, e0117246–21. doi:10.1371/journal.pone.0117246

Hsu, W. C. J., Scala, F., Nenov, M. N., Wildburger, N. C., Elferink, H., Singh, A. K., et al. (2016). CK2 Activity Is Required for the Interaction of FGF14 with Voltage-gated Sodium Channels and Neuronal Excitability. *FASEB j.* 30, 2171–2186. doi:10.1096/fj.201500161

Koes, D. R., and Camacho, C. J. (2012a). PocketQuery: Protein-Protein Interaction Inhibitor Starting Points from Protein-Protein Interaction Structure. *Nucleic Acids Res.* 40, W387–W392. doi:10.1093/nar/gks336

Koes, D. R., and Camacho, C. J. (2012b). Small-molecule Inhibitor Starting Points Learned from Protein-Protein Interaction Inhibitor Structure. *Bioinformatics* 28, 784–791. doi:10.1093/bioinformatics/btr717

Laezza, F., Gerber, B. R., Lou, J.-Y., Kozel, M. A., Hartman, H., Marie Craig, A., et al. (2007). The FGF14F145S Mutation Disrupts the Interaction of FGF14 with Voltage-Gated Na+ Channels and Impairs Neuronal Excitability. *J. Neurosci.* 27, 12033–12044. doi:10.1523/JNEUROSCI.2282-07.2007

Laezza, F., Lampert, A., Kozel, M. A., Gerber, B. R., Rush, A. M., Nerbonne, J. M., et al. (2009). FGF14 N-Terminal Splice Variants Differentially Modulate Nav1.2 and Nav1.6-encoded Sodium Channels. *Mol. Cell Neurosci.* 42, 90–101. doi:10.1016/j.mcn.2009.05.007

Lampert, A., O'Reilly, A. O., Reeh, P., and Leffler, A. (2010). Sodium Channelopathies and Pain. *Pflugers Arch. - Eur. J. Physiol.* 460, 249–263. doi:10.1007/s00424-009-0779-3

Liu, C.-j., Dib-Hajj, S. D., Renganathan, M., Cummins, T. R., and Waxman, S. G. (2003). Modulation of the Cardiac Sodium Channel Nav1.5 by Fibroblast Growth Factor Homologous Factor 1B. *J. Biol. Chem.* 278, 1029–1036. doi:10.1074/jbc.M207074200

Liu, Z., Wadsworth, P., Singh, A. K., Chen, H., Wang, P., Folorunso, O., et al. (2019). Identification of Peptidomimetics as Novel Chemical Probes Modulating Fibroblast Growth Factor 14 (FGF14) and Voltage-Gated Sodium Channel 1.6 (Nav1.6) Protein-Protein Interactions. *Bioorg. Med. Chem. Lett.* 29, 413–419. doi:10.1016/j.bmcl.2018.12.031

London, N., Raveh, B., Movshovitz-Attias, D., and Schueler-Furman, O. (2010). Can Self-Inhibitory Peptides Be Derived from the Interfaces of Globular Protein-Protein Interactions? *Proteins* 78, 3140–3149. doi:10.1002/prot.22785

London, N., Raveh, B., and Schueler-Furman, O. (2013). Druggable Protein-Protein Interactions - from Hot Spots to Hot Segments. *Curr. Opin. Chem. Biol.* 17, 952–959. doi:10.1016/j.cbpa.2013.10.011

Lou, J.-Y., Laezza, F., Gerber, B. R., Xiao, M., Yamada, K. A., Hartmann, H., et al. (2005). Fibroblast Growth Factor 14 Is an Intracellular Modulator of Voltage-Gated Sodium Channels. *J. Physiol.* 569, 179–193. doi:10.1113/jphysiol.2005.097220

Lu, H., Zhou, Q., He, J., Jiang, Z., Peng, C., Tong, R., et al. (2020). Recent Advances in the Development of Protein-Protein Interactions Modulators: Mechanisms and Clinical Trials. *Sig Transduct Target. Ther.* 5. doi:10.1038/s41392-020-00315-3

Mantegazza, M., Curia, G., Biagini, G., Ragsdale, D. S., and Avoli, M. (2010). Voltage-gated Sodium Channels as Therapeutic Targets in Epilepsy and Other Neurological Disorders. *Lancet Neurol.* 9, 413–424. doi:10.1016/S1474-4422(10)70059-4

Mantegazza, M., Gambardella, A., Rusconi, R., Schiavon, E., Annesi, F., Cassulini, R. R., et al. (2005). Identification of an Nav1.1 Sodium Channel (SCN1A) Loss-Of-Function Mutation Associated with Familial Simple Febrile Seizures. *Proc. Natl. Acad. Sci.* 102, 18177–18182. doi:10.1073/pnas.0506818102

Musa, H., Kline, C. F., Sturm, A. C., Murphy, N., Adelman, S., Wang, C., et al. (2015). SCN5A Variant that Blocks Fibroblast Growth Factor Homologous Factor Regulation Causes Human Arrhythmia. *Proc. Natl. Acad. Sci. USA* 112, 12528–12533. doi:10.1073/pnas.1516430112

Oyrer, J., Maljevic, S., Scheffer, I. E., Berkovic, S. F., Petrou, S., and Reid, C. A. (2018). Ion Channels in Genetic Epilepsy: From Genes and Mechanisms to Disease-Targeted Therapies. *Pharmacol. Rev.* 70, 142–173. doi:10.1124/pr.117.014456

Paucar, M., Lundin, J., Alshammari, T., Bergendal, A., Solders, G., Lindefeldt, M., et al. (2020). Broader Phenotypic Traits and Widespread Brain Hypometabolism in Spinocerebellar Ataxia 27. *J. Intern. Med.* 288, 103–115. doi:10.1111/joim.13052

Pitt, G. S., and Lee, S.-Y. (2016). Current View on Regulation of Voltage-Gated Sodium Channels by Calcium and Auxiliary Proteins. *Protein Sci.* 25, 1573–1584. doi:10.1002/pro.2960

Probst, V., Wilde, A. A. M., Barc, J., Sacher, F., Babuty, D., Mabo, P., et al. (2009). SCN5A Mutations and the Role of Genetic Background in the Pathophysiology of Brugada Syndrome. *Circ. Cardiovasc. Genet.* 2, 552–557. doi:10.1161/CIRCGENETICS.109.853374

Sanders, S. J., Murtha, M. T., Gupta, A. R., Murdoch, J. D., Raubeson, M. J., Willsey, A. J., et al. (2012). De Novo mutations Revealed by Whole-Exome Sequencing Are Strongly Associated with Autism. *Nature* 485, 237–241. doi:10.1038/nature10945

Savio-Galimberti, E., Gollob, M. H., and Darbar, D. (2012). Voltage-gated Sodium Channels: Biophysics, Pharmacology, and Related Channelopathies. *Front. Pharmacol.* 3 (JUL), 1–19. doi:10.3389/fphar.2012.00124

Schaefer, J., Giangrande, E., Weinberger, D. R., and Dickinson, D. (2013). The Global Cognitive Impairment in Schizophrenia: Consistent over Decades and Around the World. *Schizophrenia Res.* 150, 42–50. doi:10.1016/j.schres.2013.07.009

Shavkunov, A., Panova, N., Prasai, A., Veselenak, R., Bourne, N., Stoilova-McPhie, S., et al. (2012). Bioluminescence Methodology for the Detection of Protein-Protein Interactions within the Voltage-Gated Sodium Channel Macromolecular Complex. *ASSAY Drug Development Tech.* 10, 148–160. doi:10.1089/adt.2011.413

Shavkunov, A. S., Ali, S. R., Panova-elektronova, N. I., and Laezza, F. (2015). Split-Luciferase Complementation Assay to Detect Channel-Protein Interactions in Live Cells. *Methods Mol. Biol.*, 1278, 497–514. doi:10.1007/978-1-4939-2425-710.1007/978-1-4939-2425-7_33

Shavkunov, A. S., Wildburger, N. C., Nenov, M. N., James, T. F., Buzhdygan, T. P., Panova-Elektronova, N. I., et al. (2013). The Fibroblast Growth Factor 14·Voltage-Gated Sodium Channel Complex Is a New Target of Glycogen Synthase Kinase 3 (GSK3). *J. Biol. Chem.* 288, 19370–19385. doi:10.1074/jbc.M112.445924

Singh, A. K., Wadsworth, P. A., Tapia, C. M., Aceto, G., Ali, S. R., Chen, H., et al. (2020). Mapping of the FGF14:Nav1.6 Complex Interface Reveals FLPK as a Functionally Active Peptide Modulating Excitability. *Physiol. Rep.* 8, 1–20. doi:10.14814/phy2.14505

Tang, Z., Chen, Z., Tang, B., and Jiang, H. (2015). Primary Erythromelalgia: A Review. *Orphanet J. Rare Dis.* 10, 1–11. doi:10.1186/s13023-015-0347-1

Tapia, C. M., Folorunso, O., Singh, A. K., McDonough, K., and Laezza, F. (2020). Effects of Deltamethrin Acute Exposure on Nav1.6 Channels and Medium Spiny Neurons of the Nucleus Accumbens. *Toxicology* 440, 152488. doi:10.1016/j.tox.2020.152488

Tavassoli, T., Kolevzon, A., Wang, A. T., Curchack-Lichtin, J., Halpern, D., Schwartz, L., et al. (2014). De Novo SCN2A Splice Site Mutation in a Boy with Autism Spectrum Disorder. *BMC Med. Genet.* 15, 1–8. doi:10.1186/1471-2350-15-35

Tseng, T.-T., McMahon, A. M., Johnson, V. T., Mangubat, E. Z., Zahm, R. J., Pacold, M. E., et al. (2007). Sodium Channel Auxiliary Subunits. *J. Mol. Microbiol. Biotechnol.* 12, 249–262. doi:10.1159/000099646

Volkers, L., Kahlig, K. M., Verbeek, N. E., Das, J. H. G., van Kempen, M. J. A., Stroink, H., et al. (2011). Nav1.1 Dysfunction in Genetic Epilepsy with Febrile Seizures-Plus or Dravet Syndrome. *Eur. J. Neurosci.* 34, 1268–1275. doi:10.1111/j.1460-9568.2011.07826.x

Wadsworth, P. A., Folorunso, O., Nguyen, N., Singh, A. K., D'Amico, D., Powell, R. T., et al. (2019). High-throughput Screening against Protein:protein Interaction Interfaces Reveals Anti-cancer Therapeutics as Potent Modulators of the Voltage-Gated Na+ Channel Complex. *Sci. Rep.* 9, 1–15. doi:10.1038/s41598-019-53110-8

Wadsworth, P. A., Singh, A. K., Nguyen, N., Dvorak, N. M., Tapia, C. M., Russell, W. K., et al. (2020). JAK2 Regulates Nav1.6 Channel Function via FGF14Y158 Phosphorylation. *Biochim. Biophys. Acta (Bba) - Mol. Cel Res.* 1867, 118786. doi:10.1016/j.bbamcr.2020.118786

Wang, C., Wang, C., Hoch, E. G., and Pitt, G. S. (2011). Identification of Novel Interaction Sites that Determine Specificity between Fibroblast Growth Factor Homologous Factors and Voltage-Gated Sodium Channels. *J. Biol. Chem.* 286, 24253–24263. doi:10.1074/jbc.M111.245803

Wang, P., Wadsworth, P. A., Dvorak, N. M., Singh, A. K., Chen, H., Liu, Z., et al. (2020). Design, Synthesis, and Pharmacological Evaluation of Analogues Derived from the PLEV Tetrapeptide as Protein-Protein Interaction Modulators of Voltage-Gated Sodium Channel 1.6. *J. Med. Chem.* 63, 11522–11547. doi:10.1021/acs.jmedchem.0c00531

Wang, Q., Shen, J., Splawski, I., Atkinson, D., Li, Z., Robinson, J. L., et al. (1995). SCN5A Mutations Associated with an Inherited Cardiac Arrhythmia, Long QT Syndrome. *Cell* 80, 805–811. doi:10.1016/0092-8674(95)90359-3

White, H. V., Brown, S. T., Bozza, T. C., and Raman, I. M. (2019). Effects of FGF14 and NaVβ4 Deletion on Transient and Resurgent Na Current in Cerebellar Purkinje Neurons. *J. Gen. Physiol.* 151, 1300–1318. doi:10.1085/jgp.201912390

Woods, C. G., Babiker, M. O. E., Horrocks, I., Tolmie, J., and Kurth, I. (2015). The Phenotype of Congenital Insensitivity to Pain Due to the NaV1.9 Variant p.L811P. *Eur. J. Hum. Genet.* 23, 561–563. doi:10.1038/ejhg.2014.166

Wright, R., Malec, M., Shega, J. W., Rodriguez, E., Kulas, J., Morrow, L., et al. (2016). Deconstructing Chronic Low Back Pain in the Older Adult-step by Step Evidence and Expert-Based Recommendations for Evaluation and Treatment: Part XI: Dementia. *Pain Med.* 17, 1993–2002. doi:10.1093/pm/pnw247

Yan, H., Pablo, J. L., Wang, C., and Pitt, G. S. (2014). FGF14 Modulates Resurgent Sodium Current in Mouse Cerebellar Purkinje Neurons. *Elife* 3, e04193. doi:10.7554/eLife.04193

Yu, F. H., and Catterall, W. A. (2003). Overview of the Voltage-Gated Sodium Channel Family. *Genome Biol.* 4, 207. doi:10.1186/gb-2003-4-3-207

Conflicts of Interest: The authors declare no competing financial interest. FL is the founder and president of IonTx Inc., a start-up company focusing on developing regulators of voltage-gated Na^+ channels. However, this activity does not represent a conflict with the present study.

The remaining authors declare that the research was conducted in the absence of any commercial or financial relationships that could be construed as a potential conflict of interest.

Publisher's Note: All claims expressed in this article are solely those of the authors and do not necessarily represent those of their affiliated organizations, or those of the publisher, the editors and the reviewers. Any product that may be evaluated in this article, or claim that may be made by its manufacturer, is not guaranteed or endorsed by the publisher.

Advantages of publishing in Frontiers

OPEN ACCESS
Articles are free to read for greatest visibility and readership

FAST PUBLICATION
Around 90 days from submission to decision

HIGH QUALITY PEER-REVIEW
Rigorous, collaborative, and constructive peer-review

TRANSPARENT PEER-REVIEW
Editors and reviewers acknowledged by name on published articles

Frontiers
Avenue du Tribunal-Fédéral 34
1005 Lausanne | Switzerland

Visit us: www.frontiersin.org
Contact us: frontiersin.org/about/contact

REPRODUCIBILITY OF RESEARCH
Support open data and methods to enhance research reproducibility

DIGITAL PUBLISHING
Articles designed for optimal readership across devices

FOLLOW US
@frontiersin

IMPACT METRICS
Advanced article metrics track visibility across digital media

EXTENSIVE PROMOTION
Marketing and promotion of impactful research

LOOP RESEARCH NETWORK
Our network increases your article's readership